Stony Brook University

A Role for the Polarity Protein Par3 in ErbB2-induced Breast Cancer

A Dissertation Presented

by

Bin Xue

to

The Graduate School

in Partial Fulfillment of the

Requirements

for the Degree of

Doctor of Philosophy

in

Molecular and Cellular Biology

Stony Brook University

August 2012

Stony Brook University

The Graduate School

Bin Xue

We, the dissertation committee for the above candidate for the
Doctor of Philosophy degree, hereby recommend
acceptance of this dissertation.

Dr. Senthil K. Muthuswamy – Dissertation Advisor
Associate Professor, Cold Spring Harbor Laboratory
Professor, University of Toronto
Senior Scientist, Ontario Cancer Institute

Dr. Alea A. Mills - Chairperson of Defense
Professor, Cold Spring Harbor Laboratory

Dr. Mikala Egeblad
Assistant Professor, Cold Spring Harbor Laboratory

Dr. W. Todd Miller
Professor, Stony Brook University

Dr. Howard C. Crawford
Associate Professor, Mayo Clinic Cancer Center

This dissertation is accepted by the Graduate School

Charles Taber

Interim Dean of the Graduate School

Abstract of the Dissertation
A Role for the Polarity Protein Par3 in ErbB2-induced Breast Cancer
by
Bin Xue
Doctor of Philosophy
in
Molecular and Cellular Biology
Stony Brook University
2012

Polarity protein Partitioning defective protein 3 (Par3) is an evolutional conserved scaffold protein in metazoans. Par3 together with Par6 and aPKC form Par complex and localize at the subapical domain of epithelial cells. Par3 plays important roles during establishment of apical membrane and tight junctions in epithelia. In my thesis, I identified Par3 as a novel metastasis suppressor in breast cancer.

ErbB2, also known as HER2, is an important proto-oncogene in breast cancer. Approximately 25% of breast cancers have ErbB2 amplification or overexpression and correlate with poor prognosis. Downregulation of Par3 cooperated with ErbB2 to induce cell invasion in mammary epithelial cells *in vitro* and induced metastasis of ErbB2-induced primary mouse mammary tumors. Surprisingly, loss of Par3 induced invasive behavior in the epithelial cells was not associated with an overt epithelial mesenchymal transition. However, loss of Par3 prevented E-cadherin junction maturation and decreased cell-cell cohesion.

I identified the molecular mechanisms by which Par3 regulates E-cadherin junction maturation. Downregulation of Par3 induced spatial and temporal dysregulation of Rac activation by activating Rac-GEF Tiam1. In addition I found Par3 interacted with a branched actin polymerizing protein complex, Arp2/3 and assembles an E-cadherin-Par3-Arp2/3 at cell-cell junctions. Loss of Par3 resulted in mislocalization of Arp2/3 from cell-cell junctions. The aberrant Rac activation and disruption of Arp2/3 from cell-cell junctions induced aberrant actin cytoskeleton organization at cell-cell junctions that resulted in inhibition of maturation on E-cadherin junctions.

In human breast cancer, decrease in membrane Par3 was correlated with higher tumor grade and ErbB2 positive status. Dysregulation of Par3 was found in the metastases compared to the primary breast tumors. Together, our data suggest that loss of Par3 promotes metastatic behavior of ErbB2-induced tumor epithelial cells by decreasing cell-cell cohesion.

Table of Contents

List of Figures

List of Tables

List of Abbreviations

3D	Three-dimensional
ADH	Atypical ductal hyperplasia
AJ	Adherens junction
APKC	Atypical protein kinase C
Arp2/3	Actin related protein 2/3
BM	Basement membrane
Cdc42	Cell division control protein 42 homolog
c-MET	Mesenchymal epithelial transition factor
c-Myc	Cellular oncogene from avian myelocytomatosis
CRIB	Cdc42/Rac interactive binding
CSF-1	Colony-stimulating factor-1
DAPI	4', 6-diamidine-2-phenylinodole-dihydrochlodride
DCIS	Ductal carcinoma *in situ*
DIC	Differential interference contrast
Dlg	Discs Large
ECM	Extracellular matrix
EGFR	Epidermal growth factor receptor
EHS	Engelbreth-Holm-Swarm
EMT	epithelial-mesenchymal transition
ER	Estrogen receptor
ErbB2	v-erb-B2 erythroblastic leukemia viral oncogene homolog 2
FFPET	Formalin-fixed paraffin-embedded tissue
FKBP	FK506-binding protein
FRAP	Fluorescence recovery after photobleaching
FRET	Förster Resonance Energy Transfer
GAP	GTPase activating protein
GDI	Guanine-nucleotide dissociation inhibitor
GDP	Guanine Di-phosphate
GEF	Guanine-nucleotide exchange factor
GFP	Green fluorescent protein

GMC	Ganglion mother cell
GP135	Golgi protein 135
GTP	Guanine tri-phosphate
H&E	Hematoxylin and eosin
HA	Hemagglutinin
HELU	Hyperplastic enlarged lobular unit
HER2	Human epidermal growth factor receptor 2
HGF	Hepatocyte growth factor
IBC	Infiltrating breast carcinoma
IDC	Invasive ductal carcinomas
IF	Intermediate filament
IHC	Immunohistochemistry
IRSp53	Insulin receptor tyrosine kinase substrate p53
JAM	Junctional adhesion molecule
Lgl	Lethal(2) giant larvae
LRR	Leucin-rich repeats
LTR	Long terminal repeat
MAPK	Mitogen-activated protein kinase
MDCK	Madin-Darby canine kidney
MEC	Mammary epithelial cell
MET	Mesenchymal-epithelial transition
MMLV	Moloney murine leukemia virus
MMP	Matrix metalloproteinase
MMTV	Mouse mammary tumor virus
MOI	Multiplicity of infection
NB	Neuroblast
NGFR	Nerve growth factor receptor
NRG	Neuregulin
PanIN	Pancreatic intraepithelial neoplasia
PAR	Partitioning defective
PCP	Planar cell polarity
PDAC	Pancreatic ductal adenocarcinoma

PGK	Phosphoglycerate kinase
PH	Pleckstrin homology
PI3K	Phosphoinositide 3-kinase
PR	Progesterone receptor
PTEN	Phosphatase and tensin homolog
PyMT	Polyoma virus Middle T-Antigen
Rac1	Ras-related C3 botulinum toxin substrate
RhoA	Ras homolog gene family, member A
TDLU	Terminal ductal lobular units
TGF-α	Tumor growth factor - alpha
TGF-β	Tumor growth factor - beta
Tiam1	T Lymphoma invasion and metastasis 1
TJ	Tight junction
TP53	Tumor suppressor protein p53
TRC	The RNAi Consortium
WASp	Wiskott-Aldrich *syndrome family* protein
WAVE2	Wiskott-Aldrich syndrome protein family member 2
ZO	Zonula Occludens

Acknowledgments

First and foremost, I would like to thank my advisor Dr Senthil K. Muthuswamy for the continual advice, support and understanding throughout the years. His vision of science and dedication are truly inspiring. Working under Senthil's guidance, I am always encouraged to take challenge, think independently and constructively. The work present in this thesis could not have been achieved without his efforts and insights.

I would like to thank the members of my committee Alea Mill, Mikala Egeblad, Todd Miller and Howard Crawford, for serving on my committee and providing guidance and advices over the course of my training. I would especially like to thank Dr. Mikala Egeblad for sharing me her expertise in breast cancer and providing me the mouse tumor samples.

Thanks for the people who helped me during the project: Kannan Krishnamurthy for cell analyses and discussion; my collaborator Dr. Craig Allred for providing and analyzing the human breast cancer samples; Lixing Zhan and Avi Rosenberg for teaching me the mouse operations; Stephen Hearn in microscopy facility, Gula and Raya in histology facility, Pamela Moody in FACS facility and the staff in animal facility for their assistance. I would like to thank Mike Feigin, Jennifer Haynes and Jonathan Ipsaro for helping me with my English and editing my thesis and Charles Camarda for making these beautiful illustrations.

During my PhD period, I had the fortune to closely work with the big Muthuswamy lab, the Toronto lab and some other labs in Cold Spring Harbor Laboratory. I would like to thank all the Muthuswamy lab members, past and present, in USA and in Canada. In particular, I would like to thank Mike Feigin and Sai Dipikaa Akshinthala for their friendship and comradeship in these years, Dr. Nicholas Tonks and all his lab members for the great discussions in the labmeetings, Min Yu for mentoring me when I first joined the lab and my dear "neighbor", Dr. Yuri Lazebinik. They have been a wonderful group people to work with. In addition, I would like to thank all my friends in CSHL and my Stony Brook classmates for the help and supports in my life.

I would like to thank my parents and sister for their never-ending and selfless love.

Chapter 1
Introduction

1.1 Cell Polarity

Cell polarity is the process by which a cell establishes and maintains an asymmetric organization of cellular components and structure. A cell polarizes at multiple levels: correct positioning and orientation of the Golgi apparatus is required for transport of post-transcriptional modified proteins to their proper destinations; microtubules (MT) form a structural network to provide tracks for directional intracellular transport and form the mitotic spindle to determine chromosome segregation axes during cell division; the actin cytoskeleton provides a structural network that controls the unique shape of an individual cell, and also functions in directional intracellular transport and cell motility. At the molecular level, proteins and lipids asymmetrically organized along the plasma membrane and within the cytosol. All these elements need to be precisely integrated to form a proper polarized cell.

The ability to develop and maintain spatial asymmetry is an evolutionarily conserved property observed from yeast to humans. Almost all cell types exhibit some form of polarity, which is essential for their specialized functions. Classical examples of polarized cells include neurons that use axon-dendrite polarity to receive and propagate signals, mobile lymphocytes that use front-rear polarity to respond to cytokines and pathogens and drive towards the inflammatory area, and epithelial cells that exhibit apical-basal polarity for their structural integrity and specialized function such as secretion. Apical-basal polarity will be extensively discussed in this thesis.

During tissue morphogenesis, cells are not restricted to one type of polarity; instead, they engage in different types of cell polarity consecutively or concurrently, reflecting the complexity and plasticity of development. One example of temporal polarity transition is observed during the development of trachea in *Drosophila.* The trachea arises from dorsal trunk metameres of about 80 cells. At early stage (stage 10-12) all tracheal cells are found side-by-side and possess apical-basal polarity. During stages 13-14, cells in most branches undergo rearrangement, in which epithelial cells behave similar to mesenchymal cells with front-rear polarity to form lateral protrusions in-between individual cells and intercalate (Neumann and Affolter 2006). After these stages, intercalated cells form a dorsal branch in

which each cells show an autocellular, ‘straight-line’ and connect to the adjacent cells through adherens junction (Shaye, Casanova et al. 2008).

In epithelial cells, apical-basal polarity overlaps with other types of polarity to regulate organ homeostasis. Dividing epithelial cells can orient their spindle polarity differently to change the plane of cell division, allowing retention or release of the daughter cell from ductal structures, which is required for controlling tubule elongation or expansion (Fischer, Legue et al. 2006). In addition, epithelial cells align with their neighbors and engage in long-range patterning to maintain tissue order, a process referred to as planar cell polarity (PCP) (Zallen 2007) (Figure 1.1). During normal development, all of these polarity mechanisms need to be coordinated in a highly regulated manner.

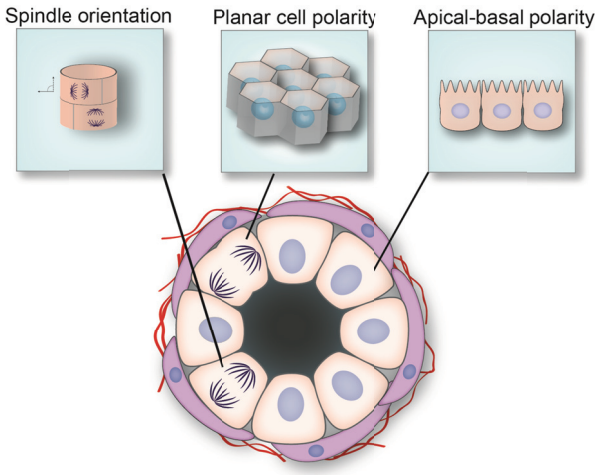

Figure 1.1. Different types of cell polarity in a epithelial ductal structure

Three different types of polarity are thought to regulate morphogenesis of epithelial ductal structure. (From left to right) Mitotic spindle polarity used for controlling positioning of daughter cells; planar cell polarity used by epithelial cells to coordinate polarity between cells; apical-basal polarity used by epithelial cells to asymmetrically distribute proteins along the apical-basal axis.

Epithelial Architecture

The epithelial tissue is one of the basic types of animal tissue, along with the connective tissue, muscle tissue and nervous tissue. Epithelial tissue lines the surface of the body and all of the internal body cavities that have a connection with the external environment at some stage. A major role for epithelial cells is to serve a protective function in maintaining physiological homeostasis of the body. However, some epithelia have evolved specialized functions including selective absorption (intestine), secretion (glands), transcellular transportation (ion-transporting epithelium) and sensory reception (taste buds). Regardless of their diverse functions, a common feature of epithelia is that they are composed of cells that are tightly bound to each other, facing two distinctive environments, and displaying a highly sophisticated type of membrane asymmetry and organelle alignment referred to as apical-basal polarity. The apical membrane, facing the outside surface of the body or in contact with the luminal space of the internal cavities, displays surface modifications such as microvilli and cilia. In contrast, the basolateral membrane scaffolds the epithelial tissue to the interior of the organism. Various cell-cell junctions, including tight junctions (TJs), adherens junctions (AJs), gap junctions, desmosomes and hemidesmosomes, regulate intercellular communication and localized to the basolateral membrane. TJs serve to limit the paracellular permeability of fluid and ions. Hemidesmosomes mediate communicate between the cells and the extracellular matrix (ECM) (Handler 1989) (Figure 1.2). In epithelial cells, the Golgi apparatus is positioned between nucleus and the apical membrane (Lacy 1957; Barr and Egerer 2005). MTs in epithelial cells do not associate with centrosomes as in other cell types; instead, MT ends are released from the centrosome after nucleation (Keating, Peloquin et al. 1997), and form bundles along the apical-basal axis, with plus ends oriented towards the basal side and minus ends oriented toward the apical side of the cells. This reorganization of MTs facilitates MT-dependent protein sorting and polarized vesicle trafficking, which is a prerequisite for development of polarized surface domains and epithelial lumen formation (Müsch 2004). As normal physiological function and tissue integrity rely on proper cell polarity, it is important to study whether changes in cell polarity could disrupt normal cellular function and cause disease, including epithelial-derived carcinoma.

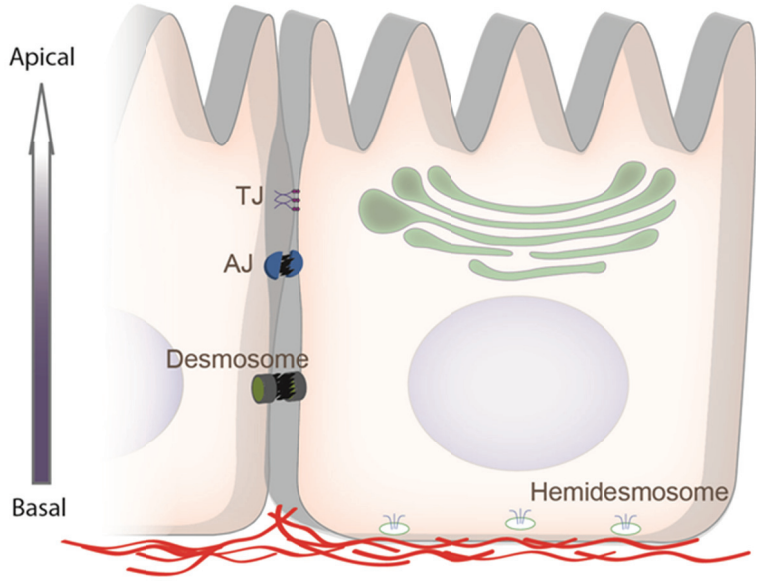

Figure 1.2. Epithelial archetucture

Illustration of typical organization of epithelial cells with apical-basal polarity. The apical membrane faces the outside surface of the body or in contact with the luminal space of the internal cavities. The basolateral membrane scaffolds the epithelial tissue to the surrounding connective tissue. Cell-cell junctions including TJs, AJs and desmosomes are localized to lateral of the membrane. Hemidesmosomes are localized at basal membrane to scaffold the cell to the ECM (red curve lines). the Golgi apparatus (green stacks) is positioned juxtaposed to the face of the nucleus proximal to the apical membrane.

1.2 Organization of Mammary Gland *In Vivo*

Anatomical Structure of the Mammary Gland

The mammary gland is an exocrine glandular epithelial structure composed of ducts that are specialized to produce and secrete milk. In the human breast, the mammary gland is composed of 15-20 irregular lobes of branched tubuloalveolar glands also known as terminal ductal lobular units (TDLU), each of which is an intact functional unit. Milk secretion originates in the lobules. Each lobule ends in a lactiferous duct that opens through a constricted orifice into the nipple (Figure 1.3. A). Near their openings, the lactiferous ducts are lined with stratified squamous epithelium, a multilayered flattened epithelium. The epithelial lining of the duct shows a gradual transition from two layers of cuboidal cells in a dilated portion to a single layer of columnar or cuboidal cells (together called luminal epithelial) through the remainder of the duct system (Figure 1.3. B). Myoepithelial cells of ectodermal origin are located within the epithelium between the surface epithelial cells and the basal lamina, and harbor progenitor/stem cells. These cells, arranged in a basketlike network, surround the secretory portion of the gland (Hennighausen and Robinson 2005; Bland and Copeland 2009; Van Keymeulen, Rocha et al. 2011) (Figure 1.3.C). The tissue between the ducts and glands, composed of adipose tissue and fibrous tissue in varying proportions, is called the "stroma".

Historically the mouse has been used as a model system to study the structure and function of breast. However, human and mouse mammary glands have some differences, mainly reflected in their TDLU structure and stromal compartment. The human TDLU comprises a small group of lobules emerging from a terminal duct, and thus resembles a cluster of grapes at the end of a stem. The mouse mammary gland consists of a single primary duct which branches into three to five secondary ducts. In adult virgin mice, the secondary ducts grow and branch off to fill the entire fat pad (Hennighausen and Robinson 2005). The stroma of the mouse mammary gland comprises a large amount of fat with small amounts of interspersed fibrous connective tissue. In contrast, human mammary epithelium is directly associated with fibrous connective tissue (Topper and Freeman 1980). Despite these differences, the bilayered ductal structure and disease development in transgenic mice are

highly comparable morphologically to those in humans, and thus provides valuable model for mammary gland development and breast cancer research (Cardiff and Wellings 1999).

Apical-Basal Polarity in Mammary Epithelial Cells

The mammary epithelial cell (MEC) shares the typical features of a ductal glandular epithelium. They are organized as one layer surrounding a lumen with the apical side facing the lumen and the basal side in contact with the surrounding basement membrane (BM), a specialized ECM structure. The cells are joined together by AJs and TJs. An AJ is a molecular connection primarily mediated by transmembrane protein epithelial cadherin (E-cadherin), the submembrane catenin complex and the associated actin cytoskeleton. E-cadherin belongs to the classical cadherin receptor family whose extracellular domain consists of five EC1-EC5 subdomains, which bind in a homophilic manner to those in adjacent cells in the presence of Ca^{2+} ions to form rod-like structures (Gumbiner, Stevenson et al. 1988; Baum and Georgiou 2011). E-cadherin is expressed in both luminal and myoepithelial cells, while another classical cadherin member, placental cadherin (P-cadherin) is restricted to myoepithelial cells (Palacios, Benito et al. 1995). The cytoplasmic domain of E-cadherin binds to the β-catenin-α-catenin complex, which provides a link to actin filaments. Catenins are not only structural components, but they are also involved in different signal transduction pathways, including the canonical Wnt pathway (Rovensky and SpringerLink 2011). In addition to AJs, epithelial cells adhere to each other and to stromal cells through desmosomes. Distinct from AJs that associate with the actin cytoskeleton, desmosomes confer their cell adhesive function by serving as binding sites for intermediate filaments (IFs) to the plasma membrane. The desmosome is composed of the transmembrane proteins Desmocollins (Dsc, three isoforms Dsc1-3) and Desmogleins (Dsg, three isoforms Dsg1-3), which belong to the classical cadherin family. In the mammary gland, desmosomal cadherins are not only expressed in the luminal epithelia, but also in myoepithelial cells in an isotype-specific manner. Dsc2 and Dsg2 are expressed both in luminal and myoepithelial cells, while Dsc3 and Dsg3 expression is restricted to the myoepithelial cells (Runswick, O'Hare et al. 2001). Functional analysis using desmosomal cadherin blocking peptides revealed that

desmosomes are not only required for cell adherence, but also are used for positioning myoepithelial cells outside of the luminal epithelial cell layer during alveolar morphogenesis (Runswick, O'Hare et al. 2001; Bissell and Bilder 2003).

Tight junctions serve to form a tight seal between adjacent cells and also to demarcate the apical and basolateral membrane domains of an epithelial cell. A growing number of proteins has been identified to be involved in TJ assembly. The integral membrane proteins that constitute the TJ strands include Occludin, claudin family proteins, and junctional adhesion molecules (JAMs). The TJ membrane proteins recruit a group of cytoplasmic proteins, which initiates downstream signaling. These cytoplasmic proteins are mainly PDZ-containing proteins, including Zonula Occludens (ZO, three isoforms ZO-1-3), and polarity proteins such as Partitioning defective 3 (Par3), Pals1 and Pals1-associated TJ protein (PATJ) (Gonzalez-Mariscal and SpringerLink 2006). In the mammary gland, the permeability of TJs is closely related to its lactogenesis function. The TJs in alveolar epithelial cells are leaky during pregnancy and become impermeable during lactation, allowing milk to be collected and stored in the lumen (Nguyen and Neville 1998; Itoh and Bissell 2003). While the functions of TJ proteins in the mammary gland are largely unknown, recent studies have shown that TJ molecules such as ZO-1 and JAM-A are directly or indirectly involved in breast cancer initiation and progression (McSherry, McGee et al. 2009; Du, Xu et al. 2010), suggesting that TJs may also be involved in diseases associated with the of mammary gland.

Epithelial organs are embedded in an organized meshwork of ECM proteins. The ECM not only provides structural support for tissues, it also guides cell development and patterning, and regulates cell fate decisions (Muschler and Streuli 2010). The ECM proteins contained in the BM include collagen, elastin, laminins, nidogens, perlecan and agrin (Hynes 2009). Collagens are the structural base of the ECM. The molecular structure of all collagens is a stiff heterotrimer containing three α-chains twisting together. This unique structure provides resistance to mechanical stretching, so called stiffness, of BMs. The common type IV collagen present in most breast BMs is a trimer of two α1 and one α2 subunits (Yurchenco 2011). Elastin, another structural component, consists of flexible polypeptide chains that are interconnected to form fibers and sheets (Rovensky and SpringerLink 2011). This stretchable property of elastin allows the tissue to maintain its shape while providing the

supporting structure. Laminins and nidogens are the proteins that mediate adhesion between the cells and the BM by directly binding cell surface proteins. Laminin is a heterotrimer containing one each of five α, four β and three γ chains, and is required for assembly of BMs. The carboxyl-terminal laminin globular (LG) domain mediates binding to cell surface receptors such as integrins and dystroglycans and is required for anchoring BM components to initiate nascent BM assembly. The amino-terminal laminin globular (LN) domain also interacts with cell surface integrins to align laminin into a triple helix parallel to the cell surface. The β and γ subunits of laminin interact with other BM proteins such as agrins and nidogens. Nidogens (entactins) bind to both laminin and collagen IV forming an additional link between laminin and BM stabilization. Agrins and perlecans provide collateral linkage between laminins and the cytoplasmic cytoskeleton.

Mammary epithelial structures are surrounded by a collagen-enriched BM matrix secreted primarily by stromal cells (Keely, Wu et al. 1995; LeBleu, MacDonald et al. 2007). The interaction of luminal cells with the BM is sufficient to initiate cell polarization. Laminin 111 (also known as laminin-1) secreted by surrounding myoepithelial cells is essential for the inner luminal cells to correctly attach to collagen and undergo polarization and lumen formation (Gudjonsson, Ronnov-Jessen et al. 2002; Bissell and Bilder 2003). Cell-matrix interactions also contribute to the functional specificity of the mammary epithelia. Specifically, single mammary epithelial cells express the milk protein β-casein when grown in laminin-rich BM, but not in a pure collagen I environment (Streuli, Bailey et al. 1991).

The recognition and adhesion of cells to the ECM is mediated by the transmembrane glycoproteins receptors called eceintegrins. All integrins are heterodimers composed of non-covalently associated α and β subunits, which both are type-I transmembrane proteins with little sequence similarity. Different integrins are required for interacting with different cell substratum: α2β1 and β4 are required for collagen, and β1-integrins (α1β1, α2β1, α3β1, α6β1, and α7β1) for laminins; therefore, they play different roles in establishing cell polarity. α2β1 and β4 integrins induce cell polarization in a Rac-dependent manner. The α3β1 integrins are implicated in positioning of mitotic spindle in epithelial cells within a cyst, which is essential for lumen formation (Myllymaki, Teravainen et al. 2011). Changes in ECM components and their receptors play important roles during cell polarization and during development.

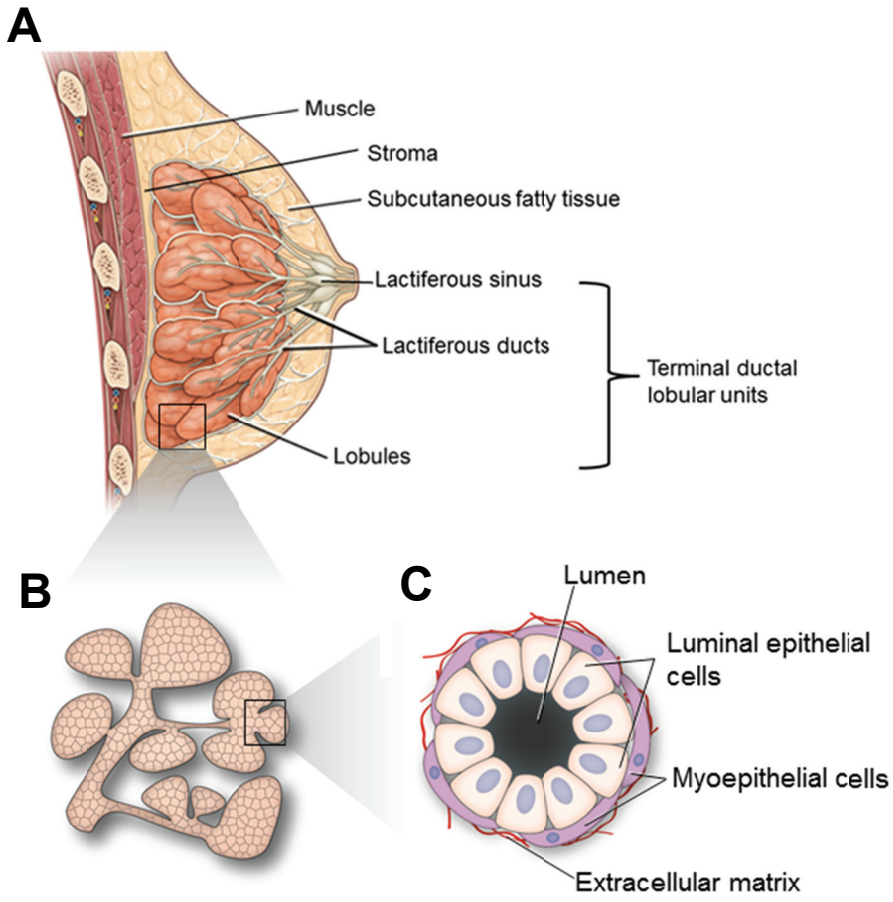

Figure 1.3. Human mammary gland structure

A) Anatomy of the human mammary gland. Each mammary gland contains 15-20 lobes. Each lobe contains a terminal ductal lobular unit and the duct drains into the nipple.

B) The TDLU structure is lined with a layer of epithelial cells.

C) The ducts consist of mammary luminal epithelial cells closely associated with an outer layer of myoepithelial cells, and surrounded by the basement membrane, a specialized ECM structure. The central lumen is where the milk is collected and stored during lactation.

1.3 *In Vitro* Models for Studying Epithelial organization

Several *in vitro* model systems have been established to study three-dimentional (3D) epithelial organization and development of cell polarity. The dog kidney epithelial cell line Madin-Darby canine kidney (MDCK) develops apical-basal polarity with functional tight junctions under specific culture conditions, and has been used in most early studies. MDCK cells can be polarized when grown at high density on a porous membrane, allowing access to the medium on both apical and basal surfaces of the epithelial cell monolayer. In this setup, the cells naturally polarize with their basal plasma membrane surface against the solid support and their apical surface facing the culture medium. (Cereijido, Robbins et al. 1978).

With the recognition of the important role of the ECM in tissue organization, new 3D culture systems where epithelial cells grown on a reconstituted BM is widely adopted to study tissue organization. The most commonly used reconstituted basement membrane in culture is Matrigel, a biologically active gelatinous protein mixture secreted by Engelbreth-Holm-Swarm (EHS) mouse sarcoma cells, and mainly composed of Laminin (56%), Collagen IV (31%) and entactin/nidogen (8%) (Kleinman and Martin 2005). Morphogenesis of human mammary epithelial cells is best modeled using MCF10A, an immortalized human breast epithelial cell line that is non-tumorigenic (Soule, Maloney et al. 1990). When grown in Matrigel, single MCF10A cells first proliferate into small clusters. After 2-3 days, the cells in direct contact with the matrix develop apical-basal polarity with the apical surface facing towards the center, and they remain polarized thereafter. Starting at day 6-8, the cells located in the center undergo apoptosis due to a lack of survival signaling from cell-ECM interaction. This cell death eventually results in the formation of a hollow lumen. This ordered sequence of events results in the formation of a polarized, growth-arrested acinar-like structure with a hollow lumen that recapitulates the glandular structure *in vivo* (Muthuswamy, Li et al. 2001). The mechanisms by which the cells achieve growth arrest and acinus limits its size are unclear. Nevertheless, several oncogenes including cyclin D1 and ErbB2 can induce escape from proliferation arrest (Debnath, Mills et al. 2002; Aranda, Haire et al. 2006). Importantly, cell death required for lumen formation is only observed in 3D, representing one distinction in the mechanisms for cell growth and death between the 2D and 3D culture conditions. Another advantage of using the 3D culture system is that each component in the ECM can be

modified to interrogate their contribution to epithelial organization. For example, collagen concentration can be increased to enhance ECM stiffness and mimic the tissue rigidity of a tumor. Epithelial cells respond to this change in ECM, and subsequently induce tension-dependent behavior such as assembly of focal adhesions, disruption of adherens junctions, and perturbation of cell polarity (Paszek, Zahir et al. 2005).

As previously described, epithelial cells switch between different types of polarity during tissue morphogenesis *in vivo*. This phenomenon can also be reconstructed in 3D culture. For instance, stimulation of MDCK cysts in collagen I-based 3D culture with hepatocyte growth factor (HGF) induces formation of branches, similar to renal tubulogenesis during embryonic development. The formation of the tubule extension is initiated by the apical-basal polarized cells switching to front-rear polarity and adopting a mesenchymal-like state. The cells re-acquire apical-basal polarity with the axis perpendicular to cells in the main duct to form branching tubule structure. (Montesano, Schaller et al. 1991; Maeshima, Zhang et al. 2000; Yu, O'Brien et al. 2003; Zegers, O'Brien et al. 2003; Zegers, Yu et al. 2003). Therefore, 3D culture can be used to study the dynamics of cell behavior during tissue morphogenesis.

1.4 Breast Cancer

In the United States, breast cancer is a leading cause of cancer death in woman between the ages of 15 and 54. According to the Centers for Disease Control and Prevention (CDC), more than 210,000 women will be diagnosed with breast cancer annually countrywide, and more than 40,000 will die from the disease. Breast cancer can be stratified based upon molecular markers to provide information about the treatment plan and disease prognosis. So far, Estrogen receptor (ER), Progesterone receptor (PR) and human epidermal growth factor receptor 2 (HER2) are the only molecular prognostic and predictive biomarkers that have been validated for routine use according to the 2007 American Society of Clinical Oncology guidelines (Zandy, Playford et al. 2007). Based on the immunohistological profile, breast cancer can be classified into four groups: 1) ER/PR+, HER2+; 2) ER/PR+, HER2−; 3) ER/PR−, HER2+, 4) ER/PR−, HER2− (Onitilo, Engel et al. 2009).

Among these subtypes, approximately two thirds of breast cancers are ER/PR+. ER/PR+ cancers are highly susceptible to chemotherapy and endocrine therapy (tamoxifen), and correlate with better patient outcome (Onitilo, Engel et al. 2009). The triple negative subtype (ER/PR−, HER2−) has the worst overall and disease-free survival. Several studies have confirmed that triple negative breast cancers are characterized by an earlier age of onset, basal-like features according to gene expression profiling, and include breast cancer type 1 susceptibility protein (BRCA1)-related breast cancer. They are also unlikely to benefit from currently available targeted therapies (Rakha, Reis-Filho et al. 2008; Onitilo, Engel et al. 2009). Approximately 25% of all breast cancers have either HER2 amplification or overexpression. The ER/PR−, HER2+ subtype has poor patient survival, very similar to the triple negative subtype. The ER/PR+, HER2+ subtype has statistically equivalent survival to the ER/PR+, HER2− subtype, but it has higher recurrence rates after chemotherapy (Onitilo, Engel et al. 2009). Overall, HER2 positivity correlates with poor patient outcome.

HER2

HER2, also known as v-erb-B2 erythroblastic leukemia viral oncogene homolog 2 (ERBB2) or Neu, is a member of the epidermal growth factor receptor (EGFR) family. The EGFR family consists of four distinct receptors: EGFR/ErbB1, HER2/ErbB2, HER3/ErbB3 and HER4/ErbB4. These receptors are transmembrane glycoproteins consisting of an extracellular ligand-binding domain, a single spanning transmembrane (TM) lipophilic domain, an intracellular juxtamembrane (JM) region and a cytoplasmic C-terminal region with tyrosine kinase (TK) activity. The classic view of EGFR activation is the ligand-induced dimerization model. In the resting state, EGFR is shown to be in its tethered conformation within the extracellular region and its kinase domain in the inactive form. Ligand binding to the extracellular domain induces receptor dimerization that brings the intracellular domains into close proximity, causes receptor to become into an "extended" conformation and promotes the association of the kinase domains into an asymmetric dimer (Ferguson, Berger et al. 2003). In the asymmetric EGFR-TK dimer, one molecule is activated through interaction of its N-lobe with the C-lobe of the cyclin-like activator on the other molecule. It is thought that the roles of the two molecules switch to activate each other (Ferguson 2008). However, tethering of the receptors is not directly related to auto-inhibition of the receptors. Mutation designed to disrupt domain II/IV tethering interaction in EGFR do not promote ligand-independent dimerization *in vitro* or activation at cell surface (Mattoon, Klein et al. 2004). It has been shown that the tethered configuration of EGFR extracellular domain need to be stabilized by multiple interactions that include intramolecular interactions of extracellular domain II/IV, backbone rigidity in the domain II/III linkage (C305/C309 disulfide bond), and additional possible restrains imposed by protein glycosylation (Dawson, Bu et al. 2007). Cancer mutations in both the extracellular region and kinase region can activate EGFR most likely by destabilizing the inactive, auto-inhibitory state (Ferguson 2008).

More than a dozen ligands have been identified to bind to EGFRs. Some of these ligands bind exclusively to EGFR, such as epidermal growth factor (EGF), transforming growth factor α (TGF-α) and amphiregulin (AREG), or bind exclusively to HER4, such as neuregulin 3 and 4 (NRG3 and NRG4). Others have a dual specificity, such as betacellulin

(BTC), heparin-binding EGF-like growth factor (HB-EGF) and epiregulin (EREG), which bind to both EGFR and HER4, or NRG1 and NRG2, which bind to both HER3 and HER4. EGFR ligands are linked to cancer. BTC and EREG are overexpressed in most breast cancers. Overexpression of TGF-α, HB-EGF and NRG2 might correlate with breast cancer progression (Yarden 2001; Revillion, Lhotellier et al. 2007; Foley, Nickerson et al. 2010). In addition, EGFR processing mechanisms are implicated in cancer. EGFR ligands, including TGF-α and HB-EGF, are expressed as transmembrane precursors that are released from the cell surface by proteinase-dependent cleavage of the extracellular domain, a process called shedding. Tumor necrosis factor-alpha converting enzyme (TACE, also known as ADAM17), which is responsible for the shedding of proTGF-α, is highly overexpressed in mammary tumors (Borrell-Pages, Rojo et al. 2003).

One of the most important gene in breast cancer is *HER2*, which was first identified in ethylnitrosourea-induced rat neuroglioblastomas (Coussens, Yang-Feng et al. 1985; Schechter, Hung et al. 1985), and subsequently found to encode a truncated version of EGFR tyrosine kinase. Overexpression of ErbB2 under the control of the long terminal repeat of moloney murine leukemia virus (MMLR) resulted in transformation of mouse NIH/3T3 fibroblasts, and thus demonstrated the role of ErbB2 as a proto-oncogene (Difiore, Pierce et al. 1987). The HER2 gene was shown to be amplified and overexpressed in human breast cancer as early as 1987 and correlate with poor prognosis.

In contrast to other EGFR family members, no ligand has been identified to directly bind to ErbB2. The extracellular domain or ErbB2 is structurally unique. It resembles the 'extended' (ligand-binding) form of EGFR with the dimerization arm exposed and readily to binds to other EGFR (GrausPorta, Beerli et al. 1997; Garrett, McKern et al. 2003). ErbB2 plays a role in EGFR signaling pathway by modulating other EGFRs activity. For example, by binding with EGFR, ErbB2 stabilizes EGFR in an activated conformation for tyrosine phosphorylation, even in the absence of ligand binding (Wada, Qian et al. 1990; Gulliford, Huang et al. 1997; Grassian, Schafer et al. 2011). ErbB3 itself has impaired tyrosine kinase activity and needs a dimerization partner to acquire signaling potential. It preferentially binds to ErbB2, and together they function as an oncogene unit to drive tumor cell proliferation (Holbro, Beerli et al. 2003). ErbB2 and ErbB4 can heterodimerize; however in this context,

ErbB2 but not ErbB4 tyrosine phosphorylation activity is required for the ErbB4 ligand NRG2 to induce cell proliferation (Mill, Zordan et al. 2011). Among the EGFRs, ErbB2-containing heterodimers are preferred over other types of heterodimers, or ErbB2 homodimers, suggesting that ErbB2 plays a central role in EGFR family-mediated signal transduction. ErbB2 used to be regarded as an 'auto-activated' receptor because of its 'extended' conformation. However, recent work on its structure has revealed that ErbB2 is closely related to the single EGF receptor family member (dEGFR) in *Drosophila melanogaster* which is tightly regulated by growth factor ligands. The auto-inhibition of dEGFR is mediated by domain I/II interactions which is common to ErbB2. This argues against the speculation that ErbB2 lacks autoinhibition, suggesting that ErbB2 needs to be stringently regulated for its normal and pathogenic function (Alvarado, Klein et al. 2009).

Dissecting the specific role of ErbB2 using an inducible ErbB2 system

Although the importance of HER2 in breast cancer had been recognized for a long time, it was not clear whether ErbB2 plays its role by promoting signaling of other EGFRs or having its own biological activity. An inducible ErbB2 homodimerization system was developed by Muthuswamy *et al.* in 1999, and used in mammary epithelial cells to distinguish the specific role of ErbB2 in mammary carcinogenesis (Muthuswamy, Gilman et al. 1999). For this system, the extracellular and transmembrane domains of the ErbB2 are replaced with the corresponding domains from the p75 low-affinity nerve growth factor receptor (p75NGFR), which prevent receptor binding to other EGFR proteins. The cytoplasmic domain of ErbB2 is linked to a synthetic ligand-binding domain from the FK506-binding protein (FKBP), and therefore allowing the chimeric ErbB2 receptor to be dimerized with the bivalent FKBP ligand AP1510 (Figure 1.4). Therefore ErbB2 can be specifically activated by homodimerization, without interacting with other EGFRs (Muthuswamy, Gilman et al. 1999). Using this method, it is found that ErbB2 homodimerization effectively induces cell transformation in Rat1 fibroblast cells and induced a five- to seven-fold higher focus-forming ability compared to ErbB1 homodimer (Muthuswamy, Gilman et al. 1999), suggesting the biological specificity of ErbB2 signaling. In addition, ErbB2, but not ErbB1 activation alters epithelial organization in mammary acini in the 3D culture (Muthuswamy, Li et al. 2001). Therefore, this ErbB2 inducible system

provides a useful tool to study the specific biological function and signaling pathway of ErbB2.

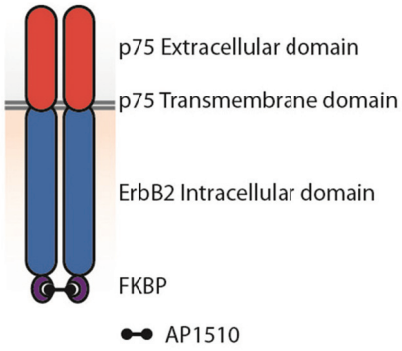

Figure 1.4. ErbB2-FKBP chimeric receptor

The illustration of the FKBP-ErbB2 receptor. The addition of AP1510 to cells expressing this chimeric receptor will result in its homodimerization.
Adopted from (Muthuswamy, Gilman et al. 1999) and (Muthuswamy, Li et al. 2001).

HER2-targeted therapy for breast cancer

The development of trastuzumab, also known as Herceptin, for the treatment of HER2-positive breast cancer is one of the major breakthroughs of medicine in the last 20 years. Trastuzumab is a humanized monoclonal antibody recognizing the extracellular domain of HER2. This therapeutic antibody was developed by scientists at Genentech 10 years after HER2 was first identified. It is a "proof of concept" confirming that tumors with specific molecular alterations can be successfully treated with targeted therapy (Delaney 1999). Seventy eight percent of patients who received trastuzumab plus chemotherapy demonstrated a survival advantage compared to patients who received chemotherapy alone (Romond, Perez et al. 2005). The women who received trastuzumab plus chemotherapy during early stage cancer had a 52% decrease in cancer recurrence (Piccart-Gebhart, Procter et al. 2005). Although trastuzumab is currently widely used, its mechanism of action is not fully understood. It is commonly agreed that binding of trastuzumab to HER2 receptors disrupts the HER2-mediated signaling caused by overexpression. Another possible

mechanism of trastuzumab is through the activation of antibody-dependent cellular cytotoxicity (Valabrega, Montemurro et al. 2007).

Not all patients overexpressing HER2 show initial response to trastuzumab therapy. Moreover, even among those who respond, resistance may be seen within 12 months, and therefore resistance to trastuzumab remains an important issue. Multiple mechanisms including activation of alternative signaling pathways such as activating insulin-like growth factor -1 receptor (IGF-1R) pathway and inhibition of PTEN pathway, loss of the extracellular domain of HER2, and upregulation of EGFR family and their ligands may contribute to the development of drug resistance (Valabrega, Montemurro et al. 2007). Because HER2 and EGFR coexpressed in ~30% of breast cancer, blockage of both receptors were used to improve patient response rates to trastuzumab and tackle the trastuzumab-resistance due to upregulation of EGFRs. Drugs including tyrosine kinase inhibitor lapatinib (GW572016) (Spector, Xia et al. 2005; Xia, Gerard et al. 2005) and Pertuzumab (2C4), a mAb directly against extracellular domain of HER2 that blocks the ability of HER2 to heterodimerize with other members of EGFR (Nahta, Hung et al. 2004) are synergetically used with trastuzumab to treat HER2+ breast cancer. Lapatinib is used both in combination of trastuzumab and as an alternative single-agent therapy for pre-surgery chemotherapy treatment. It has recently been shown that combination of trastuzumab and lapatinib significantly increase the rate of pathological complete response (Baselga, Bradbury et al. 2012).

Based on trastuzumab, a new drug, trastuzumab emtansine (T-DM1) was recently developed by Genentech. T-DM1 is composed of trastuzumab, a stable thioether linker, and the potent cytotoxic agent DM1 (derivative of maytansine). It is designed to specifically deliver the potent antimitotic drug DM1 to HER2-expressing tumor cells to induce cell death. Phase III trials of T-DM1 have shown promising prolonged progression-free survival and milder side effects compared to conventional trastuzumab. The long term effects of this formulation still need to be further evaluated (LoRusso, Weiss et al. 2011).

Changes in tissue structure during breast cancer progression

It is believed that breast cancer starts from a lesion within a TDLU that has premalignant potential, followed by a cascade of sequential molecular and morphological events that result in malignancy. The evolution of breast cancer is accompanied by continuous cytological changes, which are the basis for the histological classification used by pathologists for disease diagnosis. The diagnostic categories include the following:

- Normal TDLU: all ducts lining cells are uniform in size with normal straining characteristics.
- Hyperplastic enlarged lobular unit (HELU): excessive number of ductal groups results in enlargement of the tissue, sometimes with multilayering and slight variations in size and shape, but without significant nuclear abnormality.
- Atypical ductal hyperplasia (ADH): criteria similar to that used for HELU but with greater variation in nuclear size and shape, and irregular multilayering.
- Ductal carcinoma *in situ* (DCIS): a heterogeneous group of noninvasive neoplastic proliferations with diverse morphologies, with larger and more pleomorphic nuclei and a tendency to form microacini, cribriform spaces, or papillary structures. The cells are confined within the lumens of the mammary ducts, without evidence of invasion beyond the basement membrane into the adjacent breast stroma.
- Infiltrating breast carcinoma (IBC): previously termed carcinomas of no special type display ductal structure invading adjacent breast adipose tissue.

Only patients with DCIS and IBC receive treatment, whereas screening for ADH and HELU provide information for prediction and prevention of the disease (Figure **1.5**) (Lee, Mohsin et al. 2006; Bland and Copeland 2009). Disruption of mammary gland structure is a hallmark change associated with breast cancer. The mechanisms that induce these changes in cancerous tissue, and how disruption of tissue organization affects disease progression, remain critical areas of investigation.

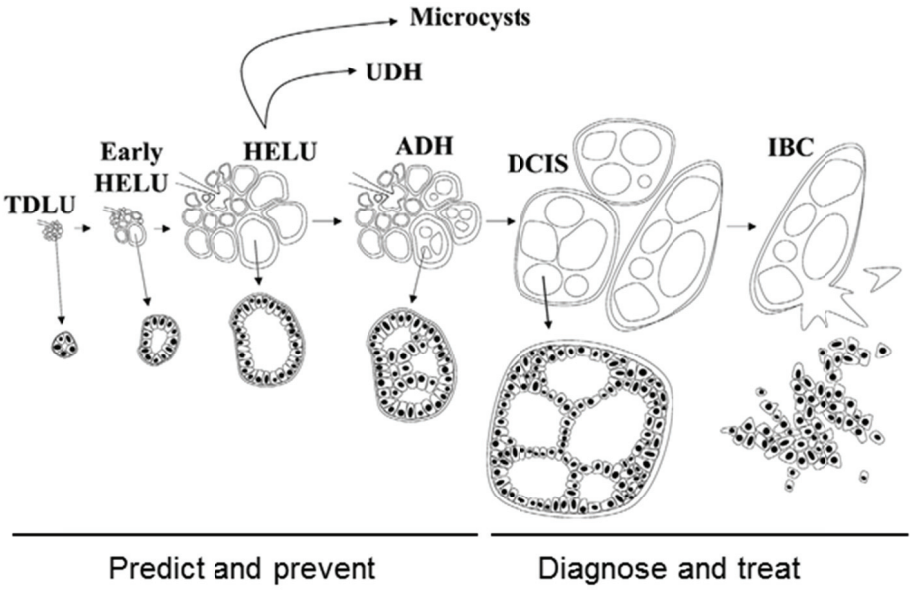

Figure 1.5. Modified Wellings-Jensen model of breast cancer progression

This figure illustrates the stepwise model of 'ductal' breast cancer progression. In this model, hyperplastic breast tissues gradually enlarge from normal TDLUs to form HELUs. HELUs occasionally differentiate to microcysts or progress to more complex lesion such as unusual ductal hyperplasia lesions (UDH) or ADHs. The staging of HELU and ADH is mainly for the purpose of disease prediction and prevention. The patients do not need to be treated. ADH may progress to DCIS as the cells continue to proliferate and distend the ductal organization, and DCIS eventually progress to IBC which is characterized by breakdown of ECM and increased motility of cancer cells.
Adopted from B*reast cancer research : BCR* 8(1): R6 (Lee, Mohsin et al. 2006).

1.5 Tumor Metastasis

With the advances in cancer prevention, early detection, and treatment, the 5-year relative overall survival rate for female breast cancer patients has improved from 63% in the early 1960s to 90% today. On the other hand, patients diagnosed with metastatic cancer still have poor survival. According to the American Cancer Society, the 5-year survival rate for woman diagnosed with localized breast cancer is 98%. However, if the cancer has already spread to lymph nodes or distant organs, the 5-year survival rate is 84% or 23% respectively. Relative survival continues to decline after 5 years (Figure **1.6**). Metastasis is the cause of 90% of human cancer deaths (Talmadge and Fidler 2010). Despite the clinical importance, little is known about the mechanisms utilized by cancer cells to metastasize; increasing research efforts are now focused on understanding and treating metastases.

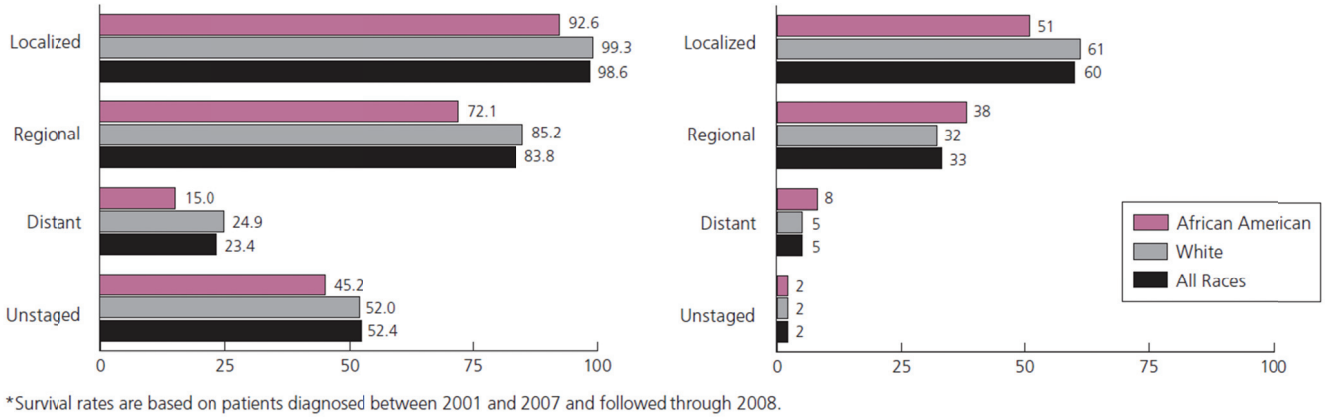

Figure 1.6. Breast cancer statistics

A) Five-year relative survival rates (%) by stage at diagnosis and race
B) Stage distribution (%) by race
Survival rates are based on patients diagnosis between 2001 and 2007 and followed through 2008.
American Cancer Society, Surveillance research, 2011

The process of tumor metastasis

The common sites for breast cancer metastasis at autopsy are lung, liver and bone (Lee 1983). To establish metastases in distant organs, cancer cells must complete a sequence of steps (Fidler 2003; Bland and Copeland 2009; Talmadge and Fidler 2010). The process of cancer metastasis involves:

- *Proliferation:* Proliferation of the primary tumor, which confers a growth advantage.
- *Angiogenesis:* Neo-vasculature is induced by tumor cells to access the circulation by outgrowth of the pre-existing vasculature or recruitment of vascular precursor cells from the circulation. This is necessary for the continued growth of a tumor.
- *Detachment:* Some tumor cells show reduced cohesion, and/or increased motility, and therefore have an increased chance of detachment from the primary tumor.
- *Invasion:* Invasion from the primary tumor involves proteolytic degradation of basement membranes and connective tissue, changes in tumor cell adherence to neighboring cells and to the ECM, and enhanced cell mobility to physically propel tumor cells through tissue and enter the blood or lymphatic vessels. This aggressive behavior could be due to a microenvironmental selective pressure, such as hypoxia, reactive oxygen species, or intrinsic genomic instability from defects in DNA damage repair machinery.
- *Intravasation/circulation/Extravasation:* Distant metastasis requires that the cancer cells enter the blood or lymphatic vessels (intravasation), get transported to the distant site through the circulation, and finally exit the vessels (extravasation). The mechanisms that control intravasation and extravasation of the vasculature are still not clear. Recent work in visualizing extravasation by tracking cells using real-time intravital imaging suggests it is a highly dynamic process involving both changes in tumor cell behavior and local vessel remodeling (Stoletov, Kato et al. 2010). In the bloodstream, the cells must adopt new survival strategies to cope with the harsh environment due to velocity-induced shear forces and constant attack from the immune system. The survived tumor cells can attach to endothelial cells where they are sheltered away from the blood flow in the capillary beds (Weiss, Grundmann et al. 1986).

- *Metastasis in distant organ:* Cancer cells must be able to grow at the new organ site. Metastasis to different organs is not a random selection; seminal work in the Massagué lab recently unveiled organ-specificity as an intrinsic property of metastatic cells (Nguyen, Bos et al. 2009) .

In order to metastasize, it is essential for cancer cells to complete all the steps described above (Figure **1.7**), each of which may be rate limiting. Failure to complete any of the steps will abort the process.

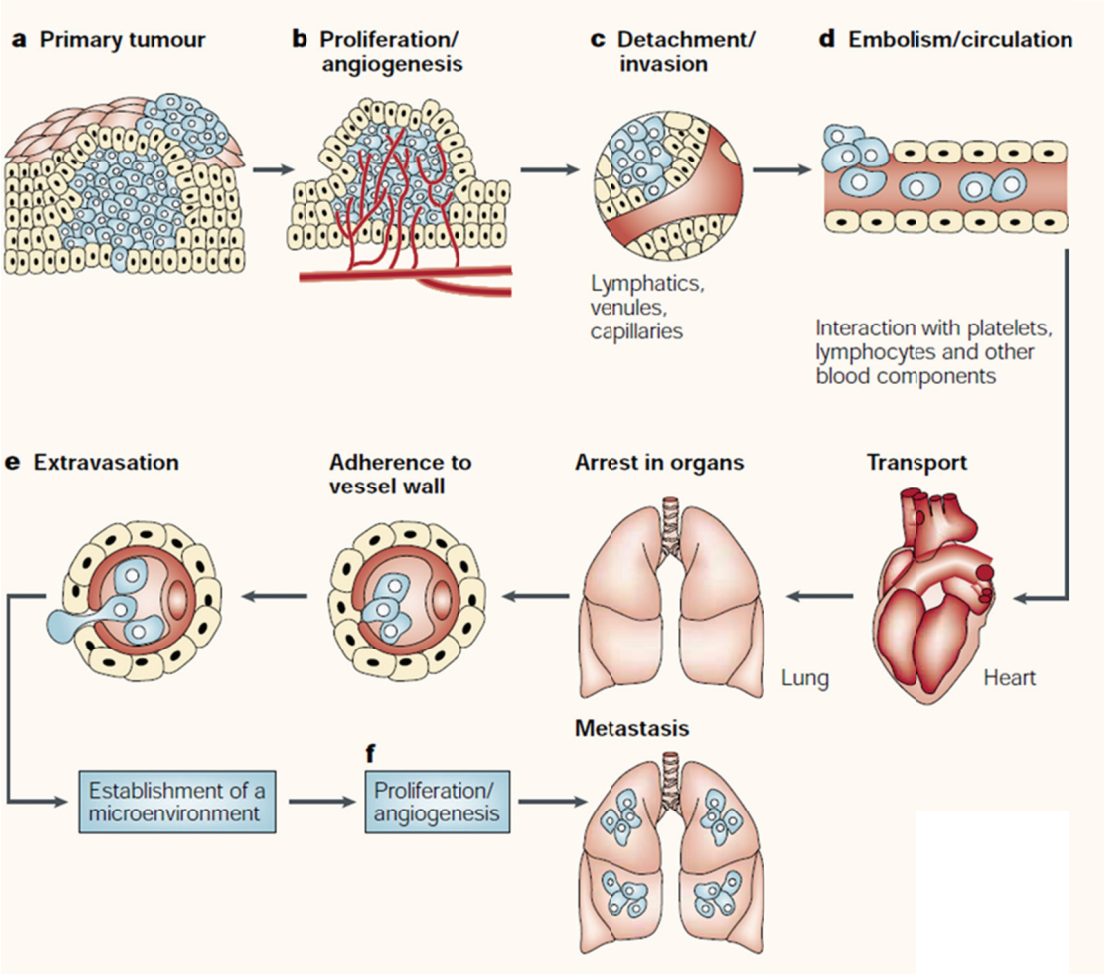

Figure 1.7. The main steps in tumor metastasis

Adopted from *Nature Reviews Cancer* 3(6): 453-458. (Fidler 2003)

Metastasis-related gene alterations

Considering that the metastatic process is a succession of individual events, it is not surprising that a large number of genes are related to metastasis. The functions of these genes are associated with different stages of cancer progression, including tumor initiation, metastasis initiation, metastasis progression, and metastasis virulence (Chiang and Massague 2008).

Functions associated with tumor initiation are provided by mutations in genes, such as those encoding KRAS, EGFR, HER2, and Phosphoinositide 3-kinase (PI3K), or inactivation of tumor suppressor genes, such as those encoding Adenomatous polyposis coli (APC), tumor suppressor protein p53 (TP53), Phosphatase and tensin homolog (PTEN), and BRCA1. Mutations of these tumor initiation genes in primary tumors provide the cancer cells a growth advantage and genomic instability, and can be inherited by metastatic cancer cells. Metastatic tumors have been shown to have more genomic alterations compared to the corresponding primary tumors (Ding, Ellis et al. 2010). For example, loss of function of the TP53, which responds to DNA damage by inducing apoptosis or arresting cell growth, promotes tumor metastasis. *TP53* is mutated or lost in 50% of cancers. C3(1)/T_{AG} transgenic mice expressing the simian virus 40 large T-antigen (T_{AG}) under the regulatory control of the prostatic steroid binding protein C3(1) gene develop mammary carcinomas several months after the appearance of dysplastic lesion. Expression levels of p53 were reduced or lost in the metastases. Inactivation of p53 in these mice by crossing C3(1)/T_{AG} transgenics with mice carrying null mutations of the p53 gene ($p53^{+/-}$) induces more aggressive mammary tumor with increased numbers and size of metastases (Maroulakou, Shibata et al. 1997). Mice carrying p53 gain of function mutation (p53+/515A) have increasing metastasis frequency in various tumors (Lang, Iwakuma et al. 2004). In pancreatic cancer mouse models, mice expressing physiological levels of oncogenic KRAS(G12D) in the pancreas only develop early ductal lesions similar to human pancreatic intraepithelial neoplasias (PanINs) (Hingorani, Petricoin et al. 2003). Additional expression of $Trp53^{R172H}$, a p53 mutation commonly observed in human pancreatic ductal adenocarcinoma (PDA), induces a high degree of genomic instability and promotes the tumor's progression into metastatic carcinoma (Hingorani, Wang et al. 2005).

Functions associated with the initiation of metastasis include induction of invasion and remodeling of the tumor microenvironment. Research done using intravital imaging has provided valuable insights into cell movement in tumors. Carcinoma cells are found to be highly dynamic within the tumors (Condeelis and Segall 2003). By comparing the motility of cells in tumors formed from the poorly metastatic MTC cell line with the highly metastatic MTLn3 cells line, it was found that tumor cells move at similar rates, but the character of the cell motility is very different (Condeelis and Segall 2003). Metastatic cancer cells show linear and fiber-associated locomotion, while non-metastatic tumor cells move randomly. Carcinoma cells in metastatic tumors are attracted towards blood vessels, where they form a layer of cells that polarize towards the vessel. This movement may correlate with intravasation and metastasis. Metastatic tumor cells can also cross the basement membrane/endothelium as intact cells, unlike non-metastatic cells, which are fragmented (Condeelis and Segall 2003). Gene expression profiling comparing metastases and primary tumors has been used extensively to search for genetic alterations required for tumor cells to metastasize. Many genes encompassing a diverse range of functions have been identified as metastasis-related genes, which might explain the changes in cancer cell behavior observed *in vivo*. Some metastasis signature genes encode key regulators of the cell motility machinery, including the actin cytoskeleton regulators cofilin, members of the Arp2/3 complex, capping protein, and cortactin (Condeelis, Singer et al. 2005; Wang, Mouneimne et al. 2006; Wang, Eddy et al. 2007; Oser, Mader et al. 2010). Other signature genes are related to ECM remodeling. Matrix metalloproteinases (MMPs), such as MMP-2 and MMP-9, which degrade collagen IV of the BM were found to be implicated in cancer invasion (Egeblad and Werb 2002). MMP-9 can also act as an angiogenic switch to increase proteolytic release of vascular endothelial growth factor A (VEGF-A) sequestered in the ECM and stimulate angiogenesis (Belotti, Paganoni et al. 2003). Expression of proteins such as TrkB induces tumor cell resistance to anoikis or “death upon detachment” and allows metastatic tumor cells to survive in the bloodstream (Douma, Van Laar et al. 2004; Kim, Koo et al. 2012). During metastasis, tumor cells recruit macrophages and other leukocytes, which may be a source of chemotactic cytokines (Dong, Kumar et al. 1997; Condeelis and Segall 2003). Colony-stimulating factor-1 (CSF-1) (Goswami, Sahai et al. 2005) and chemokine CXCL12 (Boimel, Smirnova et al. 2012) have been reported to be involved in tumor cell-macrophage

interactions by increasing microvessel density and recruiting macrophage cells to tumor sites. The genes and mechanisms used by cancer cells to metastasize vary among individuals, and even among metastases from the same individual. Therefore, further work needs to be carried out to pin down the key players and verify their functions carefully.

The last step of metastasis is colonization by the metastatic tumor cells in distant organs (Nguyen, Bos et al. 2009). Interestingly, distinct gene sets are required for organ-specific colonization. In order to understand the difference between the colonization tendencies, populations of a human breast cancer cell line with different metastatic abilities were generated and gene expression microarrays were used to determine the gene expression characteristics of cells metastasizing to lungs or bone (Minn, Gupta et al. 2005). More than 80% of women with metastatic breast cancer develop bone metastases. The ability of breast cancers to form bone metastases requires the production of osteoclast-activating factors, such as Parathyroid hormone-related protein (PTHRP), interleukin-11 (IL-11), IL-6, TNF-α and granulocyte-macrophage colony stimulating factor (GM-CSF) (Kang, Siegel et al. 2003; Smid, Wang et al. 2006; Park, Zhang et al. 2007). The second most common site of breast cancer metastasis is the lung. One of the signature genes for lung metastasis is angiopoietin-like 4 (ANGPTL4) which enhances the infiltration of tumor cells into the lungs by inducing the dissociation of endothelial cell-cell junctions (Padua, Zhang et al. 2008). In contrast, tumor cells that metastasize to the brain produce cyclooxygenase 2 (COX-2), HB-EGF and the alpha2,6-sialyltransferase ST6GALNAC5 to allow cellular passage through the blood-brain barrier (Bos, Zhang et al. 2009). Striking disparities between metastatic capabilities raise the important questions of how metastases evolve from primary tumors and which genetic determinants drive this process.

Heterogeneity of metastatic cancers

Primary tumors consist of heterogeneous populations of cells (Navin, Kendall et al. 2011). However, fully metastatic cells are rare clones. Recent genome sequencing experiments performed on matched primary and metastasis pairs have revealed that cancer cells in the metastatic site are distinct from the ones in the primary site. In pancreatic cancer, the clonal populations that give rise to distant metastases are represented within the primary

carcinoma; however, there is a genetic heterogeneity of metastases and an evolutionary relationship to the primary tumor, suggesting a requirement of additional driver mutations beyond those in the primary tumors for tumor metastasis (Campbell, Yachida et al. 2010; Yachida, Jones et al. 2010). In breast cancer, by comparing the entire genome of the primary tumor with a brain metastasis from the same patient, it was found that the overall copy number alteration was elevated in the metastasis (Ding, Ellis et al. 2010). The mutant allele range was narrowed but their frequency was enriched in the metastasis. The metastasis contained two *de novo* mutations and a large deletion not present in the primary tumor, and was significantly enriched for 20 shared mutations, indicating that the metastasis may be arisen from a minority of the cells within the primary tumor, and accumulated additional genetic alterations (Ding, Ellis et al. 2010). Both cases support the idea that the cells derived from primary tumors require additional steps to achieve a metastatic state.

Distinctive metastases in the same or different organs exhibit heterogeneity in a variety of characteristics. There are two prevalent models to explain the origin of this heterogeneity and the evolution of metastasis: the linear clonal selection progression model and the parallel evolution progression model. In the linear progression model, tumor ontogeny proceeds to full malignancy within the primary tumor microenvironment, after which tumor cell dissemination establishes a metastasis. In the parallel progression model, tumor cells depart the primary lesion before the acquisition of fully malignant phenotypes, followed by progression and metastatic growth at a distant site (Klein 2009). In human breast cancer and in HER2 and polyoma virus Middle T-Antigen (PyMT) transgenic mice, tumor cells have been shown to systematically disseminate from an early stage tumors to form micrometastases in the bone marrow and lungs (Schmidt-Kittler, Ragg et al. 2003; Balic, Lin et al. 2006; Hüsemann, Geigl et al. 2008). In pancreatic cancer, metastatic clones arise from non-metastatic cells in primary tumors and undergo further genetic modifications (Campbell, Yachida et al. 2010; Yachida, Jones et al. 2010). The results from these studies favor the latter parallel progression model. Consideration of the parallel progression model could affect therapeutic strategy. As the metastasis precursor cells in the primary tumor might not be fully malignant, gene alterations required for early progression steps such as changing cell cohesion and inducing cell invasion might provide more prognostic value. Understanding the

molecular mechanisms used by cells to disseminate and looking for biomarkers to identify those with metastatic potential in the primary tumors may benefit the diagnosis and treatment of the disease.

1.6 Disruption of Cell Polarity in Cancer

Normal tissue homeostasis is maintained in dynamic equilibrium between processes such as cell proliferation, cell death, tissue morphogenesis and differentiation. Loss of this equilibrium will initiate disease states including cancer. In the past, research interests mainly focused on understanding the mechanisms controlling cell in cancer, while the disruption of tissue organization in cancer was not well studied. One reason that tissue organization was overlooked is that the causal relationship between uncontrolled proliferation and disruption of tissue structure is unclear. There is a dynamic relationship between tissue organization and cell proliferation, where one begets the other. For example, In confluent monolayer cell culture, cell adhesion signaling crosstalks with cell cycle pathways to inhibit cell proliferate, referred to as "contact inhibition of cell division" (Takahashi and Suzuki 1996; St Croix, Sheehan et al. 1998; Stockinger, Eger et al. 2001). The interaction of integrins with the ECM can also generate signals to regulate the cell cycle and apoptosis (Howe, Aplin et al. 1998; Schwartz and Assoian 2001). Some oncogenic changes interfere with both mechanisms to disrupt the tissue homeostasis and initiate cancer. For instance, oncogenic Ras promotes cell proliferation and cooperates with TGF-β to induce epithelial-mesenchymal transition (EMT) and disrupt normal epithelial morphology (Janda, Lehmann et al. 2002; Wang, Li et al. 2009). This intertwining of tissue structure and cell growth makes it challenging to distinguish the cause and effect relationship between them.

Reconstruction of tumor phenotype in 3D culture

Studies using cultured epithelial cells grown in a three-dimensional matrix have provided surprising new insights into the relationship between cell proliferation and higher order tissue organization. Oncogenes have been shown to regulate distinct facets of cell

morphology to initiate tumorigenesis. While Cyclin D1, a known oncogene that is amplified or overexpressed in 40-50% of breast cancers (Arnold and Papanikolaou 2005), can promote cell proliferation, it is not sufficient to overcome contact inhibition of human mammary epithelial cells in monolayer cultures. However, the same cells when grown in 3D matrix fail to undergo proliferation arrest, but still retain an acinar morphology with a hollow lumen (Debnath, Walker et al. 2003). Furthermore, transgenic mouse models overexpressing Cyclin D1 in the mammary epithelium are poor at inducing tumorigenesis. These results suggest that signals that drive proliferation by deregulating proliferation control may be necessary for the cancer process but are certainly not sufficient to initiate cancer (Wang, Cardiff et al. 1994). In contrast, activation of ErbB2 led to disruption of 3D acini, reinitiation of cell proliferation in the growth-arrested 3D acini and inhibition of cell death in the lumen (Muthuswamy, Gilman et al. 1999; Muthuswamy, Li et al. 2001) (Figure 1.8). Although HER2-positive status is correlated with more aggressive forms of breast cancer (Roses, Paulson et al. 2009), the acini with ErbB2 activation specifically lack invasive properties (Muthuswamy, Li et al. 2001). Consistent with this observation, ErbB2 is overexpressed in 56% of DCIS (Hoque, Sneige et al. 2002), a type of early stage, non-invasive premalignant mammary gland lesion. This suggests that amplification of ErbB2 is not sufficient to induce metastatic disease and that additional events are required for HER2-mediatedtumor progression. Overexpression of oncogenic ErbB2 or c-Myc in MCF10A cells initiates cell translocation from ECM-contacted basal layer to the lumen, and promotes ECM-independent cell proliferation and drives clonal selection to form neoplastic outgrowth (Leung and Brugge 2012).

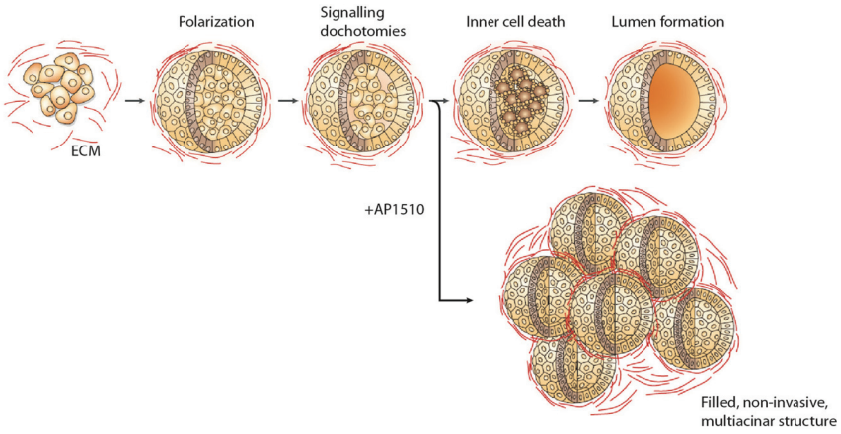

Figure 1.8. The effect of ErbB2 on 3D epithelial structure

ErbB2 homodimeriztion disrupts normal MCF10A 3D acinar structure, leading to a filled, multiacinar phenotype as results of hyperproliferation, anti-apoptotic activity and disruption of apical-basal polarity. Adopted from (Debnath and Brugge 2005).

Disruption of tissue organization during tumor progression observed in cancers can be recapitulated in the 3D culture system as well. For example, the HMT-3522 breast cancer cells display spontaneous tumorigenic in their late passage. The cells at early passage cells (S-1) are nonmalignant and form normal acini when grown in the 3D cultures. The 3D structures derive from the cells at late passage (T4-2) display disrupted tissue organization, loss of cell-cell adhesion and altered cell-ECM interaction (Briand, Petersen et al. 1987; Weaver, Petersen et al. 1997). Both β1 and β4 integrins were found upregulated in in T4-2 cells compared to S-1 cells. Treating T4-2 cells in 3D culture with β1 integrin inhibitory antibody leads to a morphological reversion to a normal phenotype with a re-organized BM and normal cell-cell junctions (Weaver, Petersen et al. 1997). Resistance to apoptosis in the nonpolarized T4-2 structures requires ligation of β4 integrin, which regulates tissue polarity, hemidesmosomes formation and NFκB activation (Weaver, Lelievre et al. 2002). There results from 3D cultures indicate the important roles of integrins play during breast cancer progression. EGFR/ErbB2 heterodimerization has been shown to promote cell invasion in 3D culture. The ability of the heterodimers to induce invasion requires EGFR-mediated activation of PI3K, Ras/mitogen-activated protein kinase (MAPK), and phosphorylation of phospholipase C gamma 1 (PLCγ1) signaling pathways (Zhan, Xiang et al. 2006). Elevated

coexpression of CSF-1 and its receptor (CSF-1R) correlates with poor prognosis in breast cancer. Co-expression of CSF-1 and CSF-1R in MCF10A induces a formation of discohesive structure in the 3D culture that is associated with the disruption of E-cadherin junctions (Wrobel, Debnath et al. 2004). Crosslinking collagen by adding ribose to the ECM can activate PI3K activity, promote focal adhesion assembly, and induce invasion in 3D culture of MCF10A cells expressing ErbB2 (Levental, Yu et al. 2009). Taken together, 3D culture systems are powerful tools for studying the mechanisms that regulate tissue organization in normal mammary gland morphogenesis and carcinoma progression.

Regulators of cell polarity

The general mechanisms of cell polarity, including its establishment and maintenance, are highly conserved through evolution from bacteria to humans. Over the past few decades, genes that are responsible for the regulation of cell polarity have been identified using genetic screens in *C. elegans* and *D. melanogaster*. The genes encoded proteins that regulate cell polarity can be grouped into three complexes according to their known localization: the subapically localized Par and Crumbs complexes, and the basolaterally localized Scribble complex.

Par complex

The Par complex consists of Par3, Par6 and atypical protein kinase C (aPKC). Par3 and Par6 are products of the *par* (*partitioning defective*) genes. Par genes were initially identified in the screenings for maternal effect lethal mutations in *C.elegans*. Mutagenesis was performed in mutant *C.elegans* strain (*egl-23* or *lin-2* heterozygote) and score for surviving F2 adults. Because *egl-23* and *lin-2* homozygot can fertilize but do not lay their eggs as they are consumed by their progeny, therefore the only expected F2 survivors are those that failed to produce F3 progeny. Using this method, six *par* genes (*par1-par6*) were discovered, mutations in which lead to defect in early egg cleavage (Kemphues, Priess et al. 1988; Kemphues 2000). The products of *par* genes have diverse molecular properties: Par-1 (MARK2) and STK11 (also known as LKB1, the homolog of *par-4* in *C.elegans*) are

serine/threonine protein kinases. Par2 (human homolog unknown) is a RING (Really Interesting New Gene) finger domain-containing protein and may function as an E3 ubiquitin ligase to connect the E2 ubiquitin-conjugated enzyme to the target protein (Moore and Boyd 2004; Hao, Boyd et al. 2006). Par5 is a 14-3-3 protein, a family of highly conserved regulatory proteins that are ubiquitously expressed in all eukaryotic cells (Morton, Shakes et al. 2002). Par3 and Par6 are scaffold proteins that contain scaffolding PDZ domains, which bind to either the C-terminus of a peptide ligand or a PDZ domain on another protein. In *C. elegans*, mutations in *par6* and *par3* display similar phenotypes including generation of equal-sized blastomeres, improper localization of P granules and SKN-1 proteins and abnormal second division cleavage patterns. In addition, Par3 protein shows abnormal symmetric localization in *par6* mutant embryos (Watts, Etemad-Moghadam et al. 1996), suggesting a connection between Par3 and Par6 .

In epithelial cells, Par3, Par6 and aPKC form a protein complex that localizes to the apical domain and regulates apical TJ formation (Hirose, Izumi et al. 2002). Par6 binds to aPKC by Phox and Bem1p (PB1)-PB1 domain interaction, and functions both as an inhibitor of aPKC kinase activity and as a targeting subunit to recruit aPKC substrates including Par3, Lgl and Pals1 (Hirano, Yoshinaga et al. 2005). Recruitment of Cell division control protein 42 homolog (Cdc42), a small GTPase of the Rho family, to the Par6-aPKC complex activates aPKC kinase activity (Joberty, Petersen et al. 2000) toward its substrates (Izumi, Hirose et al. 1998; Nagai-Tamai, Mizuno et al. 2002). Par3 binds to aPKC through its aPKC-binding domain. Although aPKC can directly bind to both Par6 and Par3 in an independent manner, it only phosphorylates Par3 but not Par6. Par3 associates with aPKC in turn reduces aPKC kinase activity measured by *in vitro* kinase assay (Lin, Edwards et al. 2000). In *Drosophila*, phosphorylation of Par3 by aPKC leads to Par3 dissociating from the apical Par6/aPKC complex. As a result, Par3 is excluded from the apical domain and localized below Par6 and aPKC at AJs. Expression of nonphosphorylatable Par3 mislocalizes to the AJs, which leads to a loss of the apical domain and an expansion of the lateral domain in epithelial cells (Morais-de-Sa, Mirouse et al. 2010), suggesting the role of Par3 in positioning the AJs in epithelia.

Crumbs complex

Another apical module, the Crumbs complex, comprises a transmembrane protein Crumbs (isoforms Crb1-3 in mammalian), the membrane-associated protein Pals1 (Mpp5 in mammalian, stardust in *Drosophila*), and Pals1-associated TJ protein (PATJ, also known as INADL) (Figure **1.9**.B). In *Drosophila*, embryos with *crumbs* mutation failed to assemble or stabilize AJs (also called zonula adherens in *Drosophila*. This lead to the breakdown of the epithelial structure and extensive cell death (Tepass, Theres et al. 1990). In mammalian cells, Crb3/Pals1/PATJ complex localizes at epithelial TJs and interacts with Par complex. MCF10A cells express little endogenous Crb3, and unable to form TJs. Expression of exogenous Crb3 induces the formation of functional TJs in MCF10A cells, demonstrating the role of Crb3 to promote TJ formation.

Scribble complex

The Scribble complex is composed of three proteins, Scribble (Scrib), Discs Large (Dlg, isoforms, Dlg1-5) and Lethal(2) giant larvae (Lgl, isoforms, LLGL1 and 2). Scrib indirectly associates with Dlg1 via a linker protein called GUK Holder, and directly binds to Lgl2 via Scrib's Leucin-rich repeats (LRR) domain (Mathew, Gramates et al. 2002) (Figure **1.9**.C). In *Drosophila*, mutations in *scrib* cause broad defects in epithelial organization and leads to embryonic lethality (Bilder and Perrimon 2000). The Scribble complex is localized to the basolateral domain, which is critical for its function, and further required for the apical confinement of polarity determinants. Mutations in *scrib* induces mislocalization of adherens junctions around the cells, which leads to the apical polarity determinants including Crb and Discs Lost (Dlt) expression unrestricted to the apical localization. These cells display aberrant cell shape and loss of the monolayer honeycomb-like organization (Bilder, Li et al. 2000). In mammalian cells, Scrib is recruited to E-cadherin at cell-cell junctions (Navarro, Nola et al. 2005) and is required for AJ formation. Knockdown of Scrib in MDCK cells results in a mesenchymal appearance at a low density with no junctions. Furthermore, Scrib knockdown cells migrate faster with no direction (Qin, Capaldo et al. 2005).

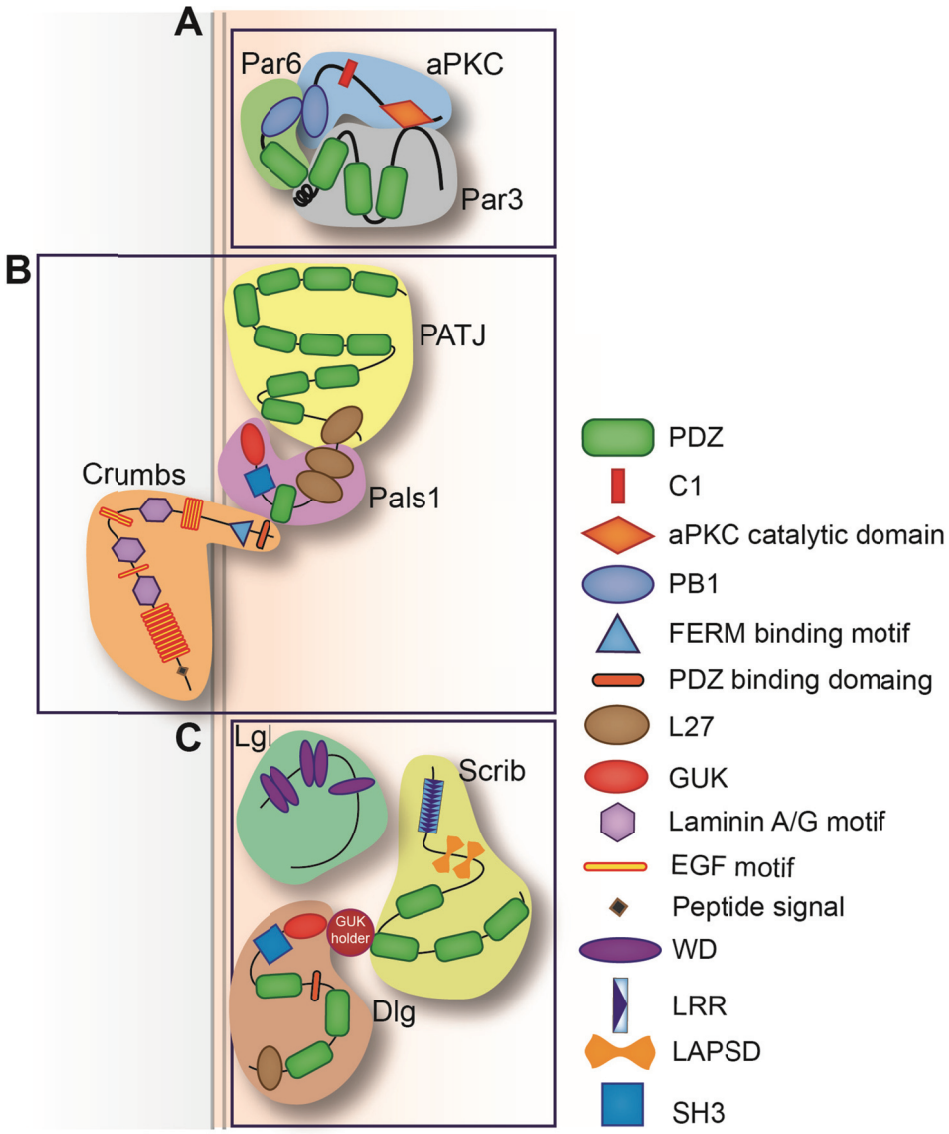

.

Figure 1.9. Cell polarity proteins in mammalian epithelia

A) Subapical Par complex: Par6 binds to aPKC through its N-terminal PB1 domain, and binds to Par3 through its PDZ domain. Par3 also interacts with aPKC through its C-terminal tail.

B) Apical Crumbs complex: the cytoplasmic tail of the transmembrane protein Crumbs interacts directly with the PDZ domain of Pals1. The interactions between Pals1 and PATJ involve the binding of the L27 domain of each protein.

C) Basolateral Scribble complex; Scrib associates indirectly with Dlg via a GUK holder protein. The interaction between Lgl and the rest of the complex is not yet clear.

Cross talk between polarity complexes

During the establishment and maintenance of cell polarity, the protein complexes extensively interact. In *Drosophila*, Scrib actively excludes Crumbs and other apical components from the basolateral domain, which is required for apical formation during embryogenesis. (Bilder and Perrimon 2000). During embryogenesis and photoreceptor apicobasal polarity remodeling, Crumbs recruits Par6 and aPKC to the membrane domain, and excludes Par3 from the subapical domain (Morais-de-Sa, Mirouse et al. 2010; Walther and Pichaud 2010; Wodarz, Krahn et al. 2010). In this process, binding of Cdc42 to Par6 is required for promoting Crb/aPKC-dependent apical exclusion of Par3, but not phosphorylation of Par3 by aPKC (Walther and Pichaud 2010). In mammalian epithelial cells, Lgl competes for Par3 in forming an independent complex with Par6/aPKC. During MDCK polarization, Lgl initially colocalizes with Par6/aPKC at the cell-cell contact region and is phosphorylated by aPKC, followed by segregation from apical Par6-aPKC after the cells are polarized. Overexpression of an aPKC kinase-deficient mutant causes mislocalization of Par6 and Lgl to the entire cell periphery. The transient interaction between Lgl and Par6/aPKC contributes to the establishment of TJs, as overexpression of Lgl2 affects TJ formation when cells are subjected to calcium switch to form TJs *de novo* (Yamanaka, Horikoshi et al. 2003). In humans, the Crumbs isoform CRB3, containing a conserved cytoplasmic domain but lacking the extracellular EGF- and laminin A-like G repeats, is preferentially expressed in epithelial tissue. CRB3 binds directly to Par6 to regulate the formation and stability of TJs *in vivo*. Overexpression of CRB3 delays TJ formation without affecting apical-basal polarity, a phenotype very similar to what is observed for Par6 overexpression (Lemmers, Michel et al. 2004).

The above studies demonstrate the complex network of interactions that occur during cell polarization and highlight the need for understanding how polarity proteins regulate polarization during tissue morphogenesis and disease.

Polarity protein alterations in cancer

Polarity proteins are frequently altered in cancer. In the Par complex, *PARD6b* is amplified and overexpressed in breast cancer (Nolan, Aranda et al. 2008). *PARD3* was recently shown to be frequently deleted in esophageal cancer cells (Zen, Yasui et al. 2009). Overexpression of aPKC is observed in multiple cancers including hepatocellular carcinoma, pancreatic adenocarcinoma and breast cancer (Huang and Muthuswamy 2010), and correlates with poor clinical prognosis in ovarian cancer (Eder, Sui et al. 2005). Par6 associates with TGFβRI to regulate TGF-β-dependent EMT; and Par6 activation correlates with breast cancer metastasis (Ozdamar, Bose et al. 2005; Viloria-Petit, David et al. 2009). The Par6/Par3 complex interacts with discoidin domain receptor 1 (DDR1) at cell-cell junctions to regulate collective migration of cancer cells (Hidalgo-Carcedo, Hooper et al. 2011). Downregulation of Crb3 was required for transformation of immortal mouse kidney cells (Karp, Tan et al. 2008), suggesting that Crb3 may function as a tumor suppressor. In the Scribble complex, Scrib was the first among the polarity proteins where it was demonstrated that its dysregulation promotes tumorigenesis (Bilder, Li et al. 2000). In breast cancer, amplification and overexpression of oncogenic c-Myc is frequently observed in early neoplastic lesions (Spandidos, Pintzas et al. 1987). Similar to cyclin D1, c-Myc induces both proliferation and apoptosis, but lacks the ability to disrupt apical-basal polarity of mammary epithelial cells (Reichmann, Schwarz et al. 1992). The expression of c-Myc in the mammary gland results in development of mammary tumors with a very long latency in 50%-80% of the mice. Scrib is mislocalized, overexpressed or downregulated in multiple cancers. Loss of Scrib or mislocalization of Scrib from cell-cell junctions cooperates with *c-myc* to block the apoptosis pathway and promote cell transformation (Zhan, Rosenberg et al. 2008). Dlg and Lgl are also mislocalized or downregulated in multiple cancers including lung, prostate, breast and colon (Huang and Muthuswamy 2010). Aberrant splicing of *LGL* and expression of the truncated protein is associated with poor differentiation and large tumor size of hepatocellular carcinoma (Lu, Feng et al. 2009). Collectively, these data implicate polarity proteins in cancer (Huang and Muthuswamy 2010).

Work from our lab for the first time uncoupled oncogene-induced cell proliferation and disruption of epithelial cell polarity. Activation of ErbB2 disrupted apical-basal polarity

by associating with Par6 and aPKC. Inhibition of the interaction between Par6 and aPKC by expressing a mutant Par6 ($Par6^{K19A}$) blocked the ability of ErbB2 to disrupt acinar organization, but was not required for cell proliferation (Aranda, Haire et al. 2006). During this process, Par3 dissociates from Par6 and aPKC. The role Par3 plays in ErbB2 induced transformation is unknown (Figure 1.10).

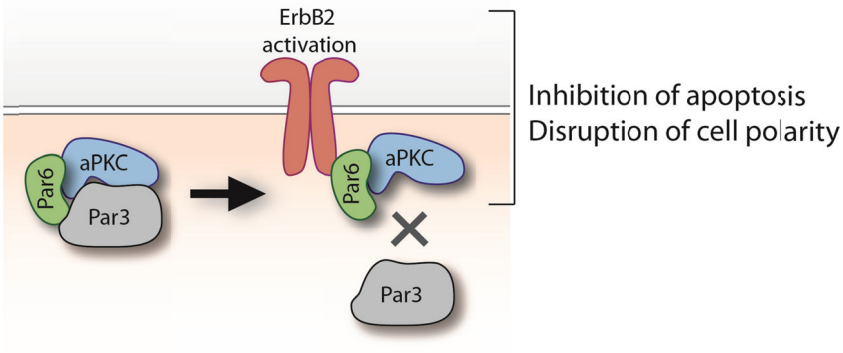

Figure 1.10. Illustration of the interaction of Par complex and activated ErbB2

Activation of ErbB2 disrupts the active Par3 complex and recruits Par6 and aPKC to the receptor by which to inhibit apoptosis and disrupt cell polarity in 3D cultures. Par3 dissociates from rest of the Par complex.

The aim of my thesis was to determine the role Par3 plays during ErbB2-induced mammary gland tumor initiation and progression. I have demonstrated that Par3 expression is lost during metastasis of ErbB2-positive breast cancers and that forced downregulation of Par3 activates a Tiam1/Rac/IRSp53/WAVE2 pathway that promotes aberrant actin remodeling at cell-cell junctions, blocks E-cadherin junction maturation, and inhibits cell-cell cohesion. Surprisingly, despite the acquisition of metastatic capacity, loss of Par3 did not induce a detectable loss of epithelial characteristics. This indicates that loss of Par3 weakens E-cadherin-mediated cell-cell adhesion to induce epithelial cells to acquire metastatic behavior, without undergoing an obvious mesenchymal transition. Our observations on the acquisition of metastatic behavior by tumor epithelial cells identify changes in cell-cell cohesion as a novel molecular step employed by epithelial cells during metastasis.

Chapter 2

Loss of Par3 Cooperates with ErbB2 to Induce Invasive Behavior in the Mammary Gland Epithelial Cells *In Vitro*

Disclosure of contribution:
Kannan Krishnamurthy performed the experiments presented in for Figure 2.3 C and Figure 2.6 B

Introduction

We have previously demonstrated that activation of ErbB2 in the human mammary epithelial cell line MCF10A, induces disruption of apical-basal polarity and formation of non-invasive abnormal structures referred to as multiaciniar structures (Muthuswamy, Li et al. 2001; Aranda, Haire et al. 2006). Par6/aPKC interaction is required for ErbB2-induced disruption of the apical-basal polarity and inhibition of apoptosis. ErbB2 activation displaces Par3 from the Par6/aPKC complex (Aranda, Haire et al. 2006). However, the role Par3 plays during ErbB2-induced transformation is unknown.

Par3 is an evolutionarily conserved protein that was first identified in *C elegans* eggs (Pellettieri and Seydoux 2002). Par3 together with Par6 and PKC3 (aPKC) localize to the anterior half of the zygote, and mutations in any of these genes disrupt the polarization and first division of the zygote (Watts, Etemad-Moghadam et al. 1996). Par3 is a signaling scaffold that contains three PDZ domains, an N-terminal dimerization domain and a C-terminal aPKC interaction domain (Etemad-Moghadam, Guo et al. 1995; Suzuki and Ohno 2006). Its PDZ domains interact with cell surface proteins such as JAM (Ebnet, Suzuki et al. 2001), Nectin (Takekuni, Ikeda et al. 2003), Par6 (Joberty, Petersen et al. 2000; Lin, Edwards et al. 2000; Suzuki, Yamanaka et al. 2001), phospholipids phosphatidylinositol 4,5-bisphosphate (PIP2), and PTEN (Nagai-Tamai, Mizuno et al. 2002; Wu, Feng et al. 2007; Feng, Wu et al. 2008). The C-terminal domain of Par3 interacts with aPKC to inhibit its kinase activity (Izumi, Hirose et al. 1998; Yamanaka, Horikoshi et al. 2001). The Par3-aPKC interaction plays important roles during both the establishment of the apical membrane and differentiation and morphogenesis of progenitor cells in the mouse mammary glands. Par3-depleted mammary progenitor cells gave rise to disrupted mammary ductal structures, characterized by ductal hyperplasia, filled lumen and disrupted end bud structures, with an expansion of $K8^+$ $K14^+$ dual positive cells and $K6^+$ progenitor cells. Re-expression of full length Par3 but not a mutant Par3 lacking the aPKC-binding domain could rescue the phenotype (Horikoshi, Suzuki et al. 2009; McCaffrey and Macara 2009). The C-terminal domain of Par3 can also interact with the Rac1 GTPase-specific GTP exchange factor (GEF) T Lymphoma invasion and metastasis (Tiam1) to inhibit its exchange activity (Mertens, Rygiel et al. 2005). This interaction was sufficient to promote TJ formation in MDCK cells

suggesting that Par3-mediated suppression of Tiam1 at the junction is required for formation of TJs (Chen and Macara 2005). A similar Par3-Tiam1-dependent, but aPKC-independent, interaction was also required for regulating dendritic spine morphogenesis. Expression of dominant negative Rac, or downregulation of Tiam1, rescued the Par3-loss phenotype, demonstrating that the ability of Par3 to inhibit Rac activation plays an important role during dendritic spine morphogenesis (Zhang and Macara 2008).

In humans, the *PAR3* gene is located on chromosome 10, at 10p11.21, and covers 705.77 kb, from 35104253 to 34398485, on the reverse strand. The gene contains 44 distinct introns (42 gt-ag, 2 gc-ag) and produces multiple splice variants. Gao et al. have identified six isoforms using human kidney cDNA (Gao, Macara et al. 2002). The longest sequence was designated as Par3a. The Par3b product differs from Par3a by an internal deletion of nine nucleotides, which results a protein lacking three amino acids (ESG, position 741-743aa). Par3c contains the same deletion and in addition lacks exons 5 and 12, as well as the end of exon 17. Par3d lacks only exon 21. Par3e lacks the nine nucleotides at the end of exon 15 in addition to exons 5, 12, 18 and 21. The splicing of exon 18 results in an amino acid substitution of a glycine by a serine in position 861 (numbering refers to Par3a). The last product, Par3f, lacks the ends of exons 15 and 17 as well as the entire exon 12. As exon 17 contains the putative aPKC phosphorylation sites, Par3c and Par3f lack the aPKC binding ability (Gao, Macara et al. 2002). Other than these isoforms, a 150 kDa short form of Par3, sPar-3, is predominantly expressed in Caco-2 cells, a colon carcinoma-derived cell line. sPar-3 associates with aPKC, but does not concentrate at the cell-cell contact region. The function of sPar-3 is unclear, but might contribute to the aberrant cell polarity noted in some diseases (Yoshii, Mizuno et al. 2005).

In this chapter, to investigate the role of Par3 in cultured mammary epithelial cells, I depleted the Par3 protein using lentiviral shRNA-mediated knockdown. I demonstrate that loss of Par3 cooperates with oncogenic ErbB2 activation to induce cell invasion without affecting cell proliferation.

Results:

2.1 Knockdown of Par3 using shRNAs

To understand if Par3 plays a role during ErbB2-induced transformation of mammary epithelial cells, I tested five independent short hairpin RNAs targeting Par3. The shRNAs were acquired from The RNAi Consortium (TRC) and constructed in the pLKO.1 vector, an HIV-based lentiviral vector containing a 21mer shRNA sequence driven by the U6 promoter allowing RNA polymerase III-dependent transcription. The shRNA lentivirus was generated and I infected MCF10A cells expressing an inducible form of the oncogenic receptor tyrosine kinase ErbB2 (10A.B2) (Muthuswamy, Gilman et al. 1999) (Figure 2.1.A). Stable cell lines were established using puromycin selection and tested for Par3 expression knockdown efficiency. The shRNA (TRCN00001118134) targeting base pair 3112-3132 was shown to be the most effective shRNA. Another shRNA targeting mouse Par3 (TRCN0000094399) was used in the experiments using primary and immortalized mouse mammary epithelial cells, and an shRNA targeting GFP was used as a non-specific RNAi control to rule-out off-target effects (Figure.2.1.B). Both shRNA and shmRNA knockdown both long (180kDa) and short (150kDa) forms of Par3 recognized by anti-Par3 antibody.

2.2 Loss of Par3 Cooperates with ErbB2 activation to induce abnormal 3D acinar structure formation

To test the effect of Par3-loss on acinar morphogenesis *in vitro*, we grew the 10A.B2 cells expressing Par3 shRNA in Matrigel-based 3D culture using the overlay method (Jayanta Debnath 2003). ErbB2 dimerizer, AP1510 was added at day 12 when the acini formed polarized growth-arrested structures. In the absence of ErbB2 activation, the acini derived from shGFP and shPar3 cells appeared to be similar, both forming well-polarized single acini with hollow lumens at day 16. Activation of ErbB2 in both shGFP and shPar3 acini disrupted normal acinar morphogenesis and induced formation of multiacinar structures. Interestingly, with ErbB2 activation, the multiacinar structures derived from shPar3 cells had a unique structure that resembled a cluster of disorganized, loosely packed cells (Figure 2.2.A). Control shGFP acini had smooth outline at the interface between the basal cell surface and

the Matrigel matrix. Differential interference contrast microscopy was used to resolve fine surface texture, and showed that the multiacinar structures derived from shPar3 cells possessed uneven surface topology, suggesting an abnormal organization with loose cell-cell junctions, which was not observed in the multiacinar structures derived from shGFP cells (Figure 2.2.B).

2.3 Loss of Par3 cooperates with ErbB2 activation to induce cell invasion

Next, the day 16 acini were immunostained for Ki-67 to analyze their proliferation rate. Both shGFP and shPar3 cells displayed similar levels of ErbB2-induced proliferation (Figure 2.3.A). Acini derived from shPar3 cells, in the absence of ErbB2 activation, showed an increased proliferation compared to shGFP cells. This result is consistent with recent observations in mouse mammary epithelial cells (McCaffrey and Macara 2009) where loss of Par3 also induced an increase in cell proliferation(Figure 2.3.A). However, loss of Par3, in the absence of ErbB2 activation, was not sufficient to induce multiacinar structures. Whereas activation of ErbB2 induced comparable numbers of multiacinar structures in both shGFP and shPar3 cells, seventeen percent of the multiacinar structures in shPar3 cells had a rough surface (Figure 2.3.B). In addition to the differences in their surface topology, the multiacinar structures derived from shPar3 cells also showed evidence of invasive protrusions (Figure 2.2.C), suggesting that loss of Par3 promoted invasive behavior in response to ErbB2 activation. To further confirm this, the cells were subjected to transwell invasion assay. In this assay, cell invasiveness can be quantitated by counting the number of cells penetrating a Matrigel basement membrane matrix and migrating through a porous membrane when seeded on culture well inserts with chemoattractant in the bottom chamber (Repesh 1989). Activation of ErbB2 induced a significant increase in invasion of shPar3 cells when compared to shGFP cells (30-fold versus 5-fold increase respectively) (Figure 2.3.C)

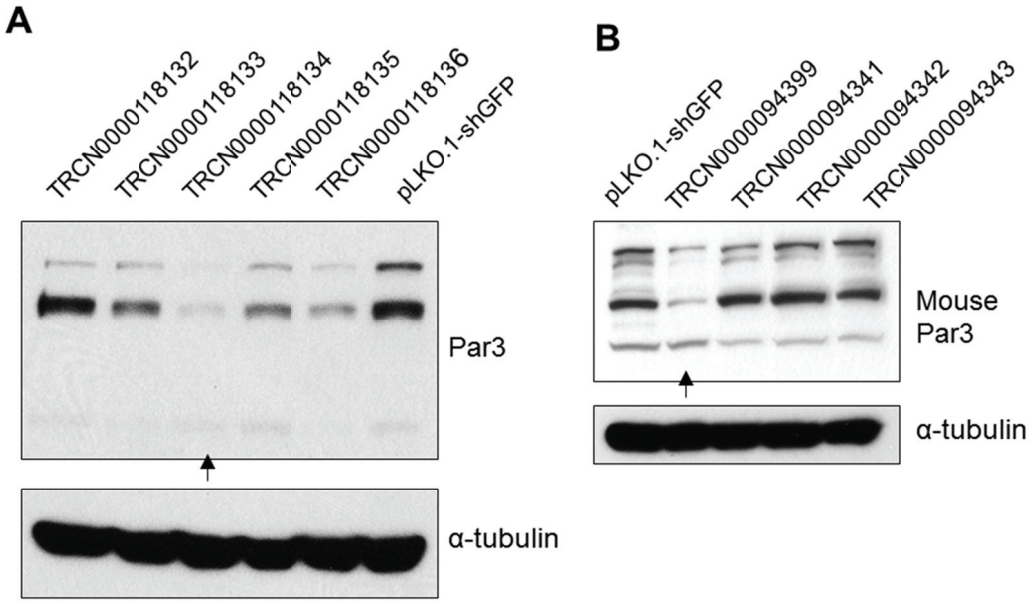

Figure 2.1. Par3 knockdown using lentiviral shRNA.

(A) Immunoblot of Par3 protein levels in 10A.B2 cells infected with virus expressing shRNA targeting GFP or one of five shRNAs targeting **P**ar3. The arrow points to the most effective shRNA.

(B) Immunoblot of Par3 protein levels in mouse mammary epithelial comma 1D cells infected with virus expressing shGFP or one of five shRNAs targeting mouse Par3.

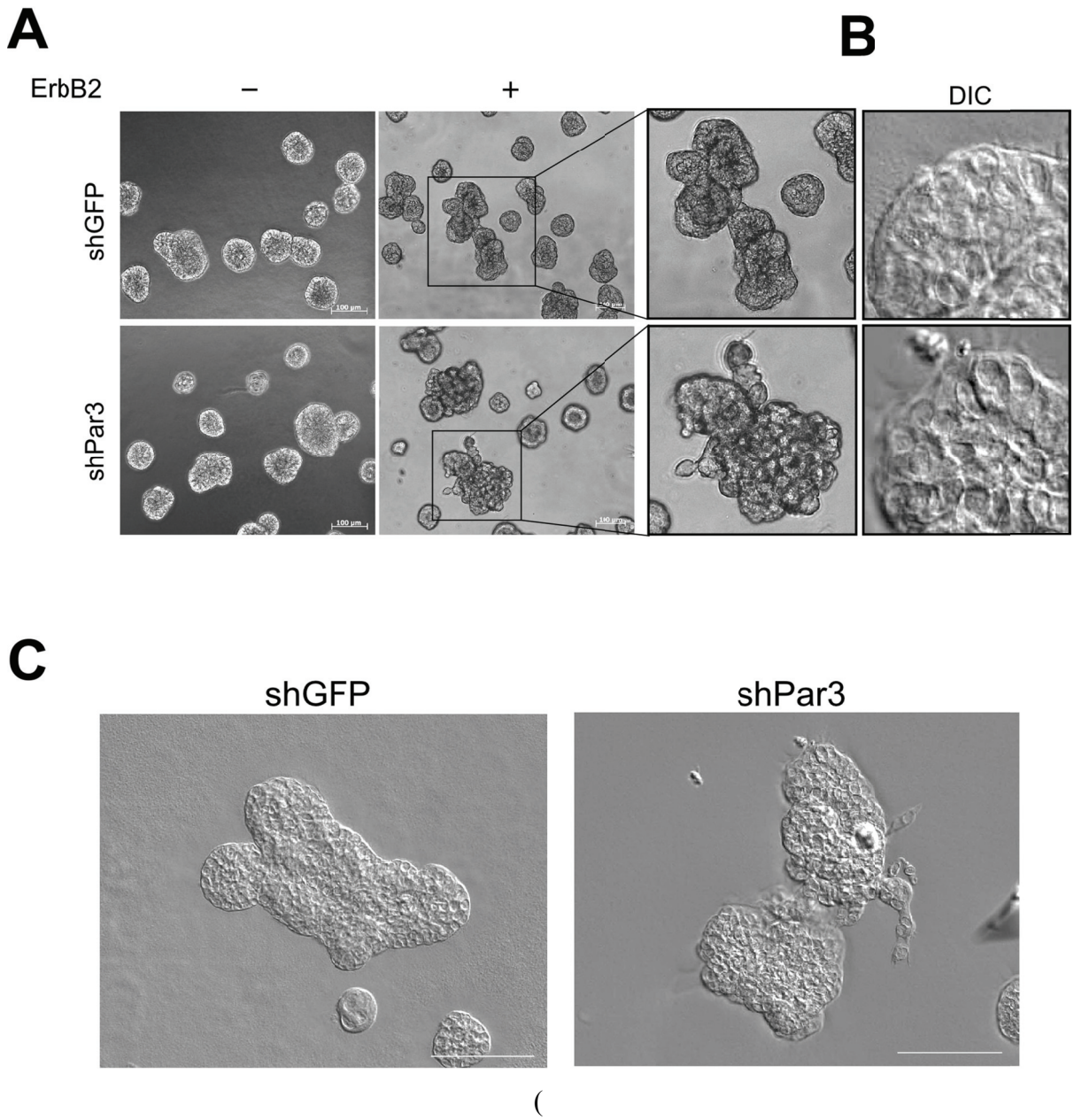

(

Figure 2.2. Loss of Par3 cooperates with ErbB2 activation to induce abnormal rough acinar structure in 3D culture.

(A) Phase contrast images of 10A.B2 day 12 acinar structures unstimulated (-) or stimulated (+) with dimerizer AP1510, a small molecule ligand to activate ErbB2, for four days (scale bar=100μm). The right panels show a higher magnification of multiacinar structures.

(B) Differential interference contrast (DIC) images showing detailed topology of the surface of acini from ErbB2-activated cells.

(C) DIC images of day 20 acinar structures stimulated with ErbB2 dimerizer for 12days (scale bar=100μm)

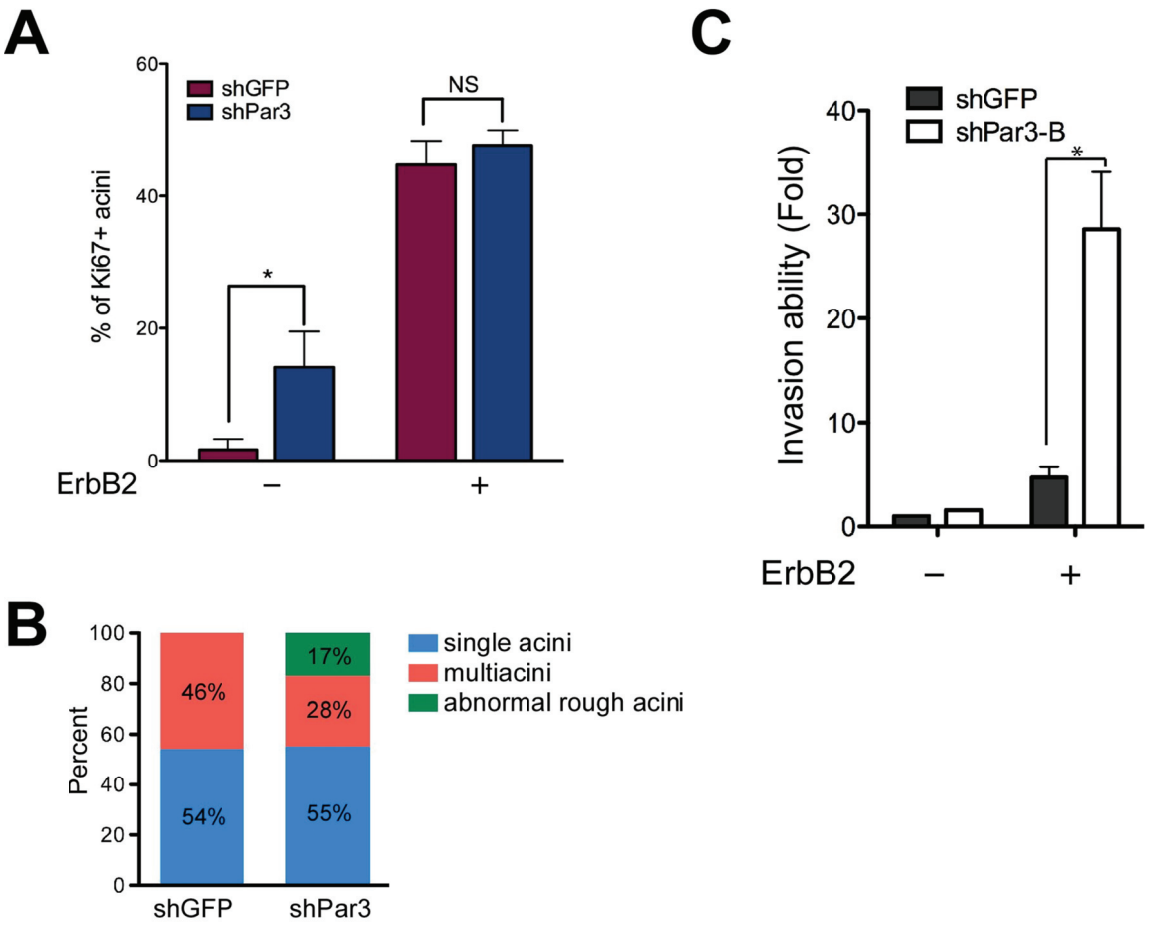

Figure 2.3. Induction of cell invasive behavior.

(A) Percentage of Ki67-positive acini. Day 16 acini from shGFP and shPar3 10A.B2 cells were grown with or without ErbB2 stimulation for 4 days and immunostained for Ki67. More than 100 structures were counted for each experiment. Error bars represent the standard error of the mean (SEM). (n=3; * represents $p<0.05$).

(B) ErbB2-activated acini were classified according to their microscopic morphology. Multiacinar structures were identified as those having three or more acinar structures abnormally organized. Abnormal rough structures were identified as those multiacinar structures having a rough surface. Percentages were determined by scoring >200 acini for each condition.

(C) 10A.B2 cells stably expressing shGFP or shPar3 were seeded for transwell invasion assays, with or without activation of ErbB2 and incubated for 48 hours. Invaded cells were quantified from three independent experiments and results are represented as fold change in invasion compared to shGFP cells without ErbB2 stimulation. (n=3; * represents $p<0.05$).

To observe the cellular morphology at the leading edge of migrating cells, we used an *in vitro* wound-healing assay. In this assay, a "wound gap" in a confluent monolayer is created by a scratch, followed by monitoring the closure of the gap by cell migration or growth towards the center of the gap. There are two advantages of this method. First, it allows the observation of cellular morphology possible, which is not possible in the transwell invasion assay. Second, since the scratch is made in confluent cell monolayers, the cells need to be released from the preexisting intercellular cohesion, which is more similar to migration *in vivo* (Rodriguez, Wu et al. 2005). In our experiments, scratches of approximately 500-μm widths were made in confluent cells grown in assay medium with or without ErbB2 activation, and gap closure was monitored by live-cell imaging for 60 hours. By the end of the time period, only shPar3 cells with ErbB2 activation had "healed" the gap (Figure 2.4). As ErbB2 activation increases cell proliferation similar in both shGFP and shPar3 cells, we can conclude that this gap closure is due to changes in cell behavior rather than cell growth. The shGFP cells were compact and migrated into the wound together forming a smooth leading edge. ErbB2 activation induced a stream of cells to migrate towards the middle. However in shPar3 cells, even without ErbB2 activation, the cells were more loosely connected despite no difference in wound healing speed compared to the control cells. ErbB2 activation caused cell less compact with each cell occupying more area, and increased their movement towards the middle. Therefore, these results are consistent with the transwell invasion assays, indicating that the loss of Par3 cooperates with ErbB2 activation to induce cell invasion and migration.

Cells can adopt different invasive strategies including individual or collective cell migration, amoeboid and mesenchymal migration (Friedl and Wolf 2003). To better understand the nature of the invasion process and further define the mechanism being used, we performed time-lapse imaging of the shPar3 cells in 3D culture with ErbB2 dimerizer for 72 hours to visualize multiacinar formation (Figure 2.5.A) and the invasion process (Figure 2.5.B). Formation of an invasive protrusion was initiated by one cell sprouting from the border of an acinus, followed by the development of a migrating structure composed of a cluster of cells without spindle-like mesenchymal transformation, suggesting that shPar3 cells move in a collective manner into the ECM.

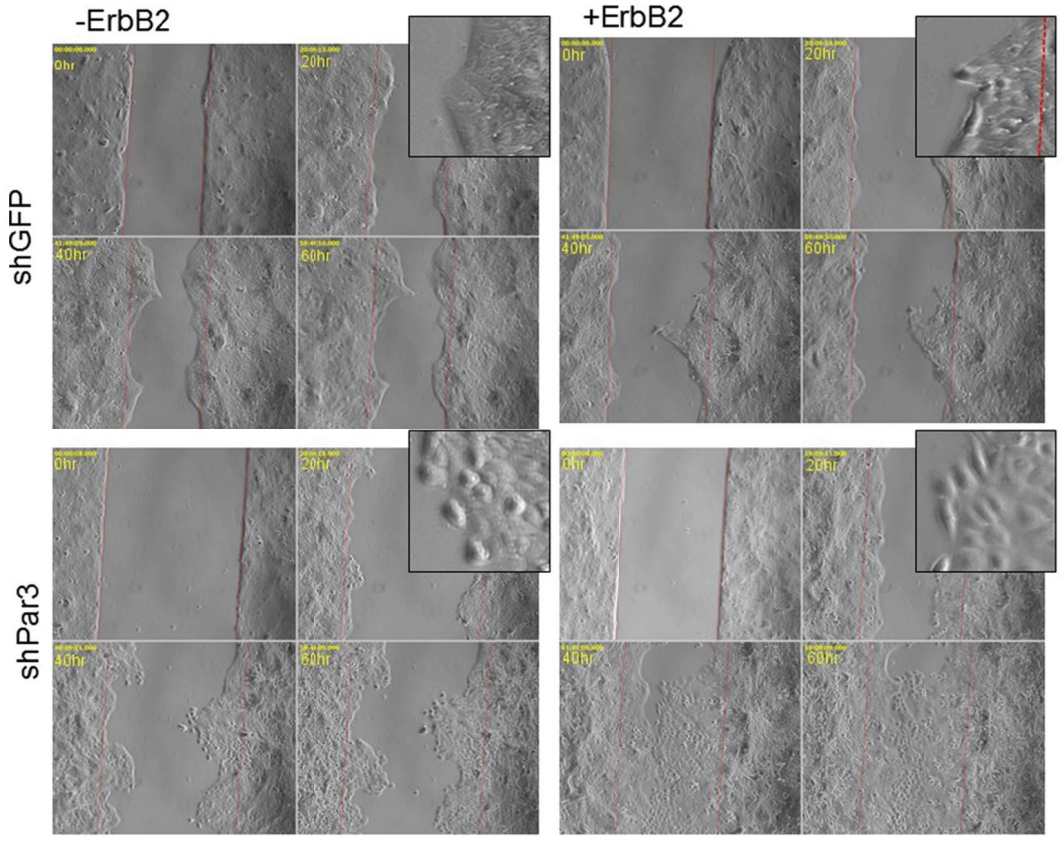

Figure 2.4. Loss of Par3 cooperates with ErbB2 activation to promote wound healing

shGFP and shPar3 cells were grown in dish with culture inserts (ibidi, LLC) until confluent, and then switched to the assay medium for 18 hours followed by removal of the insert to create the gaps. Cells were treated with or without ErbB2 dimerizer as indicated and the wound gaps were imaged every 15 minutes for 60 hours. The snapshot of 0hr, 20hr, 40hr and 60hr of each condition is shown. A red dotted line marked the edge of the gaps at 0hr time point. The boxed images are close-up areas of the leading edge of the cells from the 40hr time point images.

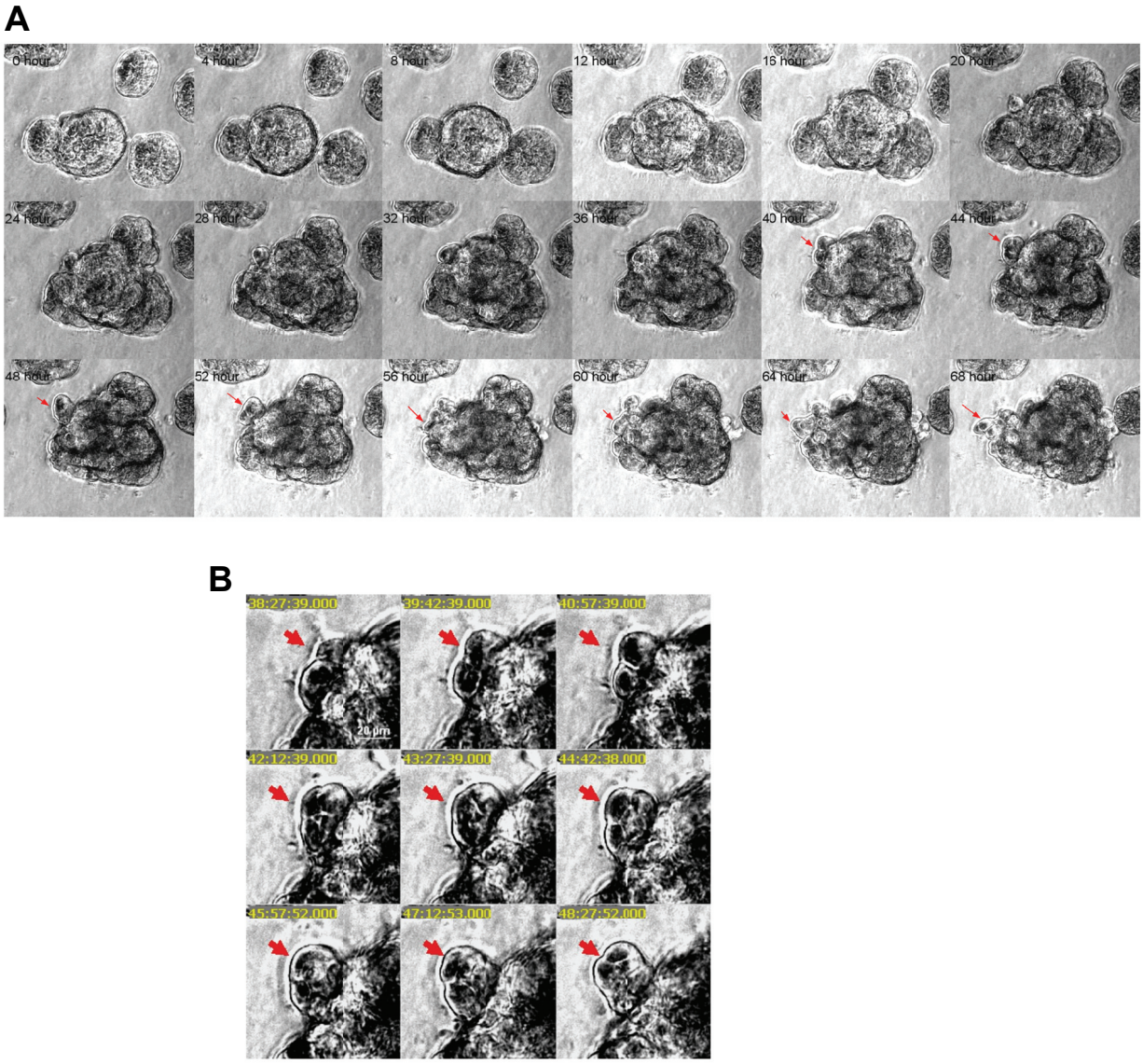

Figure 2.5. Collective migrating cells in the shPar3 3D acini.

(A) Day 8 acini from 10A.B2 shPar3 cells were treated with ErbB2 dimerizer and imaged every 15 minutes for 72 hours. The red arrows point to the protrusion formation.
(B) Higher magnification images of protrusion formation.

2.4 Loss of Par3 promotes invasive behavior in breast cancer cells

To investigate if loss of Par3 can promote invasive behavior in non-invasive human breast cancer-derived cell lines, we knocked down Par3 in T47D and SKBR3 cells (Figure 2.6.A), both of which are low-invasive breast cancer cell lines. SKBR3 cells overexpress HER2 (Price 1996). T47D and SKBR3 cells expressing shPar3 both showed a significant increase in invasion in transwell invasion assays (Figure 2.6.B). In addition, T47D cells lacking Par3, but not the parental cells, formed 3D structures with a rough topology, similar to the phenotype observed in 10A.B2 cells (Figure 2.6.C). Thus, loss of Par3 induced invasion in both ErbB2-transformed MCF10A cells and human breast tumor-derived cell lines.

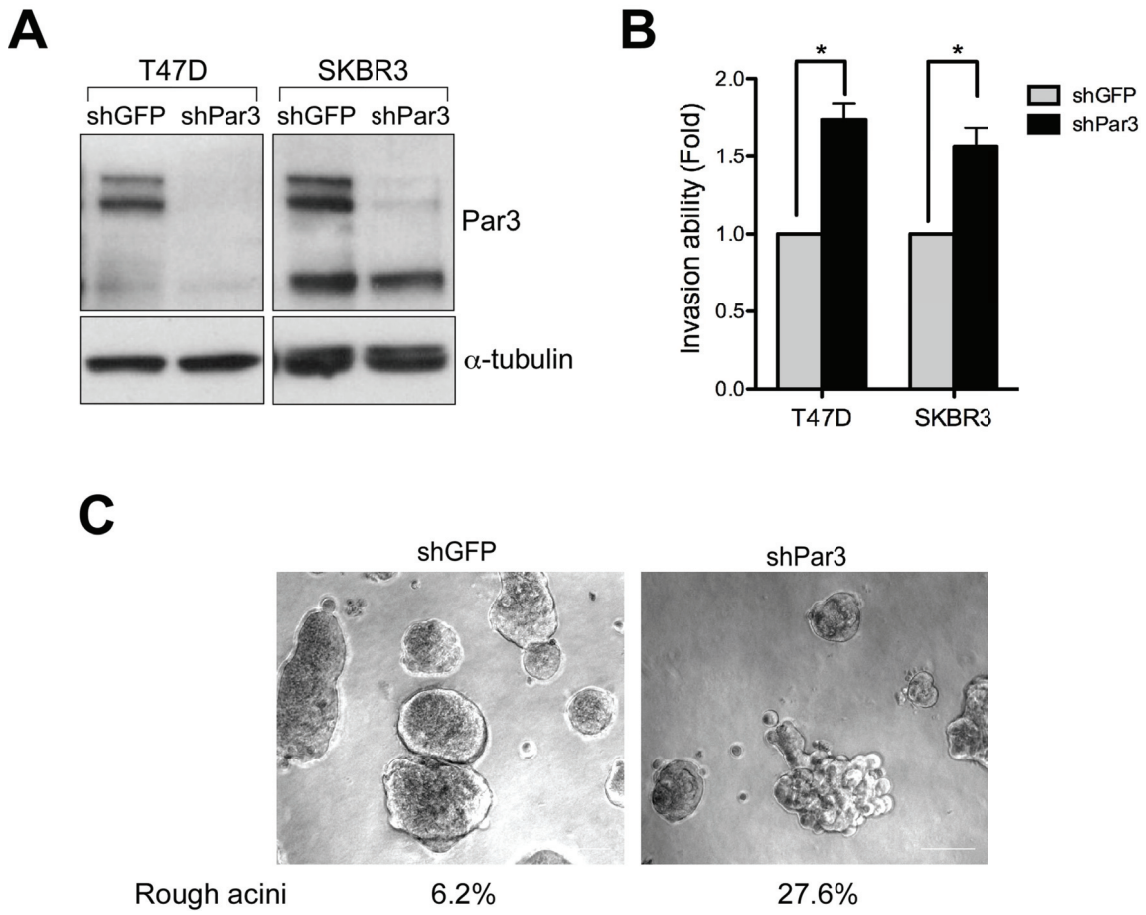

Figure 2.6. Loss of Par3 induced cell invasion in breast cancer cells

(A) Lysates from shGFP or shPar3 T47D and SKBR3 cells were analyzed for Par3 protein levels.

(B) T47D and SKBR3 cells expressing shGFP or shPar3 were seeded for transwell invasion assays and incubated for 24 hours and 72 hours respectively. Invaded cells were quantified from three independent experiments and results are represented as fold change in invasion compared to shGFP cells (n=3; *, $p<0.05$).

(C) Phase contrast images of shGFP or shPar3 T47D acini grown in Matrigel for 20 days (scale bar=100μm). The acini were classified according to their morphology. Acini with rough surface were identified as abnormal structures. The percentage of rough acini is indicated under the images. More than 50 acini were scored in each condition.

2.5 Par3 is not required for establishing the apical-basal polarity

Par3 has been shown to localize below the Par6/aPKC complex at the apical/lateral junction and is important for defining the apical/basal border during *Drosophila* cellularization. We next tested whether Par3 is required for establishing apical-basal polarity in mammalian epithelial cells. The apical-basal polarity can be visualized by immunostaining for the proteins which have polarized position in cells, including the cis-Golgi protein, GM130 and the basement membrane protein, laminin5. In the absence of ErbB2 activation, both shGFP and shPar3 cell-derived structures showed well-polarized structure, featuring apical GM130 facing the lumen and laminin5 surrounding the basal surface. ErbB2 activation induced shGFP cells to form multiacinar structures with filled lumens and intact basal laminin5. However, the shPar3 cell-derived structures had severely disrupted organization without showing any acini-like structure. The laminin5 had breakdown around the structures. Notably, the F-actin lost its normal cell peripheral structure in shPar3 cells (Figure 2.7). Therefore, loss of Par3 alone does not affect the establishment of apical-basal polarity in 10A.B2 cells.

I also investigated cell polarity using the MDCK culture system. MDCK cells can spontaneously undergo polarization when grown on a porous membrane, with the apical side facing the culture medium and basal side facing the supporting membrane. First, three microRNA30 based shRNAs against *Canis lupus familiaris* Par3 were designed and constructed in the retroviral pMSCV-LTR-hygromycin vector. Stable cell lines expressing the shRNAs were established after hygromycin selection. The expression level of Par3 was analyzed by immunoblotting. The shRNA targeting base pairs 1531-1551 (shcPar3C) was shown to be the most effective shRNA (Figure 2.8.A). The control and shcPar3 MDCK cells were seeded in the cell inserts at high density and grew for four days to allow them to be fully polarized (Figure 2.8.B). TJ protein ZO-1 was used as an apical marker and AJ protein E-cadherin was used a basolateral marker in immunostaining experiments. Z-stack images of 0.25μm thickness were acquired across the entire specimens. The z-sections at 1.0μm, 2.5μm and 4.0μm from the bottom were defined as basal; middle and apical sections, respectively. In both shGFP and shcPar3 cells, E-cadherin was restricted to the basal sections and ZO-1 was restricted to the apical sections, suggesting that cell lines were both well polarized with

the apical and basal membranes segregated. However, the staining intensity of ZO-1 and E-cadherin was lower in the Par3 knockdown cells compared to the control cells, suggesting that Par3 may regulate absolute levels of ZO-1 and E-cadherin as monitored by immunofluorescence analysis (Figure 2.8.B). Taken together, Par3 is dispensable for the establishment of apical-basal polarity.

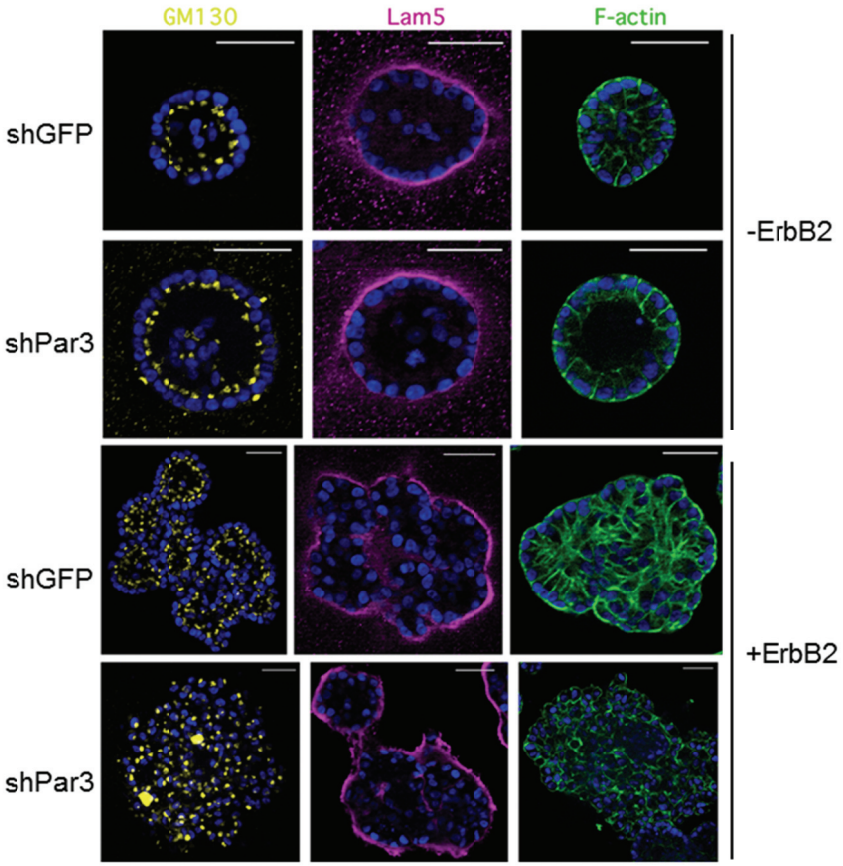

Figure 2.7. The apical-basal polarity in 10A.B2 cells

Day 16 shGFP or shPar3-derived acini with or without ErbB2 dimerizer stimulation for 8 days were stained with GM130 (yellow), a *cis*-golgi marker to mark apical orientation, laminin 5 (magenta) to mark the basal surface and phalloidin (green) to mark the actin cytoskeleton.

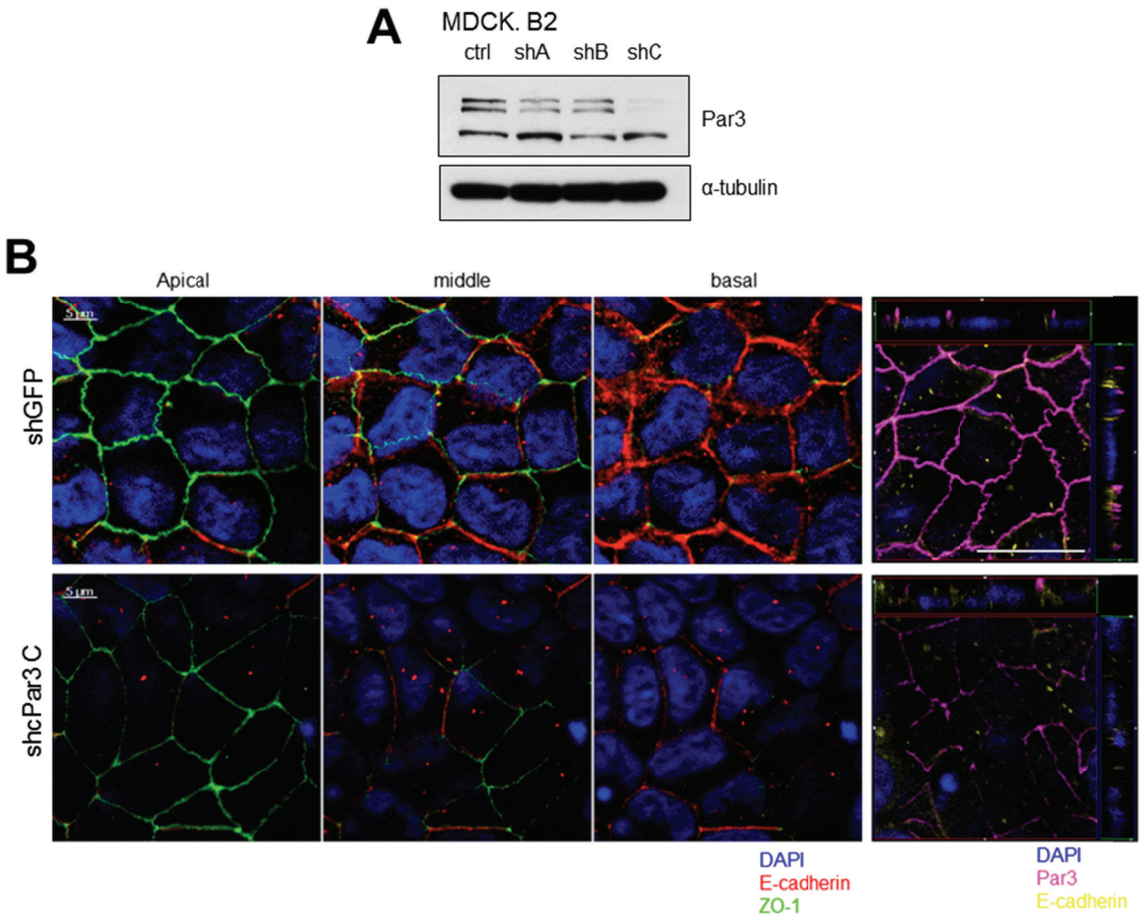

Figure 2.8. Loss of Par3 did not affect apical-basal polarity in MDCK cells

(A) Immunoblot of Par3 protein levels in MDCK cells infected with virus expressing shRNA targeting GFP and one of three shRNAs targeting *Canis lupus familiaris* Par3

(B) MDCK cells expressing shGFP or shcPar3 were seeded on 0.4μm porous membrane culture inserts and grown for four days to form a confluent polarized monolayer. The cells were fixed and immunostained for ZO-1 (green), E-cadherin (red) and Par3 (magenta). Z-stack images were acquired for each condition. The z-stack images of 4.0 μm, 2.5 μm and 1.0μm from the bottom were shown to represent the apical, middle and basal sections of the cells, respectively.

Chapter 3

Loss of Par3 Promotes Metastasis of ErbB2 Mouse Mammary Tumors *In Vivo* without Overt EMT

Introduction:

In order to understand the causal role of ErbB2 in breast cancer progression, and moreover, for developing and testing therapies targeting the receptor, several ErbB2 mouse models have been developed over the past three decades. To achieve the expression of the transgene specifically in the mammary gland, the mouse mammary tumor virus-long terminal repeat (MMTV-LTR) promoter was used as it can efficiently drive high expression of oncogenes in mammary epithelium (Stewart, Pattengale et al. 1984; Sinn, Muller et al. 1987; Mink, Ponta et al. 1990). Different strategies have been adopted to induce ErbB2 receptor activation, including expressing an active form of rat NEU (NEU-NT) (Muller, Sinn et al. 1988), the wild-type Neu proto-oncogene (Guy, Webster et al. 1992), and the active NEU receptor, which harbors a distinct in-frame deletion (NDL) (Siegel, Ryan et al. 1999). As an alternation to the MMTV-LTR promoter, some mouse models were also designed using the endogenous *erbB2* promoters to drive the oncogene (Knock-in NEU-NT) (Andrechek, Hardy et al. 2000), or a TetO conditional activation system (Moody, Sarkisian et al. 2002). These mouse models developed mammary tumors of different malignancy and pathological properties, reflecting the multifaceted contribution of the ErbB2 receptor activation to the signaling pathways and disease progression (Ursini-Siegel, Schade et al. 2007). Therefore, a model must be carefully selected to suit the research purpose.

Acquisition of invasive behavior is a prerequisite for metastasis. As loss of Par3 cooperates with ErbB2 activation to induce cell invasion *in vitro*, next we tested if downregulation of Par3 can induce metastasis of ErbB2-induced tumors *in vivo*. The ErbB2 transgenic mouse model chosen was MMTV-NDL. These mice express a Neu/ErbB2 deletion mutant (NDL), an extracellular domain mutant that promotes constitutive receptor dimerization, under the control of the MMTV-LTR (Andrechek, Hardy et al. 2000). They develop focal mammary tumors with latency as long as five months. The tumors show typical solid morphology similar to the human “solid” DCIS without central necrosis (Ursini-Siegel, Schade et al. 2007). Spontaneous lung metastases develop in these mice after 60 days following the first tumor palpation (Siegel, Ryan et al. 1999). This gives a large window assess the role of Par3 in changing tumor progression.

Acquisition of invasive behavior is frequently associated with EMT, which is defined as a process wherein cells lose epithelial traits and acquire mesenchymal characteristics. It is a process first recognized in embryonic morphogenesis; during gastrulation, invaginated mesoderm precursor cells undergo EMT to form dissociated mesoderm cells accompanied with cell shape change, and occupy the space between the epiblast and the visceral endoderm. The formation of a definitive endoderm and morphogenesis of different organs requires these cells to re-epithelize, aggregate and re-establish cell-cell adhesions and apical-basal polarity, referred to as mesenchymal-epithelial transition (MET) (Ferrer-Vaquer, Viotti et al. 2010). EMT is thought to also play important roles during the development of metastasis by providing tumor cells with the ability to escape from the primary tumor, migrate to distant regions, and invade tissues. Polarity proteins have been found to be involved in the EMT process. Transcriptional repressors that induce EMT, such as ZEB1, SNAI1, and SNAI2, directly bind to the promoter elements of cell polarity genes *CRB3* and *LGL2* and repress their mRNA expression (Davalos, Moutinho et al. 2011). In addition to being directly regulated by EMT core signals, cell polarity proteins can regulate migration and invasion by modulating signaling pathways. For example, TGF-β binds and phosphorylates Par6 at AJs, enabling recruitment of the E3 ubiquitin ligase Smurf1 to degrade the small GTPase RhoA, promote loss of TJs and cause an protrusive phenotype (Wang, Zhang et al. 2003; Ozdamar, Bose et al. 2005). Importantly, in mammary gland tumors, blockade of Par6 phosphorylation can inhibit the TGF-β pathway and suppress tumor metastasis to the lungs (Viloria-Petit, David et al. 2009). It is now believed that EMT is not a single rigid state but a highly plastic and dynamic process that involves a broad spectrum of signaling regulators. Recent results from our lab show that disruption of multiple polarity proteins in oncogene-naïve epithelial cells induces phenotypic plasticity where the cells acquire invasive behavior in response to a tumor-like microenvironment such as rigid ECM (Matrigel/type I collagen mixture) and inflammatory cytokines (IL-6 or TNF-α), while they behave like epithelial cells under normal growth factor conditions or in a bed of soft ECM (Matrigel) (Chatterjee, Seifried et al. 2012). This plastic state may be similar to previously described ‘partial-EMT’, or ‘metastable’ or ‘hybrid’ state (Thiery, Acloque et al. 2009), that is thought to allow cells to transit between epithelial and mesenchymal states.

In this chapter, we tested whether loss of Par3 affects the progression of ErbB2-induced mammary tumors *in vivo* using Par3 shRNA lentiviral transduction of primary mammary tumor cells. I demonstrate that loss of Par3 promotes ErbB2 tumor metastasis. Surprisingly, I also found that the invasive behavior of the cells was not accompanied by an overt EMT.

Results:

3.1 *Lentivirus transduction of ErbB2-induced mammary tumor cells and orthotopic transplantation*

To introduce Par3 knockdown to ErbB2-induced mammary tumor cells, we isolated the primary tumor epithelial cells from a metastasis-free MMTV-NDL mouse, then infected the tumor cells with lentivirus expressing mPar3 shRNA or control shRNA, as described in Chapter 2. The cells were infected at a multiplicity of infection (MOI) of 5 which resulted in approximately 20% of infection efficiency in the primary tumor cells at the second day (Figure 3.1). As the donor MMTV-NDL tumor cells express a constitutively activated form of NEU, the rat homolog of ErbB2 (Andrechek, Hardy et al. 2000), immunodeficient NOD/SCID mice with impaired T and B cell lymphocyte development and reduced NK activity were chosen as recipients to avoid the cross species immune rejection (Ito, Hiramatsu et al. 2002). The infected cell aggregates were injected into the No. 4 pair of mammary fat pads of NOD/SCID mice which is highly vascularized, consist of adipocytes and exhibits a histological similarity to the original tumor microenvironment. As the developing mammary parenchyma in the No.4 glands did not extend beyond the lymph node in 3- to 4-week-old mice, the entire endogenous mammary epithelial cells can be surgically removed before transplantation. The tumor onset and lung metastasis were scored.

3.2 *Loss of Par3 promotes metastasis of ErbB2-induced mammary tumors*

In the initial experiment, lentivirus expressing shGFP and shmPar3 were generated using the pLKO.1 backbone. The virus was packaged in 293T cells. The titration of viral stock was determined by infecting 293T cell with serial dilutions of the viral stock and counting viable cells after puromycin selection for 4 days. The viral supernatant containing the same amount of virus transduction unit (TU) was further concentrated to $1x10^7$ TU/ml by ultracentrifugation. The primary tumor cells were isolated from MMTV-NDL mouse that carried a tumor of $1cm^2$ without any evidence of metastasis in the lungs, and confirmed by hematoxylin and eosin (H&E) histological staining. 2500 tumor cells infected with shGFP or shmPar3 were transplanted into NOD/SCID mice. Mice injected with GFP shRNA- or mPar3 shRNA-infected cells both

developed tumors with the same latency that reached a diameter of 1.5 cm about 12 weeks after the transplantation. The mice were sacrificed and the tumors and lungs were collected for further analysis. We found that in 4 out of 7 mice the tumors derived from Par3 shRNA-infected cells developed multiple local metastases on the abdominal wall (Figure 3.2A). Metastasis was rarely (1 out of 5) observed in tumors derived from GFP shRNA-infected cells (Figure 3.2B). Knockdown of Par3 in shmPar3-derived tumors was verified by immunostaining for Par3. Analysis of H&E staining sections provided evidence that the metastatic lesions growing on the abdominal wall penetrated the muscle tissue and had poorly organized margins indicative of invasive behavior. The tumor cells in the metastatic nodules retained E-cadherin expression demonstrating that the cells had not permanently lost their epithelial properties (Figure 3.2C).

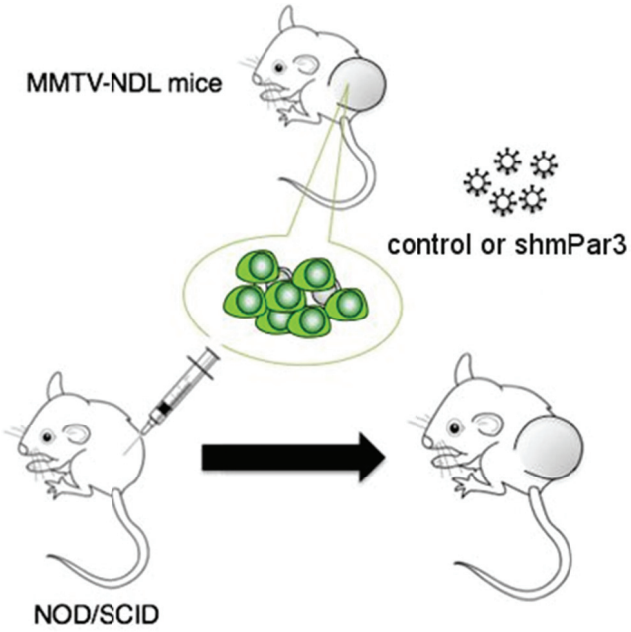

Figure 3.1. Schematic illustration of the primary mammary tumor transplantation experiments

Primary tumor cells were isolated from a tumor in an MMTV-NDL mouse, and infected with lentivirus expressing control shRNA or shRNA against mouse Par3. The infected cells were injected into the cleared mammary fat pads of NOD/SCID mice. The tumor onset and metastasis were analyzed

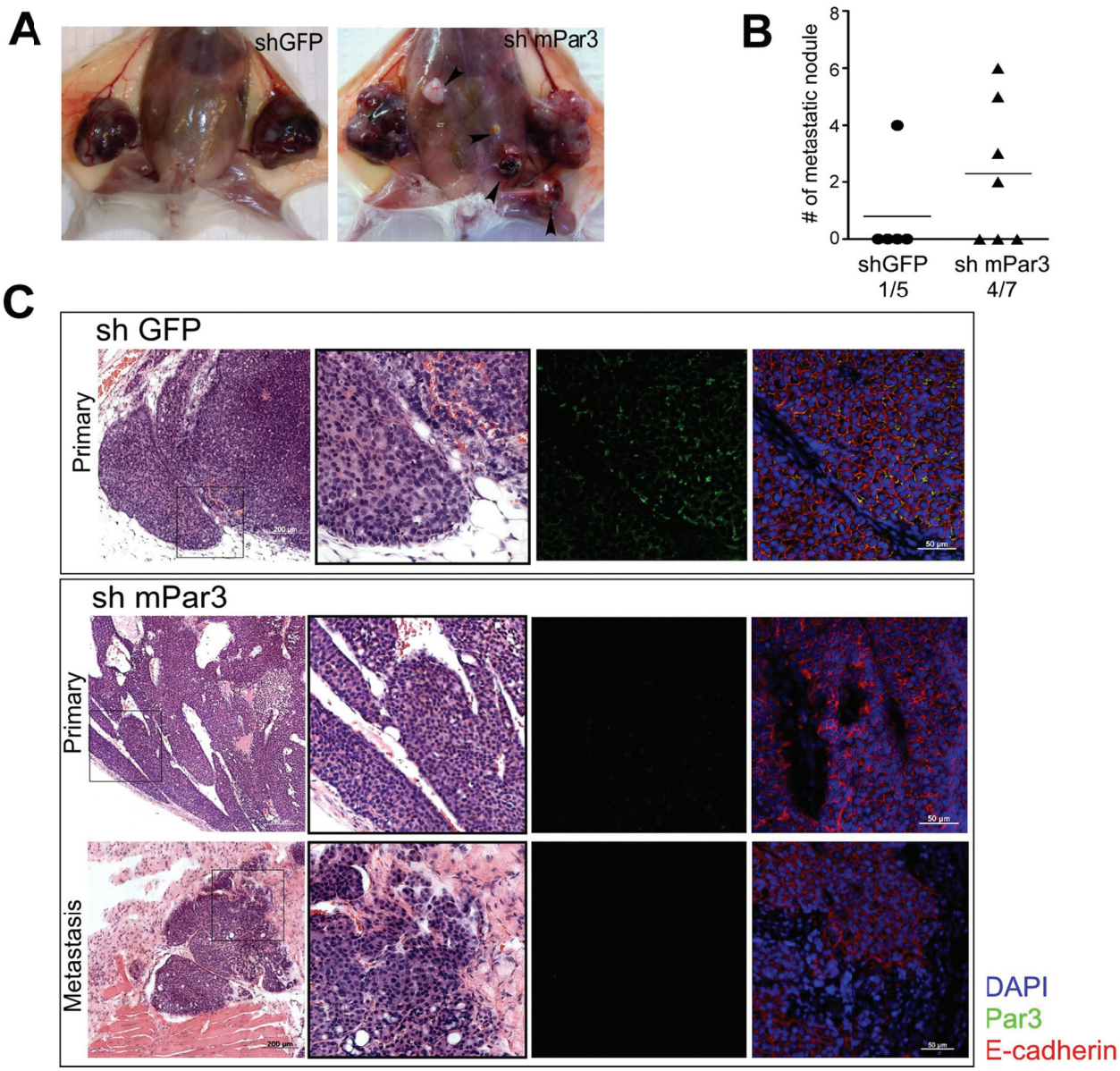

Figure 3.2. Loss of Par3 promotes ErbB2-induced local metastasis

(A) Representative tumors of mice transplanted with MMTV-NDL-tumor-derived cells infected with GFP or mPar3 shRNA lentivirus, 12 weeks after transplantation. The arrowheadss point to local metastatic nodules growing on the abdominal wall.

(B) The number of metastatic nodules in each mouse was counted and the distribution is plotted. The frequency of metastasis is indicated below the graph.

(C) Tumors and the metastatic nodules were collected and stained with H&E or immunostained for Par3 (green) and E-cadherin (red).

These results prompted us to assess the development of distant metastasis. The NDL primary tumor cells from the same stock as describe above were infected with lentivirus expressing empty vector or mPar3 shRNA in the pLKO.3G backbone in which the puromycin resistance gene was replaced by a green fluorescent protein (GFP) driven by the phosphoglycerate kinase (PGK) promoter as a reporter for infected cells. Infected cells were transplanted into pre-cleared mammary fat pads of NOD/SCID mice as previously described. Both vector and mPar3 shRNA-infected cells developed GFP-positive tumors where GFP was heterogeneously expressed (Figure 3.3.A). One cohort of mice was sacrificed 12 weeks after transplantation when the tumor size reached 1.5 cm in diameter. To extend the life span of the mice and allow distant metastasis to form, in a second cohort of mice, the primary tumor nodes were removed at week six to relieve the tumor burden and the mice were sacrificed 20 to 24 weeks after transplantation (Figure 3.3.A). The primary tumors generated by mPar3 shRNA-infected cells or the vector-infected cells did not differ significantly in total mass (approximately 1.5 grams). Fifty percent of the mice (5 out of 10) in the first cohort injected with mPar3 shRNA-infected cells developed GFP-positive lung metastases and 75% of mice (3 out of 4) in the second cohort developed lung metastasis without tumor regrowth at the primary site. In contrast, only 1 out of 10 mice developed lung metastasis in the vector-infected group (Figure 3.3.A, B). The tumors were collected and analyzed by immunostaining for Par3 and E-cadherin. Primary tumors and metastases from both vector and shmPar3 had epithelial morphology and expressed E-cadherin at cell-cell junctions. ShmPar3-derived primary tumors had decreased levels of Par3 in the selected GFP-positive region (Figure 3.3.C). This result is consistent with the previous reported observation in breast cancer that the metastases from invasive ductal carcinoma express E-cadherin with the same intensity or with an even stronger intensity than the corresponding primary tumors (Kowalski, Rubin et al. 2003). Although aberrant E-cadherin expression is commonly associated with metastasis, normal E-cadherin expression is required for a tumor to repopulate in the distant sites. So far, it is unclear whether these cells retained E-cadherin expression during dissemination or the cells lost E-cadherin initially and then regained expression of E-cadherin at the distant metastatic foci, commonly explained by EMT-MET theory. Together, these studies demonstrate that loss of Par3 was sufficient to initiate metastatic behavior in epithelial cells derived from ErbB2-induced primary mouse mammary tumors.

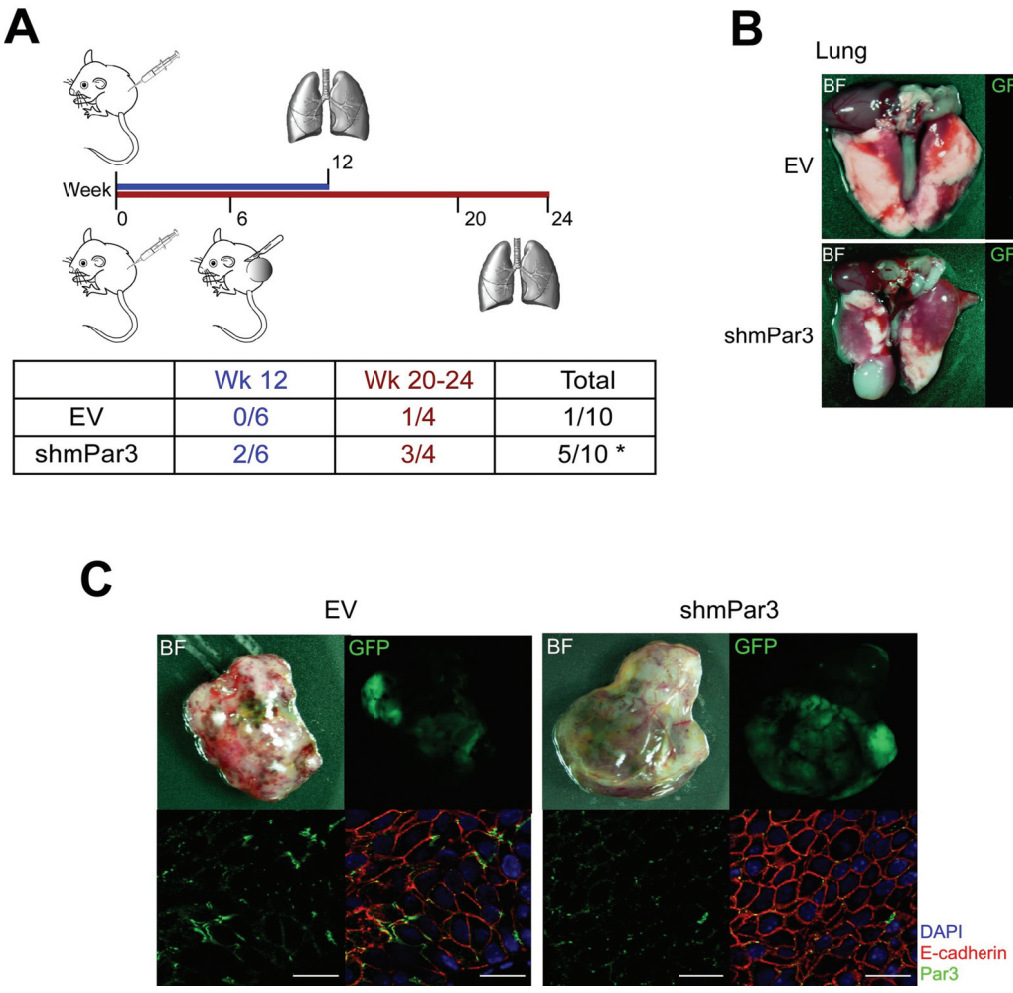

	Wk 12	Wk 20-24	Total
EV	0/6	1/4	1/10
shmPar3	2/6	3/4	5/10 *

Figure 3.3. Loss of Par3 promotes ErbB2-induced tumor metastasis

(A) Schematic illustration of the transplantation experiment (upper panel). Primary tumor cells from MMTV-NDL mice were infected with empty vector (EV) or mPar3 shRNA lentivirus with a GFP reporter and transplanted into the cleared mammary fat pads of NOD/SCID mice. Lung metastasis incidence was determined 12 weeks later, indicated in blue (n=6) for one cohort. In a second cohort of mice, primary mammary tumors were removed 6 weeks after transplantation and lung metastasis incidence was determined 20 to 24 weeks after transplantation, indicated in red (n=4). The incidence of lung metastasis is shown in the table.

(B) Representative lungs from the mice transplanted with MMTV-NDL tumor-derived primary cells infected with empty vector or mPar3 shRNA lentivirus with a GFP reporter. Lungs were collected 24 weeks after transplantation as described in Figure 3.3.A.

(C) Representative images of primary tumors collected 12 weeks after transplantation. Tumor sections were immunostained for Par3 (green) and E-cadherin (red) (scale bar=20μm).

3.3 Acquisition of the invasive behavior by loss of Par3 without associated with an overt EMT

Next, we tested if activation of in cells lacking Par3 promotes tumor metastasis by inducing EMT through observation of the cell morphology and evaluation of the mesenchymal marker expression. Treating 10A.B2 cells with TGF-β, a known inducer of EMT, led to a loss of epithelial morphology and acquisition of spindle-shaped mesenchymal morphology. In comparison, we did not observe any morphological changes associated with EMT in either shGFP or shPar3 cells in the presence or absence of ErbB2 dimerizer for four days (Figure 3.4.A). Consistent with the lack of changes in cell morphology, the mRNA expression of mesenchymal markers such as *snail, N-cadherin* and *fibronectin* was not altered by loss of Par3 or ErbB2 activation alone or in combination in 10A.B2 (Figure 3.4.B) and T47D cells (Figure 3.4.C).

EMT is also characterized by a loss of the epithelial marker E-cadherin. Loss of Par3 did not decrease expression of E-cadherin in 10A.B2, T47D or BT474 cells (Figure 3.5A). We also did not observe obvious differences in E-cadherin localization in confluent monolayers of epithelial cells (Figure 3.5.B) or in primary tumors derived from shPar3 cells (Figure 3.3.C). These observations suggest that loss of Par3 cooperates with ErbB2 to induce invasive behavior in epithelial cells without being associated with an overt EMT.

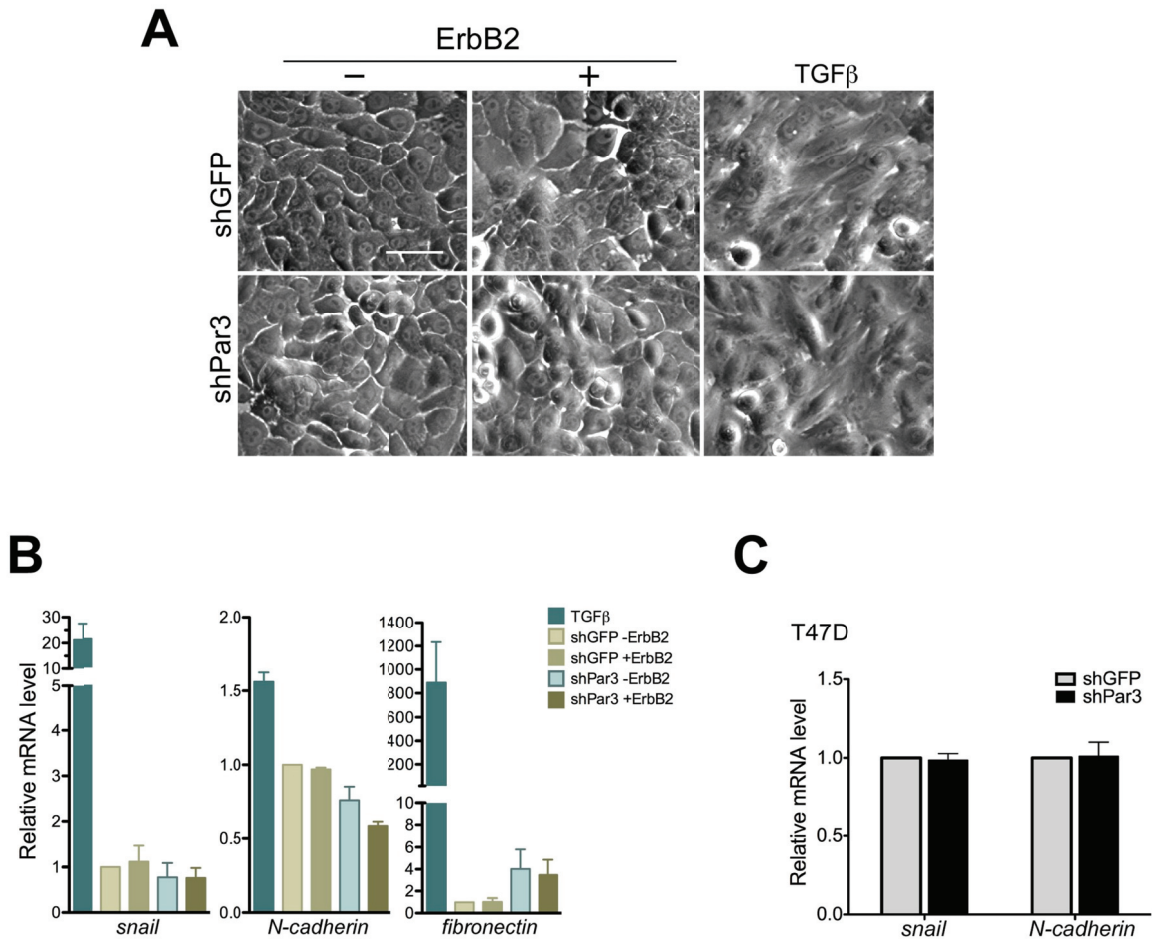

Figure 3.4. Lack of an overt mesenchymal phenotype in Par3-dificient cells

(A) Phase contrast images of shGFP or shPar3 10A.B2 cells untreated or treated with ErbB2 dimerizer, or TGF-β (5.0 ng/ml) for four days.

(B) Expression of mesenchymal markers in 10A.B2 cells was examined by quantitative PCR using primers against *snail, N-cadherin* and *fibronectin.* The data were normalized to *β-actin* mRNA levels. TGF-β stimulation was used as positive control (n=3, mean ± SD).

(C) mRNA from T47D cells was examined for *snail* and *N-cadherin* levels by quantitative PCR. The data were normalized to *β-actin* and fold changes are shown (n=3, mean ± SD).

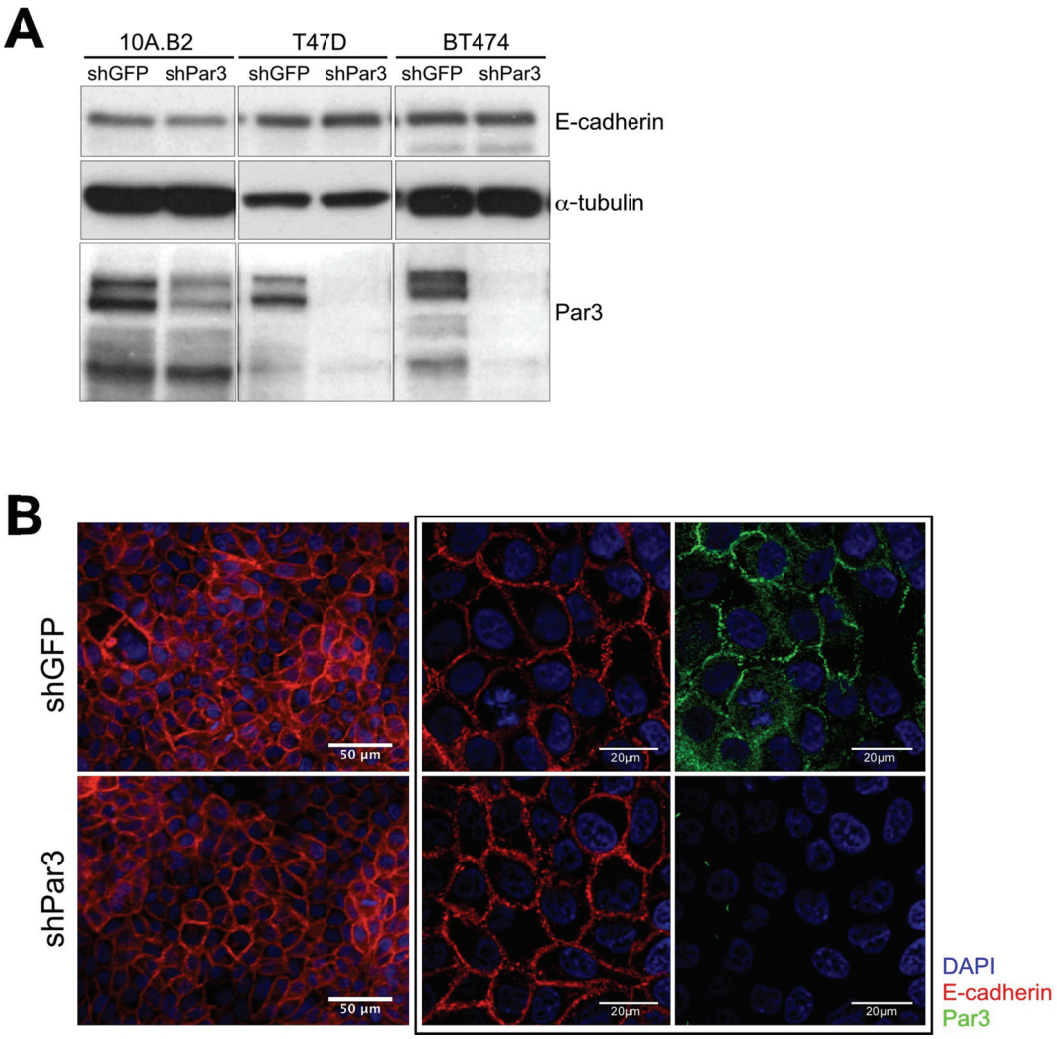

Figure 3.5. Loss of Par3 does not change E-cadherin protein expression or localization

(A) Cell lysates from confluent shGFP or shPar3 10A.B2, T47D and BT474 cells were analyzed for changes in E-cadherin protein levels.

(B) Confluent 10A.B2 cells were immunostained for E-cadherin (red) and nuclei (DAPI, Blue) (scale bar=50µm). Boxed images on the right represent cells stained for Par3 (green) and E-cadherin (red) at higher magnification (scale=20µm).

Chapter 4

Loss of Par3 Promotes Invasion by Blocking E-cadherin junction Maturation

Introduction:

Cancer cells can utilize various mechanisms to acquire invasive and migratory behavior. In primary tumors, cancer cells are packed together and they interact with neighboring cells, stromal cells and the ECM. E-cadherin mediated cell-cell interaction is the first barrier against cell mobility, and loss of cell-cell adhesion is a fundamental change that occurs during the progression of cancer to invasive disease. The suppression of E-cadherin expression and mutation of E-cadherin gene is frequently associated with metastasis in many cancers (Hirohashi 1998), and re-expression of E-cadherin in highly invasive cancer cells can block the invasiveness (Vleminckx, Vakaet et al. 1991). However, uniform strong membrane expression of E-cadherin has been seen in most invasive ductal carcinomas (IDC) and DCIS. There appears to be no correlation between E-cadherin expression levels and ErbB2 expression or tumor grade in IDC (Acs, Lawton et al. 2001). Consistent with this observation, E-cadherin expression is found to not correlate with recurrence, distant metastases, lymph node stage, vascular invasion, or prognostic group or survival in IDC patients, and therefore provides minimal prognostic value (Parker, Rampaul et al. 2001). This contradictory finding suggests that in breast ductal carcinomas, cell-cell cohesion strength may be decreased by other mechanisms without suppressing E-cadherin expression.

AJ assembly is mediated by E-cadherin, a glycoprotein with an extracellular domain and a cytoplasmic domain. The extracellular domain is composed five cadherin-motif subdomains that are used for establishing homophilic interactions between neighboring cells. The cytoplasmic domain interacts with an array of intracellular proteins including β-catenin and α-catenin, which in turn interacts with the actin-myosin cytoskeleton. One of the key features of AJs is that they are dynamic and there is a constant turnover of AJ proteins even in a stable epithelium. This dynamics nature allows cells to undergo cell shape changes and rearrange cell position while still maintaining strong adhesive strength, which is essential for organism growth and development. The dynamics of AJs can be modulated by junction assembly and AJ protein trafficking. AJ formation initiates from cortical actin polymerization to produce membrane ruffles and generate new sites of contact between cells, followed by actomyosin tension at the contact edges to generate a pulling force to expand the contact. After the initial contact is established, dynamic protrusions further propel E-cadherin interactions and clustering of other

AJ elements including polarity proteins. In the nascent junctions, actin polymerization and actomyosin tension are further required for the stabilization and maturation of the adhesive interface (Baum and Georgiou 2011). It has been shown that two spatial F-actin populations at junctions are distinguishable: junctional actin to stabilize the clustered cadherin receptor at cell-cell contacts, and peripheral thick bundles for lateral domain polarization (Zhang, Betson et al. 2005). This leads to E-cadherin distribution at two levels: stable homophilic E-cadherin *bona fide* adhesive foci and diffusing 'free' E-cadherin (Cavey, Rauzi et al. 2008) (Figure 4.1). The turnover of AJ components is also achieved by endocytosis and recycling of cadherins to the cell surface (Yap, Crampton et al. 2007). E-cadherin turnover in cultured epithelial cells can be monitored using surface biotinylation and recycling assays. It has been shown that E-cadherin is actively internalized and recycled back to the plasma membrane via a process that is dependent on clathrin-mediated endocytosis (Le, Yap et al. 1999).

Although the role of E-cadherin protein has been extensively studied in the cancer field, very little is known about the contribution of E-cadherin dynamics to AJ maintenance and cancer cell cohesion. E-cadherin dynamics are found to be significantly faster *in vivo* than *in vitro* as measured by photobleaching assays. Cancer drug dasatinib, a clinically approved Src inhibitor can reduce cell migratory behavior by stabilizing E-cadherin at cell-cell junctions *in vivo* (Serrels, Timpson et al. 2009). In this chapter, I demonstrate thatmaturation of E-cadherin requires Par3. Loss of Par3 promotes cell invasion by blocking E-cadherin maturation and weakening cell-cell adhesion strength.

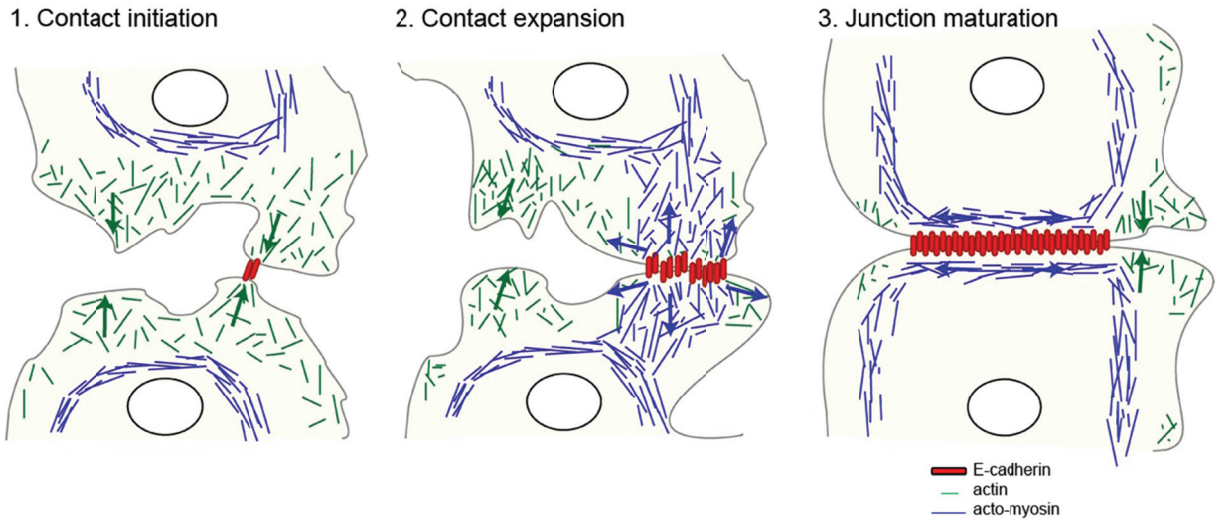

Figure 4.1. Assembly of E-cadherin homophilic adhesion complexes at adherens junction

1. Cells contact each other and E-cadherin engagement *in vitro* leads to a remodeling of the actin cytoskeleton (green), promoting lamellipodial and filopodial protrusions via Rac, Cdc42, and Arp2/3 activity.

2. These dynamic protrusions promote further E-cadherin interactions and clustering. The nascent AJs are connected to cortical actomyosin cables (blue).

3. Myosin-mediated contraction expands the region of intercellular contact and aligns cadherin–catenin complexes (red bars), leading to the maturation of the junction. (Adopted from Baum B & Georgiou M. J Cell Biol. 2011 192(6): 907–917).

Results:

4.1 Loss of Par3 weakens cell-cell adhesions

To understand the mechanism by which loss of Par3 induces invasion, we monitored ErbB2-induced changes in MCF10A cell behavior when grown in 2D culture. The cells were seeded at low density ($1x10^4$ cells per well in a 12-well plate) to allow enough time to track at least two cell cycles before reaching confluence. We tracked each cell and their progeny during colony expansion by time lapsing imaging. We found that both shGFP and shPar3 cells had the same dividing cycle time (8 hours) upon ErbB2 activation. However, the dividing shPar3 daughter cells failed to stay cohesive within a colony, whereas shGFP daughters remained proximal to each other within an epithelial island (Figure 4.2.A), suggesting a decrease in cell-cell cohesion. The migrating shPar3 cells also showed expanded lamellipodia formation at the leading edge of the cells (Figure 4.2.A).

Cadherins and integrins such as α5β1 integrins are involved in the adhesive networks and maintenance of tissue architecture (Robinson, Zazzali et al. 2003; Weber, Bjerke et al. 2011). As cells can spread on ECM in an integrin-dependent manner, a simple cell spreading assay was used to test whether this decrease in cohesiveness was due to increased motility promoted by activation of integrin signaling. shGFP and shPar3 cells were plated on Matrigel-coated coverslips in the absence or presence of ErbB2 activation and the cell area was measured. The cells did not differ in their ability to adhere and spread on a Matrigel-coated surface demonstrating that loss of Par3 did not activate integrin function (Figure 4.2.B).

To test if loss of Par3 affects cell-cell interactions, we performed a cell aggregation assay. This assay was designed to assess the strength of cell-cell adhesion without the influence of cellular adhesion to the plate (Redfield, Nieman et al. 1997).Cells were suspended in drops of media hanging from the lid of a culture dish, and the ability of cells to form aggregates was monitored. Activation of ErbB2 in shGFP cells induced a modest decrease in the size of cell clumps, indicating weakened cell cohesiveness, which is consistent with previous reports showing that activation of ErbB2 can induce a decrease in E-cadherin function (D'Souza and Taylor-Papadimitriou 1994; Kim, Yong et al. 2009). Interestingly, shPar3 cells, in the absence of

ErbB2 activation, formed aggregates that were smaller than shGFP cells and activation of ErbB2 induced dispersal of all shPar3 cell clumps (Figure 4.2.C).

4.2 Loss of Par3 compromises E-cadherin junctions

Induction of cell scattering, the dispersion of compact colonies of epithelial cells, requires the dissolution of E-cadherin-mediated cell-cell adhesions and cell mobility (Nakagawa, Fukata et al. 2001). We observed that activation of ErbB2 induced scattering of shPar3, but not the control shGFP cells (Figure 4.3.A, B). Neither shGFP nor shPar3 cells scattered in the absence of ErbB2 activation. Interestingly, when we disrupted intercellular adhesion in shGFP cells by inhibition of homophilic binding between E-cadherin extracellular domains using an E-cadherin neutralizing antibody (HECD-1) (Shimoyama, Hirohashi et al. 1989), these cells displayed a cell scattering phenotype upon ErbB2 activation, reminiscent of our observation in the shPar3 cells (Figure 4.4.A). Both shGFP cells treated with HECD-1 and shPar3 cells did not scatter in the absence of ErbB2 dimerizer, suggesting that the cell mobility also requires ErbB2 activity. Consistent with these results, overexpression of mouse E-cadherin in shPar3 10A.B2 cells blocked ErbB2-induced cell scattering (Figure 4.4.B, C). This demonstrates that cell scattering in the Par3-deficient cells was a consequence of weakened E-cadherin-mediated cell adhesion. Although in Par3-depleted cells, the E-cadherin protein level and subcellular localization was unaltered, we reasoned that the functional properties of E-cadherin junctions could be compromised in the absence Par3.

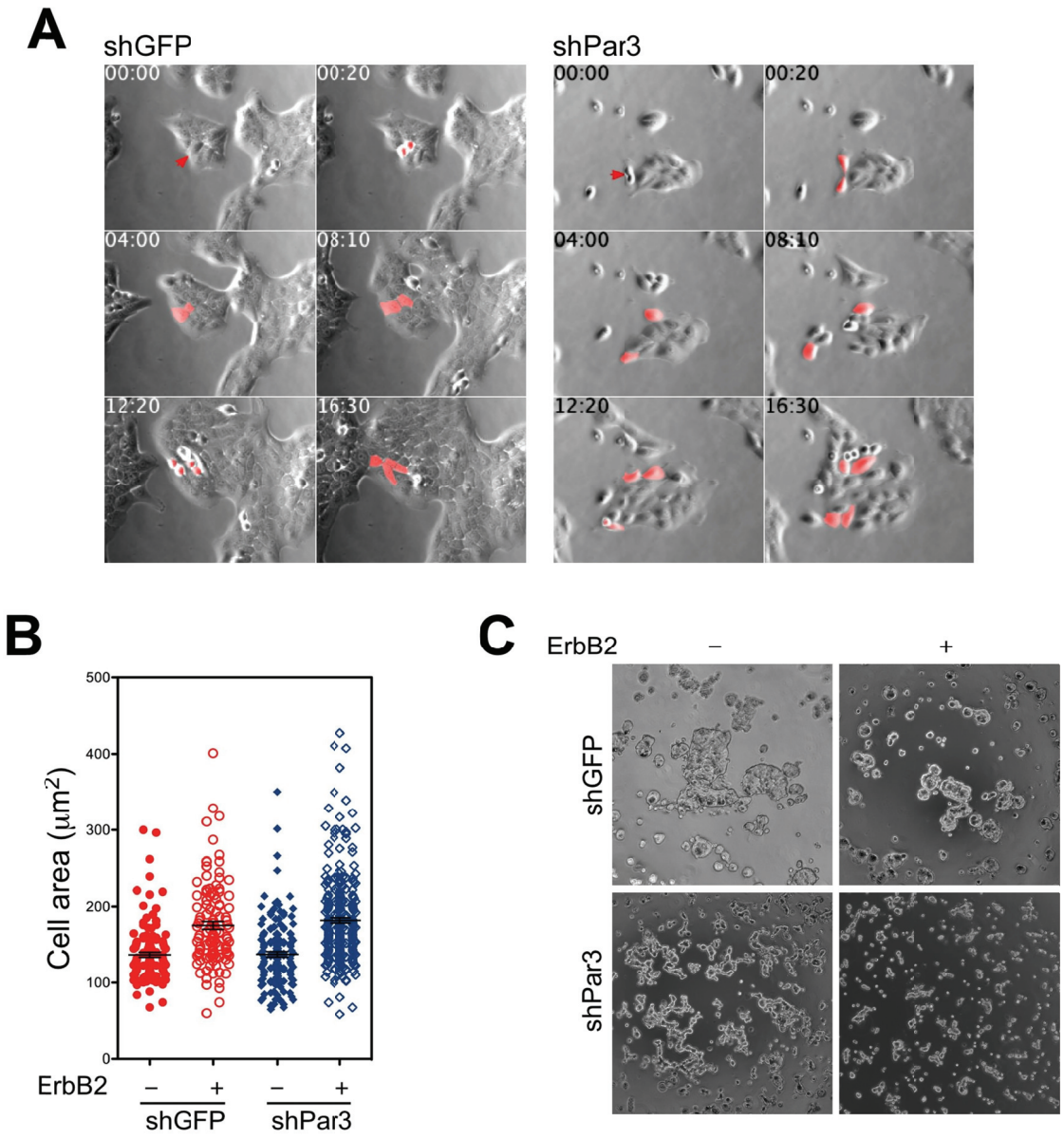

Figure 4.2. Loss of Par3 weakens cell-cell adhesions

(A) shGFP or shPar3 cells were grown on plastic dishes with ErbB2 stimulation. Images were acquired every 10 minutes for 18 hours. Still snapshots from time-lapse videos are shown. In 00:00 images, the red arrow points to a mother cell. In subsequent images, the red color tracks the progeny of the mother cell.

(B) Cell spreading assay with shGFP and shPar3 10A.B2 cells. Cells were allowed to spread on Matrigel in the presence (+) or absence (-) of dimerizer, and fixed after 1 hour. Phase contrast images were collected, and the areas of single cells were measured and presented as a scattered dot plot (Mean± SEM, >200 cells each condition).

(C) shGFP or shPar3 cells were cultured in hanging drops with (+) or without (-) ErbB2 activation, allowed to aggregate for 20 hours, and then imaged by phase contrast microscopy. Representative images from each condition are shown (n=3).

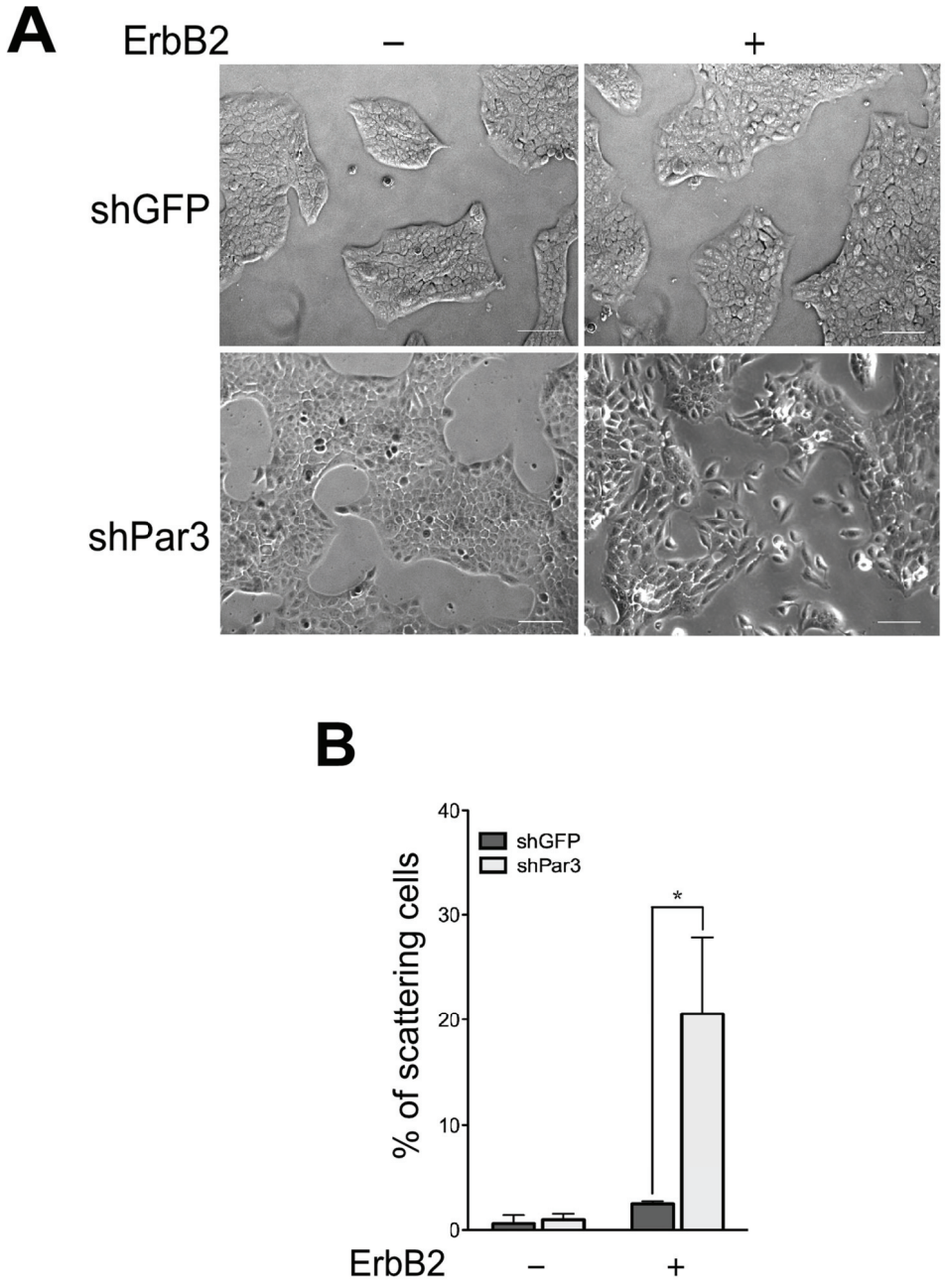

Figure 4.3. Loss Par3 cooperated with ErbB2 activation to induce cell scattering

(A) Phase contrast images of 10A.B2 shGFP or shPar3 cells growing on plastic dishes at low density, without (-) or with (+) ErbB2 stimulation for 24 hours. (Scale bar = 100μm)

(B) Quantification of cell scattering. A cell was scored as a scattered cell if it lost contact with its neighbors (n=3, mean ± SEM, >1000 cells/experiment).

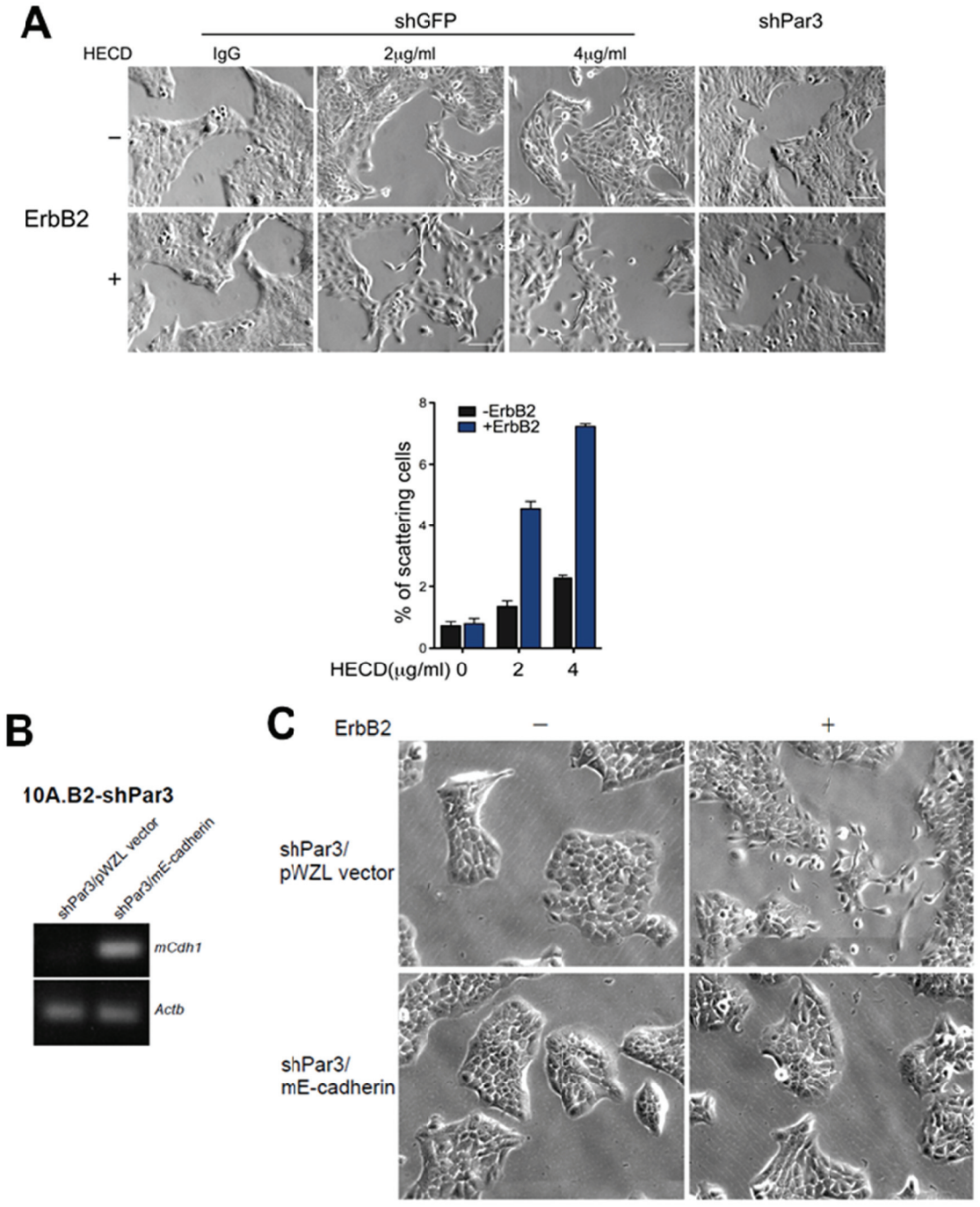

Figure 4.4. Cell scattering in Par3-deficient cells was the result of compromised E-cadherin junctions

Figure 4.4. Cell scattering in Par3-deficient cells was the result of compromised E-cadherin junctions

(A) 10A.B2 shGFP or shPar3 cells were grown on plastic dishes in the presence of a function-neutralizing antibody against E-cadherin (HECD-1) or control mIgG for 24 hours and monitored using light microscopy. The graph below represents quantification (mean±SEM) of scattered cells from three independent experiments where 400-600 cells/field were counted for each experiment.
(B) mRNA was extracted from shPar3 10A.B2 cells expressing mouse E-cadherin and analyzed for exogenous E-cadherin by RT-PCR using primers specifically against mouse *Cdh1*, but not recognizing human *CDH1*.
(C) Phase contrast images of shPar3 cells expressing control or mE-cadherin growing on plastic dishes at low density, without (-) or with (+) ErbB2 stimulation for 24 hours. (Scale bar=100μm)

4.3 Par3 is required for E-cadherin junction maturation

During the formation of E-cadherin junctions, nascent junctions are highly mobile or constantly recycle E-cadherin molecules. In contrast, mature junctions have a high fraction of immobile E-cadherin in MDCK cell monolayers (Cavey, Rauzi et al. 2008; Baum and Georgiou 2011). We tested the E-cadherin dynamics at cell-cell junctions by fluorescence recovery after photobleaching (FRAP) experiments. In these experiments, GFP conjugated E-cadherin was stably expressed in 10A.B2 cells. A small boxed region (10μm×10μm) of GFP fluorescence at the cell junction was photobleached and the recovery of E-cadherin-GFP was monitored. The kinetics of the recovery of E-cadherin can reflect the underlying dynamics. Briefly, in the FRAP fitting curve, the plateau level (a) is often lower than the pre-bleach fluorescence intensity as some of the FRAP-bleached molecules are immobile within the FRAP region. Fraction of proteins (a) that contribute to the recovery are called the 'mobile fraction' and those do not (1-a) are called the 'immobile fraction'. The index for the speed of recovery is the time it takes for the curve to reach 50% of the plateau fluorescence intensity level. Depending on the shape and area of bleaching region used in the experiment, the recovery is a combination of both E-cadherin lateral diffusion and membrane-cytoplasmic exchange (Goehring, Chowdhury et al. 2010). E-cadherin homophilic binding requires Ca^{2+}, therefore the maturation of E-cadherin junctions can be manipulated by switching cells from low calcium (immature junctions) to high calcium medium (mature junctions). We performed FRAP in the calcium-switched cells to see whether junction maturation can be monitored by FRAP. At time zero, when the junction was immature in low calcium condition, 100% of E-cadherin was recovered within five minutes after

photobleaching, demonstrating that new cell-cell junctions were composed of mobile E-cadherin molecules. Interestingly, the recovery of E-cadherin gradually decreased to only 87% and 64% at 60 min and 120 min after the cells switched to high calcium medium respectively, demonstrating that the percentage of the immobile fraction of E-cadherin increased, and mobile fraction decreased along with cell-cell junction maturation (Figure 4.5). Therefore, E-cadherin junction maturation can be quantitated using the FRAP assay.

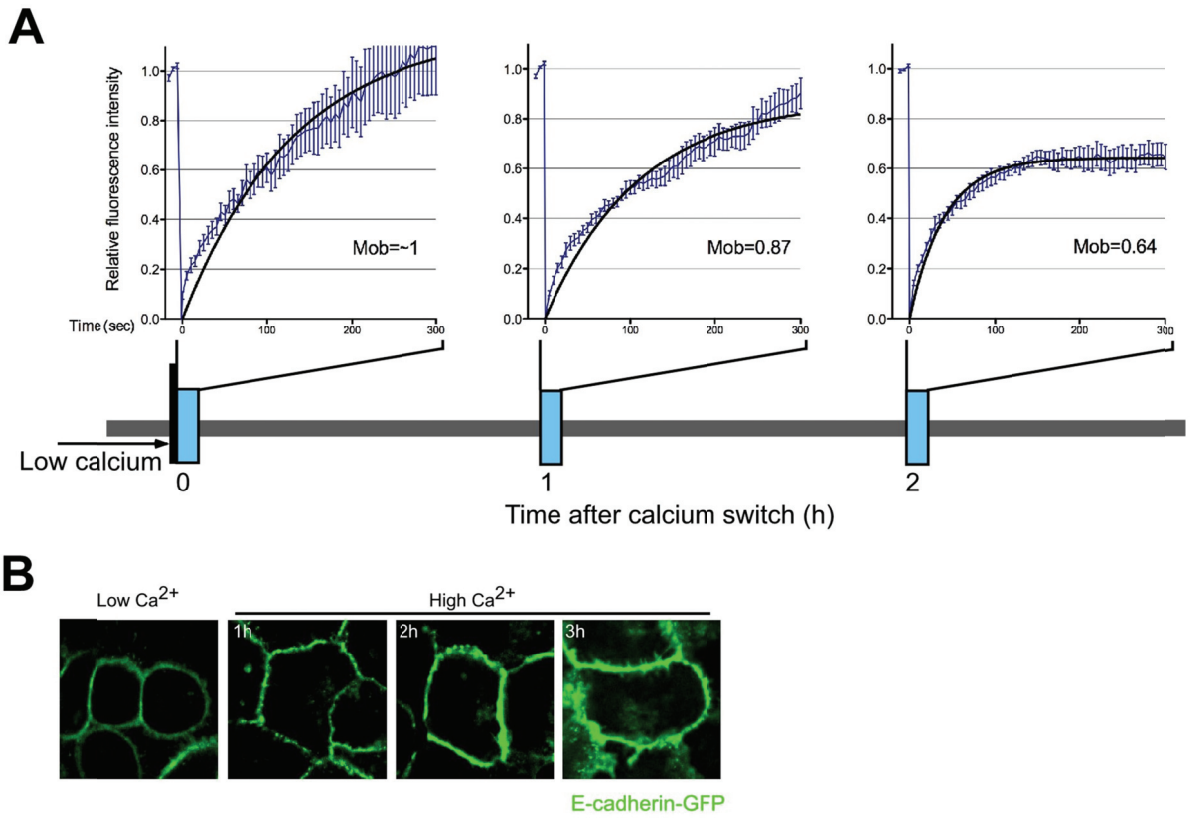

Figure 4.5. Changes in E-cadherin dynamics during junction maturation by FRAP assay

(A) FRAP analysis was performed at t=0, 60 min and 120 min after the calcium switch (n>10). The black lines indicate the best fitting curves by nonlinear regression analysis.

(B) Confluent monolayer of 10A.B2 cells expressing E-cadherin-GFP were incubated in low calcium medium for four hours and then switched to high calcium medium.

To test if loss of Par3 affects E-cadherin junction maturation in mammary epithelial cells, both control and shPar3 10A.B2 cells expressing E-cadherin-GFP were subjected to FRAP. Photobleaching analysis revealed that 50% of the GFP signal at cell-cell junctions was recovered in a confluent monolayer of control cells suggesting that 50% of E-cadherin within the junction is immobile and 50% is mobile. However, in a confluent monolayer of cells lacking Par3, 85% of the GFP signal at cell-cell junctions was recovered suggesting that only 15% of the E-cadherin junctions are immobile in cells lacking Par3 (Figure 4.6). These observations demonstrate that Par3 is required for cell-cell junction maturation. E-cadherin junctions failed to mature in mammary epithelial cells lacking Par3.

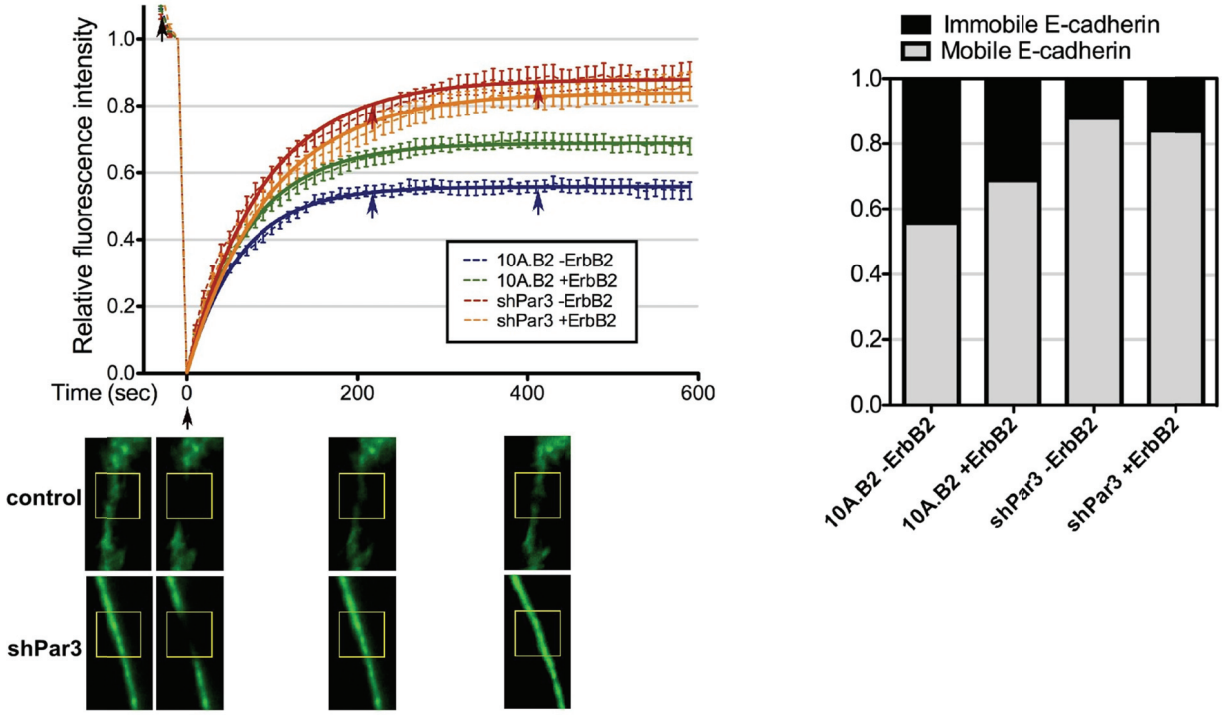

Figure 4.6. Loss of Par3 inhibits E-cadherin junction maturation

(A) FRAP was conducted in control and shPar3 10A.B2 cells expressing E-cadherin-GFP in the presence or absence of ErbB2 dimerizer (n>10). The thick lines indicate the best fitting curves of nonlinear regression analysis. Confocal sections of the cells in the absence of ErbB2 dimerizer before and after various time points after photobleaching are shown in the bottom panel. The yellow-boxed area represents the bleached areas.

(B) Quantification of immobile and mobile fractions of E-cadherin from (A).

Par3 Loss-induced Invasion Requires Rac-Mediated Alteration of Actin Cytoskeleton

Disclosure of contribution:
Kannan Krishnamurthy performed the experiments presented in for Figure5.5 C and Figure 5.13D

Introduction:

Actin microfilaments are critical components of the cytoskeletal network. Actin microfilaments (F-actin) are polarized polymers composed of globular actin (G-actin). The balance between elongation at the ATP-bound barbed end and depolymerization at the ADP-bound pointed end is called "treadmilling", which generates the pushing force. Different from microtubules, actin filaments can be nucleated and assembled into different secondary structures by a different set of actin binding proteins: the nucleator Arp2/3 complex promotes G-actin polymerization into branched F-actin; formins assemble linear F-actin, actin cross-linking proteins such as fascin and myosin combines linear filaments into thick bundles (Yang, Huang et al. 2000; Goley and Welch 2006; Kovar 2006). Both actin turnover and the secondary structure are critical for cell morphology and behavior, particularly for cell adhesion and membrane protrusion (Nurnberg, Kitzing et al. 2011).

In epithelial cells, both AJs and TJs associate with the actin cytoskeleton, which determines the maturation and strength of the junctions (Angres, Barth et al. 1996; Chu, Thomas et al. 2004). The actin-binding proteins that regulate actin assembly in turn contribute to the formation and maintenance of the junctions (Tao, Nandadasa et al. 2007). The Arp2/3 complex is an actin nucleator essential for the formation of lamellipodia and invadopodia in cancer cells (Otsubo, Iwaya et al. 2004; Lai, Szczodrak et al. 2008; Nurnberg, Kitzing et al. 2011). It has recently been shown to play an important role in both maturation and maintenance of junctions by providing the membrane stiffness and regulating junctional protein trafficking during intestinal morphogenesis in *C. elegans* (Bernadskaya, Patel et al. 2011). α-Actinin-4/focal segmental glomerulosclerosis 1 FSGS1 is required for incorporation of Arp2/3-dependent nucleation at the cell-cell juntional site and assembly of the E-cadherin-catenin complex (Tang and Brieher 2012).

The Rho-family of small GTPases, including RhoA, Rac and Cdc42 are master regulators of the actin cytoskeleton. Rho GTPases function as molecular switches to propagate the signal transduction by interacting with downstream effector molecules in their GTP-loaded "on" state. The intrinsic hydrolase activity hydrolyzes the GTP to GDP, turning the protein "off". This process is accelerated by the interaction with GAPs (GTPase activating proteins). The interaction

with guanine-nucleotide exchange factors (GEFs) facilitates the exchange of GDP to GTP (Hall 1998). Guanine-nucleotide dissociation inhibitors (GDIs) are another class of molecules that interact with Rho GTPases in the regulatory cycle. GDI binding to a Rho GTPase inhibits the dissociation ofthe guanine nucleotide and prevents activation of Rho GTPases (Spiering and Hodgson 2011) (Figure 5.1). The small GTPases each have distinct effects on the cytoskeleton and cell mobility based on *in vitro* experimental observations. Microinjection of the activated Rac1 into cells results in lamellipodial protrusions or membrane ruffles; RhoA results in the formation of stress fibers, adhesion plagues and cell contractility, and Cdc42 regulates filapodia (microspike) formation at the cell periphery (Ridley and Hall 1992; Nobes and Hall 1995). Activation of Rho GTPases needs to be tightly regulated temporally and spatially in order to generate specific and localized effects (Van Aelst and D'Souza-Schorey 1997; Kaibuchi, Kuroda et al. 1999; Gulli and Peter 2001; Jaffe and Hall 2005). To study the subcellular localization of the activity of a particular Rho GTPase, a series of biosensors based on the principle of Förster Resonance Energy Transfer (FRET) have been developed and utilized in live cells (Aoki and Matsuda 2009; Hodgson, Shen et al. 2010). Several GEFs and GAPs localize at epithelial junctions and bind to specific junctional proteins. Thus junctional proteins and small GTPases can regulate each other at junctions. For example, Rac activity is essential for E-cadherin junction formation (Braga, Machesky et al. 1997; Akhtar and Hotchin 2001). Injection of a dominant negative form of Rac (N17Rac) prevented E-cadherin stabilization at cell-cell contacts (Braga, Machesky et al. 1997). Conversely, constitutive activation of Rac induces disruption of E-cadherin junctions by promoting aberrant actin remodeling, suggesting that tight regulation of Rac activity is necessary (Chu, Thomas et al. 2004; Kraemer, Goodwin et al. 2007).

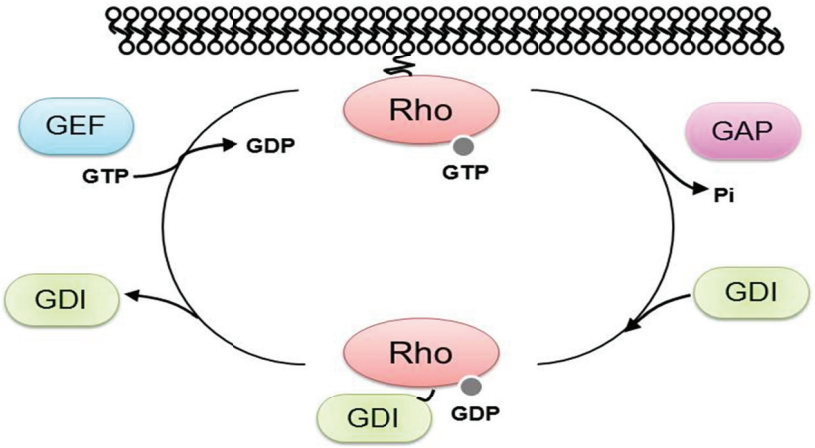

Figure 5.1. Rho family GTPases and their regulators

The temporal and spatial regulation of GTPase activity is an important element in the control of Rho GTPase signaling. The regulation takes place at three levels: GDP–GTP exchange, GTP hydrolysis and inhibition of GDP dissociation. The activation of Rho GTPases involves the exchange of GDP for GTP, which is stimulated by guanine nucleotide-exchange factors (GEFs). GEFs have various domains and determine Rho GTPase downstream signaling through binding and scaffolding of different effector molecules. The low intrinsic GTP hydrolysis activity of Rho GTPases is enhanced by the binding of GTPase-activating proteins (GAPs), resulting in an inactive GDP-bound GTPase and the shutdown of signaling. As with GEFs, most GAPs are multidomain proteins that can assemble multiprotein complexes. The release of GDP from the GTPase is blocked by guanine nucleotide-dissociation inhibitors (GDIs). GDIs also prevent membrane translocation of Rho GTPases by masking their C-terminal motifs, which are required for the interaction of Rho GTPases with anchoring phospholipids in the plasma membrane. Therefore, GDI-bound Rho GTPases are sequestered in the cytosol.

Polarity proteins have been shown to crosstalk with small GTPases to regulate cell polarization and junction formation (Feigin and Muthuswamy 2009). The direct binding between Par3 and Tiam1, a Rac-GEF is essential for tight junction assembly. TJs were disrupted and Rac1 activity was constitutively activated in the cells lacking Par3. The tight junctions could be rescued by dominant negative Rac1 or knockdown of Tiam1 (Chen and Macara 2005). In AJs,

Cdc42, Par6 and aPKC are required for junction stability via regulating WASP and Arp2/3-mediated endocytosis (Georgiou, Marinari et al. 2008). In migrating cells, the segregation of Cdc42 and Rac at the leading edge from RhoA in the back leads to different cytoskeleton structures. Cdc42 and Rac1 primarily promote branched actin nucleation, to induce protrusion formation, whereas RhoA activates ROCK to induce actomyosin contraction and tail formation (Heasman and Ridley 2008; Iden and Collard 2008). When cells attach to the ECM, focal adhesions provide the main sites for cell adhesion to the ECM, and associate with actin stress fibers to control cell movement. Assembly of stress fibers and focal adhesions are under the influence of RhoA-mediated downstream effectors such as mDia1/2 and ROCK. Par3 also is found to interact with focal adhesion kinase (FAK) in proteomic analysis and depletion of Par3 inhibits adhesion-induced activation of FAK in HeLa cells, suggesting Par3 functions to link focal adhesions, actin reorganization and cell migration (Itoh, Nakayama et al. 2010).

In this chapter, I explore the molecular mechanism utilized by Par3 to regulate the cell-cell junction maturation, and demonstrate that forced downregulation of Par3 activates a Tiam1/Rac/IRSp53/WAVE2 pathway that promotes aberrant actin remodeling at cell-cell junctions, blocks E-cadherin junction maturation and inhibits cell-cell cohesion.

Results:

5.1 Loss of Par3 induces aberrant activation of Rac

To investigate the molecular mechanism by which Par3 regulates E-cadherin junction maturation and epithelial cell behavior, first we tested if loss of Par3 changes Rac-GEF activity. Tiam1 is the only GEF identified that specifically activates Rac *in vitro* as well as *in vivo* (Michiels, Habets et al. 1995). Activation of Tiam1 requires its translocation from the cytoplasm to the plasma membrane. Its activity is regulated by different mechanisms including relief of intra-molecular inhibition, phosphorylation, and interaction with other proteins such as Par3. An active Rac-GEF assay kit, obtained from Cell Biolabs, Inc., was used to evaluate Rac activity. GEFs function by binding to a nucleotide-bound GTPase, which causes the bound nucleotide to be released, thus resulting in a nucleotide-free GEF-GTPase. This nucleotide free complex will then take up a new nucleotide after which the GEF is released from the GTPase. Because GEFs typically have a higher affinity for GDP-bound GTPases than for the corresponding GTP-bound GTPases and the ratio of GTP to GDP in cytoplasm is about 10:1, GEFs will drive the exchange from GDP-bound to GTP-bound GTPases. Based on this, the active Rac-GEF assay was designed to utilize Rac1 G15A, a nucleotide-free Rac1 mutant with high affinity for active Tiam1 (Arthur, Ellerbroek et al. 2002; Garcia-Mata, Wennerberg et al. 2006), and is conjugated to agarose beads to selectively isolate and pull-down the active form of Rac-GEF from cell lysates, namely lysates of 10A.B2 cells expressing shGFP or shPar3 grown in low growth factor media herein. Subsequently, the precipitated active Tiam1 was detected by western blot analysis. We was found that cells lacking Par3 had a dramatic increase in the basal levels of active Tiam1 in the absence of ErbB2 dimerizer (Figure 5.2.A).

We further tested whether the downstream substrate Tiam1 was affected by loss of Par3. Pulldown assays using Cdc42/Rac interactive binding (CRIB) region of p21-activated kinase (PAK) binding domain (PAK-PBD), a Rac effector protein that binds specifically to the GFP-bound form of Rac, was performed to analyze the level of active Rac (Knaus, Bamberg et al. 2007). In shPar3 cells, the Rac-GTP levels were high under unstimulated conditions compared to the levels present in shGFP cells (Figure 5.2.B). Activation of ErbB2 induced a four-fold increase in Rac-GTP levels in shGFP cells within 30 minutes, but not in shPar3 cells (Figure

5.2.C). Another small GTPase, Ras and its downstream MAPK signaling cascade, which is important for cell proliferation and invasion, was not affected by loss of Par3 on either basal level or upon ErbB2 activation, as determined by phosphorylation of Erk1/2 (Figure 5.2.C). This demonstrates that loss of Par3 shows specificity towards regulation of Rac signaling. Thus, loss of Par3 resulted in an increase in the levels of active Tiam1 and Rac-GTP.

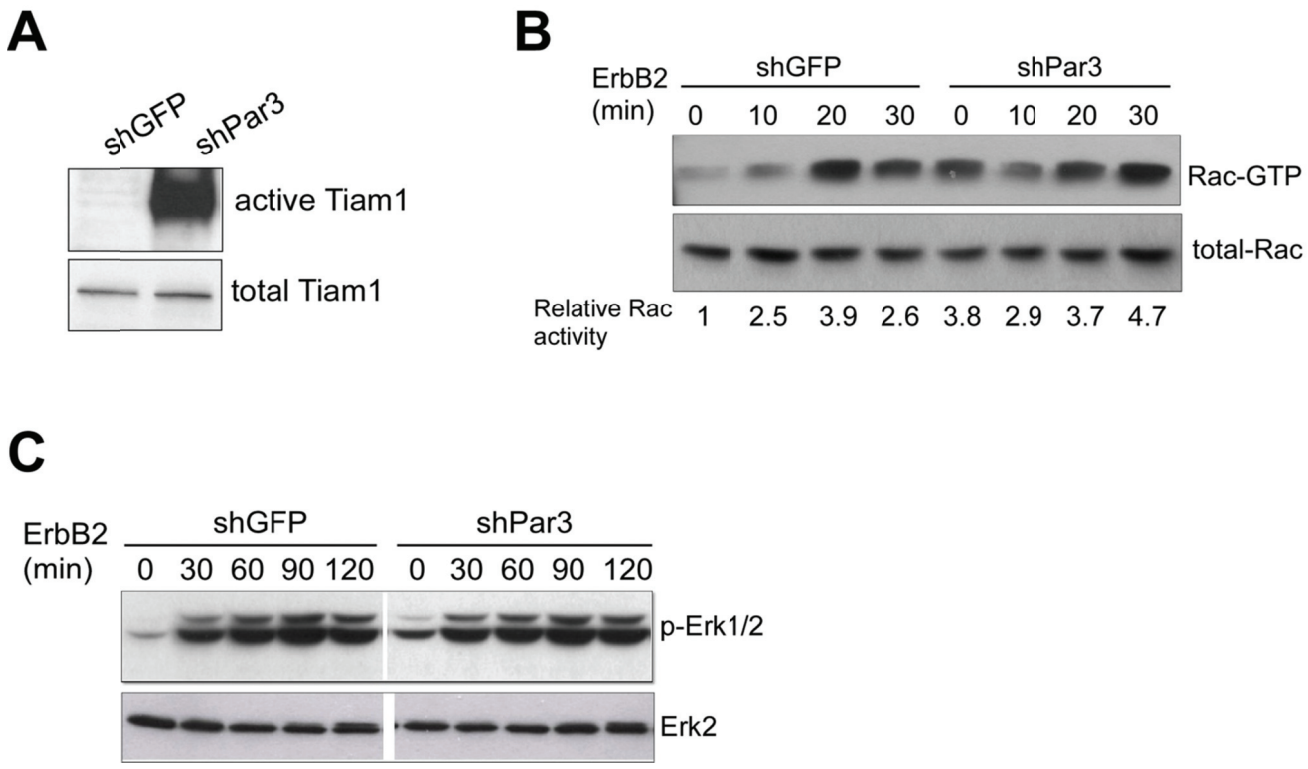

Figure 5.2. Loss of Par3 induces aberrant activation of Rac

(A) Cell lysates from shGFP or shPar3 10A.B2 cell were subjected to Tiam1 Rac-GEF activity assay. The level of active Tiam1 pulled down by Rac1 G15A agarose beads (upper panel) and total Tiam1 (lower panel) were monitored by immunoblotting with anti-Tiam1 antibody.

(B) Cell lysates, from confluent monolayers stimulated with ErbB2 dimerizer for indicated times, were incubated with GST-PAK1 agarose beads and bound active Rac (Rac-GTP) was monitored by immunoblotting with anti-Rac antibody. Total Rac levels were monitored using one tenth of the input lysate. Quantification of relative levels of Rac-GTP is shown below the blot, an average of three experiments.

(C) Cell lysates from confluent monolayers stimulated with ErbB2 for indicated times were analyzed for phosphorylated Erk1/2 (p-Erk1/2) and total Erk2 levels by immunoblot analysis.

To determine if loss of Par3 changes the spatial and temporal regulation of Rac activation in shPar3 cells, we monitored Rac activation by FRET assay using the biosensor Raichu-Rac. Raichu-Rac consists of Rac fused to CFP and the CRIB domain of PAK fused to YFP. GTP binding to Rac results in an interaction between the CRIB domain of PAK and Rac-GTP, which induces FRET emission from CFP to YFP (Itoh, Kurokawa et al. 2002) (Figure 5.3.A). The localization of Raichu-Rac fusion as monitored by CFP channel images is different from endogenous Rac and is related to local GEF activity (Itoh, Kurokawa et al. 2002). The FRET assays were conducted in confluent cell monolayers enabling the study of Rac activity at the cell junctions. In shGFP cells, Raichu-Rac was mainly localized to cell-cell junctions, whereas in shPar3 cells it showed an increase in diffuse distribution in the cytosol (Figure 5.3.B, leftmost panel). The time-lapse FRET/CFP ratio images show that ErbB2 activation induced Rac-GTP loading at cell-cell junctions in shGFP cells, which returned to basal levels by 15 minutes, whereas Rac-GTP levels were elevated diffusely throughout the cytosol in shPar3 cells and remained high at 15 minutes (Figure 5.3.B, right). These observations demonstrate that Par3 plays an important role in spatial and temporal regulation of Rac activation in mammary epithelial cells.

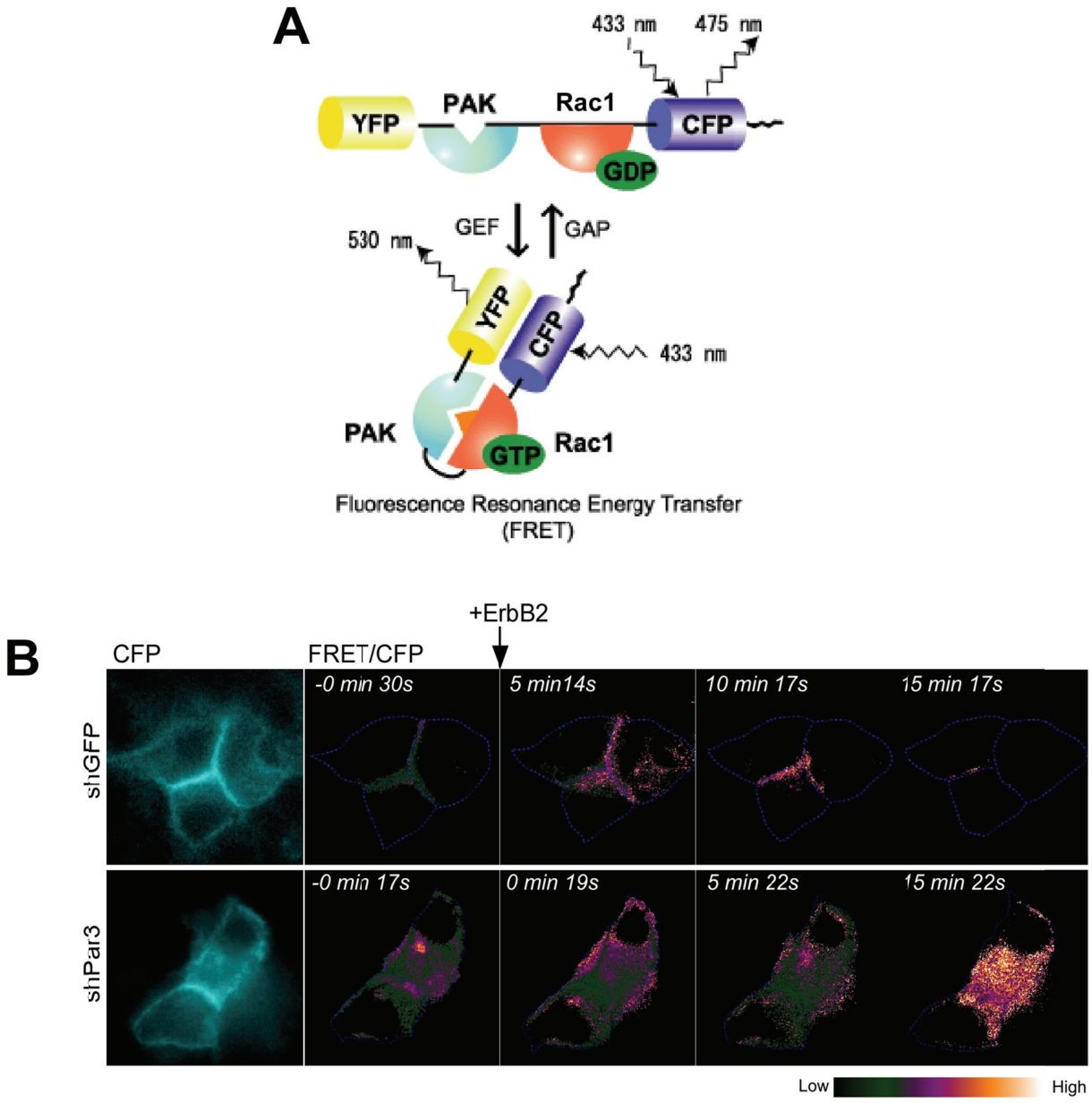

Figure 5.3. Subcellular localization of Rac activity

(A) Molecular diagram of the Raichu-Rac biosensor. Raichu-Rac has Rac as the sensor region and Pak as the ligand region. Upon GTP binding, the effector region of Rac binds to Pak, which increases FRET from CFP to YFP.

(B) Confluent 10A.B2 cells expressing Raichu-Rac were treated with ErbB2 dimerizer. CFP and FRET images were obtained before stimulation and at indicated times after stimulation. Representative FRET/CFP ratio images after background subtraction are shown. LUT colors from green to orange are used to represent the ratio, and all the images were analyzed using the same ratio range. The blue dotted lines outline the cells. The CFP images are shown on the left. Experiments were performed on at least three cells for each condition, and similar results were obtained.

5.2 Tiam1-mediated Rac activation is required for the Par3-loss induced phenotype

Next we investigated the importance of increased Tiam1/Rac signaling during invasion of shPar3 cells. A dominant-negative Tiam1 (Stam, Sander et al. 1997) or NSC23766, a pharmalogical Rac inhibitor were used to interfere with Tiam1-mediated activation of Rac. Tiam1 protein consists of 1591 amino acids and contains a Dbl homology (DH) domain followed by a pleckstrin homology (PHc) catalytic domain unit for guanine nucleotide exchanging. Tiam1-PHn-CC-Ex (393-853), a mutant of Tiam1 was used as a dominant negative Tiam1, contains an N-terminal pleckstrin homology (PHn) domain, the proximal coiled coil (CC) region, and adjacent Ex domain which is required for translocation of Tiam1 to the plasma membrane, but lacks of catalytic domains (Michiels, Stam et al. 1997; Stam, Sander et al. 1997) (Figure 5.4.A). Despite its correct localization at the plasma membrane, Tiam1-PHn-CC-Ex can interfere with endogenous Tiam1 function and inhibit Tiam1-induced cell membrane ruffling (Stam, Sander et al. 1997). We stably expressed Tiam1-PHn-CC-Ex in 10A.B2 cells. The ability of ErbB2-activated shPar3 cells to invade through Matrigel in transwell invasion assays was significantly decreased (Figure 5.4.B), and the percentage of abnormal rough acini was diminished (Figure 5.4.C).

To apply the Rac inhibitor in 10A.B2 cells, we first titrated NSC23766, a Rac inhibitor identified by a structure-based virtual screen which effectively inhibits activated Rac1 by GEF Trio or Tiam1, to the concentration (25μM) which is sufficient to decrease the high basal level of Rac-GTP observed in shPar3 cells without affecting ErbB2-induced Rac1 activation by other Rac-GEFs (Figure 5.5.A). At this concentration, NSC23766 inhibited ErbB2-induced cell invasion and cell scattering in shPar3 cells (Figure 5.5.B, C). These results demonstrate that activation of Tiam1 and the aberrant increase in Rac-GTP levels are required for the invasive behavior of shPar3 epithelial cells. To determine if the increase in basal Rac-GTP levels in shPar3 cells contributes to the incapability of E-cadherin junction maturation in shPar3 cells, FRAP analysis was performed in shPar3/E-cadherin-GFP cells treated with NSC23766. While treatment of the parental 10A.B2 cells with NSC23766 did not change the percentage of immobile fraction of E-cadherin, treatment of shPar3 cells induced a more than two fold increase in the immobile E-cadherin fraction (Figure 5.5.D), demonstrating that shPar3-induced blockade of E-cadherin junction maturation was mediated by the aberrant activation of Rac.

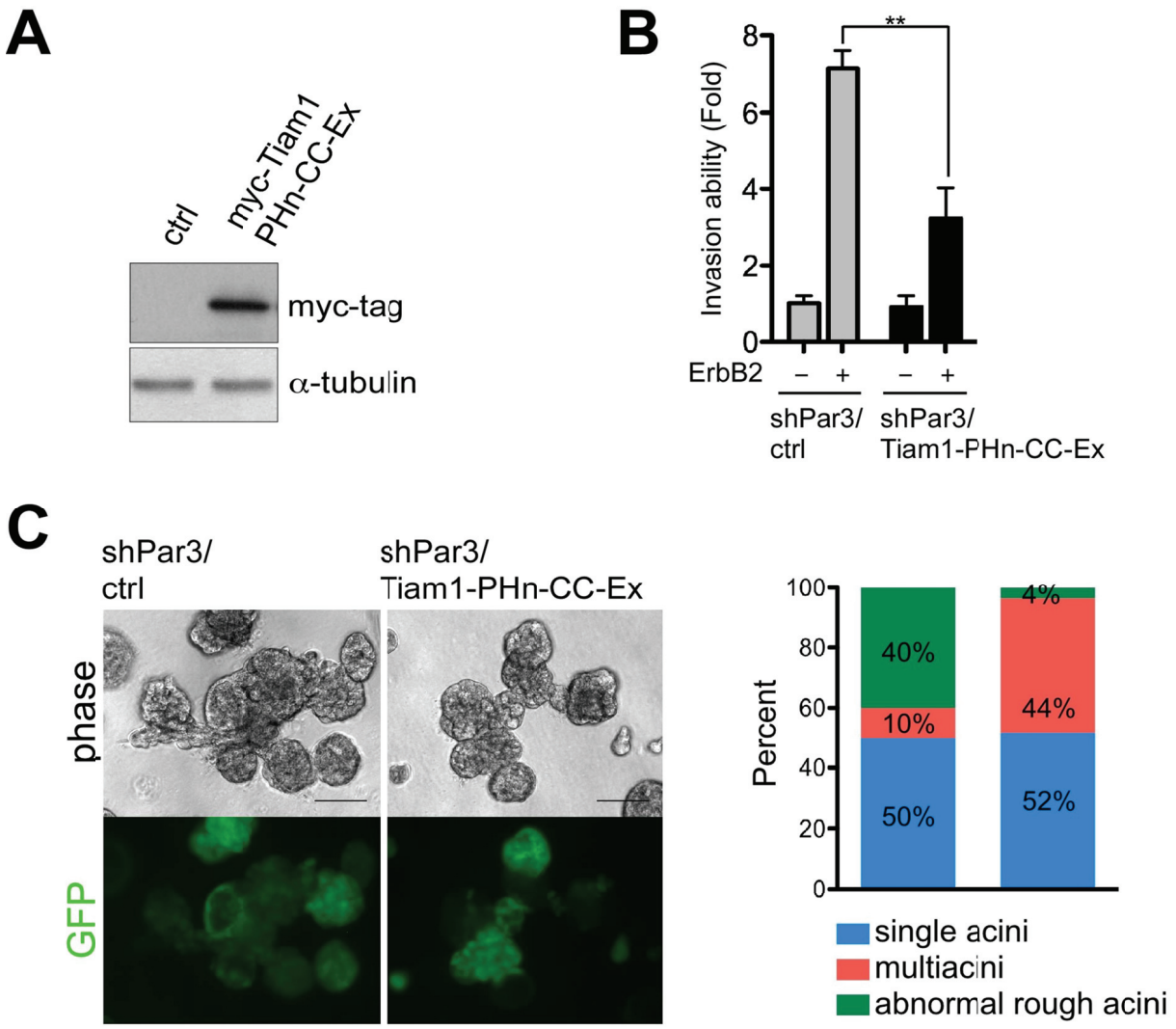

Figure 5.4. Tiam1-mediated Rac activation is required for Par3-deficient phenotype

(A) Cell lysates from 10A.B2 overexpressing control vector or myc-Tiam1-PHn-CC-Ex analyzed by immunoblot analysis for myc-tag expression (upper panel), using anti-α-tubulin as loading control.

(B) 10A.B2 shPar3 cells expressing control or Tiam1-PHn-CC-Ex vector were subjected to transwell invasion assays, with or without ErbB2 stimulation for 48 hours. Invaded cells were quantified from three independent experiments and results are presented as fold change in invasion compared to shPar3/ctrl cells without ErbB2 stimulation. (**, represents $p<0.01$).

(C) 10A.B2 Tiam1-PHn-CC-Ex cells were grown in 3D for 12 days with ErbB2 stimulation for the last four days and imaged by phase contrast and fluorescence microscopy (Scale bar=100μm). Right: Percentage of single acini, multiacini and abnormal rough acini were determined by scoring >100 for each condition.

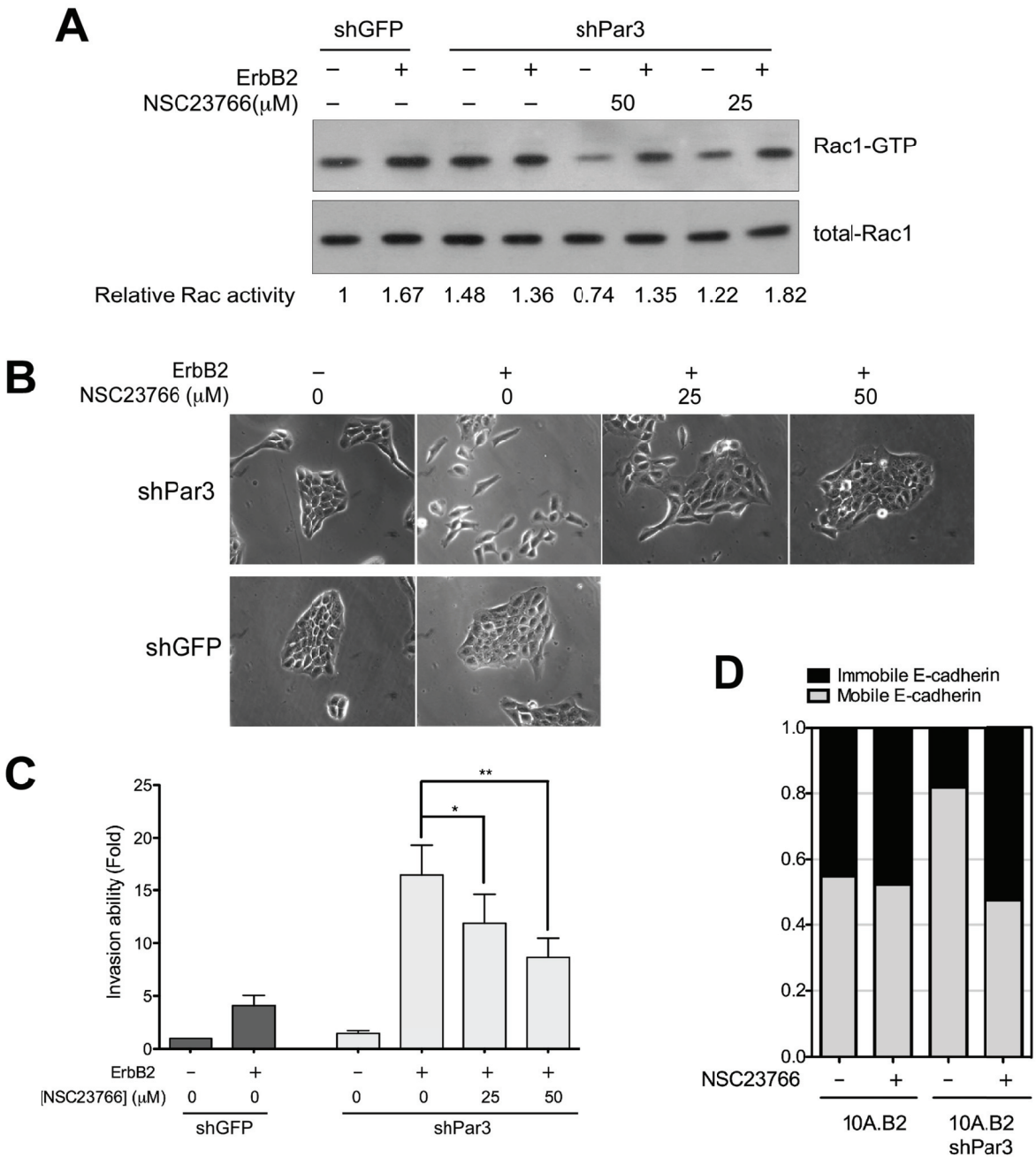

Figure 5.5. Par3-loss phenotype is mediated by aberrant Rac activity

Figure 5.5. Par3-loss phenotype is mediated by aberrant Rac activity

(A) Cell lysates from cells stimulated with ErbB2 dimerizer for 15 minutes in the absence (-) or presence (+) of different concentrations of NSC23766 (25μM and 50μM) were subjected to Rac activity assay. Quantification of relative levels of active Rac is shown below.

(B) 10A.B2 shPar3 or shGFP cells were plated in plastic dishes at low density under the indicated conditions. The cell morphology was monitored using light microscopy.

(C) 10A.B2 cells (shGFP and shPar3) were seeded for transwell invasion assays, with or without activation of ErbB2 and incubated for 48 hours. The Rac inhibitor, NSC23766, was added at the indicated concentrations at the same time as ErbB2 activation. Invaded cells were quantified from five independent experiments and results are presented as fold change in invasion compared to shGFP cells in without ErbB2 stimulation. (n=5; * represents $p<0.05$; ** represents $p<0.01$)

(D) FRAP analysis was conducted on the E-cadherin-GFP control or shPar3 10A.B2 cells in the absence or presence of 50μM NSC23766 compound (n>10). The E-cadherin immobile and mobile fractions were calculated and plotted.

5.3 ErbB2 regulates the Par3-Tiam1 complex

To understand whether the association of Par3 with Tiam1 is regulated by ErbB2, we investigated if activation of ErbB2 affects the Par3-Tiam1 interaction. As there are no good antibodies against endogenous Tiam1 suitable for immunoprecipitation, we used myc-tagged Tiam1-C1199, an N-terminal PEST sequence-truncated Tiam1 that does not produce the growth inhibitory effects observed upon expression of full length Tiam1 and allows for selection of stably expressing cells (Minard, Kim et al. 2004). Tiam1-C1199 associated with endogenous Par3 in 10A.B2 cells in the absence of ErbB2 dimerizer (Figure 5.6, the second lane from left). Activation of ErbB2 induced a 50% decrease in Par3-Tiam1 interaction at 45 minutes, demonstrating that regulation of Par3-Tiam1 interaction is a downstream target of ErbB2 activation (Figure 5.6). This Par3-Tiam1 transient dissociation is probably involved in cell junction remodeling upon ErbB2 stimulation.

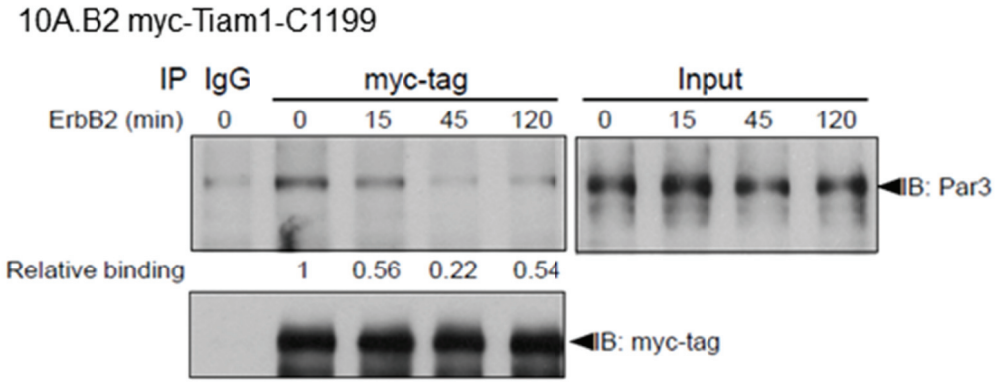

Figure 5.6. ErbB2 regulates Par3 -Tiam1 complex association

Extracts from 10A.B2 cells overexpressing myc-Tiam1 C1199 before and after ErbB2 activation for the indicated times were immunoprecipitated (IP) with control mouse IgG or anti-myc-tag antibody and immunoblotted (IB) with indicated antibodies. One tenth of the lysates were used for monitoring the level of Par3 in the input, by immunoblot as shown on the right panel.

5.4 Loss of Par3 disrupts cortical actin in epithelial cells.

Since Rac activity is known to regulate actin dynamics (Braga 2000; Yamada and Nelson 2007; Yamazaki, Oikawa et al. 2007), we investigated whether the actin cytoskeleton is affected by Par3 loss. To image the actin cytoskeleton structure, fixed cells were labeled with Alexa Fluor 488-conjugated phalloidin, a toxin from the *Amanita phallloides* mushroom that specifically binds to F-actin. F-actin was organized at cell-cell junctions to form a compact cortical actin belt in a confluent layer of shGFP epithelial cells, whereas it was loosely organized around the cellular periphery of shPar3 cells (Figure 5.7.A, left). ErbB2 activation induced a modest loosening of the cortical actin in shGFP cells and a severe disruption of cortical actin in shPar3 cells (Figure 5.7.A, right). Loss of Par3 in a normal mouse mammary cell line, Eph4, and a human cancer-derived cell line, T47D, induced detectable changes in cortical actin (Figure 5.7.B,C) demonstrating that the shPar3-induced changes in cortical actin are not specific for MCF10A cells. To determine if the relationship between Par3 loss and changes in cortical actin organization can be observed *in vivo*, we analyzed actin organization in mouse mammary tumors from the transplantation experiment described in Chapter 3. As phalloidin labeling did not give clear signals in IHC, an antibody against β-actin was used in IHC staining. Tumors generated from control vector-infected NDL tumor cells had well-organized cortical actin, whereas tumors generated from mouse shPar3-expressing cells showed loose cortical actin (Figure 5.7.D). In addition, the tumor epithelia in the spontaneous lung metastasis of MMTV-NDL mice had a dramatic disruption of cortical actin organization compared to that observed in cells within primary tumors from the same mice (Figure 5.7.E). These observations demonstrate that loss of Par3 relates to disruption of cortical actin in epithelial cells in culture and *in vivo*, which might contribute to the weakening of E-cadherin junctions.

In addition, the disruption of cortical actin organization in shPar3 cells can be partially restored by inhibition of Rac activation using NSC23766, suggesting that the aberrant Rac activation contributes to the observed Par3 loss-induced actin organization defects (Figure 5.8).

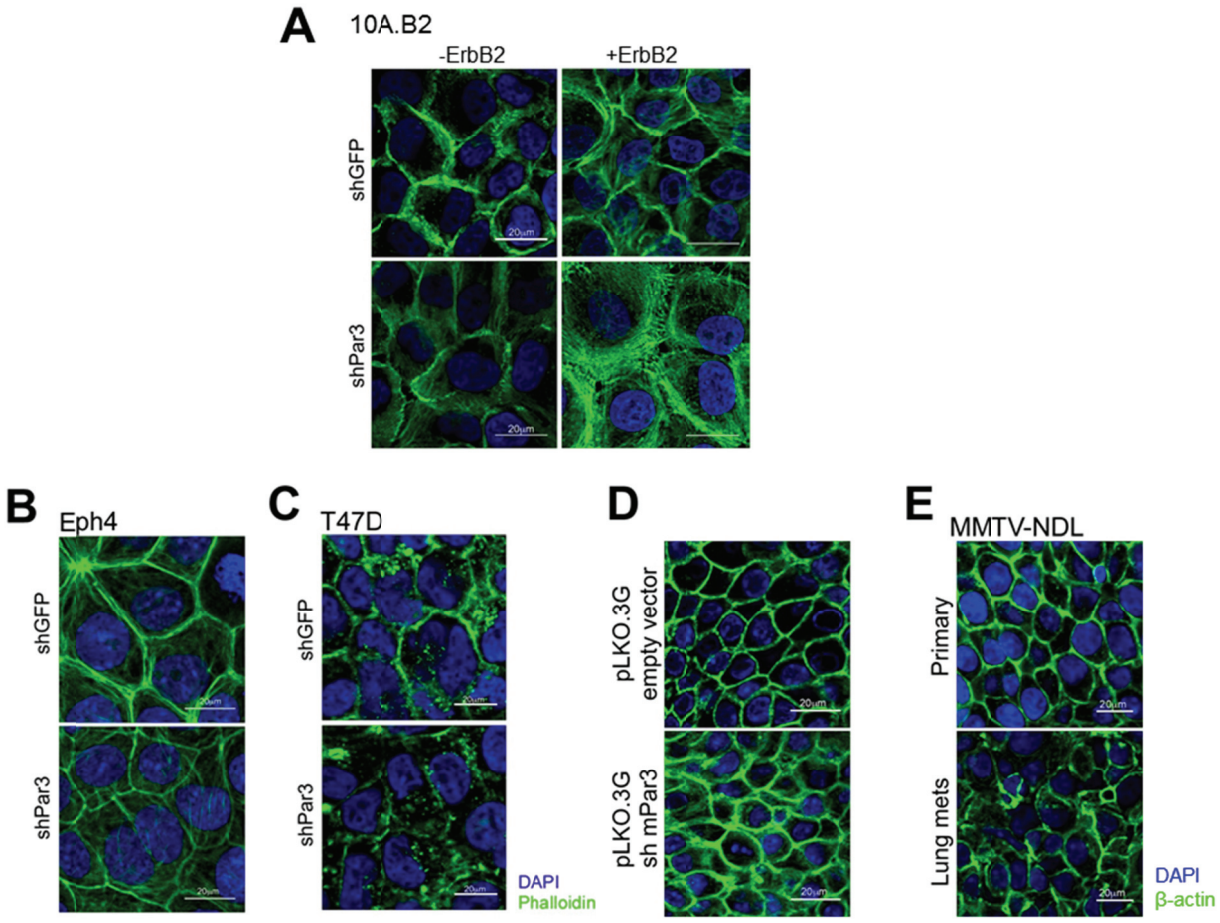

Figure 5.7. Loss of Par3 disrupts cortical actin in epithelial cells in culture and *in vivo*

Confluent monolayers of **(A)** 10A.B2, **(B)** Eph4 or **(C)** T47D cells expressing shGFP or shPar3 were labeled with Alexa Fluor 488-conjugated phalloidin for F-actin (green) and nuclei (DAPI, blue) (Scale bar=20μm). **(D)** Tissue sections of tumors generated using MMTV-NDL tumor cells infected with vector or mPar3 shRNA lentivirus, or **(E)** tissue sections from a primary tumor and paired lung metastasis from MMTV-NDL mice were immunostained for actin cytoskeleton (β-actin, green) (scale bar=20μm).

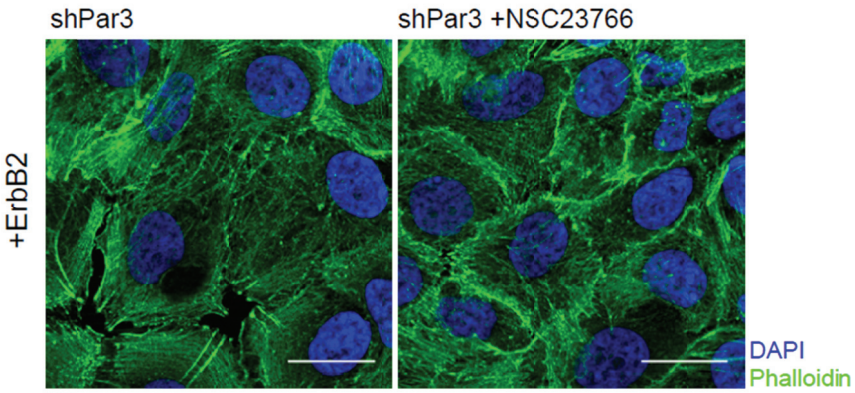

Figure 5.8. Rac inhibitor partially rescues the disorganization of cortical actin in shPar3 cells

shPar3 cells were untreated or treated with NSC23766 (50μM) for 24 hours in the presence of ErbB2 dimerizer.The cells were labeled with Alexa Fluor 488-conjugated phalloidin for F-actin (green) and nuclei (DAPI, blue) (Scale bar=20μm).

5.5 Loss of Par3 promotes actin dynamics at cell-cell junctions

To understand how loss of Par3 affects actin structure and E-cadherin junctions, we decided to study the dynamic interaction of actin and E-cadherin by visualizing these molecules. We established control or shPar3 cells stably coexpressing E-cadherin-GFP and red fluorescent protein TagRFP fused to Lifeact, a 17-amino acid peptide that specifically labels F-actin in live cells. As the peptide is derived from *Saccharomyces cerevisiae* and has no homologs in mammalian, therefore it does not interfere with actin dynamics *in vitro* and *in vivo* (Riedl, Crevenna et al. 2008). For successful live cell imaging, cells were grown in glass bottom plates until confluent and changed to assay medium for at least 18 hours to minimize the movement stimulated by cell growth factors. A high speed spinning disk microscope was employed to capture the movements of fluorescence-labeled E-cadherin and F-actin molecules in the middle section (1.5μm above bottom) of the cell junctions at 10 frames per minute. We found that in the control cells, E-cadherin (green) colocalized with F-actin (red) to form a continuous, smooth junctional structure of even thickness. During the 10 minutes of time-lapse imaging, we did not observe any noticeable change in the overall organization of F-actin or E-cadherin suggesting that the junctions were of relatively stable thickness (Figure 5.9.A). However, in shPar3 cells F-

actin organization was complex with a cortical belt and additional thin actin filaments adjacent to the cortical belt, similar to the structures reported in immature cell-cell contacts (Zhang, Betson et al. 2005). During the 10 minutes of time-lapse imaging, E-cadherin moved concomitantly with F-actin at cell-cell junctions of shPar3 cells in a highly dynamic pattern with oscillating protrusions and retractions (Figure 5.9.A, lower box) . Kymograph analysis of Lifeact-TagRFP from representative regions in control and shPar3 cells revealed that the average speed of actin protrusions at cell-cell junctions in shPar3 cells was 4-5 fold higher compared to that observed in control cells (Figure 5.9.B, C). These observations provide direct evidence that loss of Par3 promotes dynamic remodeling of F-actin and E-cadherin at cell-cell junctions. Loss of Par3 mislocalizes the actin nucleator Arp2/3 complex

In mammalian cells, the Arp2/3 complex attaches the sides and pointed ends of existing actin filaments at a fixed angle of 70º and organizes actin filaments into a branched network (Mullins, Heuser et al. 1998; Volkmann, Amann et al. 2001). Actin nucleation by the Arp2/3 complex is essential for formation of lamellipodia and invadopodia in cancer cells (Otsubo, Iwaya et al. 2004; Lai, Szczodrak et al. 2008; Nurnberg, Kitzing et al. 2011). The Arp2/3 complex consists of seven protein subunits, including Arp2, Arp3, ARPC1B/p41-ARC, ARPC2/p34-ARC, ARPC3/p21-ARC, ARPC4/p20-ARC and ARPC5/p16-ARC. We immunostained for the ARPC2 subunit to represent the subcellular localization of the Arp2/3 complex as the ARPC2 antibody gave the best staining signal (Welch, DePace et al. 1997). In the mouse mammary epithelial Eph4 cells, Par3 loss induces a breakage of ARPC2 staining at cell-cell junctions (Figure 5.10). Immunohistochemistry (IHC) analysis of mouse tissues yielded reproducible signals. In normal mammary glands from FVB mice, ARPC2 was localized at cell-cell junctions and along the apical actin ring (Figure 5.11.A). Interestingly, tumors (n=2) derived from control vector-infected MMTV-NDL tumor cells had ARPC2 at cell-cell junctions, whereas tumors (n=2) derived from shPar3 cells displayed diffuse cytosolic ARPC2 distribution in all cells analyzed (Figure 5.11.B). We also investigated if changes in ARPC2 were selected for during spontaneous lung metastasis observed in the MMTV-NDL mammary tumors. ARPC2 was localized to cell-cell junctions in the primary tumors of MMTV-NDL mice, while the spontaneous lung metastasis (n=2) had mislocalization of ARPC2 from cell-cell junctions in all cells analyzed (Figure 5.11.B). Interestingly, endogenous ARPC2 and Par3 co-

immunoprecipitated with each other. ARPC2 co-immunoprecipitated E-cadherin and Par3 in 10A.B2 cells (Figure 5.12). Thus, our results demonstrate that Par3 is required for localizing the Arp2/3 actin nucleator complex to cell-cell junctions.

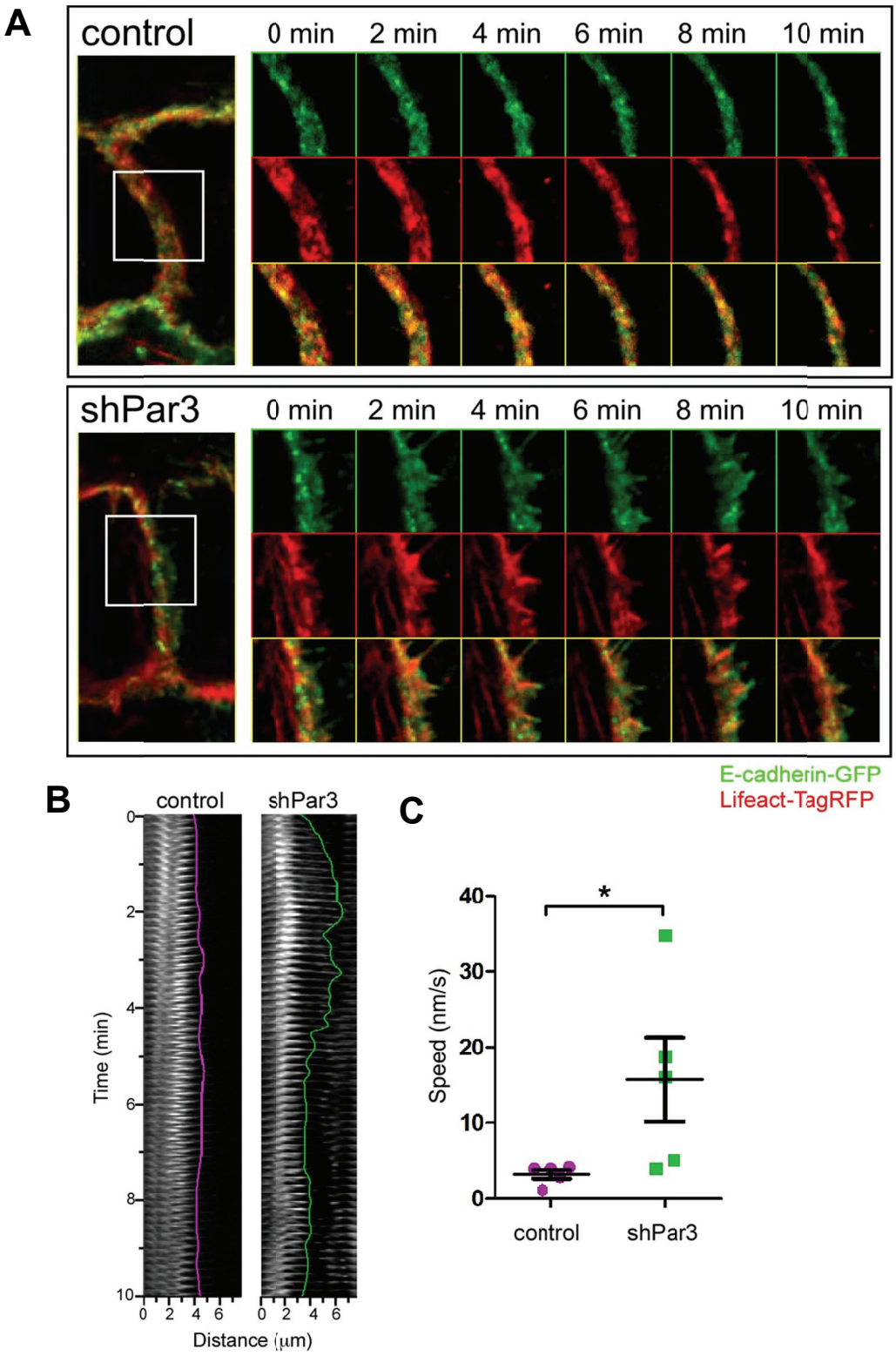

Figure 5.9. Loss of Par3 induces changes in actin and E-cadherin dynamics at cell-cell junctions

Figure 5.9. Loss of Par3 induces changes in actin and E-cadherin dynamics at cell-cell junctions

(A) Confluent monolayers of control and shPar3 10A.B2 cells stably co-expressing E-cadherin-GFP and TagRFP-Lifeact were imaged every 5 seconds for 10 minutes. Representative images of cell-cell junctions are shown (left panels). The right panels show time-lapse montages at 2 minute intervals of an area delineated by a white box in the cell-cell junction images in the left panel.

(B) Kymograph of a representative region of TagRFP-Lifeact at the cell-cell junctions in control cells (top) or shPar3 cells (bottom).

(C) The mean speed of five protrusions was measured from kymographs and shown in the graph. *, $P<0.05$.

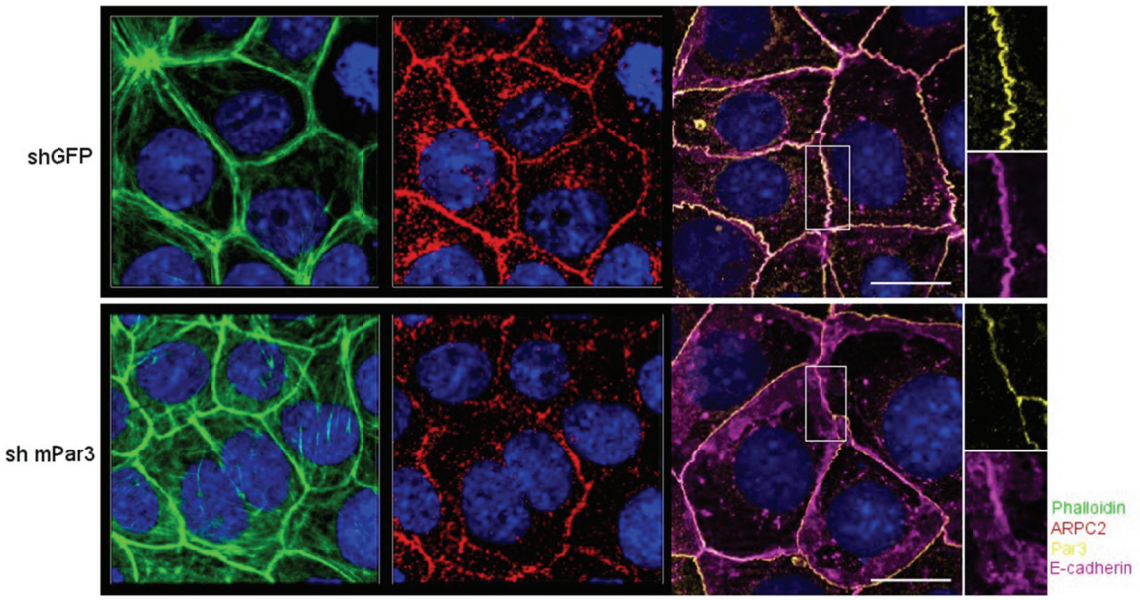

Figure 5.10. Loss of Par3 mislocalizes the junctional ARPC2 in Eph4 cells

Confluent monolayers of mouse mammary epithelial cell, Eph4 expressing shGFP or shmPar3 was immunostained for ARPC2 (red), E-cadherin (magenta) and Par3 (yellow). Cells were stained with Phalloidin (green) for actin cytoskeleton and DAPI (blue) for nuclei. (scale bar=20μm).

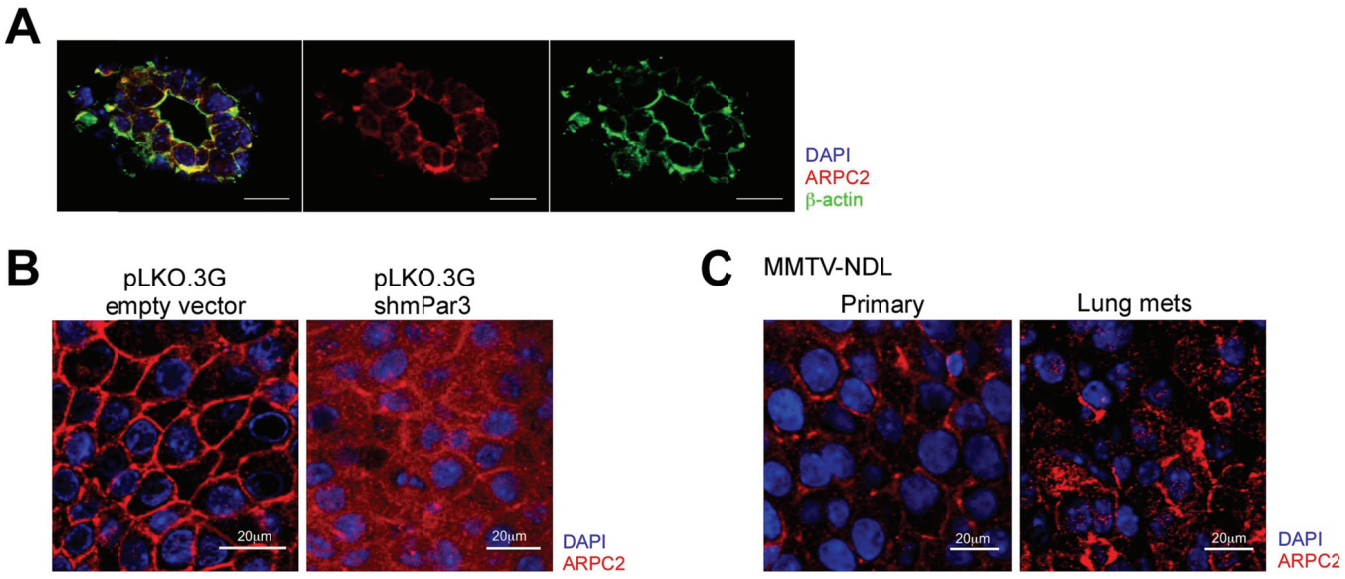

Figure 5.11. Loss of Par3 mislocalizes Arp2/3 in mouse tissue

(A) Images of tissue sections from normal mammary gland from FVB mouse immunostained for ARPC2 (red) and β-actin (green).

(B) Tissue sections from tumors generated using MMTV-NDL tumor cells infected with empty vector or mPar3 shRNA lentivirus.

(C) Tissue sections from a primary tumor and paired lung metastasis from MMTV-NDL mice were immunostained for ARPC2 (red) (scale bar=20μm).

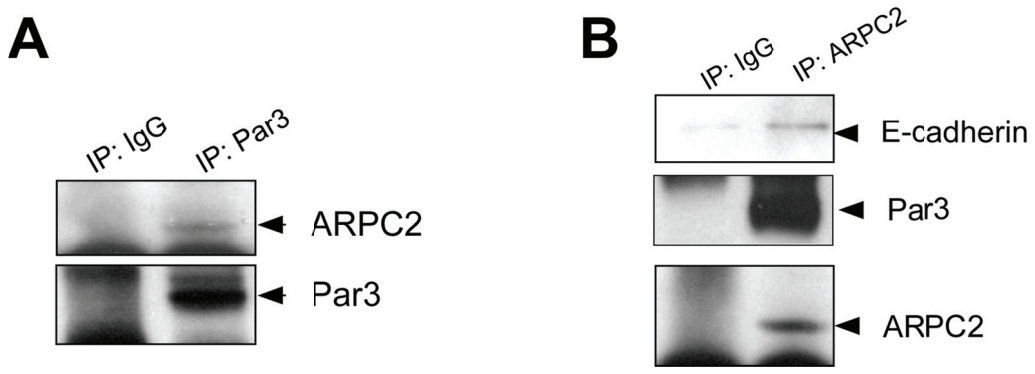

Figure 5.12. Interaction of Arp2/3, Par3 and E-cadherin.

Cell lysates from confluent monolayers of control 10A.B2 cells were immunoprecipitated using anti-Par3 **(A)** or anti-ARPC2 **(B)** antibodies and the immunoprecipitates were immunoblotted as indicated. Rabbit IgG was used as non-specific control in both experiments.

5.6 Loss of Par3 engages IRSp53-WAVE2 pathway to regulate cell invasion

Next we investigated if Rac mediated its effect by regulating Arp2/3 complex activity. The nucleation activity of Arp2/3 is activated by members of Wiskott-Aldrich syndrome family protein including WASp, N-WASp, WAVE and WASH proteins. All the WASP proteins contain a VCA domain named for its three sub-elements, the verprolin (V) homology, central (C) hydrophobic and acidic (A) regions, by which they strongly stimulate Arp2/3-mediated actin nucleation. Among the WASps, WAVE proteins are the only protein family functioning downstream of Rac GTPase (Padrick and Rosen 2010). The bridge connecting Rac-GTP to the Arp2/3 complex is the insulin receptor tyrosine kinase substrate p53 (IRSp53) (Miki, Yamaguchi et al. 2000). The N-terminus of IRSp53 binds to Rac-GTP while the C-terminal SH3 domain binds to the SH3-binding site in the large proline-rich domain (PRD) of WAVE2 to form a trimolecular complex that promotes Arp2/3-mediated branched actin polymerization in response to an increase in Rac-GTP level (Nakagawa, Miki et al. 2003; Yamagishi, Masuda et al. 2004; Millard, Bompard et al. 2005) (Figure 5.13.A). IRSp53 and WAVE2 have been shown to bind to each other. We found that Par3 associated with IRSp53 and WAVE2 complex (Figure 5.13.B), as determined by co-immunoprecipitation analysis. To determine if the IRSp53-WAVE2 interaction is involved in Par3-mediated regulation of actin dynamics, we stably expressed myc-tagged IRSp53 full length or a dominant-negative construct lacking the SH3 domain (ΔSH3) that cannot couple Rac-GTP to the WAVE2/Arp2/3 complex in 10A.B2 shPar3 cells (Figure 5.13.C). Expression of ΔSH3 IRSp53 in shPar3 cells suppressed the ErbB2-induced cell invasion. In addition, expression of full length IRSp53 also inhibited invasion (Figure 5.13.D). We did not anticipate full length IRSp53 to function as a dominant negative in this context; however it is likely due the ability of full length to function as competitive inhibitor for Rac-GTP. We have also tested another WASp member, WASp using the dominant negative WASp (WASp-CA), in which the peptide of the CA region by itself binds the Arp2/3 complex but lacks the binding sites for G-actin, and therefore acts as inhibitor of WASp and N-WASp (Zhang, Wu et al. 2005). Expression of WASp-CA did not change cell invasion in shPar3 cells (data not shown), suggesting that N-WASp and WASp are not involved in Par3-loss induced cell invasion. Taken together, these results identify IRSp53-WAVE2 as an important mediator of Par3 loss-induced changes in cytoskeleton and cell invasion.

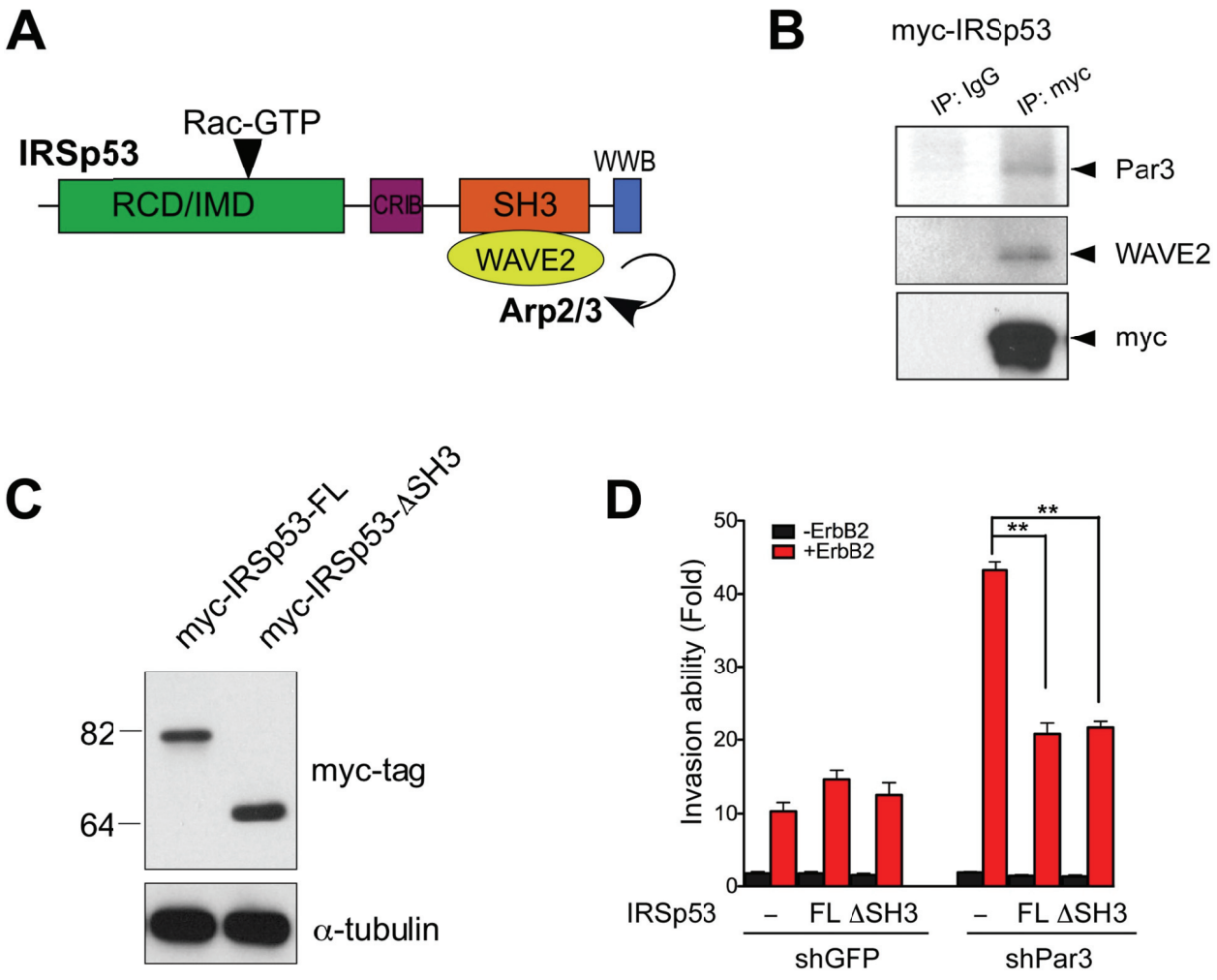

Figure 5.13. Loss of Par3 engages an IRSp53 pathway to induce cell invasion

(A) A schematic diagram showing IRSp53 and its interaction with Rac and WAVE2.

(B) Cell lysates from confluent monolayers of 10A.B2 cells expressing full length myc-IRSp53 were immunoprecipitated with anti-myc-tag antibody and the immunoprecipitates were immunoblotted as indicated. Mouse IgG was used as non-specific control.

(C) Lysates from 10A.B2 cells overexpressing vector or myc-IRSp53 full length or ΔSH3 mutant were immunoblotted using anti-myc-tag antibodies.

(D) shGFP and shPar310A.B2 cells stably expressing empty vector or full length myc-IRSp53 or ΔSH3 were seeded for transwell invasion assays, with or without activation of ErbB2 and incubated for 48 hours. Invaded cells were quantified from three independent experiments and results are represented as fold change in invasion compared to shGFP cells without ErbB2 stimulation (n=3; ** represents $p<0.01$).

Deregulation of Par3 in Human Breast Cancer

Disclosure of contributions:
Dr. D.Craig Allred provided the human breast cancer samples in Table 6-2, Table 6-3, Figure 6-3 and Figure 6.4 and performed Allred Score analysis for the IHC staining.

Introduction

The results from cell lines and MMTV-NDL mice strongly suggest an association between loss of Par3 and human breast cancer progression. In this chapter, we investigate the status of Par3 in human breast cancers, and whether there is a correlation between dysregulation of Par3 and breast cancer progression. To address these questions, we have performed four experiments to measure Par3 mRNA or protein levels in human breast cancer cells:

1) Analyze Par3 protein levels in different cell lines derived from human breast cancer.
2) Compare *PARD*3 mRNA levels between normal breast tissue and human breast cancer using the Oncomine web-based meta-analysis.
3) Analyze Par3 protein expression by immunohistochemistry in human invasive breast cancers.
4) Compare Par3 protein expression levels between paired primary breast tumors and distant metastases.

Results

6.1 Par3 expression levels in breast cancer cell lines

We selected a collection of well-studied breast cancer cell lines, including BT474, MDA-MB-453, T47D, SKBR3 and SUM159PT. The origin, properties and characteristics of each cell line are listed in Table 6-1. The Par3 and E-cadherin expression in the non-tumorigenic MCF10A and the cancer cell lines was evaluated by immunoblotting. First, we noticed that control MCF10A cells and BT474 and T47D cell lines derived from ductal carcinomas retained E-cadherin expression. However, E-cadherin levels were decreased in BT474 cells, and completely depleted in MDAMB453, SKBR3 and SUM159PT (Figure 6.1, middle panel). It has been reported that the E-cadherin gene is deleted in SKBR3 cells (Hajra, Ji et al. 1999) and silenced in SKBR3 cells (Hiraguri, Godfrey et al. 1998). Consistent with the E-cadherin levels, only BT474 and T47D form compact epithelial islets, but E-cadherin negative cells do not form islets. Par3 is expressed in all the cell lines, and does not show obvious correlation with the level

of E-cadherin (Figure 6-1). Except in SKBR3 cells, Par3 expression is lower in the cancer cell lines compared to non-tumorigenic MCF10A cells (Figure 6.1, top panel). This result suggests that Par3 protein levels are altered in breast cancer cells.

Table 6-1 Characteristics of the breast cancer cell lines.

Cell Line	Gene Cluster	ER	PR	HER2	TP53	Source	Tumor Type	Age (yrs)	Ethnicity
BT474	Lu	+	[+]	+	+	P.Br	IDC	60	W
MDAMB453	Lu	-	[-]		$-^{WT}$	PE	AC	48	W
T47D	Lu	+	[+]		$++^{M}$	PE	IDC	54	
SKBR3	Lu	-	[-]	+	+	PE	AC	43	W
SUM159PT	BaB	[-]	[-]		[-]	P.Br	AnCa		

Abbreviations: AC, Adenocarcinoma; AnCa, Anaplastic Carcinoma; BaB, Basal B; IDC, Invasive Ductal Carcinoma; Lu, Luminal; MC, metaplastic carcinoma; P.Br, primary breast; PE, Pleural Effusion; W=Caucasian.

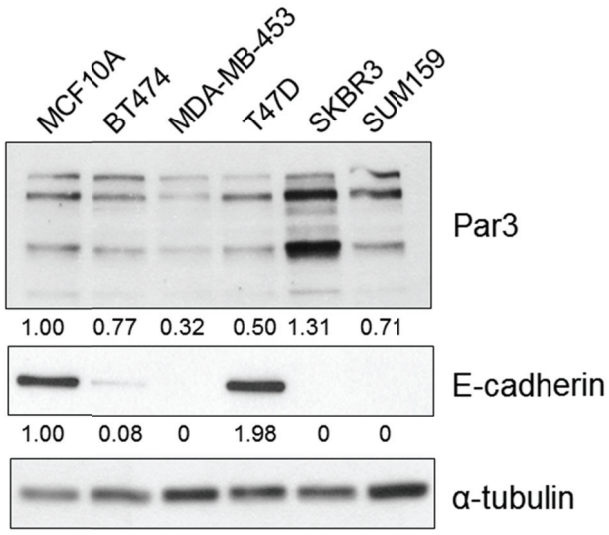

Figure 6.1. Par3 and E-cadherin protein levels in breast cancer cell lines

Cell lysates from indicated breast cancer cell lines were collected and analyzed for Par3 and E-cadherin protein expression by immunoblot analysis. The relative abundance of each protein was normalized to α-tubulin and indicated as fold changes relative to non-tumorigenic MCF10A cells.

6.2 Analysis of PARD3 mRNA level in human breast cancer using the Oncomine Database

Next, we used the Oncomine web-based meta-analysis (Oncomine™, Compendia Bioscience, Ann Arbor, MI) (Rhodes, Yu et al. 2004), to investigate *PARD3* mRNA expression levels in normal breast tissue and human breast cancer. Only studies where the difference in expression was highly significant ($p<0.001$) were selected for this analysis. Expression studies from the TCGA (The Cancer Genome Atlas) used 4 reporters (DNA probes) for *PARD3*. While two reporters (A-23-P201963 and A-23-P201964) met our significance criteria, two reporters (A-24-P35478 and A-23-P35479) did not. Both reporters that met our selection criteria showed *PARD3* expression to be downregulated by 1.7 to 1.9 fold in invasive breast cancer (IBC), invasive ductal cancer (IDC) and invasive lobular cancer (ILC) compared to the expression levels in normal breast tissue (Figure 6.2). The reporters that did not meet the criteria did not show a notable fold change in expression (<1.15 fold) between normal tissue and cancer. In another independent study, where one reporter met our significance criteria, IDC had a 2.8 fold

decrease in *PARD3* expression compared to the levels in normal breast (Zhao, Langerod et al. 2004). In addition, a third study showed that *PARD3* level is downregulated by 1.4 fold in IDC compared to DCIS (p=0.018) (Radvanyi, Singh-Sandhu et al. 2005). The latter study supports the notion that downregulation of *PARD3* mRNA level is associated with invasive progression in breast carcinomas (Figure 6.2).

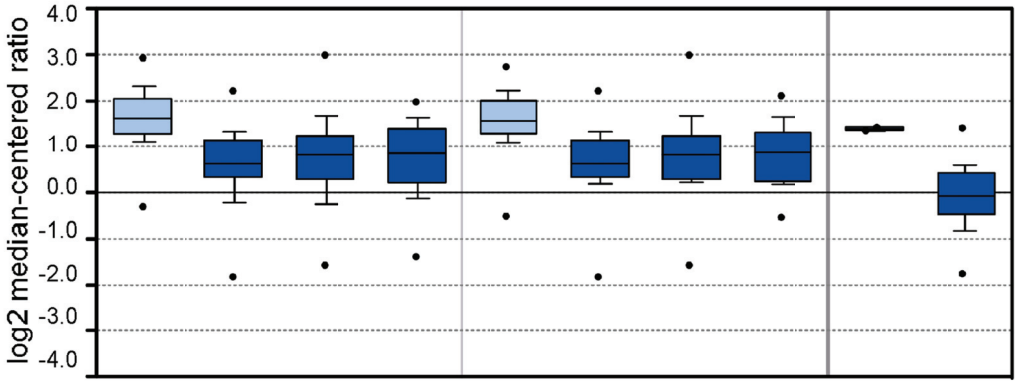

Class	Breast	IBC	IDC	ILC	Breast	IBC	IDC	ILC	Breast	IDC
N	61	76	392	36	61	76	392	36	2	37
P-value (Cancer vs. Breast)		6.18E-16	4.20E-17	7.86E-8		9.26E-17	1.18E-19	4.68E-8		9.37E-15
Fold change (Cancer vs. Breast)		-1.952	-1.815	-1.802		-1.928	-1.802	-1.744		-2.789
Reporter ID	A_23_P201963				A_23_P201964				1693642	
Analysis	TCGA Breast				TCGA Breast				Zhao Breast	

Figure 6.2. Pard3 mRNA profile in Oncomine database

Comparison of *Pard3* mRNA expression between invasive breast cancer and normal breast using Oncomine™ (Compendia Bioscience, Ann Arbor, MI) database. Analyses that met the significance threshold (P<0.001) are presented as a box and whisker plot. The P-value, fold change, reporter (DNA probe) identification (reporter ID) and study reference are listed. Abbreviations: N: Number of samples, IBC: Invasive breast carcinoma, IDC: Invasive ductal breast carcinoma, ILC: Invasive lobular carcinoma.

6.3 Correlation between loss of Par3 and tumor characteristics in invasive breast cancer

To better understand the relationship between Par3 expression and tumor characteristics in IBC, we analyzed tissue microarray samples for Par3 protein expression by IHC. The study utilized formalin-fixed paraffin-embedded tissue (FFPET) samples of human invasive breast cancers (IBCs; n=98) assembled on tissue microarrays (Lampkin and Allred 1990). Histological

grade of the IBCs was determined using the method of Scarff-Bloom-Richardson as modified by Elston-Ellis (Elston and Ellis 2002; Elston and Ellis 2002). The grade is obtained through a composition sum by assigning score based on the nuclear pleomorphism, a mitotic index, and a tubular assessment. The overall grades from 1 to 3 are described as "highly differentiated, moderately differentiated, and poorly differentiated". This histologic grade is strongly associated with both breast cancer-specific survival and disease-free survival, and provides a strong prognostic value for patients with invasive breast cancer (Rakha, El-Sayed et al. 2008). In this system, grade 1, 2 and 3 tumors reoccurred with a median time of 88, 42 and 23 months, respectively. It was often found that low and intermediate grade carcinomas often recur as higher grade tumors. Thus, this system also reflects individual tumor aggressiveness and predicts tumor progression (Cserni 2002). ER and HER2 oncogene expression were evaluated by IHC using comprehensively standardized and validated assays (Harvey, Clark et al. 1999; Wolff, Hammond et al. 2007; Hammond, Hayes et al. 2010). ER (nuclear) was quantified using the Allred Score (range 0-8; positive >2; Figure 6.3A) (Harvey, Clark et al. 1999). HER2 was quantified using the Dako HercepTest Score (0-3+; negative = 0/1+; indeterminate = 2+; positive = 3+) (Wolff, Hammond et al. 2007). Par3 expression was evaluated by indirect immunofluorescence using anti-Par3 antibody. To understand the relationship between Par3 and tumor characteristics, we quantified changes in membrane-localized Par3 using the Allred Score [Total Score (TS) range 0-8]. An Allred score of 3 corresponds to as few as 10% cells with weak membrane signal and an Allred score of 7 indicates strong membrane Par3 in more than 66% of cells (Figure 6.3B). The statistical significance of the association between mean Par3 expression levels in samples within each subgroup (Grade, ER +/- and HER2) was determined utilizing the Student's t test. As shown in Table 6-2, Par3 membrane localization was significantly decreased in IBCs associated with clinically aggressive prognostic factors, including higher histological grade, negative ER status, and positive HER2 status. Thus, decreases in membrane-localized Par3 correlated with higher tumor grade and ErbB2-positive status, which are strong indicators of poor clinical prognosis.

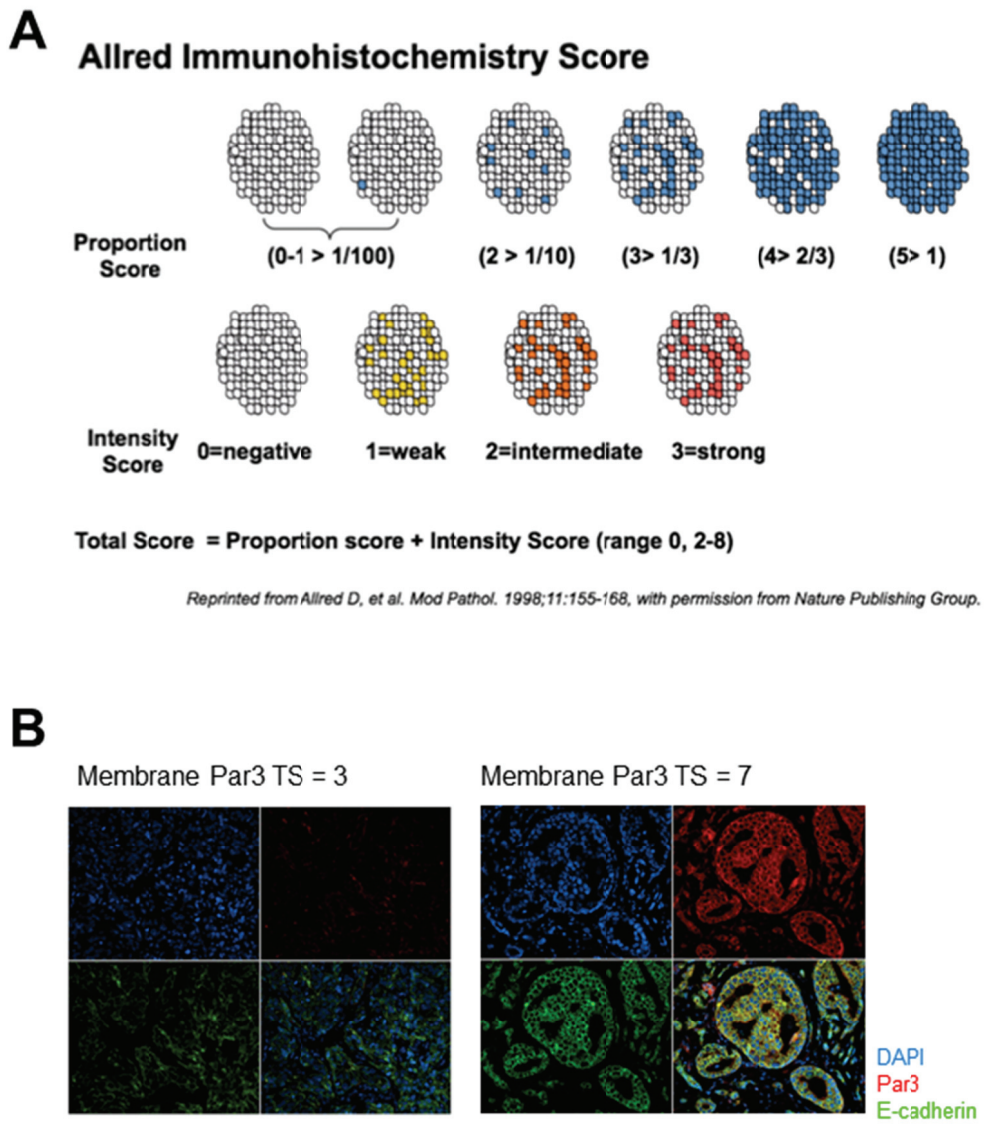

Figure 6.3. IHC scoring system and staining of Par3 expression in human breast cancer samples

(A) Allred IHC scoring system. This scoring system assigns a numerical value to both the overall stain intensity and the staining pattern; the two values are simply added to produce the final Allred score**.**

(B) IHC for Par3 protein expression representing a low (Total Score, TS=3) and high (TS=7) Allred score (Par3: green, E-cadherin: red, nuclei: DAPI, blue).

Table 6-2 Characteristics of human invasive breast cancer samples for Par3 membrane expression levels

Characteristics of Human Invasive Breast Cancer Samples For Par3 Membrane Expression Levels			
Characteristic	Total (N=98)	Mean membrane Par3 TS[§]	P value[¶]
Tumor Histological Grade			
Grade 1	36	6.08 ± 1.40	
Grade 2	42	5.83 ± 1.58	
Grade 3	20	4.94 ± 2.14	
Grade 1 *vs.* Grade 3.			0.0202*
ER status			
ER-pos	70	5.96 ±1.52	
ER-neg	28	5.21 ± 1.97	
ER-pos *vs.* ER-neg			0.0478*
HER2 status			
HER2-neg (0/1+)	86	5.86 ± 1.6	
HER2-pos (2+/3+)	12	4.92 ± 2.11	
HER2-pos (3+)	9	4.33 ± 2.12	
HER2-neg vs. HER2-pos (2+/3+)			0.0734
HER2-neg vs. HER2-pos (3+)			0.0096**

[§] Plus-minus values are mean±SD.
[¶] Two-tailed t test
Significance level *<0.05, **<0.01

6.4 Downregulation of Par3 in human breast cancer metastasis

As metastatic tumor cells originate from primary tumors and accumulate additional genetic alterations, the genetic alterations related to metastasis are enriched in the metastases. To address if changes in Par3 expression is related to breast cancer metastasis, we compared the Par3 expression level between the primary tumor and metastasis from the same patient. We obtained 14 primary breast tumor and metastasis pairs from the St. Louis Breast Tissue Registry in collaboration with Dr. Craig Allred. The metastases were derived from various organs including lung, liver, brain, skin, lymph node and pleura (Table 6-3). Expression of Par3 was analyzed by IHC using indirect immunofluorescence. Expression of membrane-localized Par3 in the primary tumor and metastasis from the same patient were analyzed using the Allred score. The results demonstrate that eight out of 14 metastases have a decrease in the level of membrane Par3 expression (BST>MET) compared to matched primary tumors (Figure 6.4.A). Two out of 14 metastases show no change in levels of Par3 (BST=MET) (Figure 6.4.B), and four out 14 metastases show an increase in the levels of Par3 (BST<MET) (Figure 6.4.C) when compared to the Par3 levels in matched primary tumors (Table 6-3). Using the binomial test with a null assumption that Par3 has the random distribution to increase, decrease or remain unchange in the metastasis compared to the primary tumor, the calculation produced a probability of 0.0174 of statistical significance only for the BST>MET group, but not for the BST=MET or BST<MET groups, suggesting a tendency of downregulation of Par3 in the metastases. These observations provide direct evidence to suggest a correlation between a decrease in membrane Par3 expression and metastasis.

Table 6-3 Characteristics of human primary breast and metastasis pairs for Par3 membrane expression level

Case #	Met type	BST.membrane			MET.membrane			
		PS	IS	TS	PS	IS	TS	
1	Neck lymph node	2	2	4	0	0	0	↓
2	Lung met	2	2	4	0	0	0	↓
3	Neck lymph node	0	0	0	1	2	3	↑
4	Lung met	2	2	4	2	2	4	→
5	Liver met	3	2	5	3	2	5	→
6	Pleura met	1	1	2	2	2	4	↑
7	Cervical lymph node	1	2	3	0	0	0	↓
8	Brain met	4	2	6			0	↓
9	Skin (left arm) met	5	2	7	3	2	5	↓
10	Pleura met	2	2	4	0	0	0	↓
11	Neck met	1	2	3	0	0	0	↓
12	Supraclavicular lymph node met	1	2	3	2	2	4	↑
13	Skin (right shoulder) met	3	2	5	2	2	4	↓
14	Pleura met	2	2	4	3	2	5	↑
	Mean ± SD	3.86±1.7			2.43±2.24			

:

PS: Propotion score; IS: Intensity score; TS: Total score in Allred IHC score system.
BST: Primary breast tumor; MET: Metastasis

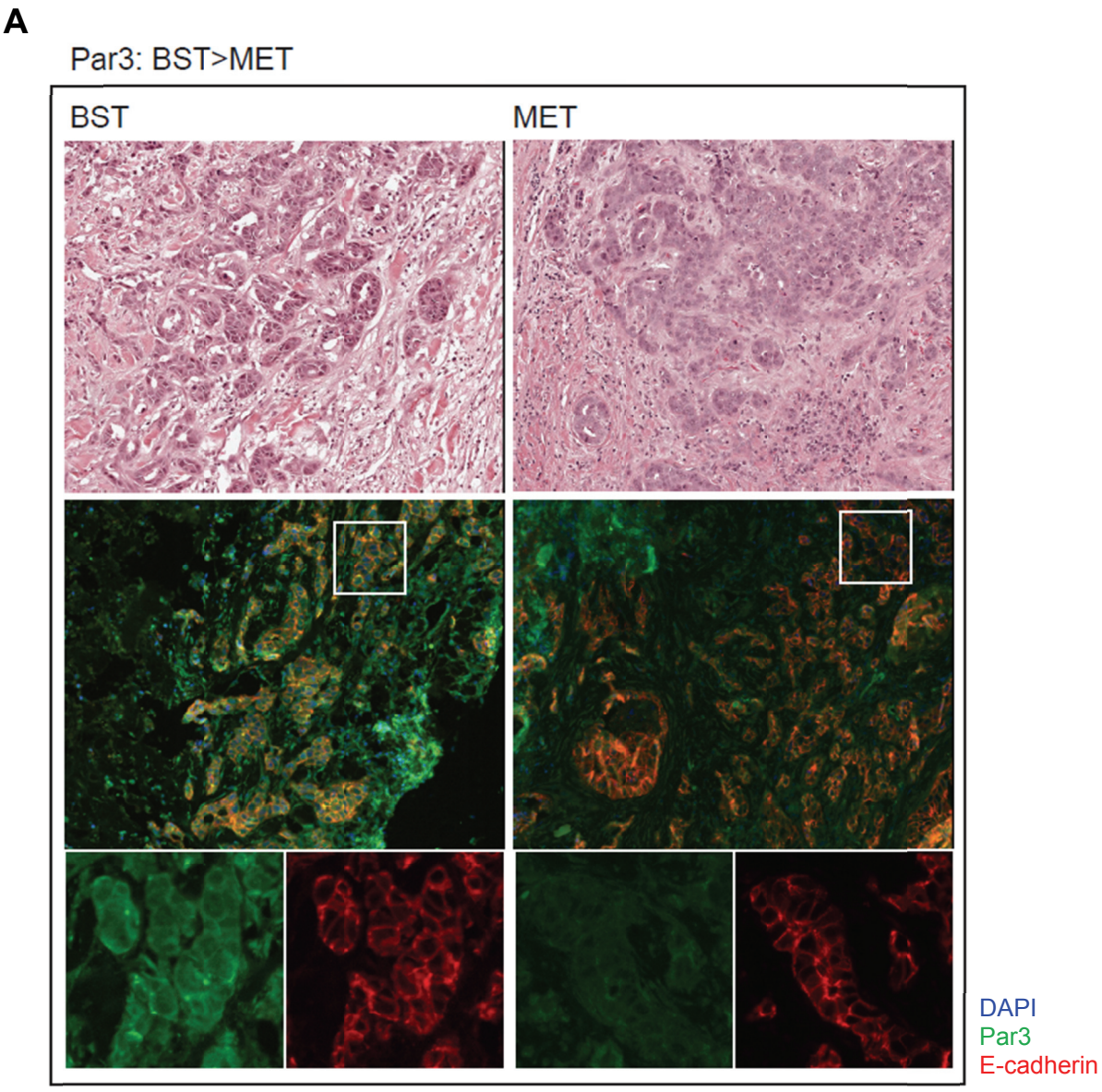

Figure 6.4. Expression of membrane Par3 in matched primary breast tumors and metastases

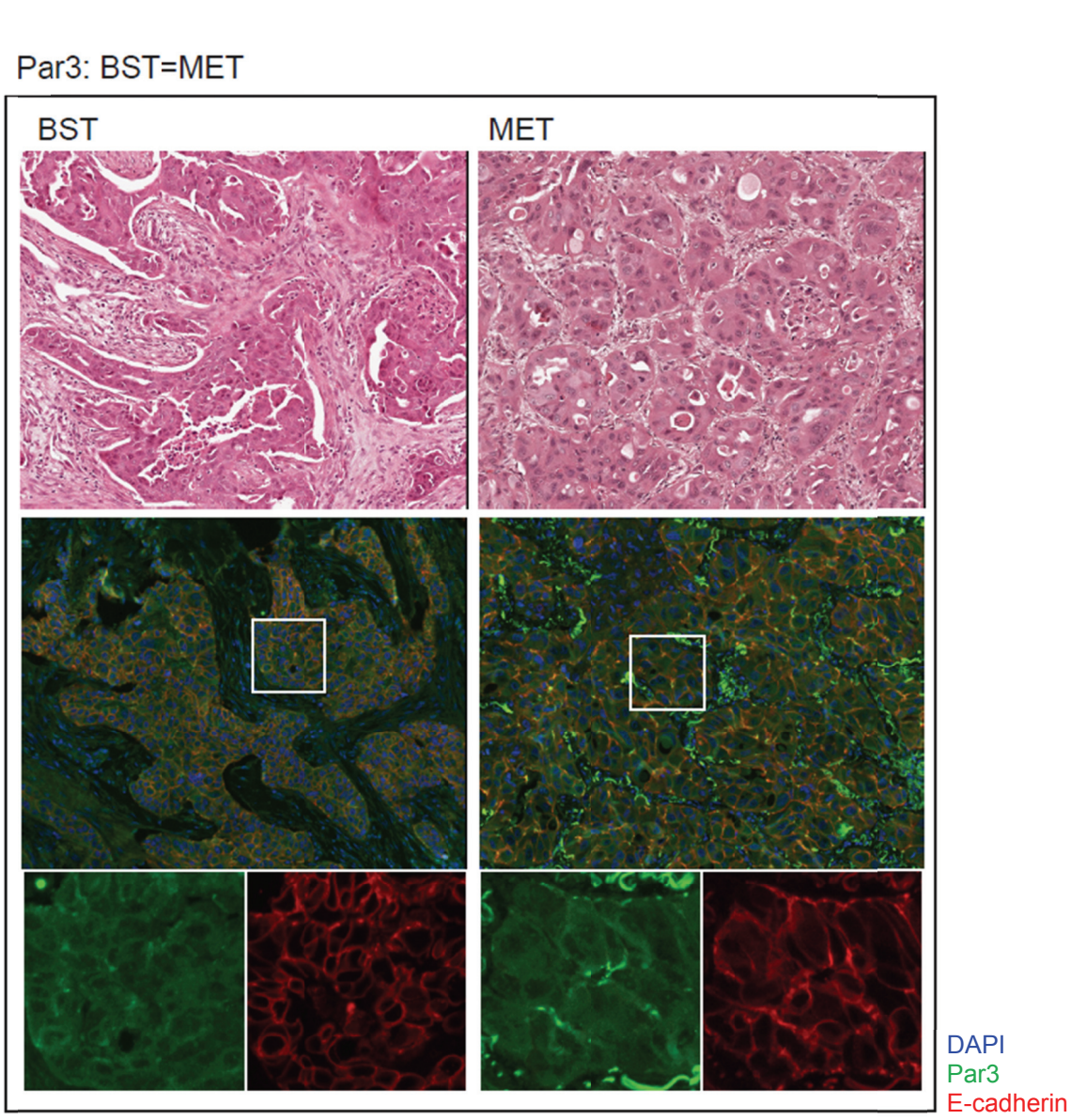

Figure 6.4. Expression of membrane Par3 in matched primary breast tumors and metastases

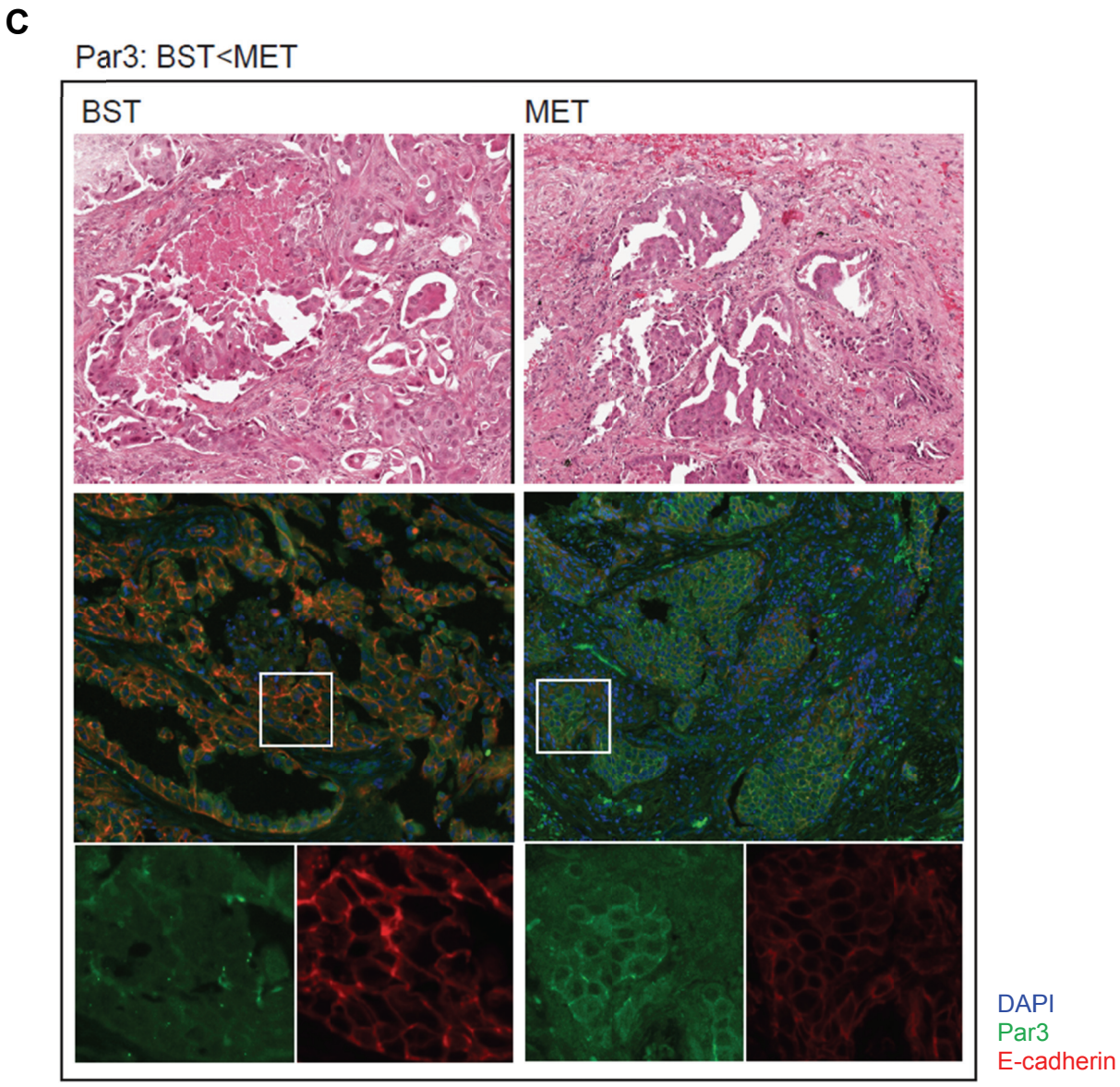

Figure 6.4. Expression of membrane Par3 in matched primary breast tumors and metastases

IHC for Par3 (green) and E-cadherin (red) in the primary breast tumor (BST) and metastasis (MET) paired samples.

(A) A representative pair in which metastasis has a decrease in the level of membrane Par3 expression compared to matched the primary tumor (B>M).

(B) A representative pair in which Par3 protein expression is at the same level in the primary BST and the MET (B=M).

(C) A representative pair in which metastasis has an increase in the level of membrane Par3 expression compared to matched the primary tumor (B<M).

Materials and Methods

Plasmids

shRNAs

The shRNA constructs against human and mouse Par3 were obtained from TRC lentiviral shRNA library (Open Biosystems, Thermo Scientific). TRC ID numbers of individual clones of efficient knockdown effect are listed as below:

shPar3-TRCN0000118134, from TRC-Hs1.0 (Human), targeting human *PAR3* (locus: NM 019619.3) 3112-3132bp
sequence:
5'- CCGGGCCATCGACAAATCTTATGATCTCGAGATCATAAGATTTGTCGATGGCTTT TTG-3'

shmPar3-TRCN0000094399, from TRC-Mm1.0 (Mouse), targeting mouse *Par3* (locus: NM_001013580.3) 3404-3424bp.
sequence:
5'- CCGGCCAGTTTATCTCTATCACTTTCTCGAGAAAGTGATAGAGATAAACTGGTTT TTG-3',

Lentiviral pLKO.3G vector which contains an eGFP marker instead of puromycin selectable marker was obtained from Christophe Benoist and Diane Mathis through Addgene (Addgene plasmid 14748, http://www.addgene.org/14748/). mshPar3 were amplified using oligos containing EcoRI and PacI sites from TRC vector and subcloned into pLKO.3G vector.

Retroviral microRNA30 based RNA interference vectors targeting expression of *Canis lupus familiaris* Par3 in MDCK cells were designed as follows: 97-nucleotide oligonucleotide was synthesized containing a 5' miR30 flanking sequence - a sense strand *cPar3* target sequence - a common miR30 loop sequence- an antisense strand *cPar3* and a common 3' miR30 flanking sequence. The oligo sequence for shRNA template strands used was as follows:

cPar3-C, targeting <u>*canis*</u> Par3 (locus: XM_535141)1531-1551bp:

5'- TGCTGTTGACAGTGAGCGACCAAGGGAACTGAATGCAGAGTAGTGAAGCCACAG ATGTACTCTGCATTCAGTTCCCTTGGGTGCCTACTGCCTCGGA-3'.

The sequence was amplified using polymerase chain reaction (PCR) with primers that recognize the miR30 flanking sequence containing XhoI and EcoRI restriction enzyme sites.

5'miR30PCRXhoIF

5'- CAGAAGGCTCGAGAAGGTATATTGCTGTTGACAGTGAGCG -3'

3'miR30PCREcoRIF
5'- CTAAAGTAGCCCCTTGAATTCCGAGGCAGTAGGCA -3'

The PCR product was cloned into the pMSCV–LTR-hygromycin vector. Preparation of virus, infection and selection were performed as previously described (Debnath, Muthuswamy et al. 2003).

Expression vectors

p^{CMV}LifeAct-TagRFP was purchased from ibidi GmbH and subcloned into XhoI/HpaI sites of pMSCV-LTR-blasticidin vector (kindly provided by Yuri Lazebnik, Cold Spring Harbor Laboratory, Cold Spring Harbor, NY)..

Tiam1-PHn-Ex-CC was generated by PCR amplification of pK-Tiam1-PHn-CC-Ex (Kindly provided by Ian G. Macara, University of Virginia School of Medicine, Charlottesville, VA) using the following primers as an EcoRV/MfeI fragment:

Forward: CTA GTA GCG ATA TCC ATG GGA AAC GCA
Reverse: GCA TAC TAC AAT TGC TAT CAC GCG TCT GA
The PCR fragments were cloned into HpaI/EcoRI sites of pMSCV-PIG-Myc vector (kindly provided by Scott Lowe, Cold Spring Harbor Laboratory, Cold Spring Harbor, NY).

IRSp53 full length and ΔSH3 mutant was amplified from cDNA clone (Open Biosystems, Clone Id: 4125501) with following primers as BamHI/EcoRI fragments

IRSp53 full length:
Forward: 5'- ATT CGG ATC CGA TGT CTC TGT CT -3'
Reverse: 5' - TCG AGA ATT CTC ACA CTG TGG ACA -3'
IRSp53 ΔSH3:
Forward: 5'- ATT CGG ATC CGA TGT CTC TGT CT -3'
Reverse: 5'- TCG AGA ATT CTC ACG AGC GAG GCA GAG T-3'
The PCR fragments were cloned into pMSCV-PIG-Myc vector.

Preparation of retrovirus infection and selection were performed as previously described

(Debnath, Muthuswamy et al. 2003) and can also refer to the Nolan Laboratory website in Stanford http://www.stanford.edu/group/nolan/retroviral_systems/retsys.html for the detailed protocol.

pLKO.1-shRNAs and pLKO.3G-shRNA lentivirus production and infection were performed using the protocol provided by The RNAi Consortium (Moffat, Grueneberg et al. 2006) http://www.broadinstitute.org/rnai/public/resources/protocols.

Antibodies and Reagents

Antibodies were purchased from commercial sources and listed in Supplemental Data. Growth factor reduced Matrigel (BD Transduction Laboratories) was used for 3D culture and transplantation experiments. Small molecule ligand AP1510 (ARIAD Pharmaceuticals) was used to activate the chimeric ErbB2 receptor in 10A.B2 cells as previously described (Muthuswamy, Gilman et al. 1999). Recombinant human TGF-β (Abcam) and Rac inhibitor NSC23766 (Calbiochem) were used as described.

Antibodies used in this study were Par3 (Upstate Biotechnology), α-tubulin (Sigma), E-cadherin (BD Transduction Labs), GM130 (BD Transduction Labs), Rac1 (BD Transduction Labs), phospho-Erk 1/2 (Cell Signaling Technologies), Erk2 (BD Transduction Labs), Laminin 5 (Millipore Corporation), Myc-tag (Cell Signaling Technologies), Ki67 (Zymed), Her2 clone 3B5 (Calbiochem), HECD-1 (Calbiochem), p34/ARPC2 (Millipore Corporation) and fluorophore-conjugated secondary antibodies (Molecular Probes). Alexa 488 labeled Phalloidin (Invitrogen) was used to detect F-actin.

Cell Culture

10A.B2 cells were generated and cultured as previously described (Muthuswamy, Li et al. 2001). T47D, BT474, SKBR3 and Eph4 cells were cultured according to the protocol provided by ATCC. Populations of cells expressing either shGFP or shPar3 were generated by

lentiviral/retroviral infection and selected with antibiotics. Three-dimensional (3D) culture of 10A.B2 cells, inducible ErbB2 activation and indirect immunofluorescence of 3D acini were performed as described earlier (Muthuswamy, Gilman et al. 1999; Debnath, Muthuswamy et al. 2003; Xiang and Muthuswamy 2006). 3D culture of T47D cells, cells were seeded in Matrigel using the same embedding technique except replacing the medium with T47D growth medium (RPMI1640, 8μg/ml, 10% FBS) in 2500 cells/well.

Quantitative PCR

Total RNA was isolated under indicated conditions using TRIzol reagent following the manufacturer's protocol (Invitrogen). 1.0 μg of RNA was reverse transcribed with the TaqMan kit (Applied Biosystems) to generate cDNA. The resulting cDNA was used for quantitative real-time PCR using SYBR Green PCR Mix (Applied Biosystems) in triplicate. The data were gathered on the Applied Biosystems 7900HT Fast Real-Time PCR system. Fluorescence measurements during the extension step of PCR cycles were used to calculate threshold cycle values. Fold changes in mRNA abundance were calculated by a comparative threshold cycle method (Schmittgen and Livak 2008) using *β-actin* mRNA as an internal control for each sample. Results are expressed as fold change in expression compared to shGFP cells. Primer sequences used are as follows:

fibronectin forward:	5'- GAG GGG ACC TGC AGC CAC AA -3'
fibronection reverse:	5'- TTC GCA ACC TGC GGG AAA AA-3'
human β-actin forward:	5'-TTC AAC ACC CCA GCC ATG-3'
human β-actin reverse:	5'-GCC AGT GGT ACG GCC AGA-3'
snail forward:	5'-TGC AGG ACT CTA ATC CAA GTT TAC C-3'
snail reverse:	5'-GTG GGA TGG CTG CCA GC-3'
N-cadherin forward:	5'-GAC GGT TCG CCA TCC AGA C-3'
N-cadherin reverse:	5'-TCG ATT GGT TTG ACC ACG G-3'
mouse E-cadherin forward:	5'-GCC GGA GAG GCA CCT GGA GA-3'
mouse E-cadherin reverse:	5'-GCC GGC CAG TGC ATC CTT CA-3'

Immunoblotting

Immunoblot analysis was performed as previously outlined (Muthuswamy, Li et al. 2001; Debnath, Muthuswamy et al. 2003; Xiang and Muthuswamy 2006).

Immunoprecipitation

10A.B2 cells were lysed in in TNE buffer (25 mM Hepes, 150 mM NaCl, 0.5 mM EDTA, 5 mM MgCl2, 1% Triton X-100, 1 mM Na_3VO_4, 100 μg/mL aprotinin, 2.5 μg/mL leupeptin, and 1 μg/mL pepstatin). Lysates were collected by scraping the plates and were centrifuged at 15,000×g for 15 minutes at 4ºC. Protein concentration was measured using the Biorad protein assay. 1mg total protein were incubate with indicated antibodies for 4 hours at 4ºC and the immune complex was then captured by Protein G Sepharose beads (GE Healthcare Life Science). The immunoprecipitated proteins were further analyzed by SDS-PAGE and immunoblotting to determine protein interactions (Muthuswamy, Li et al. 2001).

Transwell Invasion Assay

Invasion assays were performed in transwell filters using 8μm pore size, growth factor reduced Matrigel invasion chambers (BD Biosciences, Cat# 354483). ShGFP and shPar3 10A.B2 cells were starved overnight in assay medium (MCF10A medium with 2.0 % horse serum and no EGF) before splitting. 1×10^5 cells in assay medium were added on top of the chamber. AP1510 was added to both top and bottom chambers to activate ErbB2. For experiments with the Rac inhibitor NSC23766, the inhibitor of indicated concentration was added at the indicated concentrations to both the top and bottom chamber. For invasion assays using T47D cells, a similar protocol was followed except that the cells were starved overnight in the serum-free RPMI 1640 medium before seeding. RPMI 1640 + 10.0 % FBS was added to the lower chamber during invasion assay. After 24 hours (for T47D cells) or 48 hours (for 10A.B2 cells) the chambers were washed once with PBS and fixed with 4.0% PFA. Non-invading cells on the top of the filter were removed with a cotton swab and invaded cells on the bottom of the filter were

stained with 5.0 mg/ml 4,6-diamidino-2-phenylindole (DAPI) to visualize nuclei. The number of invaded cells in five different fields was counted under 20× magnification, and the mean for each condition determined. Results are expressed as fold change in invasion compared to shGFP without activation of ErbB2. Experiments were repeated a minimum of three times.

Hanging Drop Assay

Aggregation assays were done as previously described (Redfield, Nieman et al. 1997) with minor modifications. Briefly, 10A.B2 cells were trypsinized and resuspended at a density of 2.5×10^5 cells/ml in the assay medium, and then passed through a 40μm nylon cell strainer. ErbB2 dimerizer is added to this single cell suspension as needed. 20μl drops of medium, containing 5,000 cells/drop, were pipetted onto the inner surface of the lid of a 12 well culture plate. The lid was then quickly flipped over and placed on the plate so that the drops were hanging from the lid with the cells suspended within them. To prevent evaporation, 2.0 ml serum-free culture medium was placed in the well. After 20 hours at 37°C, the lid of the plate was inverted and photographed using a ZEISS inverted tissue culture microscope at 20× magnification.

Cell Spreading Assay

The cells were trypsinized, washed twice with chilled PBS to remove all traces of trypsin, and resuspended in chilled assay medium. The cell suspensions were incubated for 40 min at 37°C in the tissue culture incubator with the cap loose to maintain the pH of the medium. The cells (5×10^4/well in case of 12-well plates) were then directly transferred onto Matrigel-coated coverslips in 12-well tissue plates and allowed to adhere at 37°C for 2.0 hours. After incubation, unattached cells were removed by washing with PBS. Adherent cells were fixed with 4% PFA. Membrane protrusion and spreading were recorded using ZEISS inverted tissue culture microscope at 20× magnification. The average surface area per cell was measured using ImageJ software.

Rac-GTP Pulldown Assay

Confluent layer of cells were starved with assay medium overnight before ErbB2 activation stimulation. Assays were performed using the Rac1 activation assay kit (Cell Biolabs) according to the manufacturer's instructions. Briefly, cells were washed with ice-cold PBS and lysed with buffer containing 25mM HEPES (pH 7.4), 150mM NaCl, 10% glycerol, 1.0mM EDTA, 1.0% NP40, 10mM $MgCl_2$, 1.0mg/ml aprotinin and 1.0mM PMSF for 20 minutes on ice. Lysates were centrifuged at 15,000 × g. for 10 minutes. 0.5mg of protein was incubated with 10μg of PAK-PBD agarose bead slurry for 1.0 hour with gentle agitation. The beads were washed three times with lysis buffer. All the procedure was performed at 4.0°C. The resulting beads were resuspended in and the pull-down supernatant was analyzed by immunoblotting with anti-Rac1 antibody.

Tiam1 Activity Assay

Assays were performed using the active Rac-GEF assay kit (Cell Biolabs) according to the manufacturer's instructions. Briefly, cells were washed with ice-cold PBS and lysed with buffer containing 20mM HEPES (pH 7.5), 150mM NaCl, 1.0% Trition X-100, 5mM $MgCl_2$, 1.0mg/ml aprotinin and 1.0 mM PMSF for 20 minutes on ice. Lysates were centrifuged at 14,000 x g at 4 ºC for 10 minutes. 0.5 mg of protein was incubated with 40μg of Rac1 G15A agarose bead slurry for 1.0 hour with gentle agitation at 4 ºC. The beads were washed three times with ice-cold lysis buffer and boiled with 40μl 2 × SDS-PAGE sample buffer. The resulting pull-down supernatant was analyzed by immunoblotting with anti-Tiam1 antibody.

Fluorescence recovery after photobleaching (FRAP) analysis

10A.B2 cells expressing E-cadherin-GFP were seeded in the glass bottom 6-well plate (MetTek Corporation) at 5×10^5 per well density and grown for 72 hours into a confluent monolayer and starved with no-phenol red assay medium for 18 hours. FRAP experiments were

performed using spinning disk microscopy (Perkin Elmer spinning disk microscope, Perkin Elmer Inc; operated by the Velocity 5.4.1) with an APON 60×, 1.49NA oil immersion lens (Olympus) and the cells were maintained at 37ºC in 5.0% CO_2 during imaging. Excitation of GFP was carried out at a 488nm laser line of an argon laser. Before photobleaching, three images were acquired at 5 seconds interval. A selected region (10.0 μm x 10.0 μm) was bleached by a 5.0 milliseconds single laser pulse (UltraVIEW PK Device) at 80% laser transmission power. Recovery images were collected using 20% laser transmission power for 10 minutes at a scanning rate of 12 time points per minute. In ErbB2 activation condition, ErbB2 dimerizer was added 5 minutes before the first pre-bleaching image acquired. The average intensity was determined in the photobleaching region and normalized to the initial intensity before bleaching using ImageJ with Stacks-T functions- FRAP profiler plugin.

Raichu-Rac Förster Resonance Energy Transfer (FRET) Assay

1×10^6 cells were transiently transfected with 2μg pRaichu-Rac plasmid using Amaxa® Cell Line Nucleofector® Kit L (Lonza) with Program X-001. The electroporated cells were transferred into a 24-well glass bottom plate (In Vitro Scientific) at 1×10^5 cell/well density in growth medium. 20 hours after transfection, cells were starved in assay medium overnight. Cells were imaged on a Zeiss Axiovert 200M wide-field microscope at 63× magnification maintained at 37ºC in 5.0% CO_2 supplied with no-phenol red assay medium. For dual-emission ratio, we used an ET436/20× excitation filter, a T515LP diachronic mirror, an ET520LP emission filter for FRET channel, and an ET636/20× excitation filter, a T455LP dichroic mirror and an ET480/40m emission filter for CFP channel (Chroma Technology Crop). FRET, CFP and phase contrast channels were sequentially collected before add the ErbB2 stimulation and every 5 minutes after ErbB2 activated. The FRET channel and CFP channel exposure time was 80 milliseconds when the digital gain was set to 2^4. After background extraction, the ratio image was created with ImageJ PixFRET plugin (Feige, Sage et al. 2005).

Immunofluorescence Microscopy

Cells were plated on glass coverslips at (1×10^5/well in case of 12-well plates) and cultured for designated incubation times and cell treatments. Cells were fixed in 4% PFA, permeabilized using 0.1% Triton X-100, and blocked with 1% bovine serum albumin in IF wash buffer. Cells were incubated with primary antibody overnight at 4°C and then treated with fluorophore-conjugated secondary antibody for 1 hour at room temperature and then stained with DAPI. The slides were mounted and examined by fluorescence microscopy (Axiovert 200M and Apotome imaging, Carl Zeiss).

Tumor Immunohistochemistry (IHC) and Image Analysis

Paraffin-embedded mouse samples or human tissue slides were deparaffinized in xylene twice for five minutes each. Antigen retrieval was performed using a pressure cooker to boil the sample in Trilogy™ buffer (Cell Marque) for 15 min. Samples were blocked with 10% goat serum in 0.1% Triton X-100:PBS for 1.0 hr. Staining with Par3, E-cadherin, ErbB2, ARPC2 antibodies in blocking buffer was performed in a humidified chamber for 4 hours at room temperature followed by 3x10 minutes wash with IF buffer. Samples were incubated with fluorophore-conjugated secondary antibody for 1.0 hours at room temperature in blocking buffer and followed by 3×10 minutes wash, and then stained with DAPI. Microscopy was performed on Zeiss LSM710 microscope or Aperio Scanscope. Identical microscope parameters were applied to paired primary tumors and metastasis. The nonspecific fluorescence of the background, using sample only labeled with same fluorophore conjugated secondary antibody, was determined as the threshold value.

In human tumor samples, ER (nuclear) was quantified using the Allred Score (range 0-8; positive >2) (Harvey, Clark et al. 1999). HER2 was quantified using the Dako HercepTest Score (0-3+; negative = 0/1+; indeterminate = 2+; positive = 3+) (Wolff, Hammond et al. 2007). Membrane Par 3 was also quantified using the Allred Score (range 0-8) for each sample. Total Score (TS) = Proportion score (range 0-5) + Intensity Score (range 0-3) (Allred, Harvey et al. 1998).

Primary Mammary Tumor Cell Transplantation

Tumors of 1.5 cm in diameter were excised from metastasis-free MMTV-NDL mice. Single primary mammary tumor cells were prepared as described previously (Zhang, Behbod et al. 2008). Isolated cells were maintained in DMEM/F12 medium containing 2.0 % BSA, MEGM Singlequot (Lonza), 20 ng/ml basic fibroblast growth factor (bFGF) (Sigma-Aldrich), 4.0 μg/ml heparin (Sigma-Aldrich). The lentivirus used to infect the primary cells were first concentrated by ultracentrifuging the lentivirus supernatant collected as previously described at 100,000 × g for 1h45min and resuspending the virus pellet to 200μl. The detailed protocol was previously described (Welm, Dijkgraaf et al. 2008) and refer to Zena Werb website (http://werblab.ucsf.edu/sites/werblab.ucsf.edu/files/protocol%20pdfs/Lentiviral%20Production.pdf). Isolated cells were infected with concentrated shRNA lentivirus (MOI=5) in the ultra-low attachment plates (Corning, Corning, NY). Infected cells were maintained in 37°C in the tissue culture incubator for two days. At the day of the transplantation, the cells were dissociated into single cells using Dispase II (Roche Applied Science) and resuspended at 2,500 cell/10μl in RPMI and 1:1 mixed with Matrigel. Three week old female NOD/SCID mice were anesthetized and the number 4 and 9 inguinal mammary fat pads were cleared of endogenous epithelium by removing the tissue between the nipple and the lymph node following established procedures (Ehmann, Guzman et al. 1987). Then, 2,500 cells in 20μl RPMI:Matrigel were injected into the pre-cleared fat pads and the incision was closed with sutures. Mice were palpated weekly for tumor onset, starting two weeks after the operation. Mice were dissected 12 weeks after surgery when all tumors reached 1.5-2.0 cm in diameter. Or the primary tumors were surgical removed six weeks after transplantation to prolong the survival and dissected 20-24 weeks after the initial transplantation. All tumors were imaged using stereo fluorescence microscope (Leica) and collected for IHC.

Conclusions and Discussion:

An association of metastatic cell with decreased cell cohesion was recognized as early as 1944 by Coman (Coman 1944). However, cell adhesion molecule E-cadherin has been shown to have moderate to strong membrane expression in invasive ductal carcinomas, and fail to provide prognostic value (Acs, Lawton et al. 2001; Parker, Rampaul et al. 2001). My results from Par3 unveil an alternative mechanism by which cancer cells decrease cell cohesion without suppressing membrane E-cadherin protein levels. In cohesive cells, Par3 was localized to the adherens junction and was required to maintain the junction strength. Downregulation of Par3 decreased cell cohesion by activation of Tiam1 and an increase in levels of Rac-GTP in the cytosol, which led to aberrant actin remodeling and inhibition of E-cadherin adherens junction maturation. Inhibition of aberrant Rac activation restored E-cadherin junction maturation and blockade cell invasion. Par3 was present in a complex with E-cadherin and the Arp2/3. Downregulation of Par3 led to mislocalization of the Arp2/3 complex to the cytoplasm both in culture and *in vivo*, demonstrating a role for Par3 as a regulator of actin remodeling (Figure 8.1). In conclusion, my results identify the Par3 polarity protein as a metastasis suppressor that controls cell-cell cohesion by modulating Rac-GTP and actin dynamics at cell-cell junctions. Loss of Par3 allows tumor cells to detach from neighboring cells and further acquire invasiveness, which is required for the initiation of metastasis (Figure 1.7). From breast cancer therapy point of view, the proteins involved in regulating actin for tuning E-cadherin junction dynamics might be metastatic prognostic marker candidates and potential drug targets.

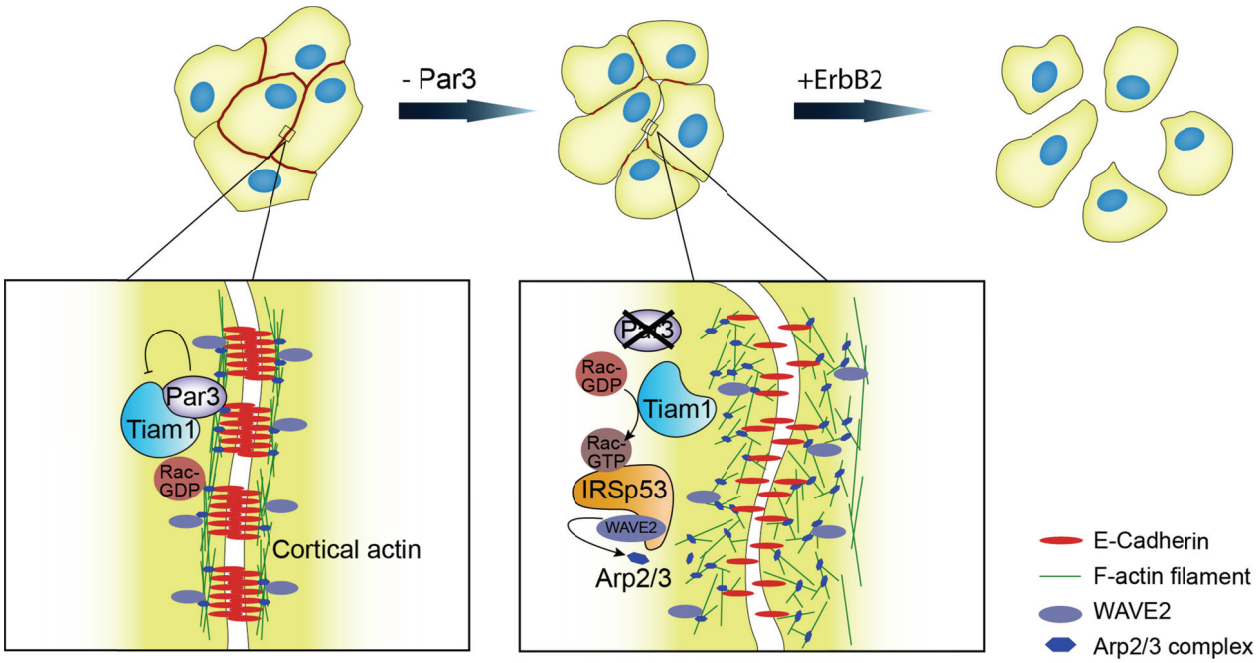

Figure 8.1. Proposed model for dysregulation of Par3 induced invasiveness in ErbB2-transformed cells.

Normal levels of Par3 inhibit the GEF Tiam1 and regulate Rac and Arp2/3 activity at cell-cell junction to promote formation of stable cortical actin and facilitate E-cadherin junction maturation (left). Downregulation of Par3 leads to activation of Tiam1 and constitutive increase of Rac-GTP in cytoplasm, mislocalizing and activating Arp2/3, in turn induces loss of compact cortical F-actin at cell-cell junctions and inhibition of E-cadherin junction maturation (middle).Activation of ErbB2 in the non-cohesive cells leads to cell invasion (right).

Discussion

My results provide new insights into mechanisms by which ErbB2-positive cancers progress. During human breast cancer progression (Figure 1.6), overexpression of ErbB2 is not observed in non-cancerous lesions such as hyperplasia and dysplastic lesions (Allred, Clark et al. 1992). In contrast, overexpression of ErbB2 is present in 56% of non-invasive DCIS, especially in 77% of the comedo DCIS, a subtype that is frequently associated with higher nuclear grade, aneuploidy, and a higher proliferation rate, and is clinically more aggressive (Allred, Clark et al. 1992; Bland and Copeland 2009). However, only 15% of IDC overexpressed ErbB2, suggesting a more important role of ErbB2 in initiation than in progression of ductal carcinomas (Allred,

Clark et al. 1992). Consistent with this possibility, transgenic mouse models overexpressing ErbB2 develop DCIS-like mammary tumors that metastasize infrequently (Ursini-Siegel, Schade et al. 2007). On the other hand, ErbB2 overexpression/amplification in breast cancer correlates with poor patient outcome (Reis-Filho et al. 2008), suggesting that although ErbB2 by itself is not sufficient to drive metastatic disease, it may cooperate with other events to promote progression. The nature and the identity of the events that cooperate with ErbB2 to promote metastasis are poorly understood.

Several members of the 14-3-3 protein family have been shown to be involved in ErbB2 tumor progression. The 14-3-3 protein family comprises a large number of highly conserved, small, acidic polypeptides of 28~33 kDa that are found in all eukaryotic species (Hurd, Fan et al. 2003; Nance 2005). In humans, seven 14-3-3 isoforms have been identified, which are β, γ, ε, η, σ, τ (sometimes referred to as θ) and ζ. Most of them are expressed in all tissues except 14-3-3σ, whose expression is restricted to epithelial cells. Among them, the *14-3-3σ* gene is frequently` lost in ErbB2-amplified breast cancer. Loss of 14-3-3σ resulted in a loss of epithelial polarity and ErbB2 tumor progression (Ling, Zuo et al. 2010) (See Appendix). In contrast, another 14-3-3 protein, 14-3-3ζ, is co-overexpressed with ErbB2 in DCIS. Overexpression of 14-3-3ζ reduced cell adhesion and increased migration by activating the TGF-β/Smad pathway that leads to EMT. Breast tumors overexpressing both ErbB2 and 14-3-3ζ showed higher rates of metastatic recurrence (Lu, Guo et al. 2009). Par3 has been shown to bind to 14-3-3σ and 14-3-3ζ, which is essential for the maintenance of cell polarity and cell junctions (Hurd, Fan et al. 2003; Benzinger, Muster et al. 2005; Ling, Zuo et al. 2010). These observations taken together with our results described in this thesis suggest that the Par3/14-3-3 signaling module is an important regulator of metastasis in ErbB2-overexpressing breast cancers.

Accumulating evidence has suggested that the EMT process, typically associated with normal development, may be a critical process in tumor progression (Thiery, Acloque et al. 2009). During normal development, epithelial cells lose adhesion and polarity, delaminate, and acquire an invasive, mesenchymal phenotype, thus facilitating migration to a site appropriate for organ formation (Thiery, Acloque et al. 2009). During neoplasia, a similar process is thought to occur at the tumor margins, allowing for cell invasion and eventual metastatic dissemination of cancer cells (Thiery 2002; Brabletz, Jung et al. 2005; Guarino, Rubino et al. 2007; Thiery,

Acloque et al. 2009). Recent studies using lineage-tracing reporters in the KrasG12D model for pancreatic ductal adenocarcinoma (PDAC) demonstrate a role for EMT during the development of metastasis. Even the pancreatic intraepithelial neoplasms (PanINs), the most common premalignant precursors for PDAC, harbor the cells that are predetermined to metastasize and migrate away from the pre-neoplasm into the surrounding tissue, as well as present EMT features such as loss of E-cadherin, upregulation of ZEB1, and elongated cell shape (Rhim, Mirek et al. 2012). However, our results from this study demonstrate that acquisition of metastatic behavior in Par3-loss cells was not accompanied by a gain of overt mesenchymal characteristics. The difference between KRasG12D-induced tumors in pancreas and ErbB2-induced tumors in breast suggests a tissue and oncogene-context specific role for EMT during metastasis. It also raises the possibility that tumors are unique from each other in the way they metastasize and the underlying mechanisms.

During normal development and cancer progression, many processes involve only transient loss of epithelial polarity without full acquisition of mesenchymal characteristics, referred to as partial-EMT. Among 18 human or mouse cell lines tested in culture, TGF-β, a strong EMT inducer, can only induce two cell lines (NMuMG and MCT cells) to undergo a complete EMT, accomplishing both morphological change and loss of E-cadherin (Brown, Aakre et al. 2004) . Some cells including Colo357, Panc-1 and HaCaT did not change morphology in response to TGF-β. Some cells lines such as HEK an HMEC-1012 displayed spindle-shape morphology but still retained junctional E-cadherin (Brown, Aakre et al. 2004), suggesting that EMT is a multistep process and requires complex regulation. The EMT transcription factors TWIST1 and TWIST2 are both important regulators of embryogenesis. Both *TWIST1* and *TWIST2* mRNA were overexpressed in MMTV-ErbB2-derived primary mammary tumors in mouse and a variety of human cancer-derived cell lines. Cells expressing TWIST1 or TWIST2 alone only induced partial-EMT with an incomplete decrease of E-cadherin and a modest increase of the mesenchymal intermediate filament vimentin. In contrast, expression of both TWIST1 (or TWIST2) and oncogenic H-Ras^{V12} (or ErbB2) triggered a complete loss of E-cadherin and an increase of vimentin, resulting in an acquisition of invasive properties and increasing the risk of metastatic dissemination (Ansieau, Bastid et al. 2008). In our study, it is also possible that shPar3 cells underwent a partial-EMT. As there are no specific markers to

define partial-EMT, we cannot rule out the possibility for partial-EMT during metastasis of shPar3 cells in culture and *in vivo*. Nevertheless, our study suggests that tumor epithelial cells can acquire metastatic potential in the absence of an overt mesenchymal phenotype, which adds an additional perspective to our understanding of cancer metastasis.

Tumor cell dyscohesion is known to correlate with metastatic disease in breast cancers and melanoma (Yu, Cajulis et al. 1998; Roxanis and Chow 2010). Our data suggest that loss of Par3 induces a constitutively high Rac-GTP level that promotes aberrant actin remodeling at cell-cell junctions and compromises cell-cell cohesion. We speculate that unregulated activation of the Arp2/3 complex as a result of deregulation of Par3 or other actin modulators may promote aberrant actin remodeling and compromise cell-cell cohesion to induce metastatic behavior of epithelial cells. Consistent with this possibility, dysregulation of proteins that modulate actin nucleation such as Arp2/3 and its upstream activators is frequently observed in multiple cancers and strongly correlates with cell invasion (Condeelis, Singer et al. 2005; Nurnberg, Kitzing et al. 2011). For example, coexpression of Arp2 and WAVE2 predicts poor outcome in invasive breast cancers (Iwaya, Norio et al. 2007). Elevated expression of both Cdc42 and Arp2/3 have been observed in invasive cells, and enhances N-WASp-dependent Arp2/3 activity, thereby leading to increased invadopodia dynamics and cell invasion (Mizutani, Miki et al. 2002; Yamaguchi, Lorenz et al. 2005). Loss of Arp2/3 inhibitors may also promote aggressive cancers. Consistent with this possibility, the genomic region containing α-catenin, an inhibitor of Arp2/3 (Drees, Pokutta et al. 2005), was deleted in three out of three metastases but retained in matched primary basal breast cancers (Ding, Ellis et al. 2010). It is possible that loss of α-catenin in cancer cells can lead to sustained Arp2/3 activity, which can inhibit cell cohesion and promote metastatic behavior (Benjamin and Nelson 2008). Therefore, Arp2/3 and its regulators are implicated in cancer metastasis. Understanding the mechanisms of actin regulation during tumor progression will provide us new insights into tumor cell behavior *in vivo*, which may result in new strategies for treatment of metastatic diseases.

Metastatic carcinomas are known to have significant loss of polarity, disordered differentiation and loss of lineage-specific markers. Although these changes can be highly pleomorphic, cells within the primary tumor as well as cells that migrate away from the primary tumor tend to retain significant epithelial characteristics such as expression of epithelial keratins,

mucins and E-cadherin (Thompson, Newgreen et al. 2005). Furthermore, the tumors growing at the sites of metastasis tend to retain epithelial characteristics (Thompson, Newgreen et al. 2005). It is thought that the tumor epithelium undergoes EMT during invasion and regains its epithelial state at the metastatic site by undergoing a MET (Thiery, Acloque et al. 2009). Our observations identify regulation of E-cadherin junction maturation, changes in cortical actin organization and cell-cell cohesion as an alternative avenue for tumor epithelial cells to metastasize. Deeper and broader understanding of the mechanisms by which epithelia deregulate cell-cell cohesion and acquire metastatic-epithelial properties will help to search for novel predictive biomarkers of tumors with metastatic potential and to delineate novel strategies to prevent metastasis.

Future Directions

Our study of the role of Par3 polarity protein in tumor progression opens more exciting questions. The obvious questions include: Does loss of Par3 occur in the primary breast tumor prior to metastasis or during tumor metastasis? How can cells with low Par3 levels be identified? How are Par3 levels regulated and what drives cells to dysregulate Par3? How does Par3 regulate the actin cytoskeleton? Moreover, is Par3 involved in regulating metastasis of other tumor types in addition to HER2-positive ductal breast carcinomas?

8.1 Intratumor heterogeneity

Breast cancer is a heterogeneous disease. Between tumors, there are numerous morphological and molecular variations, which provide the base for tumor classification, disease prognosis and design of individualized therapies. With the latest development of the techniques to widely study small populations of cells or even single cell genome, evidence is emerging that cancer cells within human tumors frequently display heterogeneity of various traits related to tumorigenesis, drug resistance, angiogenic and metastatic potential (Polyak, Shipitsin et al. 2009). The recent work in renal carcinomas shows the primary tumor has extensive spatial tumor heterogeneity of branching evolutional relationship. The tumor cells in the metastasis site

resemble some subclones in the primary tumor but accumulating additional genetic alterations (Gerlinger, Rowan et al. 2012). As we have observed the differences of Par3 levels between primary and metastasis sites, the question arises as to whether loss of Par3 occurs in the primary site or during the metastasis dissemination? To address this question, we can collect circulating tumor cells from human patients or mice, and examine Par3 expression in them. As we have only compared the protein levels of Par3 in human breast cancer samples in our study, it is still unclear whether Par3 is dysregulated at the genomic level or the post-transcriptional level and how the dysregulation occurs. In Gerlinger's work, a histone H3K36 methyltransferase SETD2 was found to be commonly lost in the metastases and in the precursor region of the primary tumor, but not in the other parts of primary tumor (Gerlinger, Rowan et al. 2012), suggesting that the chromatin remodeling is also changed during tumor progression. Therefore, it could also be important to take the epigenetic mechanism of gene silencing into consideration. Dysregulation of other polarity proteins like Scribble, or Dlg1 cooperates with oncogenes to induce invasive behavior (Chatterjee, Seifried et al. 2012). Further investigations into other polarity proteins will help to understand the bigger picture of dysregulation of cell polarity mechanisms during tumor progression.

8.2 Phosphorylation as a biochemical mechanism for regulating Par3 function

There is emerging evidence for protein phosphorylation as a key mechanism by which polarity proteins are regulated. It has been shown that phosphorylation of Par3 by aPKC at serines 827 and 114 regulates the interaction of Par3-aPKC and 14-3-3ζ (Hirose, Izumi et al. 2002; Hurd, Fan et al. 2003). EGF-induced tyrosine phosphorylation of Par3 (Tyr 1127) via c-Src and c-Yes reduces the association of Par3 with LIM kinase 2 and regulates tight junction assembly (Wang, Du et al. 2006). Drosophila Aurora A kinase binds and phosphorylates Par3 at Ser 962, which is required for Par3 to establish neuron polarity (Khazaei and Püschel 2009). Rho-kinase/ROCK/ROK, an effector of RhoA, phosphorylates Par3 at Thr833 and disrupts its interaction with aPKC and Par6 at the leading edge of migrating cells (Nakayama, Goto et al. 2008). In 10A.B2 cells, I found that Par3 was phosphorylated at both tyrosine and serine upon ErbB2 activation (Figure 8.2). It is not clear whether this Par3 phosphorylation is involved in

actin cytoskeleton regulation and maintaining the junction strength during ErbB2 activation. Future work can be carried out to identify the phosphorylation sites and investigate the role of Par3 phosphorylation in cell-cell junction regulation and tumor progression. A finer understanding of the biochemical regulation of Par3 might provide a potential therapeutic approach.

8.3 Par3 mislocalization

While examining Par3 protein levels in human breast cancer samples, we also observed that Par3 was mislocalized to the cytoplasm in a small portion of samples (Figure 8.3). In these tumor cells, although the total Par3 expression level was high, the E-cadherin junction was severely disrupted. Correct localization of polarity proteins has been shown as an important requirement for their functions. For instance, junctional localization of Scrib is crucial for its protein function. A point mutation in the LRR domain of Scrib can mislocalize it from cell-cell junctions, leading to defects in cell polarization. In breast cancer, more than half of DCIS has mislocalization of Scribble protein, suggesting the importance of correct localization of Scrib for normal tissue organization (Zhan, Rosenberg et al. 2008). Likewise, it is possible that mislocalization of Par3 impairs its function and is implicated in the disease. It will be important to use available cancer genome data and look for mutations in Par3 and other polarity proteins that can potentially cause protein mislocalization and further characterize the effects of these mutations. As described in Chapter 2, sPar3, a splicing variant of Par3, shows cytoplasmic localization in mature epithelial cells, differing from full length Par3. Studies also need to be focused on gaining knowledge of the splicing machinery in regulating Par3 and cell polarity.

8.4 Cooperation with other oncogenic alterations

In this study, we mainly focused on the role of Par3 in ErbB2-induced breast cancer. Although the induction of invasive behavior in shPar3 cells requires ErbB2 activation, loss of Par3 alone is already sufficient to alter the actin dynamics and weaken the cell-cell junctions. In

addition, pioneer work done in *Drosophila* shows a synergetic induction of metastatic behavior between oncogenic RasV12 and inactivation of Par3 (Bazooka) (Pagliarini and Xu 2003). Taken together, this evidence suggests that Par3 may play a role in tumor progression mediated by other oncogenes, and is not limited to breast tissue. Additional work will be required to define the role of Par3 polarity protein in tumors of different tissue type and oncogenic background.

8.5 Biomarkers for tumor cell cohesion

Here our results uncovered a new mechanism employed by tumor cells to break cell-cell cohesion and initiate metastasis. More significantly, we found ARPC2 as a marker to identify those "epithelial-like" cells with weakened cell-cell cohesion and metastable potential. This raises the possibility that a new class of molecules including the actin modulators can be employed as biomarkers for pre-metastatic tumor cells with decreased cohesion. Clinically, this will pose challenges on the current diagnostic procedure including the biopsy sampling issue, choosing the biomarkers that can represent the metastatic capability, application of new techniques to measure cell cohesion mechanically, and development of new IHC scoring system to include protein sublocalization as a parameter. As technology evolves, more analyses will give way to methods aimed at acquiring cell morphological information at the individual cell level, which will shed light into the capture of early metastatic cells.

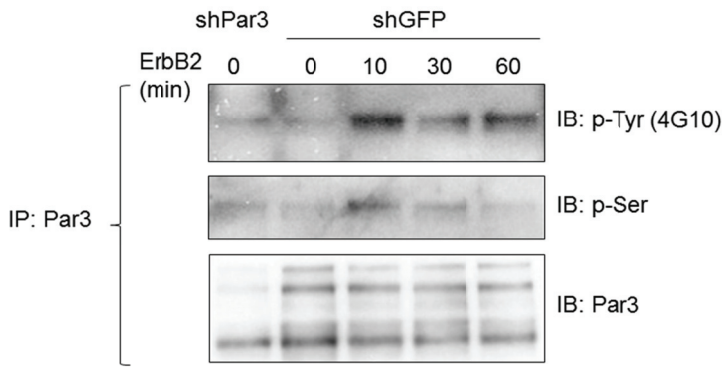

Figure 8.2. Phosphorylation of Par3 upon ErbB2 activation

Confluent monolayers of 10A.B2 cells were stimulated with ErbB2 dimerizer for the indicated time period. Par3 was immunoprecipitated and immunoblots were probed for phospho-tyrosine or phospho-serine.

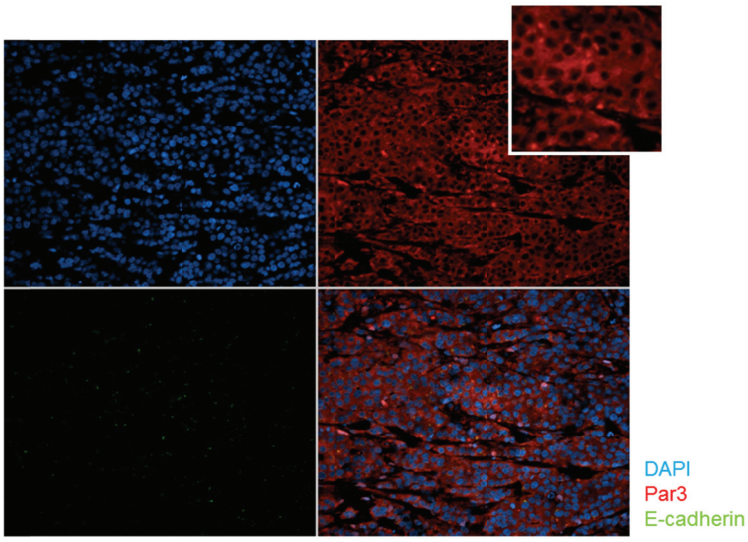

Figure 8.3. Mislocalization of Par3 in human breast cancer sample

Representative image of mislocalized Par3 protein from IHC staining for Par3 (red) and E-cadherin (green) protein human IBC tumor microarray samples.

Reference List

ACS, G., T. J. LAWTON, ET AL. (2001). Differential expression of E-cadherin in lobular and ductal neoplasms of the breast and its biologic and diagnostic implications. *American journal of clinical pathology* **115**(1): 85-98.

AKHTAR, N. AND N. A. HOTCHIN (2001). RAC1 regulates adherens junctions through endocytosis of E-cadherin. *Mol Biol Cell* **12**(4): 847-862.

ALLRED, D. C., G. M. CLARK, ET AL. (1992). Overexpression of HER-2/ *neu* and its relationship with other prognostic factors change during the progression of in situ to invasive breast cancer. *Human pathology* **23**(9): 974-979.

ALLRED, D. C., J. M. HARVEY, ET AL. (1998). Prognostic and predictive factors in breast cancer by immunohistochemical analysis. *Mod Pathol* **11**(2): 155-168.

ALVARADO, D., D. E. KLEIN, ET AL. (2009). ErbB2 resembles an autoinhibited invertebrate epidermal growth factor receptor. *Nature* **461**(7261): 287-291.

ANDRECHEK, E. R., W. R. HARDY, ET AL. (2000). Amplification of the neu/erbB-2 oncogene in a mouse model of mammary tumorigenesis. *Proc. Natl Acad. Sci. USA* **97**(7): 3444-3449.

ANGRES, B., A. BARTH, ET AL. (1996). Mechanism for transition from initial to stable cell-cell adhesion: kinetic analysis of E-cadherin-mediated adhesion using a quantitative adhesion assay. *J Cell Biol* **134**(2): 549-557.

ANSIEAU, S., J. BASTID, ET AL. (2008). Induction of EMT by Twist Proteins as a Collateral Effect of Tumor-Promoting Inactivation of Premature Senescence. *Cancer Cell* **14**(1): 79-89.

AOKI, K. AND M. MATSUDA (2009). Visualization of small GTPase activity with fluorescence resonance energy transfer-based biosensors. *Nature protocols* **4**(11): 1623-1631.

ARANDA, V., T. HAIRE, ET AL. (2006). Par6-aPKC uncouples ErbB2 induced disruption of polarized epithelial organization from proliferation control. *Nat Cell Biol* **8**(11): 1235-1245.

ARNOLD, A. AND A. PAPANIKOLAOU (2005). Cyclin D1 in Breast Cancer Pathogenesis. *Journal of clinical oncology : official journal of the American Society of Clinical Oncology* **23**(18): 4215-4224.

ARTHUR, W. T., S. M. ELLERBROEK, ET AL. (2002). XPLN, a Guanine Nucleotide Exchange Factor for RhoA and RhoB, But Not RhoC. *Journal of Biological Chemistry* **277**(45): 42964-42972.

BALIC, M., H. LIN, ET AL. (2006). Most early disseminated cancer cells detected in bone marrow of breast cancer patients have a putative breast cancer stem cell phenotype. *Clinical*

cancer research : an official journal of the American Association for Cancer Research **12**(19): 5615-5621.

BARR, F. A. AND J. EGERER (2005). Golgi positioning: are we looking at the right MAP? *J Cell Biol* **168**(7): 993-998.

BASELGA, J., I. BRADBURY, ET AL. (2012). Lapatinib with trastuzumab for HER2-positive early breast cancer (NeoALTTO): a randomised, open-label, multicentre, phase 3 trial. *The Lancet* **379**(9816): 633-640.

BAUM, B. AND M. GEORGIOU (2011). Dynamics of adherens junctions in epithelial establishment, maintenance, and remodeling. *J Cell Biol* **192**(6): 907-917.

BELOTTI, D., P. PAGANONI, ET AL. (2003). Matrix metalloproteinases (MMP9 and MMP2) induce the release of vascular endothelial growth factor (VEGF) by ovarian carcinoma cells: implications for ascites formation. *Cancer Res* **63**: 5224-5233.

BENJAMIN, J. M. AND W. J. NELSON (2008). Bench to bedside and back again: molecular mechanisms of alpha-catenin function and roles in tumorigenesis. *Seminars in cancer biology* **18**(1): 53-64.

BENTON, R. AND D. S. JOHNSTON (2003). *Drosophila* PAR-1 and 14-3-3 Inhibit Bazooka/PAR-3 to Establish Complementary Cortical Domains in Polarized Cells. *Cell* **115**(6): 691-704.

BENZINGER, A., N. MUSTER, ET AL. (2005). Targeted proteomic analysis of 14-3-3 sigma, a p53 effector commonly silenced in cancer. *Molecular & cellular proteomics : MCP* **4**(6): 785-795.

BERNADSKAYA, Y. Y., F. B. PATEL, ET AL. (2011). Arp2/3 promotes junction formation and maintenance in the Caenorhabditis elegans intestine by regulating membrane association of apical proteins. *Mol Biol Cell* **22**(16): 2886-2899.

BILDER, D., M. LI, ET AL. (2000). Cooperative regulation of cell polarity and growth by Drosophila tumor suppressors. *Science* **289**(5476): 113-116.

BILDER, D. AND N. PERRIMON (2000). Localization of apical epithelial determinants by the basolateral PDZ protein Scribble. *Nature* **403**(6770): 676-680.

BISSELL, M. J. AND D. BILDER (2003). Polarity determination in breast tissue: desmosomal adhesion, myoepithelial cells, and laminin 1. *Breast cancer research : BCR* **5**(2): 117-119.

Bland, K. I. and E. M. Copeland (2009). The breast comprehensive management of benign and malignant diseases. Philadelphia, PA, Saunders/Elsevier.

BOIMEL, P., T. SMIRNOVA, ET AL. (2012). Contribution of CXCL12 secretion to invasion of breast cancer cells. *Breast cancer research : BCR* **14**.

BORRELL-PAGES, M., F. ROJO, ET AL. (2003). TACE is required for the activation of the EGFR by TGF-[alpha] in tumors. *EMBO J* **22**(5): 1114-1124.

BOS, P. D., X. H. F. ZHANG, ET AL. (2009). Genes that mediate breast cancer metastasis to the brain. *Nature* **459**(7249): 1005-U1137.

BRABLETZ, T., A. JUNG, ET AL. (2005). Opinion: migrating cancer stem cells - an integrated concept of malignant tumour progression. *Nat Rev Cancer* **5**(9): 744-749.

BRAGA, V. (2000). Epithelial cell shape: cadherins and small GTPases. *Exp Cell Res* **261**(1): 83-90.

BRAGA, V. M., L. M. MACHESKY, ET AL. (1997). The small GTPases Rho and Rac are required for the establishment of cadherin-dependent cell-cell contacts. *J Cell Biol* **137**(6): 1421-1431.

BRIAND, P., O. W. PETERSEN, ET AL. (1987). A new diploid nontumorigenic human breast epithelial cell line isolated and propagated in chemically defined medium. *In vitro cellular & developmental biology : journal of the Tissue Culture Association* **23**(3): 181-188.

BROWN, K., M. AAKRE, ET AL. (2004). Induction by transforming growth factor-beta1 of epithelial to mesenchymal transition is a rare event in vitro. *Breast cancer research : BCR* **6**(3): R215-231.

CAMPBELL, P. J., S. YACHIDA, ET AL. (2010). The patterns and dynamics of genomic instability in metastatic pancreatic cancer. *Nature* **467**(7319): 1109-1113.

CARDIFF, R. D. AND S. R. WELLINGS (1999). The comparative pathology of human and mouse mammary glands. *J Mammary Gland Biol Neoplasia* **4**(1): 105-122.

CAVEY, M., M. RAUZI, ET AL. (2008). A two-tiered mechanism for stabilization and immobilization of E-cadherin. *Nature* **453**(7196): 751-756.

CEREIJIDO, M., E. S. ROBBINS, ET AL. (1978). Polarized monolayers formed by epithelial cells on a permeable and translucent support. *J Cell Biol* **77**(3): 853-880.

CHATTERJEE, S., L. SEIFRIED, ET AL. (2012). Dysregulation of cell polarity proteins synergize with oncogenes or the microenvironment to induce invasive behavior in epithelial cells. *PLoS ONE* **7**(4): e34343.

CHEN, X. AND I. G. MACARA (2005). Par-3 controls tight junction assembly through the Rac exchange factor Tiam1. *Nat Cell Biol* **7**(3): 262-269.

CHIANG, A. C. AND J. MASSAGUE (2008). Molecular Basis of Metastasis. *New Engl J Med* **359**(26): 2814-2823.

CHU, Y. S., W. A. THOMAS, ET AL. (2004). Force measurements in E-cadherin-mediated cell doublets reveal rapid adhesion strengthened by actin cytoskeleton remodeling through Rac and Cdc42. *J Cell Biol* **167**(6): 1183-1194.

COMAN, D. R. (1944). Decreased Mutual Adhesiveness, a Property of Cells from Squamous Cell Carcinomas. *Cancer Research* **4**(10): 625-629.

CONDEELIS, J. AND J. SEGALL (2003). Intravital imaging of cell movement in tumours. *Nat Rev Cancer* **3**: 921-951.

CONDEELIS, J., R. SINGER, ET AL. (2005). The great escape: when cancer cells hijack the genes for chemotaxis and motility. *Annu Rev Cell Dev Bi* **21**: 695-1413.

COUSSENS, L., T. L. YANG-FENG, ET AL. (1985). Tyrosine kinase receptor with extensive homology to EGF receptor shares chromosomal location with neu oncogene. *Science* **230**(4730): 1132-1139.

CSERNI, G. (2002). Tumour histological grade may progress between primary and recurrent invasive mammary carcinoma. *Journal of clinical pathology* **55**(4): 293-297.

D'SOUZA, B. AND J. TAYLOR-PAPADIMITRIOU (1994). Overexpression of ERBB2 in human mammary epithelial cells signals inhibition of transcription of the E-cadherin gene. *Proc Natl Acad Sci U S A* **91**(15): 7202-7206.

DAVALOS, V., C. MOUTINHO, ET AL. (2011). Dynamic epigenetic regulation of the microRNA-200 family mediates epithelial and mesenchymal transitions in human tumorigenesis. *Oncogene*.

DAWSON, J., Z. BU, ET AL. (2007). Ligand-induced structural transitions in ErbB receptor extracellular domains. *Structure (London, England : 1993)* **15**(8): 942-954.

DEBNATH, J., K. R. MILLS, ET AL. (2002). The role of apoptosis in creating and maintaining luminal space within normal and oncogene-expressing mammary acini. *Cell* **111**(1): 29-40.

DEBNATH, J., S. K. MUTHUSWAMY, ET AL. (2003). Morphogenesis and oncogenesis of MCF-10A mammary epithelial acini grown in three-dimensional basement membrane cultures. *Methods* **30**(3): 256-268.

DEBNATH, J., S. J. WALKER, ET AL. (2003). Akt activation disrupts mammary acinar architecture and enhances proliferation in an mTOR-dependent manner. *J Cell Biol* **163**(2): 315-326.

DELANEY, P. (1999). HER-2 : The Making of Herceptin, a Revolutionary Treatment for Breast Cancer. *Journal of the National Cancer Institute* **91**(15): 1329-1330.

DIFIORE, P. P., J. H. PIERCE, ET AL. (1987). Erbb-2 Is a Potent Oncogene When Overexpressed in Nih/3t3 Cells. *Science* **237**(4811): 178-182.

DING, L., M. J. ELLIS, ET AL. (2010). Genome remodelling in a basal-like breast cancer metastasis and xenograft. *Nature* **464**(7291): 999-1005.

DONG, Z., R. KUMAR, ET AL. (1997). Macrophage-derived metalloelastase is responsible for the generation of angiostatin in Lewis lung carcinoma. *Cell* **88**: 801-811.

DOUMA, S., T. VAN LAAR, ET AL. (2004). Suppression of anoikis and induction of metastasis by the neurotrophic receptor TrkB. *Nature* **430**(7003): 1034-1039.

DREES, F., S. POKUTTA, ET AL. (2005). Alpha-catenin is a molecular switch that binds E-cadherin-beta-catenin and regulates actin-filament assembly. *Cell* **123**(5): 903-915.

DU, D., F. XU, ET AL. (2010). The tight junction protein, occludin, regulates the directional migration of epithelial cells. *Dev Cell* **18**(1): 52-63.

EBNET, K., A. SUZUKI, ET AL. (2001). The cell polarity protein ASIP/PAR-3 directly associates with junctional adhesion molecule (JAM). *EMBO J* **20**(14): 3738-3748.

EDER, A. M., X. SUI, ET AL. (2005). Atypical PKCι contributes to poor prognosis through loss of apical-basal polarity and Cyclin E overexpression in ovarian cancer. *Proc Natl Acad Sci U S A* **102**(35): 12519-12524.

EGEBLAD, M. AND Z. WERB (2002). New functions for the matrix metalloproteinases in cancer progression. *Nat Rev Cancer* **2**: 161-235.

EHMANN, U. K., R. C. GUZMAN, ET AL. (1987). Cultured mouse mammary epithelial cells: normal phenotype after implantation. *J Natl Cancer Inst* **78**(4): 751-757.

ELSTON, C. W. AND I. O. ELLIS (2002). Pathological prognostic factors in breast cancer. I. The value of histological grade in breast cancer: experience from a large study with long-term follow-up. *Histopathology* **41**(3A): 154-161.

ELSTON, C. W. AND I. O. ELLIS (2002). Pathological prognostic factors in breast cancer. I. The value of histological grade in breast cancer: experience from a large study with long-term follow-up. C. W. Elston & I. O. Ellis. Histopathology 1991; 19; 403-410. *Histopathology* **41**(3A): 151-152, discussion 152-153.

ETEMAD-MOGHADAM, B., S. GUO, ET AL. (1995). Asymmetrically distributed PAR-3 protein contributes to cell polarity and spindle alignment in early C. elegans embryos. *Cell* **83**(5): 743-752.

FARRAR, M. A., I. ALBEROL, ET AL. (1996). Activation of the Raf-1 kinase cascade by coumermycin-induced dimerization. *Nature* **383**(6596): 178-181.

FARRAR, M. A., S. H. OLSON, ET AL. (2000). Coumermycin-induced dimerization of GyrB-containing fusion proteins. *Methods in enzymology* **327**: 421-429.

FEIGE, J. N., D. SAGE, ET AL. (2005). PixFRET, an ImageJ plug-in for FRET calculation that can accommodate variations in spectral bleed-throughs. *Microscopy research and technique* **68**(1): 51-58.

FEIGIN, M. AND S. MUTHUSWAMY (2009). Polarity proteins regulate mammalian cell-cell junctions and cancer pathogenesis. *Current Opinion in Cell Biology* **21**: 694-700.

FENG, W., H. WU, ET AL. (2008). Par-3-mediated junctional localization of the lipid phosphatase PTEN is required for cell polarity establishment. *J Biol Chem* **283**(34): 23440-23449.

FERGUSON, K. (2008). Structure-based view of epidermal growth factor receptor regulation. *Annual review of biophysics* **37**: 353-373.

FERGUSON, K., M. BERGER, ET AL. (2003). EGF activates its receptor by removing interactions that autoinhibit ectodomain dimerization. *Mol Cell* **11**: 507-517.

FERRER-VAQUER, A., M. VIOTTI, ET AL. (2010). Transitions between epithelial and mesenchymal states and the morphogenesis of the early mouse embryo. *Cell Adhesion & Migration* **4**(3): 447-457.

FIDLER, I. (2003). The pathogenesis of cancer metastasis: the 'seed and soil' hypothesis revisited. *Nat Rev Cancer* **3**: 453-461.

FISCHER, E., E. LEGUE, ET AL. (2006). Defective planar cell polarity in polycystic kidney disease. *Nat Genet* **38**(1): 21-23.

FOLEY, J., N. K. NICKERSON, ET AL. (2010). EGFR signaling in breast cancer: bad to the bone. *Seminars in cell & developmental biology* **21**(9): 951-960.

FRIEDL, P. AND K. WOLF (2003). Tumour-cell invasion and migration: diversity and escape mechanisms. *Nat Rev Cancer* **3**(5): 362-374.

GAO, L., I. G. MACARA, ET AL. (2002). Multiple splice variants of Par3 and of a novel related gene, Par3L, produce proteins with different binding properties. *Gene* **294**(1-2): 99-107.

GARCIA-MATA, R., K. WENNERBERG, ET AL. (2006). Analysis of activated GAPs and GEFs in cell lysates. *Methods Enzymol* **406**: 425-437.

GARRETT, T. P., N. M. MCKERN, ET AL. (2003). The crystal structure of a truncated ErbB2 ectodomain reveals an active conformation, poised to interact with other ErbB receptors. *Mol Cell* **11**(2): 495-505.

GEORGIOU, M., E. MARINARI, ET AL. (2008). Cdc42, Par6, and aPKC Regulate Arp2/3-Mediated Endocytosis to Control Local Adherens Junction Stability. *Current Biology* **18**(21): 1631-1638.

GERLINGER, M., A. J. ROWAN, ET AL. (2012). Intratumor heterogeneity and branched evolution revealed by multiregion sequencing. *The New England journal of medicine* **366**(10): 883-892.

GODFREY, J. C. AND K. E. PRICE (1972). Structure-activity relationships in coumermycins. *Advances in applied microbiology* **15**: 231-296.

GOEHRING, N. W., D. CHOWDHURY, ET AL. (2010). FRAP Analysis of Membrane-Associated Proteins: Lateral Diffusion and Membrane-Cytoplasmic Exchange. *Biophysical Journal* **99**(8): 2443-2452.

GOLEY, E. D. AND M. D. WELCH (2006). The ARP2/3 complex: an actin nucleator comes of age. *Nat Rev Mol Cell Biol* **7**(10): 713-726.

Gonzalez-Mariscal, L. and SpringerLink (2006). Tight junctions. Molecular biology intelligence unit. Georgetown, Tex. New York, N.Y., Landes Bioscience/Eurekah.com ; Springer Science+Business Media**:** 224 p.

GOSWAMI, S., E. SAHAI, ET AL. (2005). Macrophages promote the invasion of breast carcinoma cells via a colony-stimulating factor-1/epidermal growth factor paracrine loop. *Cancer Res* **65**: 5278-5361.

GRASSIAN, A. R., Z. T. SCHAFER, ET AL. (2011). ErbB2 stabilizes epidermal growth factor receptor (EGFR) expression via Erk and Sprouty2 in extracellular matrix-detached cells. *J Biol Chem* **286**(1): 79-90.

GRAUSPORTA, D., R. R. BEERLI, ET AL. (1997). ErbB-2, the preferred heterodimerization partner of all ErbB receptors, is a mediator of lateral signaling. *EMBO J* **16**(7): 1647-1655.

GUARINO, M., B. RUBINO, ET AL. (2007). The role of epithelial-mesenchymal transition in cancer pathology. *Pathology* **39**(3): 305-318.

GUDJONSSON, T., L. RONNOV-JESSEN, ET AL. (2002). Normal and tumor-derived myoepithelial cells differ in their ability to interact with luminal breast epithelial cells for polarity and basement membrane deposition. *J Cell Sci* **115**(Pt 1): 39-50.

GULLI, M. P. AND M. PETER (2001). Temporal and spatial regulation of Rho-type guanine-nucleotide exchange factors: the yeast perspective. *Genes Dev* **15**(4): 365-379.

GULLIFORD, T. J., G. C. HUANG, ET AL. (1997). Reduced ability of transforming growth factor-alpha to induce EGF receptor heterodimerization and downregulation suggests a mechanism of oncogenic synergy with ErbB2. *Oncogene* **15**(18): 2219-2223.

GUMBINER, B., B. STEVENSON, ET AL. (1988). The role of the cell adhesion molecule uvomorulin in the formation and maintenance of the epithelial junctional complex. *J Cell Biol* **107**(4): 1575-1587.

GUY, C. T., M. A. WEBSTER, ET AL. (1992). Expression of the neu protooncogene in the mammary epithelium of transgenic mice induces metastatic disease. *Proc Natl Acad Sci U S A* **89**(22): 10578-10582.

HAJRA, K. M., X. JI, ET AL. (1999). Extinction of E-cadherin expression in breast cancer via a dominant repression pathway acting on proximal promoter elements. *Oncogene* **18**(51): 7274-7279.

HALL, A. (1998). Rho GTPases and the Actin Cytoskeleton. *Science* **279**(5350): 509-514.

HAMMOND, M. E., D. F. HAYES, ET AL. (2010). American Society of Clinical Oncology/College of American Pathologists guideline recommendations for immunohistochemical testing of estrogen and progesterone receptors in breast cancer (unabridged version). *Archives of pathology & laboratory medicine* **134**(7): e48-72.

HANDLER, J. S. (1989). Overview of epithelial polarity. *Annu Rev Physiol* **51**: 729-740.

HAO, Y., L. BOYD, ET AL. (2006). Stabilization of cell polarity by the C. elegans RING protein PAR-2. *Dev Cell* **10**(2): 199-208.

HARVEY, J. M., G. M. CLARK, ET AL. (1999). Estrogen receptor status by immunohistochemistry is superior to the ligand-binding assay for predicting response to adjuvant endocrine therapy in breast cancer. *Journal of clinical oncology : official journal of the American Society of Clinical Oncology* **17**(5): 1474-1481.

HEASMAN, S. J. AND A. J. RIDLEY (2008). Mammalian Rho GTPases: new insights into their functions from in vivo studies. *Nat Rev Mol Cell Biol* **9**(9): 690-701.

HENNIGHAUSEN, L. AND G. W. ROBINSON (2005). Information networks in the mammary gland. *Nat Rev Mol Cell Biol* **6**(9): 715-725.

HIDALGO-CARCEDO, C., S. HOOPER, ET AL. (2011). Collective cell migration requires suppression of actomyosin at cell-cell contacts mediated by DDR1 and the cell polarity regulators Par3 and Par6. *Nat Cell Biol* **13**(1): 49-58.

HINGORANI, S., E. PETRICOIN, ET AL. (2003). Preinvasive and invasive ductal pancreatic cancer and its early detection in the mouse. *Cancer Cell* **4**: 437-487.

HINGORANI, S., L. WANG, ET AL. (2005). Trp53R172H and KrasG12D cooperate to promote chromosomal instability and widely metastatic pancreatic ductal adenocarcinoma in mice. *Cancer Cell* **7**: 469-552.

HIRAGURI, S., T. GODFREY, ET AL. (1998). Mechanisms of Inactivation of E-Cadherin in Breast Cancer Cell Lines. *Cancer Res* **58**(9): 1972-1977.

HIRANO, Y., S. YOSHINAGA, ET AL. (2005). Structure of a Cell Polarity Regulator, a Complex between Atypical PKC and Par6 PB1 Domains. *The Journal of biological chemistry* **280**(10): 9653-9661.

HIROHASHI, S. (1998). Inactivation of the E-cadherin-mediated cell adhesion system in human cancers. *Am J Pathol* **153**(2): 333-339.

HIROSE, T., Y. IZUMI, ET AL. (2002). Involvement of ASIP/PAR-3 in the promotion of epithelial tight junction formation. *J Cell Sci* **115**(Pt 12): 2485-2495.

HODGSON, J. G., T. MALEK, ET AL. (2005). Copy Number Aberrations in Mouse Breast Tumors Reveal Loci and Genes Important in Tumorigenic Receptor Tyrosine Kinase Signaling. *Cancer Res* **65**(21): 9695-9704.

HODGSON, L., F. SHEN, ET AL. (2010). Biosensors for characterizing the dynamics of rho family GTPases in living cells. *Current protocols in cell biology / editorial board, Juan S. Bonifacino ... [et al.]* **Chapter 14**: Unit 14 11 11-26.

HOLBRO, T., R. R. BEERLI, ET AL. (2003). The ErbB2/ErbB3 heterodimer functions as an oncogenic unit: ErbB2 requires ErbB3 to drive breast tumor cell proliferation. *Proc Natl Acad Sci U S A* **100**(15): 8933-8938.

HOLGADO-MADRUGA, M., D. R. EMLET, ET AL. (1996). A Grb2-associated docking protein in EGF- and insulin-receptor signalling. *Nature* **379**(6565): 560-564.

HOQUE, A., N. SNEIGE, ET AL. (2002). HER-2/neu Gene Amplification in Ductal Carcinoma In Situ of the Breast. *Cancer Epidemiology Biomarkers & Prevention* **11**(6): 587-590.

HORIKOSHI, Y., A. SUZUKI, ET AL. (2009). Interaction between PAR-3 and the aPKC-PAR-6 complex is indispensable for apical domain development of epithelial cells. *J Cell Sci* **122**(Pt 10): 1595-1606.

HOWE, A., A. APLIN, ET AL. (1998). Integrin signaling and cell growth control. *Curr Opin Cell Biol* **10**(2): 220-231.

HUANG, L. AND S. K. MUTHUSWAMY (2010). Polarity protein alterations in carcinoma: a focus on emerging roles for polarity regulators. *Curr Opin Genet Dev* **20**(1): 41-50.

HURD, T. W., S. FAN, ET AL. (2003). Phosphorylation-dependent binding of 14-3-3 to the polarity protein Par3 regulates cell polarity in mammalian epithelia. *Curr Biol* **13**(23): 2082-2090.

HÜSEMANN, Y., J. B. GEIGL, ET AL. (2008). Systemic Spread Is an Early Step in Breast Cancer. *Cancer cell* **13**(1): 58-68.

HYNES, R. O. (2009). The Extracellular Matrix: Not Just Pretty Fibrils. *Science* **326**(5957): 1216-1219.

IDEN, S. AND J. G. COLLARD (2008). Crosstalk between small GTPases and polarity proteins in cell polarization. *Nat Rev Mol Cell Biol* **9**(11): 846-859.

ITO, M., H. HIRAMATSU, ET AL. (2002). NOD/SCID/gamma(c)(null) mouse: an excellent recipient mouse model for engraftment of human cells. *Blood* **100**(9): 3175-3182.

ITOH, M. AND M. J. BISSELL (2003). The organization of tight junctions in epithelia: implications for mammary gland biology and breast tumorigenesis. *J Mammary Gland Biol Neoplasia* **8**(4): 449-462.

ITOH, N., M. NAKAYAMA, ET AL. (2010). Identification of focal adhesion kinase (FAK) and phosphatidylinositol 3-kinase (PI3-kinase) as Par3 partners by proteomic analysis. *Cytoskeleton (Hoboken)* **67**(5): 297-308.

ITOH, R. E., K. KUROKAWA, ET AL. (2002). Activation of rac and cdc42 video imaged by fluorescent resonance energy transfer-based single-molecule probes in the membrane of living cells. *Mol Cell Biol* **22**(18): 6582-6591.

IWAYA, K., K. NORIO, ET AL. (2007). Coexpression of Arp2 and WAVE2 predicts poor outcome in invasive breast carcinoma. *Mod Pathol* **20**(3): 339-343.

IZUMI, Y., T. HIROSE, ET AL. (1998). An atypical PKC directly associates and colocalizes at the epithelial tight junction with ASIP, a mammalian homologue of Caenorhabditis elegans polarity protein PAR-3. *J Cell Biol* **143**(1): 95-106.

JAFFE, A. B. AND A. HALL (2005). Rho GTPases: biochemistry and biology. *Annu Rev Cell Dev Biol* **21**: 247-269.

JANDA, E., K. LEHMANN, ET AL. (2002). Ras and TGF[beta] cooperatively regulate epithelial cell plasticity and metastasis: dissection of Ras signaling pathways. *J Cell Biol* **156**(2): 299-313.

JAYANTA DEBNATH, S. K. M., AND JOAN S. BRUGGE (2003). Morphogenesis and oncogenesis of MCF-10A mammary epithelial acini grown in three-dimensional basement membrane cultures *Methods* **Volume 30**(Issue 3): 256-268.

JOBERTY, G., C. PETERSEN, ET AL. (2000). The cell-polarity protein Par6 links Par3 and atypical protein kinase C to Cdc42. *Nat Cell Biol* **2**(8): 531-539.

KAIBUCHI, K., S. KURODA, ET AL. (1999). Regulation of the cytoskeleton and cell adhesion by the Rho family GTPases in mammalian cells. *Annu Rev Biochem* **68**: 459-486.

KANG, Y. B., P. M. SIEGEL, ET AL. (2003). A multigenic program mediating breast cancer metastasis to bone. *Cancer Cell* **3**(6): 537-549.

KARP, C. M., T. T. TAN, ET AL. (2008). Role of the Polarity Determinant Crumbs in Suppressing Mammalian Epithelial Tumor Progression. *Cancer Res* **68**(11): 4105-4115.

KEATING, T. J., J. G. PELOQUIN, ET AL. (1997). Microtubule release from the centrosome. *Proc Natl Acad Sci U S A* **94**(10): 5078-5083.

KEELY, P., J. WU, ET AL. (1995). The spatial and temporal expression of the alpha 2 beta 1 integrin and its ligands, collagen I, collagen IV, and laminin, suggest important roles in mouse mammary morphogenesis. *Differentiation; research in biological diversity* **59**(1): 1-13.

KEMPHUES, K. (2000). PARsing embryonic polarity. *Cell* **101**(4): 345-348.

KEMPHUES, K. J., J. R. PRIESS, ET AL. (1988). Identification of genes required for cytoplasmic localization in early C. elegans embryos. *Cell* **52**(3): 311-320.

KHAZAEI, M. R. AND A. W. PÜSCHEL (2009). Phosphorylation of the Par Polarity Complex Protein Par3 at Serine 962 Is Mediated by Aurora A and Regulates Its Function in Neuronal Polarity. *The Journal of biological chemistry* **284**(48): 33571-33579.

KIM, I. Y., H. Y. YONG, ET AL. (2009). Overexpression of ErbB2 induces invasion of MCF10A human breast epithelial cells via MMP-9. *Cancer Lett* **275**(2): 227-233.

KIM, Y. N., K. H. KOO, ET AL. (2012). Anoikis resistance: an essential prerequisite for tumor metastasis. *International journal of cell biology* **2012**: 306879.

KLEIN, C. A. (2009). Parallel progression of primary tumours and metastases. *Nat Rev Cancer* **9**(4): 302-312.

KLEINMAN, H. K. AND G. R. MARTIN (2005). Matrigel: basement membrane matrix with biological activity. *Seminars in cancer biology* **15**(5): 378-386.

Knaus, U. G., A. Bamberg, et al. (2007). Rac and Rap GTPase Activation Assays. **412:** 59-67.

KOVAR, D. R. (2006). Molecular details of formin-mediated actin assembly. *Curr Opin Cell Biol* **18**(1): 11-17.

KOWALSKI, P. J., M. A. RUBIN, ET AL. (2003). E-cadherin expression in primary carcinomas of the breast and its distant metastases. *Breast cancer research : BCR* **5**(6): R217-222.

KRAEMER, A., M. GOODWIN, ET AL. (2007). Rac is a dominant regulator of cadherin-directed actin assembly that is activated by adhesive ligation independently of Tiam1. *Am J Physiol Cell Physiol* **292**(3): C1061-1069.

LACY, D. (1957). The Golgi apparatus in neurons and epithelial cells of the common limpet Patella vulgata. *The Journal of biophysical and biochemical cytology* **3**(5): 779-796.

LAI, F. P., M. SZCZODRAK, ET AL. (2008). Arp2/3 complex interactions and actin network turnover in lamellipodia. *EMBO J* **27**(7): 982-992.

LAMPKIN, S. R. AND D. C. ALLRED (1990). Preparation of Paraffin Blocks and Sections Containing Multiple Tissue Samples Using a Skin Biopsy Punch. *J Histotechnol* **13**(2): 121-122.

LANG, G. A., T. IWAKUMA, ET AL. (2004). Gain of function of a p53 hot spot mutation in a mouse model of Li-Fraumeni syndrome. *Cell* **119**(6): 861-872.

LE, T. L., A. S. YAP, ET AL. (1999). Recycling of E-cadherin: a potential mechanism for regulating cadherin dynamics. *J Cell Biol* **146**(1): 219-232.

LEBLEU, V. S., B. MACDONALD, ET AL. (2007). Structure and Function of Basement Membranes. *Experimental Biology and Medicine* **232**(9): 1121-1129.

LEE, S., S. K. MOHSIN, ET AL. (2006). Hormones, receptors, and growth in hyperplastic enlarged lobular units: early potential precursors of breast cancer. *Breast cancer research : BCR* **8**(1): R6.

LEE, Y.-T. N. (1983). Breast carcinoma: Pattern of metastasis at autopsy. *Journal of surgical oncology* **23**(3): 175-180.

LEMMERS, C., D. MICHEL, ET AL. (2004). CRB3 binds directly to Par6 and regulates the morphogenesis of the tight junctions in mammalian epithelial cells. *Mol Biol Cell* **15**(3): 1324-1333.

LEUNG, C. T. AND J. S. BRUGGE (2012). Outgrowth of single oncogene-expressing cells from suppressive epithelial environments. *Nature* **482**(7385): 410-413.

LEVENTAL, K. R., H. YU, ET AL. (2009). Matrix crosslinking forces tumor progression by enhancing integrin signaling. *Cell* **139**(5): 891-906.

LIN, D., A. S. EDWARDS, ET AL. (2000). A mammalian PAR-3-PAR-6 complex implicated in Cdc42/Rac1 and aPKC signalling and cell polarity. *Nat Cell Biol* **2**(8): 540-547.

LING, C., D. ZUO, ET AL. (2010). A novel role for 14-3-3sigma in regulating epithelial cell polarity. *Genes Dev* **24**(9): 947-956.

LOCK, L. S., C. R. MAROUN, ET AL. (2002). Distinct Recruitment and Function of Gab1 and Gab2 in Met Receptor-mediated Epithelial Morphogenesis. *Molecular Biology of the Cell* **13**(6): 2132-2146.

LoRusso, P. M., D. Weiss, et al. (2011). Trastuzumab emtansine: a unique antibody-drug conjugate in development for human epidermal growth factor receptor 2-positive cancer. *Clin Cancer Res* **17**(20): 6437-6447.

Lu, J., H. Guo, et al. (2009). 14-3-3zeta Cooperates with ErbB2 to promote ductal carcinoma in situ progression to invasive breast cancer by inducing epithelial-mesenchymal transition. *Cancer Cell* **16**(3): 195-207.

Lu, X. F., X. J. Feng, et al. (2009). Aberrant Splicing of Hugl-1 Is Associated with Hepatocellular Carcinoma Progression. *Clinical cancer research : an official journal of the American Association for Cancer Research* **15**(10): 3287-3296.

Maeshima, A., Y. Q. Zhang, et al. (2000). Hepatocyte growth factor induces branching tubulogenesis in MDCK cells by modulating the activin-follistatin system. *Kidney Int* **58**(4): 1511-1522.

Maroulakou, I. G., M.-A. Shibata, et al. (1997). Reduced p53 dosage associated with mammary tumor metastases in C3(1)/TAG transgenic mice. *Molecular Carcinogenesis* **20**(2): 168-174.

Maroun, C. R., M. Holgado-Madruga, et al. (1999). The Gab1 PH Domain Is Required for Localization of Gab1 at Sites of Cell-Cell Contact and Epithelial Morphogenesis Downstream from the Met Receptor Tyrosine Kinase. *Molecular and cellular biology* **19**(3): 1784-1799.

Maroun, C. R., M. A. Naujokas, et al. (2000). The Tyrosine Phosphatase SHP-2 Is Required for Sustained Activation of Extracellular Signal-Regulated Kinase and Epithelial Morphogenesis Downstream from the Met Receptor Tyrosine Kinase. *Molecular and cellular biology* **20**(22): 8513-8525.

Mathew, D., L. S. Gramates, et al. (2002). Recruitment of scribble to the synaptic scaffolding complex requires GUK-holder, a novel DLG binding protein. *Curr Biol* **12**(7): 531-539.

Mattoon, D., P. Klein, et al. (2004). The tethered configuration of the EGF receptor extracellular domain exerts only a limited control of receptor function. *Proc Natl Acad Sci U S A* **101**(4): 923-928.

McCaffrey, L. M. and I. G. Macara (2009). The Par3/aPKC interaction is essential for end bud remodeling and progenitor differentiation during mammary gland morphogenesis. *Genes Dev* **23**(12): 1450-1460.

McSherry, E. A., S. F. McGee, et al. (2009). JAM-A expression positively correlates with poor prognosis in breast cancer patients. *International Journal of Cancer* **125**(6): 1343-1351.

MERTENS, A. E., T. P. RYGIEL, ET AL. (2005). The Rac activator Tiam1 controls tight junction biogenesis in keratinocytes through binding to and activation of the Par polarity complex. *J Cell Biol* **170**(7): 1029-1037.

MICHIELS, F., G. G. HABETS, ET AL. (1995). A role for Rac in Tiam1-induced membrane ruffling and invasion. *Nature* **375**(6529): 338-340.

MICHIELS, F., J. C. STAM, ET AL. (1997). Regulated membrane localization of Tiam1, mediated by the NH2-terminal pleckstrin homology domain, is required for Rac-dependent membrane ruffling and C-Jun NH2-terminal kinase activation. *J Cell Biol* **137**(2): 387-398.

MIKI, H., H. YAMAGUCHI, ET AL. (2000). IRSp53 is an essential intermediate between Rac and WAVE in the regulation of membrane ruffling. *Nature* **408**(6813): 732-735.

MILL, C. P., M. D. ZORDAN, ET AL. (2011). ErbB2 Is Necessary for ErbB4 Ligands to Stimulate Oncogenic Activities in Models of Human Breast Cancer. *Genes & Cancer* **2**(8): 792-804.

MILLARD, T. H., G. BOMPARD, ET AL. (2005). Structural basis of filopodia formation induced by the IRSp53/MIM homology domain of human IRSp53. *EMBO J* **24**(2): 240-250.

MILLER, K. G., L. F. LIU, ET AL. (1981). A homogeneous type II DNA topoisomerase from HeLa cell nuclei. *The Journal of biological chemistry* **256**: 9334.

MINARD, M. E., L.-S. KIM, ET AL. (2004). The Role of the Guanine Nucleotide Exchange Factor Tiam1 in Cellular Migration, Invasion, Adhesion and Tumor Progression. *Breast Cancer Research and Treatment* **84**(1): 21-32.

MINK, S., H. PONTA, ET AL. (1990). The long terminal repeat region of the mouse mammary tumour virus contains multiple regulatory elements. *Nucleic acids research* **18**(8): 2017-2024.

MINN, A., G. GUPTA, ET AL. (2005). Genes that mediate breast cancer metastasis to lung. *Nature* **436**(2bd6ebca-c15f-0519-c259-a0861f46baf4): 518-542.

MIZUTANI, K., H. MIKI, ET AL. (2002). Essential role of neural Wiskott-Aldrich syndrome protein in podosome formation and degradation of extracellular matrix in src-transformed fibroblasts. *Cancer Res* **62**(3): 669-674.

MOFFAT, J., D. A. GRUENEBERG, ET AL. (2006). A lentiviral RNAi library for human and mouse genes applied to an arrayed viral high-content screen. *Cell* **124**(6): 1283-1298.

MONTAGNA, C., E. R. ANDRECHEK, ET AL. (2002). Centrosome abnormalities, recurring deletions of chromosome 4, and genomic amplification of HER2/neu define mouse mammary gland adenocarcinomas induced by mutant HER2/neu. *Oncogene* **21**(6): 890-898.

MONTESANO, R., G. SCHALLER, ET AL. (1991). Induction of epithelial tubular morphogenesis in vitro by fibroblast-derived soluble factors. *Cell* **66**(4): 697-711.

MOODY, S. E., C. J. SARKISIAN, ET AL. (2002). Conditional activation of Neu in the mammary epithelium of transgenic mice results in reversible pulmonary metastasis. *Cancer Cell* **2**(6): 451-461.

MOORE, R. AND L. BOYD (2004). Analysis of RING finger genes required for embryogenesis in C. elegans. *Genesis* **38**(1): 1-12.

MORAIS-DE-SA, E., V. MIROUSE, ET AL. (2010). aPKC phosphorylation of Bazooka defines the apical/lateral border in Drosophila epithelial cells. *Cell* **141**(3): 509-523.

MORTON, D. G., D. C. SHAKES, ET AL. (2002). The Caenorhabditis elegans par-5 gene encodes a 14-3-3 protein required for cellular asymmetry in the early embryo. *Dev Biol* **241**(1): 47-58.

MULLER, W. J., E. SINN, ET AL. (1988). Single-step induction of mammary adenocarcinoma in transgenic mice bearing the activated c-neu oncogene. *Cell* **54**(1): 105-115.

MULLINS, R. D., J. A. HEUSER, ET AL. (1998). The interaction of Arp2/3 complex with actin: nucleation, high affinity pointed end capping, and formation of branching networks of filaments. *Proc Natl Acad Sci U S A* **95**(11): 6181-6186.

MÜSCH, A. (2004). Microtubule Organization and Function in Epithelial Cells. *Traffic* **5**(1): 1-9.

MUSCHLER, J. AND C. H. STREULI (2010). Cell-matrix interactions in mammary gland development and breast cancer. *Cold Spring Harb Perspect Biol* **2**(10): a003202.

MUTHUSWAMY, S. K., M. GILMAN, ET AL. (1999). Controlled dimerization of ErbB receptors provides evidence for differential signaling by homo- and heterodimers. *Mol Cell Biol* **19**(10): 6845-6857.

MUTHUSWAMY, S. K., D. LI, ET AL. (2001). ErbB2, but not ErbB1, reinitiates proliferation and induces luminal repopulation in epithelial acini. *Nat Cell Biol* **3**(9): 785-792.

MYLLYMAKI, S. M., T. P. TERAVAINEN, ET AL. (2011). Two distinct integrin-mediated mechanisms contribute to apical lumen formation in epithelial cells. *PLoS ONE* **6**(5): e19453.

NAGAI-TAMAI, Y., K. MIZUNO, ET AL. (2002). Regulated protein-protein interaction between aPKC and PAR-3 plays an essential role in the polarization of epithelial cells. *Genes to Cells* **7**(11): 1161-1171.

NAGAI-TAMAI, Y., K. MIZUNO, ET AL. (2002). Regulated protein-protein interaction between aPKC and PAR-3 plays an essential role in the polarization of epithelial cells. *Genes Cells* **7**(11): 1161-1171.

NAHTA, R., M.-C. HUNG, ET AL. (2004). The HER-2-Targeting Antibodies Trastuzumab and Pertuzumab Synergistically Inhibit the Survival of Breast Cancer Cells. *Cancer Research* **64**(7): 2343-2346.

NAKAGAWA, H., H. MIKI, ET AL. (2003). IRSp53 is colocalised with WAVE2 at the tips of protruding lamellipodia and filopodia independently of Mena. *Journal of Cell Science* **116**(12): 2577-2583.

NAKAGAWA, M., M. FUKATA, ET AL. (2001). Recruitment and activation of Rac1 by the formation of E-cadherin-mediated cell-cell adhesion sites. *Journal of Cell Science* **114**: 1829-1838.

NAKAYAMA, M., T. M. GOTO, ET AL. (2008). Rho-Kinase Phosphorylates PAR-3 and Disrupts PAR Complex Formation. *Dev Cell* **14**(2): 205-215.

NANCE, J. (2005). PAR proteins and the establishment of cell polarity during C. elegans development. *Bioessays* **27**(2): 126-135.

NAVARRO, C., S. NOLA, ET AL. (2005). Junctional recruitment of mammalian Scribble relies on E-cadherin engagement. *Oncogene* **24**(27): 4330-4339.

NAVIN, N., J. KENDALL, ET AL. (2011). Tumour evolution inferred by single-cell sequencing. *Nature* **472**: 90-94.

NEUMANN, M. AND M. AFFOLTER (2006). Remodelling epithelial tubes through cell rearrangements: from cells to molecules. *Embo Rep* **7**(1): 36-40.

NGUYEN, D., P. BOS, ET AL. (2009). Metastasis: from dissemination to organ-specific colonization. *Nat Rev Cancer* **9**: 274-358.

NGUYEN, D. A. AND M. C. NEVILLE (1998). Tight junction regulation in the mammary gland. *J Mammary Gland Biol Neoplasia* **3**(3): 233-246.

NGUYEN, D. X., P. D. BOS, ET AL. (2009). Metastasis: from dissemination to organ-specific colonization. *Nat Rev Cancer* **9**(4): 274-284.

NOBES, C. D. AND A. HALL (1995). Rho, rac, and cdc42 GTPases regulate the assembly of multimolecular focal complexes associated with actin stress fibers, lamellipodia, and filopodia. *Cell* **81**(1): 53-62.

NOLAN, M. E., V. ARANDA, ET AL. (2008). The Polarity Protein Par6 Induces Cell Proliferation and Is Overexpressed in Breast Cancer. *Cancer Res* **68**(20): 8201-8209.

NURNBERG, A., T. KITZING, ET AL. (2011). Nucleating actin for invasion. *Nat Rev Cancer* **11**(3): 177-187.

ONITILO, A. A., J. M. ENGEL, ET AL. (2009). Breast Cancer Subtypes Based on ER/PR and Her2 Expression: Comparison of Clinicopathologic Features and Survival. *Clin Med Res* **7**(1-2): 4-13.

OSER, M., C. MADER, ET AL. (2010). Specific tyrosine phosphorylation sites on cortactin regulate Nck1-dependent actin polymerization in invadopodia. *Journal of cell science* **123**: 3662-3735.

OTSUBO, T., K. IWAYA, ET AL. (2004). Involvement of Arp2/3 complex in the process of colorectal carcinogenesis. *Mod Pathol* **17**(4): 461-467.

OZDAMAR, B., R. BOSE, ET AL. (2005). Regulation of the polarity protein Par6 by TGFbeta receptors controls epithelial cell plasticity. *Science* **307**(5715): 1603-1609.

PADRICK, S. B. AND M. K. ROSEN (2010). Physical Mechanisms of Signal Integration by WASP Family Proteins. *Annual Review of Biochemistry, Vol 79* **79**: 707-735.

PADUA, D., X. ZHANG, ET AL. (2008). TGFbeta primes breast tumors for lung metastasis seeding through angiopoietin-like 4. *Cell* **133**: 66-143.

PAGLIARINI, R. A. AND T. XU (2003). A Genetic Screen in Drosophila for Metastatic Behavior. *Science* **302**(5648): 1227-1231.

PALACIOS, J., N. BENITO, ET AL. (1995). Anomalous expression of P-cadherin in breast carcinoma. Correlation with E-cadherin expression and pathological features. *Am J Pathol* **146**(3): 605-612.

PARK, B. K., H. L. ZHANG, ET AL. (2007). NF-kappa B in breast cancer cells promotes osteolytic bone metastasis by inducing osteoclastogenesis via GM-CSF. *Nature Medicine* **13**(1): 62-69.

PARKER, C., R. S. RAMPAUL, ET AL. (2001). E-cadherin as a prognostic indicator in primary breast cancer. *Br J Cancer* **85**(12): 1958-1963.

PASZEK, M. J., N. ZAHIR, ET AL. (2005). Tensional homeostasis and the malignant phenotype. *Cancer Cell* **8**(3): 241-254.

PELLETTIERI, J. AND G. SEYDOUX (2002). Anterior-posterior polarity in C-elegans and Drosophila - PARallels and differences. *Science* **298**(5600): 1946-1950.

PICCART-GEBHART, M., M. PROCTER, ET AL. (2005). Trastuzumab after adjuvant chemotherapy in HER2-positive breast cancer. *New Engl J Med* **353**(3cc0e2ea-02c3-64af-b676-9b25f2188ede): 1659-1731.

POLYAK, K., M. SHIPITSIN, ET AL. (2009). Breast tumor heterogeneity: causes and consequences. *Breast cancer research : BCR* **11 Suppl 1**: S18.

PRICE, J. E. (1996). Metastasis from human breast cancer cell lines. *Breast Cancer Res Treat* **39**(1): 93-102.

QIN, Y., C. CAPALDO, ET AL. (2005). The mammalian Scribble polarity protein regulates epithelial cell adhesion and migration through E-cadherin. *J Cell Biol* **171**(6): 1061-1071.

RADVANYI, L., D. SINGH-SANDHU, ET AL. (2005). The gene associated with trichorhinophalangeal syndrome in humans is overexpressed in breast cancer. *Proc Natl Acad Sci U S A* **102**(31): 11005-11010.

RAKHA, E. A., M. E. EL-SAYED, ET AL. (2008). Prognostic Significance of Nottingham Histologic Grade in Invasive Breast Carcinoma. *Journal of clinical oncology : official journal of the American Society of Clinical Oncology* **26**(19): 3153-3158.

RAKHA, E. A., J. S. REIS-FILHO, ET AL. (2008). Basal-like breast cancer: a critical review. *J Clin Oncol* **26**(15): 2568-2581.

REDFIELD, A., M. T. NIEMAN, ET AL. (1997). Cadherins promote skeletal muscle differentiation in three-dimensional cultures. *J Cell Biol* **138**(6): 1323-1331.

REICHMANN, E., H. SCHWARZ, ET AL. (1992). Activation of an inducible c-FosER fusion protein causes loss of epithelial polarity and triggers epithelial-fibroblastoid cell conversion. *Cell* **71**(7): 1103-1116.

REPESH, L. A. (1989). A new in vitro assay for quantitating tumor cell invasion. *Invasion & metastasis* **9**(3): 192-208.

REVILLION, F., V. LHOTELLIER, ET AL. (2007). ErbB/HER ligands in human breast cancer, and relationships with their receptors, the bio-pathological features and prognosis. *Annals of oncology : official journal of the European Society for Medical Oncology / ESMO*: mdm431.

RHIM, A. D., E. T. MIREK, ET AL. (2012). EMT and Dissemination Precede Pancreatic Tumor Formation. *Cell* **148**(1): 349-361.

RHODES, D., J. YU, ET AL. (2004). ONCOMINE: a cancer microarray database and integrated data-mining platform. *Neoplasia (New York, N.Y.)* **6**(1): 1-6.

RIDLEY, A. J. AND A. HALL (1992). The Small Gtp-Binding Protein Rho Regulates the Assembly of Focal Adhesions and Actin Stress Fibers in Response to Growth-Factors. *Cell* **70**(3): 389-399.

RIEDL, J., A. H. CREVENNA, ET AL. (2008). Lifeact: a versatile marker to visualize F-actin. *Nature methods* **5**(7): 605-607.

ROBINSON, E. E., K. M. ZAZZALI, ET AL. (2003). α5β1 integrin mediates strong tissue cohesion. *Journal of Cell Science* **116**(2): 377-386.

RODRIGUEZ, L. G., X. WU, ET AL. (2005). Wound-healing assay. *Methods Mol Biol* **294**: 23-29.

ROMOND, E., E. PEREZ, ET AL. (2005). Trastuzumab plus adjuvant chemotherapy for operable HER2-positive breast cancer. *New Engl J Med* **353**: 1673-1757.

ROSES, R. E., E. C. PAULSON, ET AL. (2009). HER-2/neu Overexpression as a Predictor for the Transition from In situ to Invasive Breast Cancer. *Cancer Epidemiology Biomarkers & Prevention* **18**(5): 1386-1389.

Rovensky, Y. A. and SpringerLink (2011). Adhesive interactions in normal and transformed cells. New York, Humana Press**:** 1 online resource.

ROXANIS, I. AND J. CHOW (2010). Cellular cohesion as a prognostic factor in malignant melanoma: a retrospective study with up to 12 years follow-up. *Modern Pathol* **23**(4): 502-510.

RUNSWICK, S. K., M. J. O'HARE, ET AL. (2001). Desmosomal adhesion regulates epithelial morphogenesis and cell positioning. *Nat Cell Biol* **3**(9): 823-830.

SCHECHTER, A. L., M. C. HUNG, ET AL. (1985). The neu gene: an erbB-homologous gene distinct from and unlinked to the gene encoding the EGF receptor. *Science* **229**(4717): 976-978.

SCHMIDT-KITTLER, O., T. RAGG, ET AL. (2003). From latent disseminated cells to overt metastasis: genetic analysis of systemic breast cancer progression. *Proc Natl Acad Sci U S A* **100**(13): 7737-7742.

SCHMITTGEN, T. D. AND K. J. LIVAK (2008). Analyzing real-time PCR data by the comparative C(T) method. *Nature protocols* **3**(6): 1101-1108.

SCHWARTZ, M. A. AND R. K. ASSOIAN (2001). Integrins and cell proliferation. *Journal of cell science* **114**(14): 2553-2560.

SEIDEN-LONG, I., R. NAVAB, ET AL. (2008). Gab1 but not Grb2 mediates tumor progression in Met overexpressing colorectal cancer cells. *Carcinogenesis* **29**(3): 647-655.

SERRELS, A., P. TIMPSON, ET AL. (2009). Real-time Study of E-Cadherin and Membrane Dynamics in Living Animals: Implications for Disease Modeling and Drug Development. *Cancer Research* **69**(7): 2714-2719.

SHAYE, D. D., J. CASANOVA, ET AL. (2008). Modulation of intracellular trafficking regulates cell intercalation in the Drosophila trachea. *Nature cell biology* **10**(8): 964-970.

SHIMOYAMA, Y., S. HIROHASHI, ET AL. (1989). Cadherin cell-adhesion molecules in human epithelial tissues and carcinomas. *Cancer Res* **49**(8): 2128-2133.

SIEGEL, P. M., E. D. RYAN, ET AL. (1999). Elevated expression of activated forms of Neu/ErbB-2 and ErbB-3 are involved in the induction of mammary tumors in transgenic mice: implications for human breast cancer. *EMBO J* **18**(8): 2149-2164.

SINN, E., W. MULLER, ET AL. (1987). Coexpression of Mmtv/V-Ha-Ras and Mmtv/C-Myc Genes in Transgenic Mice - Synergistic Action of Oncogenes Invivo. *Cell* **49**(4): 465-475.

SMID, M., Y. X. WANG, ET AL. (2006). Genes associated with breast cancer metastatic to bone. *Journal of clinical oncology : official journal of the American Society of Clinical Oncology* **24**(15): 2261-2267.

SOULE, H. D., T. M. MALONEY, ET AL. (1990). Isolation and Characterization of a Spontaneously Immortalized Human Breast Epithelial Cell Line, MCF-10. *Cancer Res* **50**(18): 6075-6086.

SPANDIDOS, D., A. PINTZAS, ET AL. (1987). Elevated expression of the myc gene in human benign and malignant breast lesions compared to normal tissue. *Anticancer research* **7**(6): 1299-1304.

SPECTOR, N. L., W. XIA, ET AL. (2005). Study of the Biologic Effects of Lapatinib, a Reversible Inhibitor of ErbB1 and ErbB2 Tyrosine Kinases, on Tumor Growth and Survival Pathways in Patients With Advanced Malignancies. *Journal of clinical oncology : official journal of the American Society of Clinical Oncology* **23**(11): 2502-2512.

SPIERING, D. AND L. HODGSON (2011). Dynamics of the Rho-family small GTPases in actin regulation and motility. *Cell Adh Migr* **5**(2): 170-180.

ST CROIX, B., C. SHEEHAN, ET AL. (1998). E-Cadherin-dependent growth suppression is mediated by the cyclin-dependent kinase inhibitor p27(KIP1). *J Cell Biol* **142**(2): 557-571.

STAM, J. C., E. E. SANDER, ET AL. (1997). Targeting of Tiam1 to the plasma membrane requires the cooperative function of the N-terminal pleckstrin homology domain and an adjacent protein interaction domain. *J Biol Chem* **272**(45): 28447-28454.

STAM, J. C., E. E. SANDER, ET AL. (1997). Targeting of Tiam1 to the Plasma Membrane Requires the Cooperative Function of the N-terminal Pleckstrin Homology Domain and an Adjacent Protein Interaction Domain. *Journal of Biological Chemistry* **272**(45): 28447-28454.

STEWART, T. A., P. K. PATTENGALE, ET AL. (1984). Spontaneous Mammary Adenocarcinomas in Transgenic Mice That Carry and Express Mtv/Myc Fusion Genes. *Cell* **38**(3): 627-637.

STOCKINGER, A., A. EGER, ET AL. (2001). E-cadherin regulates cell growth by modulating proliferation-dependent beta-catenin transcriptional activity. *J Cell Biol* **154**(6): 1185-1196.

STOLETOV, K., H. KATO, ET AL. (2010). Visualizing extravasation dynamics of metastatic tumor cells. *J Cell Sci* **123**(Pt 13): 2332-2341.

STREULI, C. H., N. BAILEY, ET AL. (1991). Control of mammary epithelial differentiation: basement membrane induces tissue-specific gene expression in the absence of cell-cell interaction and morphological polarity. *J Cell Biol* **115**(5): 1383-1395.

SUZUKI, A. AND S. OHNO (2006). The PAR-aPKC system: lessons in polarity. *J Cell Sci* **119**(Pt 6): 979-987.

SUZUKI, A., T. YAMANAKA, ET AL. (2001). Atypical protein kinase C is involved in the evolutionarily conserved par protein complex and plays a critical role in establishing epithelia-specific junctional structures. *J Cell Biol* **152**(6): 1183-1196.

TAKAHASHI, K. AND K. SUZUKI (1996). Density-dependent inhibition of growth involves prevention of EGF receptor activation by E-cadherin-mediated cell-cell adhesion. *Exp Cell Res* **226**(1): 214-222.

TAKEKUNI, K., W. IKEDA, ET AL. (2003). Direct binding of cell polarity protein PAR-3 to cell-cell adhesion molecule nectin at neuroepithelial cells of developing mouse. *J Biol Chem* **278**(8): 5497-5500.

TALMADGE, J. E. AND I. J. FIDLER (2010). AACR Centennial Series: The Biology of Cancer Metastasis: Historical Perspective. *Cancer Res* **70**(14): 5649-5669.

TANG, V. W. AND W. M. BRIEHER (2012). alpha-Actinin-4/FSGS1 is required for Arp2/3-dependent actin assembly at the adherens junction. *J Cell Biol* **196**(1): 115-130.

TAO, Q., S. NANDADASA, ET AL. (2007). G-protein-coupled signals control cortical actin assembly by controlling cadherin expression in the early Xenopus embryo. *Development* **134**(14): 2651-2661.

TEPASS, U., C. THERES, ET AL. (1990). crumbs encodes an EGF-like protein expressed on apical membranes of Drosophila epithelial cells and required for organization of epithelia. *Cell* **61**(5): 787-799.

THIERY, J. P. (2002). Epithelial-mesenchymal transitions in tumour progression. *Nat Rev Cancer* **2**(6): 442-454.

THIERY, J. P., H. ACLOQUE, ET AL. (2009). Epithelial-mesenchymal transitions in development and disease. *Cell* **139**(5): 871-890.

THOMPSON, E. W., D. F. NEWGREEN, ET AL. (2005). Carcinoma invasion and metastasis: a role for epithelial-mesenchymal transition? *Cancer Res* **65**(14): 5991-5995; discussion 5995.

TOPPER, Y. J. AND C. S. FREEMAN (1980). Multiple hormone interactions in the developmental biology of the mammary gland. *Physiol Rev* **60**(4): 1049-1106.

URSINI-SIEGEL, J., B. SCHADE, ET AL. (2007). Insights from transgenic mouse models of ERBB2-induced breast cancer. *Nat Rev Cancer* **7**(5): 389-397.

URSINI-SIEGEL, J., B. SCHADE, ET AL. (2007). Insights from transgenic mouse models of ERBB2-induced breast cancer. *Nat Rev Cancer* **7**(5): 389-397.

VALABREGA, G., F. MONTEMURRO, ET AL. (2007). Trastuzumab: mechanism of action, resistance and future perspectives in HER2-overexpressing breast cancer. *Annals of oncology : official journal of the European Society for Medical Oncology / ESMO* **18**(6): 977-984.

VAN AELST, L. AND C. D'SOUZA-SCHOREY (1997). Rho GTPases and signaling networks. *Genes Dev* **11**(18): 2295-2322.

VAN KEYMEULEN, A., A. S. ROCHA, ET AL. (2011). Distinct stem cells contribute to mammary gland development and maintenance. *Nature* **479**(7372): 189-193.

VILORIA-PETIT, A. M., L. DAVID, ET AL. (2009). A role for the TGFbeta-Par6 polarity pathway in breast cancer progression. *Proc Natl Acad Sci U S A* **106**(33): 14028-14033.

VLEMINCKX, K., L. VAKAET, JR., ET AL. (1991). Genetic manipulation of E-cadherin expression by epithelial tumor cells reveals an invasion suppressor role. *Cell* **66**(1): 107-119.

VOLKMANN, N., K. J. AMANN, ET AL. (2001). Structure of Arp2/3 complex in its activated state and in actin filament branch junctions. *Science* **293**(5539): 2456-2459.

WADA, T., X. L. QIAN, ET AL. (1990). Intermolecular association of the p185neu protein and EGF receptor modulates EGF receptor function. *Cell* **61**(7): 1339-1347.

WALTHER, R. F. AND F. PICHAUD (2010). Crumbs/DaPKC-dependent apical exclusion of Bazooka promotes photoreceptor polarity remodeling. *Curr Biol* **20**(12): 1065-1074.

WANG, H. R., Y. ZHANG, ET AL. (2003). Regulation of cell polarity and protrusion formation by targeting RhoA for degradation. *Science* **302**(5651): 1775-1779.

WANG, T. C., R. D. CARDIFF, ET AL. (1994). Mammary hyperplasia and carcinoma in MMTV-cyclin D1 transgenic mice. *Nature* **369**(6482): 669-671.

WANG, W., R. EDDY, ET AL. (2007). The cofilin pathway in breast cancer invasion and metastasis. *Nat Rev Cancer* **7**(471c663a-ccb1-0eb2-4f3c-a26cbe50e8a5): 429-469.

WANG, W., G. MOUNEIMNE, ET AL. (2006). The activity status of cofilin is directly related to invasion, intravasation, and metastasis of mammary tumors. *J Cell Biol* **173**: 395-799.

WANG, X.-Q., H. LI, ET AL. (2009). Oncogenic K-Ras regulates proliferation and cell junctions in lung epithelial cells through induction of cyclooxygenase-2 and activation of metalloproteinase-9. *Molecular Biology of the Cell* **20**(3): 791-800.

WANG, Y., D. DU, ET AL. (2006). Tyrosine phosphorylated Par3 regulates epithelial tight junction assembly promoted by EGFR signaling. *EMBO J.* **25**: 5058-5070.

WATTS, J., B. ETEMAD-MOGHADAM, ET AL. (1996). par-6, a gene involved in the establishment of asymmetry in early C. elegans embryos, mediates the asymmetric localization of PAR-3. *Development (Cambridge, England)* **122**(10): 3133-3140.

WEAVER, V. M., S. LELIEVRE, ET AL. (2002). beta4 integrin-dependent formation of polarized three-dimensional architecture confers resistance to apoptosis in normal and malignant mammary epithelium. *Cancer Cell* **2**(3): 205-216.

WEAVER, V. M., O. W. PETERSEN, ET AL. (1997). Reversion of the malignant phenotype of human breast cells in three-dimensional culture and in vivo by integrin blocking antibodies. *J Cell Biol* **137**(1): 231-245.

WEBER, G. F., M. A. BJERKE, ET AL. (2011). Integrins and cadherins join forces to form adhesive networks. *Journal of Cell Science* **124**(8): 1183-1193.

WEIDNER, K. M., S. DI CESARE, ET AL. (1996). Interaction between Gab1 and the c-Met receptor tyrosine kinase is responsible for epithelial morphogenesis. *Nature* **384**: 173-176.

WEISS, L., E. GRUNDMANN, ET AL. (1986). Haematogenous metastatic patterns in colonic carcinoma: an analysis of 1541 necropsies. *The Journal of pathology* **150**(3): 195-203.

WELCH, M. D., A. H. DEPACE, ET AL. (1997). The Human Arp2/3 Complex Is Composed of Evolutionarily Conserved Subunits and Is Localized to Cellular Regions of Dynamic Actin Filament Assembly. *The Journal of Cell Biology* **138**(2): 375-384.

WELM, B. E., G. J. DIJKGRAAF, ET AL. (2008). Lentiviral transduction of mammary stem cells for analysis of gene function during development and cancer. *Cell Stem Cell* **2**(1): 90-102.

WODARZ, A., M. P. KRAHN, ET AL. (2010). Formation of a Bazooka-Stardust complex is essential for plasma membrane polarity in epithelia. *J Cell Biol* **190**(5): 751-760.

WOLFF, A. C., M. E. HAMMOND, ET AL. (2007). American Society of Clinical Oncology/College of American Pathologists guideline recommendations for human epidermal growth factor

receptor 2 testing in breast cancer. *Archives of pathology & laboratory medicine* **131**(1): 18-43.

WOLFF, A. C., M. E. H. HAMMOND, ET AL. (2007). American Society of Clinical Oncology/College of American Pathologists guideline recommendations for human epidermal growth factor receptor 2 testing in breast cancer. *Journal of clinical oncology : official journal of the American Society of Clinical Oncology* **25**(1): 118-145.

WROBEL, C., J. DEBNATH, ET AL. (2004). Autocrine CSF-1R activation promotes Src-dependent disruption of mammary epithelial architecture. *J Cell Biol* **165**(2): 263-273.

WU, H., W. FENG, ET AL. (2007). PDZ domains of Par-3 as potential phosphoinositide signaling integrators. *Mol Cell* **28**(5): 886-898.

XIA, W., C. M. GERARD, ET AL. (2005). Combining lapatinib (GW572016), a small molecule inhibitor of ErbB1 and ErbB2 tyrosine kinases, with therapeutic anti-ErbB2 antibodies enhances apoptosis of ErbB2-overexpressing breast cancer cells. *Oncogene* **24**(41): 6213-6221.

XIANG, B. AND S. K. MUTHUSWAMY (2006). Using three-dimensional acinar structures for molecular and cell biological assays. *Methods Enzymol* **406**: 692-701.

YACHIDA, S., S. JONES, ET AL. (2010). Distant metastasis occurs late during the genetic evolution of pancreatic cancer. *Nature* **467**(7319): 1114-1117.

YAMADA, S. AND W. J. NELSON (2007). Localized zones of Rho and Rac activities drive initiation and expansion of epithelial cell-cell adhesion. *J Cell Biol* **178**(3): 517-527.

YAMAGISHI, A., M. MASUDA, ET AL. (2004). A novel actin bundling/filopodium-forming domain conserved in insulin receptor tyrosine kinase substrate p53 and missing in metastasis protein. *J Biol Chem* **279**(15): 14929-14936.

YAMAGUCHI, H., M. LORENZ, ET AL. (2005). Molecular mechanisms of invadopodium formation: the role of the N-WASP-Arp2/3 complex pathway and cofilin. *J Cell Biol* **168**(3): 441-452.

YAMANAKA, T., Y. HORIKOSHI, ET AL. (2003). Mammalian Lgl Forms a Protein Complex with PAR-6 and aPKC Independently of PAR-3 to Regulate Epithelial Cell Polarity. *Curr Biol* **13**(9): 734-743.

YAMANAKA, T., Y. HORIKOSHI, ET AL. (2001). PAR-6 regulates aPKC activity in a novel way and mediates cell-cell contact-induced formation of the epithelial junctional complex. *Genes Cells* **6**(8): 721-731.

YAMASAKI, S., K. NISHIDA, ET AL. (2003). Gab1 is required for EGF receptor signaling and the transformation by activated ErbB2. *Oncogene* **22**(10): 1546-1556.

YAMAZAKI, D., T. OIKAWA, ET AL. (2007). Rac-WAVE-mediated actin reorganization is required for organization and maintenance of cell-cell adhesion. *Journal of cell science* **120**(Pt 1): 86-100.

YANG, C., M. HUANG, ET AL. (2000). Profilin enhances Cdc42-induced nucleation of actin polymerization. *J Cell Biol* **150**(5): 1001-1012.

YANG, H., R. ZHAO, ET AL. (2006). 14-3-3σ, a p53 regulator, suppresses tumor growth of nasopharyngeal carcinoma. *Molecular Cancer Therapeutics* **5**(2): 253-260.

YAP, A. S., M. S. CRAMPTON, ET AL. (2007). Making and breaking contacts: the cellular biology of cadherin regulation. *Curr Opin Cell Biol* **19**(5): 508-514.

YARDEN, Y. (2001). The EGFR family and its ligands in human cancer: signalling mechanisms and therapeutic opportunities. *European Journal of Cancer* **37**(Supplement 4): 3-8.

YOSHII, T., K. MIZUNO, ET AL. (2005). sPAR-3, a splicing variant of PAR-3, shows cellular localization and an expression pattern different from that of PAR-3 during enterocyte polarization. *Am J Physiol Gast and Liver Phys* **288**(3): G564-570.

YU, G. H., R. S. CAJULIS, ET AL. (1998). Tumor cell (dys)cohesion as a prognostic factor in aspirate smears of breast carcinoma. *American journal of clinical pathology* **109**(3): 315-319.

YU, W., L. E. O'BRIEN, ET AL. (2003). Hepatocyte growth factor switches orientation of polarity and mode of movement during morphogenesis of multicellular epithelial structures. *Molecular Biology of the Cell* **14**(2): 748-763.

YURCHENCO, P. D. (2011). Basement membranes: cell scaffoldings and signaling platforms. *Cold Spring Harb Perspect Biol* **3**(2).

ZALLEN, J. A. (2007). Planar polarity and tissue morphogenesis. *Cell* **129**(6): 1051-1063.

Zandy, N. L., M. Playford, et al. (2007). Abl tyrosine kinases regulate cell cell adhesion through Rho GTPases. **104:** 17686-17691.

ZEGERS, M. M., L. E. O'BRIEN, ET AL. (2003). Epithelial polarity and tubulogenesis in vitro. *Trends Cell Biol* **13**(4): 169-176.

ZEGERS, M. M. P., W. YU, ET AL. (2003). Hepatocyte growth factor switches orientation of polarity and mode of movement during morphogenesis of multicellular epithelial structures. *Molecular Biology of the Cell* **14**(2): 748-763.

ZEN, K., K. YASUI, ET AL. (2009). Defective expression of polarity protein PAR-3 gene (PARD3) in esophageal squamous cell carcinoma. *Oncogene* **28**(32): 2910-2918.

ZHAN, L., A. ROSENBERG, ET AL. (2008). Deregulation of Scribble Promotes Mammary Tumorigenesis and Reveals a Role for Cell Polarity in Carcinoma. *Cell* **135**(5): 865-878.

ZHAN, L., B. XIANG, ET AL. (2006). Controlled Activation of ErbB1/ErbB2 Heterodimers Promote Invasion of Three-Dimensional Organized Epithelia in an ErbB1-Dependent Manner: Implications for Progression of ErbB2-Overexpressing Tumors. *Cancer Res* **66**(10): 5201-5208.

ZHANG, H. AND I. G. MACARA (2008). The PAR-6 polarity protein regulates dendritic spine morphogenesis through p190 RhoGAP and the Rho GTPase. *Dev Cell* **14**(2): 216-226.

ZHANG, J., M. BETSON, ET AL. (2005). Actin at cell-cell junctions is composed of two dynamic and functional populations. *J Cell Sci* **118**(23): 5549-5562.

ZHANG, M., F. BEHBOD, ET AL. (2008). Identification of tumor-initiating cells in a p53-null mouse model of breast cancer. *Cancer Res* **68**(12): 4674-4682.

ZHANG, W., Y. WU, ET AL. (2005). Activation of the Arp2/3 complex by N-WASp is required for actin polymerization and contraction in smooth muscle. *Am J Physiol Cell Physiol* **288**(5): C1145-1160.

ZHAO, H., A. LANGEROD, ET AL. (2004). Different gene expression patterns in invasive lobular and ductal carcinomas of the breast. *Mol Biol Cell* **15**(6): 2523-2536.

Appendix

Antibiotic-inducible ErbB2 system

While chimeric ErbB2 inducible system (Muthuswamy, Li et al. 2001) resolve the question of the specificity of ErbB2-mediated signaling during tumor transformation and disruption of cell polarity in breast cancer, this system has two limitations. First, the ErbB2 dimerizer AP1510 has not been tested in animal, therefore this inducible system cannot be further used to generate ErbB2-inducible transgenic mouse. Second, this receptor has its HER2 extracellular domain replaced by p75NGFR extracellular domain, and therefore cannot be recognized by trastuzumab, the HER2 targeting drug which known to disrupt HER2 mediated signaling by binding to the extracellular domain of HER2. Thus this chimeric receptor system cannot be used in studying the drug resistance and cancer recurrence. To solve these two problems, I developed a new inducible ErbB2 construct which contains a wild type HER2 containing its original extracellular domain and can be activated by an antibiotic drug.

To achieve the dimerizer controlled activation of ErbB2, I adopted the coumermycin-GyrB dimerization strategy. Antibiotic coumermycin A1 (Figure 9.1) produced from *Streptomyces* binds to bacterial DNA gyrase B subunit (GyrB) with a stoichiometry of 1:2, thus act as a natural dimerizer. By fusing ErbB2 with GyrB, the receptor can be homo-dimerized and activated by coumermycin in a nanomolar concentration. Coumermycin has several advantages. First, this antibiotic drug targets prokaryotic enzyme, but no high-affinity endogenous binding targets exist in normal eukaryotic cells (Miller, Liu et al. 1981). Extensive pharmacological tests of coumermycin have been done both in rodents and dogs. At concentrations that exhibit significant antibacterial activity, coumermycin has no overt toxicity (Godfrey and Price 1972). Therefore it can be safely applied in mouse experiment. Second, coumermycin exhibits good pharmacokinetic properties, with a reported serum half-life in mice of 5.5 hours (Farrar, Olson et al. 2000). Last but not least, coumermycin is commercially available from Sigma-Aldrich Co. LLC. This strategy was previously used to dimerize Raf and study its activation of MAPK signaling (Farrar, Alberol et al. 1996).

First, I constructed the HER2-2×GyrB expression vector containing a full length HER2 followed by two copies of GyrB (1-220aa) and hemagglutinin (HA) tag following the procedure as shown in the flow chart (Figure 9.2).

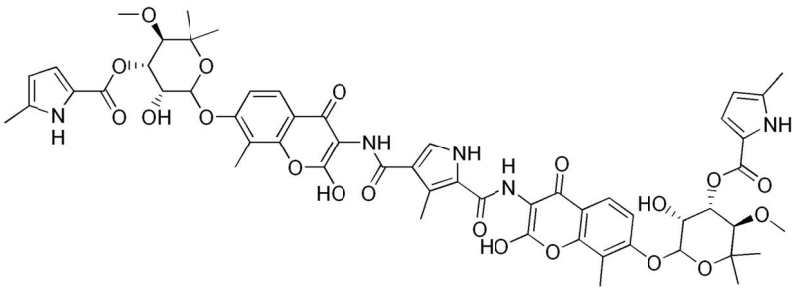

Figure 9.1. Chemical structure of coumermycin A1

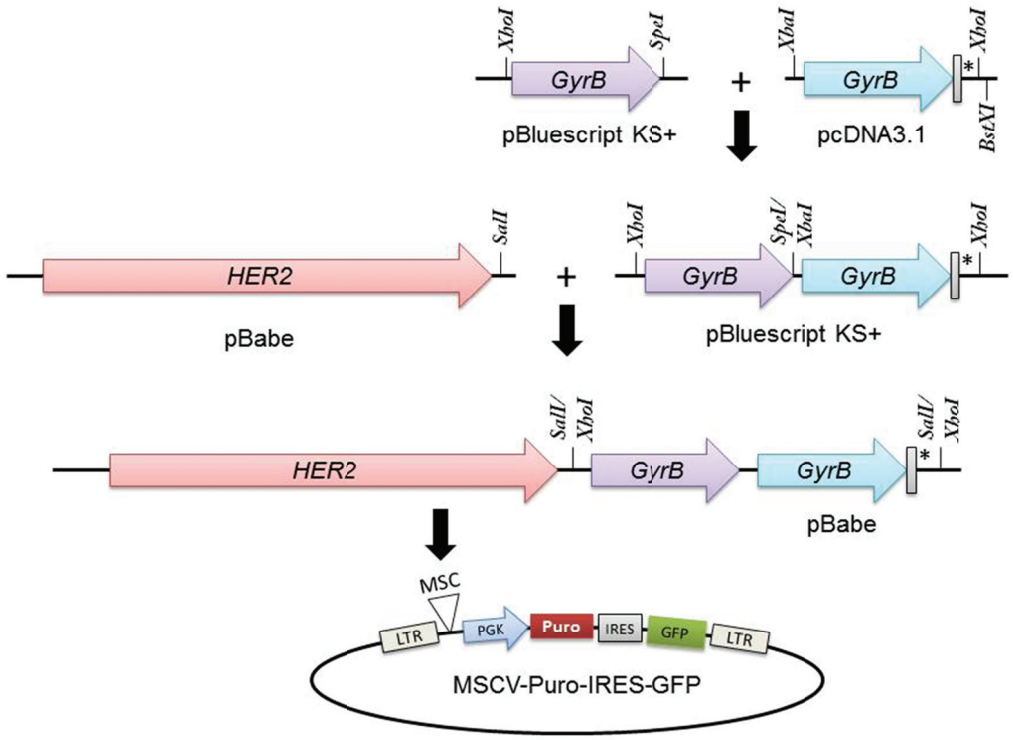

Figure 9.2. Schematic diagram of pMSCV-PIG-HER2-2×GyrB cloning procedure

The first GyrB (2-220aa) was amplified from GyrB cDNA using the following primers:
GyrB XhoI forward: 5'- ATCGCTCGAGTCTAGATCGAATTCTTATGA -3'
GyrB SpeI reverse: 5'- ATTAACTAGTGGATCCGCCTTCATAGTGGAAGT -3'
The PCR fragment was cloned into SpeI sites of pBluescript KS+ vector (pKS-GyrB1).

The second GyrB (2-220aa) was amplified using the following primers:
GyrB forward:
5'-AAGCGTCGACGAATTCTCTAGAAGCAATTCTTATGACTCCTCCA-3'
GyrB-HA reverse:
5'-AACGCTCGAGTACGTATCATTAAGCGTAATCTGGAACATCGTATGGGTAGCCTT
CAAGTGGAAGT -3'
The PCR fragment containing HA-tag and stop codon was cloned into XbaI/SnaBI site of pcDNA3.1 vector (pcDNA-GyrB2-HA).

The GyrB2-HA in pcDNA3 vector was released using XbaI/XhoI and cloned into SpeI/XhoI sites of pKS-GyrB1 to generate pKS-2×GyrB vector.

A SalI site was created at the 3' flanking region of HER2 in a pBabe vector using the primers (pBabe-HER2-SalI):
HER2 SalI forward; 5'-GGTCTGGACGTGCCAGTGGTCGACCAGAAACTCATCTCTG -3'
HER2 SalI reverse: 5'- CAGAGATGAGTTTCTGGTCGACCACTGGCACGTCCAGACC -3'

2×GyrB-HA was released from pKS-2×GyrB using XhoI and cloned into SalI site of pBabe-HER2-SalI vector. The construct containing a insert of correct direction was selected and verified by sequencing.

In order to select infected cells and get high expression level, the gene were constructed into pMSCV-PIG, a retrovirual expression vector containing puromycin resistant gene for antibiotic selection and a GFP marker. HER2-2×GyrB was amplified by PCR using the following primers and cloned into XhoI site of pMSCV-PIG:
HER2-2G forward: 5'- ACATCTCGAGATGGAGCTGGCGGCCTTG -3'

HER2-2G reverse: 5’- ATTCCTCGAGTACGTATCATTAAGCGTAATC -3’
The final expression clone was selected and verified by sequencing the entire gene.

Retrovirus expressing HER2-2×GyrB was produced using the final construct. A MCF10A cell line stably expressing HER2-2×GyrB, named as 10A.G2, was generated by infecting parental MCF10A cells with the virus and followed by puromycin selection. To test the expression of HER2-2×GyrB and the activity of the receptor in response to coumermycin, 10A.G2 cells were stimulated with two different doses of coumermycin for half hour and analyzed for tyrosine phosphorylation level of exogenous HER2-GyrB (Figure 9.3). The fusion protein pulled down by anti-HA antibody was recognized by ErbB2 antibody, demonstrating the expression of the correct fusion protein. The receptor showed most phosphorylation level upon 10nM of coumermycin stimulation, suggesting that HER2-GyrB can be dimerized and activated by coumermycin.

To determine whether this fusion protein would have the same activity as the ErbB2-FKBP chimeric protein which was previously used, 10A.G2 cells were tested in 3D culture system to see whether the cells could form multi-acinar structure upon coumermycin stimulation. Using immunofluorescence staining, it showed that the GFP positive cells expressed exogenous HA-tagged ErbB2 (Figure 9.4.A). The acini composed by the GFP and HA positive cells demonstrated multi-acini structures after treated with coumermycin at the optimized concentration, whereas formed normal single acini without stimulation. The GFP negative cells did not respond to the coumermycin as expected (Figure 9.4.B). This inducible ErbB2 construct requires more validation *in vivo* and *in vitro* and can be further used for generating inducible-ErbB2 transgenic mouse.

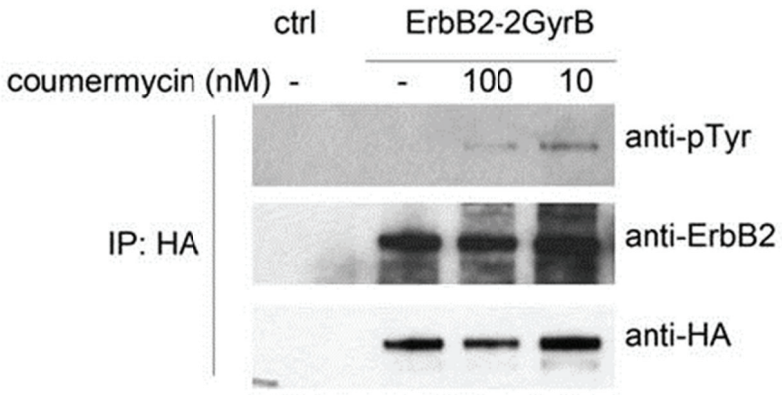

Figure 9.3. Coumermycin induced activation of HER2-2×GyrB

Confluent monolayers of 10A.G2 cells were stimulated untreated or treated with 100nM and 10nM coumermycin respectively for 0.5 hour. Cell lysates were collected and immunoprecipitated using anti-HA antibody. The precipitated proteins were immunoblotted as indicated

.

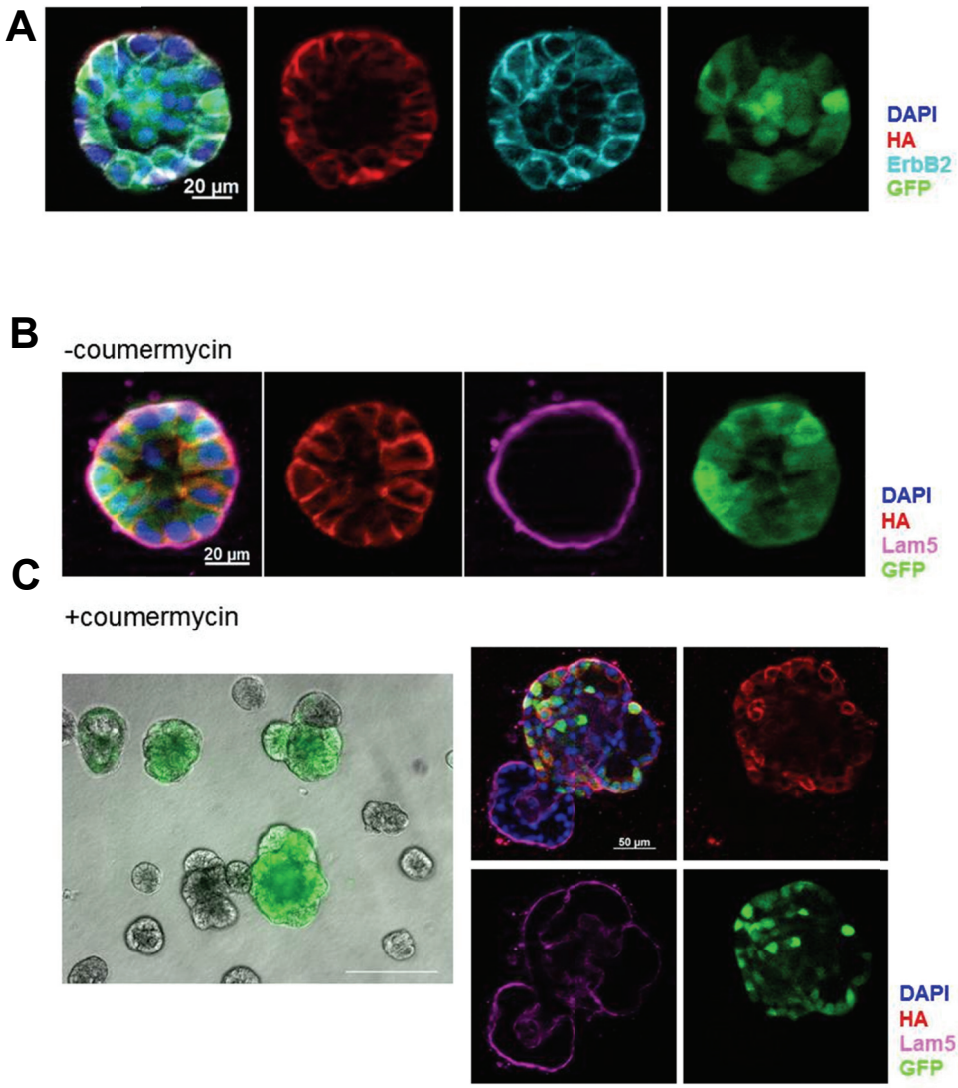

Figure 9.4. Coumermycin stimulation induced formation of multiacini structure of 10A.G2 cells in 3D culture

Day 16 10A.G2 acini without coumermycin treatment were immunostained for HA (red)/ErbB2 (cyan) **(A)** or HA (red)/Lam5 (magenta) **(B)**. The images show the representative staining of a GFP positive acinus (scale bar=20µm).
(C) Day16 10A.G2 acini treated with 10nM coumermycin for 8 days were immunostained for HA (red)/Lam5 (magenta). The phase contrast and GFP image of the representative image was shown on the left (scale bar=50µm).

Disruption of cell polarity in mammary epithelial cell lacking 14-3-3σ

A novel role for 14–3–3σ in regulating epithelial cell polarity

Chen Ling[1,2,3], Dongmei Zuo[1,2,3], Bin Xue[4,5], Senthil Muthuswamy[4,5,6]and William J. Muller[1,2,3,7]

Author Affiliations

[1]Department of Biochemistry, McGill University, Montreal, Quebec H3A 1A3, Canada;

[2]Goodman Cancer Centre, McGill University, Montreal, Quebec H3A 1A3, Canada;

[3]Faculty of Medicine, McGill University Cancer Research, Montreal, QC H3A 1A3, Canada;

[4]Cold Spring Harbor Laboratory, Cold Spring Harbor, New York 11724, USA;

[5]Stony Brook University, Cold Spring Harbor, New York 11724, USA;

[6]University of Toronto, Ontario Cancer Institute (OCI), Princess Margaret Hospital, Toronto, Ontario, M5G 2M9, Canada

Correspondence should be addressed to W.J. Muller (William.muller@mcgill.ca)

In HER2+ breast cancer, the elevated levels of ErbB2 are due to genomic amplification of the *ErbB2* proto-oncogene. To mimic the events involved in ErbB2-induced mammary tumor progression, the ErbB2 knock-in ($ErbB2^{KI}$) transgenic mouse model was established by expressing a Cre-inducible activated *erbB2* under the transcriptional control of the endogenous *erbB2* promoter (Andrechek, Hardy et al. 2000). Strikingly, the mammary tumor generated from these mice all bear amplified copies of the activated *erbB2* (Andrechek, Hardy et al. 2000) and further correlated with selective genomic amplification of the activated *erbB2* allele (Montagna, Andrechek et al. 2002; Hodgson, Malek et al. 2005). In addition to *erbB2* amplification, deletion of chromosome 4 was frequently observed in $ErbB2^{KI}$ tumors (Hodgson, Malek et al. 2005). 14-3-3σ, a 14-3-3 protein family member, was among the deleted genes. As a putative tumor suppressor which can be upregulated by p53 in response to DNA damage, the 14-3-3σ gene product is involved in cell-cycle checkpoint control and blocks DNA synthesis by inhibiting Akt pathway (Yang, Zhao et al. 2006). These evidences suggest that ErbB2 induced tumors may further cooperate with 14-3-3σ ablation to promote tumor progression.

In the initial experiment, overexpressing 14-3-3σ in TM15 cells, an established breast cancer cell line derived from mammary tumors of $ErbB2^{KI}$, decreased cell motility in Boyden chamber and wound healing assay, suggesting restoration of 14-3-3σ significantly impairs ErbB2-induced breast cancer metastasis. Knockdown 14-3-3σ in MCF-10A and MDCK cells by siRNA resulted in cells forming solid structure that lacked a discernible lumen, suggesting that down-regulation of 14-3-3σ results in the loss of epithelial polarity (Lu, Guo et al. 2009).

In order to verify the effect of 14-3-3σ in the regulation of epithelial polarity *in vivo*, a mouse model have 14-3-3σ deleted in the luminal epithelial compartment (MMTV-Cre/*14-3-3*$\sigma^{F/F}$) was established. Histological examination of virgin mammary glands revealed that the mammary ducts derived from 14-3-3σ deficient mice had multiple layers of CK8+ luminal epithelial cells, in contrast to a single layer of luminal cells in the wild type mice. To investigate whether the multilayer epithelial phenotype in the 14-3-3σ-deficient gland is related to a loss of epithelial polarity, the primary mammary gland epithelial cells from control and 14-3-3σ-deficient mice were isolated and grown on 0.4μm porous membrane transwell for four days till they fully reached confluence. The cells were stained for ZO-1 and E-cadherin to analyze the apical-basal polarity in the cells. In contrast to the control cells, 14-3-3σ-deficient epithelial cells

displayed disrupted cell junctions at apical and basal layers (Figure 9.5.A). Quantification of cells with placement of ZO-1 at apical layer and E-cadherin at basal layer as polarized cell revealed that the percentage of polarized cell were dramatically reduced in 14-3-3σ-deficient cells compared with the wild-type controls (Figure 9.5.B), indicating that 14-3-3-σ is required for correct cell polarity. Furthermore, Par3 could be detected to readily in physical complex with 14-3-3σ protein. 14-3-3σ MDCK cells showed lower Par3 at the cytoplasm membrane (Lu, Guo et al. 2009). Together, these data suggest that Par3 is involved in 14-3-3σ regulation of epithelial polarity. These observations taken together with the results of Par3 described in this thesis suggest the implication of Par3/14-3-3σ in metastasis of ErbB2-overexpressing breast cancer.

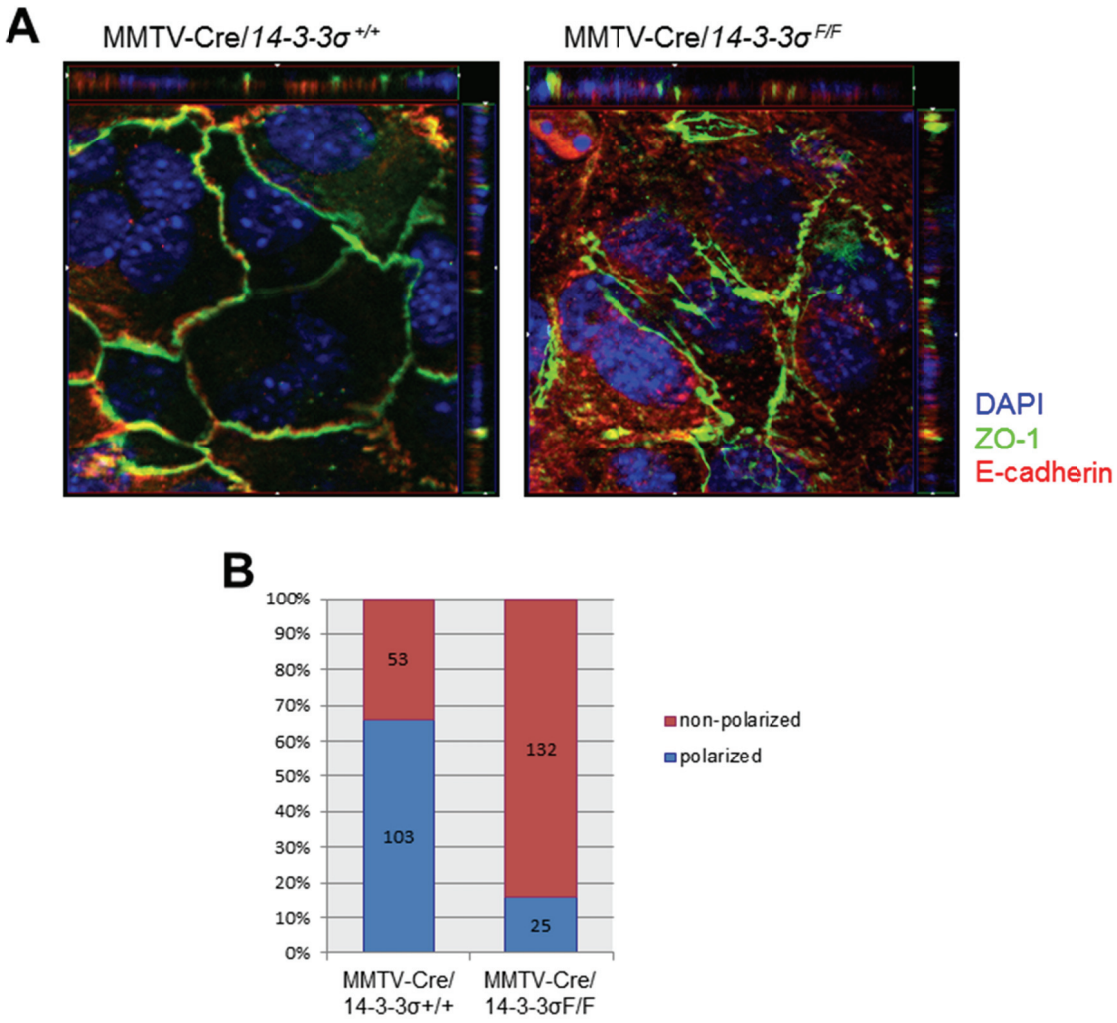

Figure 9.5. Primary mammary epithelial cells lacking 14-3-3σ have disrupted epithelial polarity

(A) Representative immunofluorescence images of control mammary epithelial cells (MMTV-Cre/*14-3-3σ*$^{+/+}$) and 14-3-3σ-deleted cells (MMTV-Cre/*14-3-3σ*$^{F/F}$) in transwell monolayer culture. ZO-1 (green) was stained for apical tight junctions. E-cadherin (red) was stained for basolateral adherens junction. Nuclei were counterstained with DAPI (blue).

(B) Quantification of polarized and nonpolarized epithelial cells. The ability of the cells to localized ZO-1 to the apical border was analyzed using XZ optical sections.

The signaling adapter Gab1 regulates cell polarity by acting as a PAR protein scaffold

Ziqiang Yang[1], Bin Xue[2,3], Masataka Umitsu[1], Mitsuhiko Ikura[1,4], Senthil K. Muthuswamy[1,2,3,4,] Benjamin G. Neel[1,4]

Author Affiliations

1Campbell Family Cancer Research Institute, Ontario Cancer Institute, Princess Margaret Hospital, University Health Network, Toronto, ON, Canada

2Cold Spring Harbor Laboratory, One Bungtown Road, Cold Spring Harbor, NY;

3Department of Molecular and Cellular Biology, Stony Brook University, Stony Brook, NY;

4Department of Medical Biophysics, University of Toronto, Toronto, ON, Canada

Correspondence should be addressed to Ziqiang Yang (zyang@uhnresearch.ca)

Grb2-associated binding protein 1 (GAB1) is a pleckstrin homology (PH) domain-containing docking protein that is believed to function downstream of receptors for growth factors and cytokines. The Gab1 belongs to the Gab family proteins which lack enzymatic activity, but become phosphorylated on tyrosine residue upon activation by external stimuli, providing binding sites for multiple proteins and involving in signal transduction (Holgado-Madruga, Emlet et al. 1996). For example, Gab1 is the major downstream of the Met receptor in epithelial cells (Weidner, Di Cesare et al. 1996). Gab1 is localized to cell-cell junctions via PH domain in MDCK cells. Gab1 is recruited to Met by HGF stimulation, coupled with the p85 subunit of PI3-kinase and responsible for Met-dependent PI3K activity, which leads to cell scattering (Maroun, Holgado-Madruga et al. 1999; Lock, Maroun et al. 2002). The Gab1-dependent recruitment of SHP-2 is required for sustained MAPK activity and HGF-induced epithelial morphogenesis (Maroun, Naujokas et al. 2000). Gab1 function is also co-opted in cancers. ErbB2-induced cell transformation requires Gab1mediated ERK activation (Yamasaki, Nishida et al. 2003). Gab1 is required for stimulating tumor growth in Met overexpressing DLD-1 colon carcinomas cells (Seiden-Long, Navab et al. 2008).

In MDCK cells, Gab1 was found to associate with Par1b through a region between amino acid 152-250. Deletion of this region (Gab1Δ152-250) markedly reduced Gab1-Par1b interaction. In addition to Par1b, Gab1 also bond to Par3, in turn interacted with aPKC. The region for Par3 binding lies between amino acid 301-400. However, when cells co-expressed Par1b and Par3, less Par3 co-immunoprecipitate with Gab1, suggesting Par1b interfere with the interaction of Gab1 and Par3. Par1 has been reported to phosphorylate Par3 and restrict Par3 to tight junction (Benton and Johnston 2003). To test whether Par1b affects the Gab1 interacting with Par3 depended on Par3 phosphorylation, a phosphorylation-resistant mutant Par3 were tested and found its interaction with Gab1 was unaffected by Par1b, indicating that Par1b disrupts Gab1/Par3 interaction by phosphorylating Par3. In addition, Par1b kinase activity was enhanced through Gab1 binding.

The involvement of Par proteins prompted us to test whether Gab1 is involved in regulation of epithelial polarity. Previous studies showed that Par1 depletion results in shortening of the lateral membrane. Because Gab1 and Par1 form a complex and Gab1 positively regulates Par1 kinase activity, I assessed the effect of Gab1 on apical-basal polarity. Control and GAB1-

KD MDCK cells were polarized on the porous filters, then immunostained for ZO-1, E-cadherin and gp135, an apical surface glycoprotein. We found that the lateral membrane (as revealed by E-cadherin) was shortened in GAB1-KD cells compared to the control cells (Figure 9.6). Gab1-depletion also increased the thickness of TJs without affecting the overall cell polarity, as determined by even staining of gp135 on the apical surface.

The Gab1-depleted cells then were reconstituted with wild type Gab1 or its Par1b- or Par3-binding deficient mutants and analyzed for the polarity. As Gab1 proteins were substantially overexpressed in the reconstituted cells, overexpression of WT Gab1 resulted in a severe loss of polarity, where ZO-1 diffused to the basolateral domain, disrupted apical surface shown by gp135 staining and abolished epithelial cobblestone morphology (Figure 9.7.A). Quantification of cell polarity by counting the cells with correct placement of ZO-1 at apical layer and E-cadherin at basal layer as polarized cell revealed that 80% of the Gab1-overexpressing cells were non-polarized (Figure 9.7.B). By contrast, ZO-1 and E-cadherin remained well-segregated in the cells expressing Gab1 mutants lacking Par1b- or Par3-binding domains (Figure 9.7.A). Cell polarity were only partially lost in these cells. Thus, Gab1 overexpression disrupts apical-basal polarity in a Par1b- and Par3-dependent manner. Further experiments to analyzed TJ formation by measuring trans-epithelial electrical resistance (TER) in calcium switch experiments shows that Gab1-KD cells attained a higher TER than control cells, whereas Gab1-overexpressing cells decrease TER, suggesting TJ formation is regulated by Gab1.In conclusion, these results identify Gab1 as a negative polarity that function as a scaffold for modulating Par protein complex on the lateral membrane in epithelial cells.

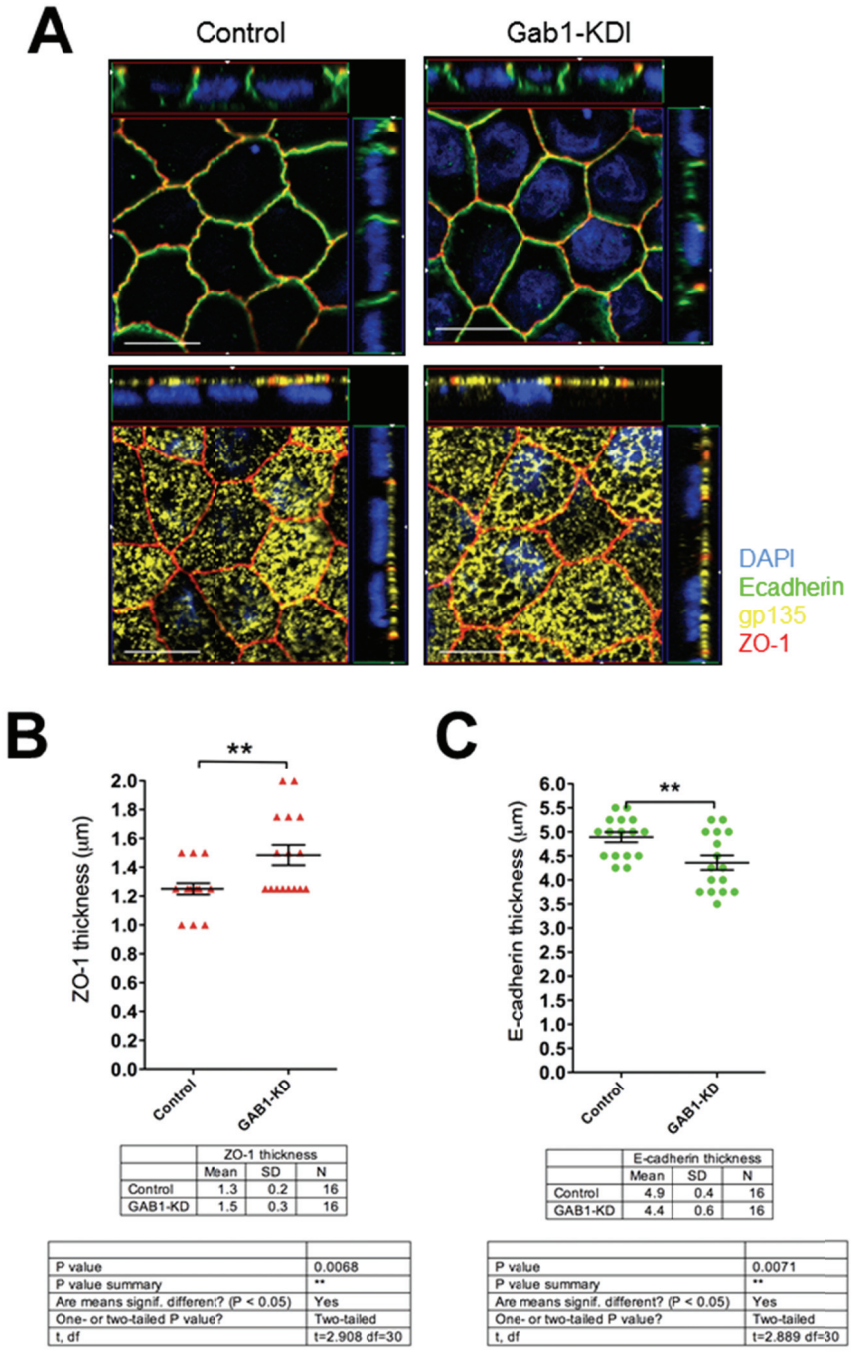

	ZO-1 thickness		
	Mean	SD	N
Control	1.3	0.2	16
GAB1-KD	1.5	0.3	16

P value	0.0068
P value summary	**
Are means signif. differen? (P < 0.05)	Yes
One- or two-tailed P value?	Two-tailed
t, df	t=2.908 df=30

	E-cadherin thickness		
	Mean	SD	N
Control	4.9	0.4	16
GAB1-KD	4.4	0.6	16

P value	0.0071
P value summary	**
Are means signif. different? (P < 0.05)	Yes
One- or two-tailed P value?	Two-tailed
t, df	t=2.889 df=30

Figure 9.6. Gab1 regulates cell polarity

(A) Control and GAB1-KD MDCK II cells were cultures on transwell filters for 3 days. The cells were immunostained for ZO-1 (red)/E-cadherin or ZO-1 (red)/gp135 (yellow).

(B) Quantification of TJ thickness (ZO-1 staining) and lateral membrane height (E-cadherin staining).

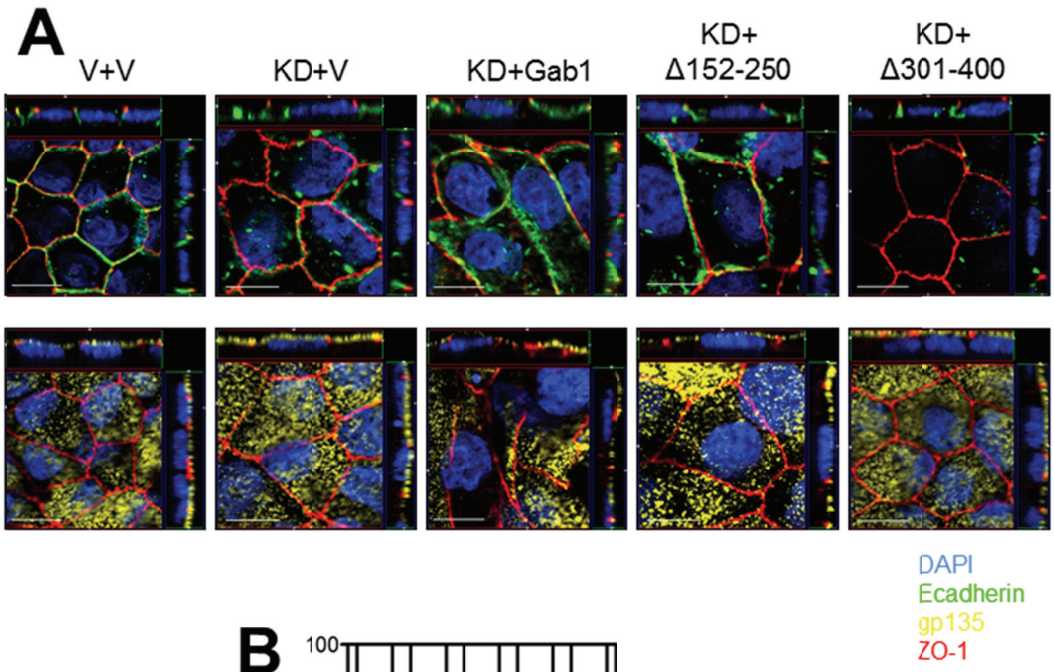

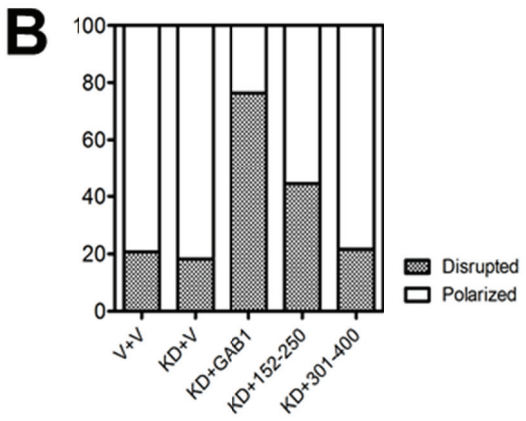

	Disrupted	Polarized
V+V	20.72727	79.27273
KD+V	18.22660	81.77340
KD+GAB1	76.41509	23.58491
KD+152-250	44.36090	55.63910
KD+301-400	21.56863	78.43137

Figure 9.7. Overexpression of Gab1 disrupts epithelial polarity

GAB1-KD MDCK II cells reconstituted with WT Gab1 or the indicated mutants were cultures on transwell filter for 3 days.

(A) The cells were immunostained for ZO-1 (red)/E-cadherin or ZO-1 (red)/gp135 (yellow).

(B) Quantification of polarized cell in these cells.